Russian Original Vol. 32, No. 4, April, 1972

Translation published November, 1972

SATEAZ 32(4) 303-434 (1972)

SOVIET ATOMIC ENERGY

АТОМНАЯ ЭНЕРГИЯ
(ATOMNAYA ÉNERGIYA)

TRANSLATED FROM RUSSIAN

CONSULTANTS BUREAU, NEW YORK

SOVIET ATOMIC ENERGY

Soviet Atomic Energy is a cover-to-cover translation of *Atomnaya Énergiya*, a publication of the Academy of Sciences of the USSR.

An arrangement with Mezhdunarodnaya Kniga, the Soviet book export agency, makes available both advance copies of the Russian journal and original glossy photographs and artwork. This serves to decrease the necessary time lag between publication of the original and publication of the translation and helps to improve the quality of the latter. The translation began with the first issue of the Russian journal.

Consultants Bureau journals appear about six months after the publication of the original Russian issue. For bibliographic accuracy, the English issue published by Consultants Bureau carries the same number and date as the original Russian from which it was translated. For example, a Russian issue published in December will appear in a Consultants Bureau English translation about the following June, but the translation issue will carry the December date. When ordering any volume or particular issue of a Consultants Bureau journal, please specify the date and, where applicable, the volume and issue numbers of the original Russian. The material you will receive will be a translation of that Russian volume or issue.

Subscription
$75.00 per volume (6 issues)
2 volumes per year
(Add $5 for orders outside the United States and Canada.)

Single Issue: $30
Single Article: $15

CONSULTANTS BUREAU, NEW YORK AND LONDON

227 West 17th Street
New York, New York 10011

Davis House
8 Scrubs Lane
Harlesden, NW10 6SE
England

Published monthly. Second-class postage paid at Jamaica, New York 11431.

SOVIET ATOMIC ENERGY

A translation of *Atomnaya Énergiya*
Translation published November, 1972

Volume 32, Number 4 April, 1972

CONTENTS

CONTENTS

(continued)

Engl./Russ.

CONTENTS

(continued)

The Russian press date (podpisano k pechati) of this issue was 3/29/1972. Publication therefore did not occur prior to this date, but must be assumed to have taken place reasonably soon thereafter.

ON THE OCCASION OF THE SEVENTIETH BIRTHDAY OF ACADEMICIAN VIKTOR IVANOVICH SPITSYN

The editorial staff of Atomnaya Énergiya warmly greets Academician Viktor Ivanovich Spitsyn on the occasion of his 70th birthday, and wishes him excellent health, long years of life, and creative successes.

Translated from Atomnaya Énergiya, Vol. 32, No. 4, p. 267, April, 1972.

REVIEWS

PROBLEMS OF SAFETY OF NUCLEAR POWER PLANTS*

V. A. Sidorenko

UDC 621.039.51

Problems of safety of nuclear power plants occupied one of the most prominent places among the subjects discussed at the IV Geneva Conference.

Of 505 reports read at the Conference, 78 dealt with safety. In accordance with the topics they discussed, these reports can be arbitrarily divided into five groups:

1. Discussion of the general scientific and engineering aspects of nuclear power plant safety including a study of the fundamental approach to safety control (so-called "philosophy of safety") (24 reports).
2. Legislation concerning safety, norms, standards, and legal problems associated with the division of responsibilities, etc., (nine reports).
3. Effect of nuclear power on the environment including a discussion of the actual conditions prevailing at nuclear power plant sites (23 reports).
4. Scientific and engineering problems associated with the removal of radioactive waste and its burial (eight reports).
5. Effects of radiation on living organisms, radiation protection and shielding (14 reports).

Approximately the same attention has been devoted to two aspects of nuclear safety: the effect on environment and handling of nuclear waste (3rd and 4th groups, 31 reports) and the scientific and engineering principles of nuclear plant safety and setting up norms for safety control (1st and 2nd groups, 33 reports).

The materials presented at the Conference reflect considerable advances in nuclear safety control: the problem is now much better understood, technical and organizational measures of safety control have improved, and a reliable basis has been provided for nuclear safety taking into account the expected growth of nuclear energy.

The expected growth of nuclear power focussed attention on the effect on the environment of nuclear engineering in general and of specific power plants whose operation proved the adequacy of the safety measures provided. One conclusion that follows from the discussion is that the radioactivity level in the vicinity of nuclear power plants and fuel processing plants is very low and that the amount of radioactive waste is considerably less than allowed by national supervisory and legislative organs for every specific plant. Detailed information on the environmental effects of atomic installations was presented in the American Report No. 087†, English Report No. 512, West German Report No. 399, etc. For example, the annual waste of radioactive materials of commercial nuclear power plants in 1970 in the USA amounted to 0.14-25% and 0.002-6.5% of the allowed level of liquid and gaseous waste (Report No. 087). Even now it is possible to design nuclear reactors with a radioactive waste level as low as desired. British experience indicates that fuel processing plants produce the greatest amount of radioactive waste. Many countries have undertaken special studies whose aim is the reduction of radioactive discharge from future high-output fuel processing plants.

* Review of papers presented at the IV International Conference on Peaceful Uses of Atomic Energy, Geneva, 1971.

† Lists of reports presented at the Geneva Conference were published in the October issues of Atomnaya Énergiya (Soviet Reports) and Atomnaya Tekhnika za Rubezhom (foreign reports) in 1971.

Translated from Atomnaya Énergiya, Vol. 32, No. 4, pp. 269-272, April, 1972. Original article submitted January 13, 1972.

By considering the possible ways of penetration of radioactive products into the surroundings, and by comparing environmental pollution due to nuclear and fossil fuels, the authors of the Soviet Report No. 684 arrived at the conclusion that nuclear energy allows the conservation of a reasonably clean environment; what is more, replacement of fossile-fuel power by nuclear power should lead to a considerably lower level of contamination of the surroundings by toxic materials and so improve the environment.

Despite the optimistic prospects of the present and future states of nuclear safety, all reports call for still more stringent measures to ensure the safety of nuclear power plants with respect to both "actual" and "potential" radiation dangers (reduction of allowed radioactive-discharge levels and improvement of the reliability of safety devices and radioactivity containment devices). This trend is associated with the ever increasing number of nuclear power plants and their location in densely populated areas.

Perfection of safety systems, including containment devices, proceeds in the direction of higher device efficiency and reduced size and cost. This is quite pressing as the rise in the cost of nuclear power plants is due largely to the additional safety measures necessary to meet the more stringent requirements.

Another feature characteristic of modern trends is the increasingly important role of equipment reliability in securing actual plant safety and in reducing the probability of accidents. Although these aspects of the problem of safety are not entirely new, they have become recently of primary importance together with safety measures that can be termed "obvious." Of independent significance is the supervision of plant equipment at all stages, from its manufacture to utilization. The accumulated operational experience helped to improve methods of continuous supervision and periodic inspection of nuclear plants (ultrasonic flaw detection, noise monitoring, etc.).

As follows from the reports, particular attention is now devoted to specific solutions to key technological safety problems that are revealed in studies of the possible developments of dangerous processes in nuclear plants especially under emergency conditions.

The basic trends in nuclear plant safety were discussed in USA reports (Nos. 038, 040) from the point of view of "protection in depth" which includes the following steps in the provision of nuclear safety: securing equipment reliability, provision of technological and circuit impossibility of dangerous consequences of any single failure or damage, limitation of the consequences of any possible emergency case.

The fact that problems of nuclear plants safety are complex and many-sided and have no single universal solution has been stressed in many reports. In particular, one cannot expect that security can be provided only by high-quality equipment (much better than used in conventional power plants) or only by ensuring containment of the effects of possible emergencies (such as isolation of the plant). The problem must be considered from all its aspects.

The implementation of the safety-in-depth principle can be seen in the different approaches to nuclear plant safety.

In one of the possible variants all systems and equipment of the plant are divided into three functional parts: the reactor proper, equipment and systems that ensure its normal operation; "external" protection systems that reduce the possibility of hazardous deviation of plant parameters from their design values and protect the plant in case of failure of normal operating devices; systems whose task is to reduce as much as possible the consequences of any potential accident. The safety of nuclear power plants is ensured by independent and reliable performance of all these three functional parts.

In a different approach, safety-in-depth is ensured by different independent and reliable "barriers" that prevent penetration of fission fragments to inhabited areas: from the fuel to coolant, from the coolant to the reactor location, from the power plant location to the surroundings, and finally from the surroundings by various means to the population.

The development of specific concepts and criteria of safety in several countries merits special attention.

The desirability of a numerical and probabilistic approach to the evaluation and standardization of nuclear safety has been recently frequently stressed together with the fact that the amount of statistical data on the performance of nuclear power plant equipment is still insufficient. The expensiveness of putting this approach into practice and the importance of international cooperation for the solution of this problem has been pointed out in the French Report No. 579. The Conference proved beyond doubt that the necessity of a

numerical approach to safety analysis is now generally accepted, but that, at the same time, the feasibility of a probabilistic approach to safety standardization is still treated with reserve. Numerical methods of estimating equipment reliability and accident probability are quite advanced and should be widely used in design practice of nuclear power plants. These methods make it possible to compare various approaches and to select optimum solutions in the design of safety equipment and devices. However, there is apparently no sufficient basis for a numerical treatment of the standardization of nuclear plant safety in the immediate future. In the West German Report No. 364 attention is called to the fact that throughout a normal life span all existing nuclear power plants are unable to provide sufficient statistical data for very grave accidents whose probability is estimated as 10^{-7} per year; in such cases the numerical approach becomes meaningless.

The most frequently used concept in safety control is still the concept of the "basic design accident." Perfection of this concept is partially evident in the fact that attempts are made to apply probabilistic methods in selecting the basic design accident. One of the most important advances in this field is the use of not only "the maximum probable accident" but of a full spectrum of possible accidents of which the basic design accident is one. This is done in order to protect the plant not only against major but little probable potential dangers but also against real dangers presented by much more probable equipment failures. An effective and systematic approach to the analysis of the spectrum of emergency situations is the so-called "failure tree." This method reveals all situations that are liable to result from any specific failure or damage. The failure tree makes it possible to demonstrate and evaluate numerically various combinations of serious damages that can lead to an emergency situation.

In aqueous reactors the basic design accident is still assumed to be the total disruption of the main pipeline of the circulating loop. The possibility of reactor vessel rupture is also considered. Some designs (e.g., in West Germany) even consider the probability of an accident involving vessel damage. The most probable location of vessel damage is considered to be the region where the circulating loop pipes are connected to the vessel. An analysis of the probability of crack development in the vessel makes it possible to take into account in the design defects in the vessel that can cause leakages much smaller than resulting from a burst in the main pipeline (West German Report No. 364).

A modification of the basic design accident concept was described in the Canadian Report No. 150. The plant safety is evaluated by quantitatively analyzing the frequency of occurrence of probable hazardous processes in the system, but the use of specific maximum radiation exposure of the population is based on two principal schemes of accident occurrence: a single failure in standard technological equipment with the preservation of full capability of accident prevention and containment devices or the coincidence of failure of both the standard operating system and the accident prevention system. In the first case maximum radiation exposure is that acceptable for normal operation; the second case involves the use of special maximum radiation exposure rates.

The available design and operational experience made it possible to find many specific solutions in various safety control systems (USA Report No. 040). For example, methods have been developed for the construction of equipment and buildings resistant to earthquakes (Japanese Report No. 226, Swiss Report No. 672), hurricanes, floods, and other natural disasters. There is also the experience of building a nuclear power plant near an airfield where the danger of collision or fire caused by an airplane accident must be taken into account. Instruments and a program have been developed for monitoring the spread of radioactivity in the locality surrounding nuclear power plants.

Devices have been developed for aqueous reactors which monitor and if necessary suppress effects associated with xenon power fluctuations (such as, for example, absorbing rods of partial length); fixed intermitent absorbers are used for canceling the positive temperature coefficient of the moderator reactivity. Comprehensive programs have been developed for analyzing the vibrations of intravessel devices in the course of start-up tests for the detection and elimination of weak points. Specific solutions aimed at improving the construction reliability, provision of continuous and periodic supervision, and ensurance of operating efficiency under emergency conditions are incorporated in the design of reactor cooling systems, of buildings and containment installations, of safety control systems, monitoring and measuring apparatus, and other systems.

Among problems that require further research are:

development of flaws in steel structures of circulation loops;

thermal interaction of fuel and coolant, in particular the heat exchange crisis (British Report No. 477);

embrittlement of thick steel samples (including thermal shock in case of emergency cooling of the reactor core);

performance of safety systems under emergency conditions;

critical parameters and power (this can be said to be a "perennial" problem);

the probability of natural phenomena which must be allowed for in the design of nuclear power plants;

improvement of the safety systems of core cooling (USA Reports Nos. 040 and 039);

conditions of heat removal in time of and after emergencies involving the loss of coolant;

hydrodynamic effects in the reactor vessel and in the cooling loop in case of large leakages;

improvement of remote monitoring methods of the equipment state in the course of reactor operation and perfection of ultrasonic methods;

melting of the reactor core (West German Reports Nos. 365 and 364).

Special attention has been devoted to the safety of fast-neutron reactors. In sodium-cooled fast reactors characteristic hazardous events in which a single failure or damage is liable to cause grave consequences are damages in the primary loop, sodium ignition, chain damage of fuel elements, the passage of large gas bubbles through the core, etc. Accordingly, in the analysis of various design accidents (fast reactivity buildup, stoppage of coolant circulation, etc.), and in the development of protective measures particular attention was given to the study of such phenomena as the formation of voids in sodium, interaction of the coolant with molten fuel, the mechanism of the spread of fuel element damage, the Doppler effect, the formation and spread of aerosols in connection with sodium ignition (USA Report No. 041).

In conclusion, one should stress once more the generally accepted importance of the creation of a system of norms and rules for all stages of the design, equipment manufacture, construction, operation, and maintenance of nuclear power plants. The reaction of such a system of norms and rules is a continuous process. Besides this work, which is conducted by the Atomic Energy Commission for the development of general rules, criteria, specifications, procedures, etc., with the participation of 1200 representatives of 400 organizations, work is going on in the USA on the creation of a system of 78 most important nuclear standards. The development is now being concluded of the first ten standards to which belong:

secondary criteria for pressurized-water reactors;

secondary criteria for boiling water reactors;

criteria for taking into account seismic effects in the location and design of power reactors;

qualification and training of nuclear power plant personnel;

specifications of periodic test in nuclear power plants;

specifications on prestart and startup tests of nuclear power plants;

criteria and practical measures for securing quality performance of nuclear power plants, etc.

One thousand and five hundred nuclear standards are to be developed in the next decade. Experience indicates that nuclear power plants can be and are designed to operate reliably and safely. The development and introduction into practical use of a system of norms and standards should consolidate the present level of technology and extend it successfully to other fields.

PEACEFUL USE OF ATOMIC ENERGY AND THE ENVIRONMENT*

U. A. Izraél'

UDC 621.039.77

With the rapid development of nuclear power engineering and a large-scale introduction of atomic energy in industry and daily life it is inevitable that mankind would be affected by nuclear radiation and radioactive products would get into natural media. These problems appear in the production of nuclear fuel and atomic power, in reprocessing fuel, and in handling wastes and isotopes.

Numerous estimates show that by the year 2000 the generation of electrical power from atomic power plants (APP) will exceed 3 mill. MW and will comprise ~50% of the entire electric power generation.

At present the number of APP is increasing in many countries.

One of the most important conditions for extending the network of APP consists in ensuring the safety of operation of these power plants from the point of view of the effect on the environment.

Estimates show that the main source of radiation effect on man (at present and in future) is the contamination due to the production of atomic energy [1]. Besides, it is necessary to consider specific thermal contamination of the natural media in the operation of APP.

A large attention is being devoted to these problems. The effect of radioactive contaminants on the environment is being investigated extensively and the problems appearing in these investigations are discussed in international meetings and symposia [2, 3]. At the IV Geneva conference on the peaceful use of atomic energy many papers were devoted to this problem. In two meetings of the special section on "The effect on the environment and the reaction of the population" 12 papers (of which three were from Soviet authors) were read and in addition six papers (two by Soviet authors) were presented in abstract form. A number of papers, presented in other sections, were also related to this problem (for example, papers on working out the principle for locating APP and the choice of safe areas for APP).

It was noted at the conference that the problems of the effect of radioacitve substances on man and the biosphere as a whole are focal in the peaceful use of atomic energy.

It is clear from the papers presented at the conference that extensive investigations are being carried out in different countries on the possible ways of incidence of radioactive products into the environment and their interaction with the biosphere and the migration of isotopes to human body through different biological chains. On one hand careful measurements and study of the behavior of radioactive products penetrating into the environment from reactors and plants are being made; on the other hand the interaction of the radio nuclides with the natural media are being studied in a general way.

The Soviet papers discussed in detail the results of the study of biological effect and behavior of radioactive products in agricultural cycles [4] and in forest plantations [5]. Extra-root entry of radio nuclides into plants and also their assimilation by plants from the soil and passage to livestocks is discussed.

During global fall-outs of long-life radioactive products the maximum amount of radio nuclides is retained in agricultural plants. It is found that the maximum content of radio nuclides in harvest is observed after the period of formation of the productive organs (for example, the radio nuclide content in wheat is maximum when the wheat attains milk ripeness).

*Review of papers presented at the IV International Conference on Peaceful Uses of Atomic Energy, Geneva, 1971.

Translated from Atomnaya Energiya, Vol. 32, No. 4, pp. 273-277, April, 1972. Original article submitted January 31, 1972.

The assimilation of radio nuclides by agricultural plants from soil is characterized by the following figures: the contaminated area from which the radioisotope is assimilated (per kg of the product) is hundreds of cm^2 for Zr^{95}, tens of cm^2 for W^{185}, a few cm^2 for Cs^{137}, Sr^{90}, and Fe^{59}, a few tenths or hundredths of cm^2 for Ce^{144}, Ru^{106}, Zr^{95}, and varies between a few tenths to a few thousandths of cm^2 for Pu^{239}, U^{235}, Pm^{147}, Y^{91}.

For extra-root incidence the radio nuclide content in a wheat grain is ten times higher than in the case of their assimilation from soil. In respect of the concentration in milk and meat radio nuclides form a descending series $I^{131} > Mo^{99} > Sr^{89} > Ba^{140}$.

The limiting fall-out intensities of radio isotopes and their content in soil, at which the annual incidence of nuclides into human organism along with food does not exceed the limiting admissible value, are estimated as: for Sr^{90} – 1.5 mCi/month·km^2 (content 2 Ci/km^2), for I^{131} – 0.5 mCi/day·km^2. It is shown that the main degree of radiational affliction of grain cereals is caused in the forming ears.

The problems of migration of radio nuclides in forests, radiation decrease in forests and the effect of radioactive fall-outs on bio-organisms under the forest cover are discussed in [5]. The results of the investigations show that the forest, as a part of the landscape, is among one of the most sensitive biological systems to radioactive fall-out.

The results of a 15 year study of the behavior of radio nuclides, falling into water and earth ecosystems during the operation of a reactor in model experiments at Oak Ridge laboratory in USA, are presented in [6]. For water systems the isotopes Sr^{90}, Cs^{137}, Co^{60}, and T^3 (sometimes Ru^{106}, Sb^{125}, and Zn^{65}) are typical; for forest and field systems Co^{60}, Sr^{90}, Zn + Nb^{95}, Ru^{106}, Cs^{137}, and Ce^{144} are typical.

The results of studies of dilution and diffusion of radio nuclides in sea water, and also of the possibility of incidence of these products in sea organisms (Co^{60}, Fe^{59}, and Mn^{54}) are presented in Indian [7] and Japanese [8] papers.

The background radiation situation and also the dose from medicinal procedures in different countries are discussed in some papers. For instance, it is shown that the natural background from the radiation from mountain rocks and cosmic rays comprises 120 mrem/yr [9]; the intake of radiation through medicine gives an average genetic dose of 20-37 mrem/yr [9, 10], while the global fall-outs from the past tests of nuclear weapons give an average dose of 10 mrem/yr [9].

The radioactive contamination of ocean waters and the behavior of some radio nuclides in sea water are estimated in a Soviet paper [11]. In 1966-1967 on the whole there was a decrease in the contamination of the surface waters of Pacific and Atlantic oceans. The amount of Sr^{90}, going deep into Pacific ocean, exceeds the fall-out during this period. Technogenic radioactive regions have been detected (for instance, near the west coast of North America, close to the mount of Columbia river). The results of the study of physicochemical and biological processes, which control radioactivity, are interesting. It is found that the accumulation of iron in suspended matter in oceans leads to the transformation of a number of radio nuclides (Y^{91}, Ce^{144}, Nb^{95}) in the suspended fraction. In the presence of iron the coefficient of accumulation of these isotopes by plankton increases by an order of magnitude. This shows that the disposal of radioactive wastes into oceans presents a definite hazard and can not be recommended (however, Japan, for example, does not adhere to this practice) [8].

It is obvious that no branch of industry has such a control and measures of protection against the possibility of contamination of the environment as the nuclear power industry.

A careful control of exposure of the population to radiation, the study of contamination of the environment, and the measures of protection of the population are discussed in [8, 10, 12, 13] and other papers.

It is shown in [13, 14] that detailed investigations of the contamination of the environment are carried out around APP: investigations of agricultural vegetations, drinking water, precipitations, water organisms, and fishes, domestic and wild animals, and so forth. The problems of utilization of ground, the settlement density, meteorology, geology, seismology, hydrography, hydrology of the region are also studied. It is especially important to know what is the admissible limit of dilution of water and air basins near APP by liquid and gaseous wastes. These investigations are necessary for the prognosis of possible contamination of environment at present and in future.

The construction of APP almost excludes the possibility of ejection of fission products into the environment during their normal operation. Only the gaseous isotopes Ar^{41}, Xe^{133}, Kr^{85}, H^3 [1] and very

insignificant amount of I^{131} can get into the atmosphere. Gaseous ejections of C^{14} and I^{129} (latter with $T_{1/2} = 1.7 \cdot 10^7$ yr is formed during the processing of nuclear fuel) are described in [13]. Liquid disposals contain H^3 and in very small quantities also Mn^{54}, Co^{58}, Co^{60}, Sr^{89}, Sr^{90}, Ru^{106}, Sb^{125}, Cs^{134}, Cs^{137}, Ba^{140} [1, 13].

The number and amount of ejections varies in wide limits during the operation of reactors. The average amount of liquid waste in reactors in USA and England in 1966-1969 was 6-11 Ci/yr (maximum up to 27 Ci/yr), tritium up to 3700 Ci/yr, noble gases up to $3.8 \cdot 10^5$ Ci/yr (mainly Ar^{41} up to $2 \cdot 10^5$ Ci/yr), which comprises about 24-28% of the admissible level for liquid wastes and 15% for gaseous wastes [1].

The largest yield of noble gases is observed in the operation of boiling water reactors (BWR) and in gas cooled reactors (GCR); the smallest yield is observed in reactors cooled by pressurized water (PWR). The pattern is reversed for the yield of tritium in the operation of these reactors.

Thus the ejections from the American BWR in 1968 comprised [13] 240 thousand Ci/yr, of which Xe^{133} was 9000 Ci, Kr^{85} 3 Ci, H^3, 0.2 Ci, and I^{131} 0.02 Ci. The annual liquid disposal was 2 Ci H^3, 0.6 Ci Co^{68}, and 0.9 Ci Co^{60}. Gaseous ejections of the American PWR during the year was 14 Ci H^3, 3 Ci Kr^{85}; the total gaseous ejection comprised 10^3-10^4 Ci, while the liquid disposals were estimated at 1000 Ci H^3.

The fuel treatment plants discharge Kr^{85} in appreciable quantities. In liquid discharges Ru^{106}, uranium, plutonium, americium, and curium have been detected [13]. The concentrations of radio nuclides in liquid discharges comprise $1.4 \cdot 10^{-10}$-$2.2 \cdot 10^{-6}$ mCi/cm^3.

The ejection of noble gases into the atmosphere by Canadian reactors comprises an average of 6400 Ci/day from the first reactors and up to 440 Ci/day from the new reactors; the ejection of tritium is up to 30 Ci/day (ejection of I^{131} is in all 10^{-5}-10^{-3} Ci/day and about 10^{-2} Ci/day in the oldest reactor.

The amount of tritium in liquid discharges goes up to 15 Ci/day. In old reactors the ejection of Sr^{90} (up to 7.5 mCi/day) is observed; Cs^{134}, Cs^{137}, and Co^{60} ($6 \cdot 10^{-8}$ mCi/cm^3 on the average) are also present.

At the beginning of 1971 the gas ejection at four APP of Japan comprised $8 \cdot 10^{-4}$-11 mCi/sec (up to 1000 Ci/day. At "Mishana" APP the ejections in February 1971 comprised 0.1 Ci/day. Liquid discharges were up to 7-1200 mCi/month [8].

Such ejections lead only to an insignificant concentration of radio nuclides in the environment. Thus the concentrations in expendable surface waters of some APP in the USA reached 100-270 nCi/liter, 2-6 nCi H^3/ml in drinking water, up to 0.6 nCi Co^{60}/g in fish, up to 120 nCi Mn^{54}/g in precipitations, and up to 57 nCi Co^{60}/ml in vegetables [13]. A concentration of 1 nCi Co^{60}/g was observed in the organisms of sea shells in the vicinity of one Japanese APP [8].

From the ejections mentioned above the population living in the immediate vicinity of an APP can receive only a small dose of radiation. Thus the maximum doses of external radiation from ejections (mainly Ar^{41}) from the tubes of Canadian APP in 1968 was up to 0.26 rem/yr at a distance of 1 km, and 0.037 rem/yr at 4.8 km. The total integral dose of radiation of the entire population at a distance up to 50 km is 16 man·rem/yr [14]. At a Japanese APP the dose at a distance of 1.5 km for constant wind and gaseous ejection of 7500 mCi/yr is 7 mrem/yr [8].

In 1968 at an Americal BWR the dose of external radiation at a distance of 2 km was 10 mrem/yr; the maximum dose of internal radiation received by fishes in the region of fuel treatment plants was 4 mrem/yr [13].

Specialists of different countries use the standards recommended by the International Commission on protection from radioactivity (ICRP) in the design and construction of APP. However, there is a system of licensing and additional requirements in the zone of construction of APP. They amount, for example, [9], to the following: for the atomic industry in FRG a genetic dose of 2 ber in 30 years (instead of 5 ber according to ICRP) is acceptable.

For long-range planning the dose from gaseous ejections for the population is restricted to 1 rem in 30 years or 30 mrem/yr. It is assumed that for different persons the dose must be approximately the same.

At new plants charcoal filters and delay lines for gaseous ejections are used for purification. For liquid wastes also (in future planning) the acceptable dose is 1 rem in 30 years, uniformly distributed among the external radiation, internal radiation in drinking water, and internal radiation in cereal requirements.

Individual enterprises are allowed an ejection of liquid wastes not exceeding 5-20 Ci/yr (without considering tritium). The concentrations of radio nuclides in river water must not exceed 10-30 nCi/liter, and 3000 nCi/liter of tritium (from all the sources excluding global fall-outs). Drainage water with concentration larger than $5 \cdot 10^{-4}$ mCi/ml must be cleaned before disposal [9]. In Canada it is stipulated that an additional condition, that the genetic dose be no more than 10^4 man · rem/yr, must be fulfilled for each reactor [14]. The concentration of radioactivity in water, discharged into oceans, must be below 10^{-7} μCi/cm^3 [8].

In some papers a desire is expressed that radioactive discharges from APP be as low as practically possible [8, 15].

In [14] it is estimated that, if the ejections from APP cause 20% of the ICRP admissible dose, then $3.4 \cdot 10^4$ man · rem is received per million of population, or the maximum dose is $4.5 \cdot 10^4$ man · rem per 2000 MW of electrical power per year taking into consideration the growth of power production in future.

The radiation doses of the entire world population from the radioactive products of APP up to the year 2000 are estimated in [1, 16].

It is calculated that by 2000 up to 500 MCi of tritium will go into the environment per year (from which the dose for each man will be up to 0.04 mrem/yr); the corresponding input of I^{129} will be $6.3 \cdot 10^4$ Ci (radiation dose for one man 0.2 mrem/yr) and of Kr^{85} $7 \cdot 10^3$ MCi (dose 0.4 mrem/yr) at a level of power production of 4260 GW/yr [1].

Thus, at present the radiation doses from radioactive materials produced in the process of peaceful uses of atomic energy are small and appreciably below the admissible levels recommended by international organizations.

However, a sharp increase in the power generation from nuclear sources (almost by a factor of 200) by the year 2000 forces one to consider carefully the possibilities of contamination of the environment. According to some estimates the doses on global scale may comprise about 1% of the values of the natural background, which is smaller than its variations. Different conditions over the globe, permeation of isotopes and their passage along biological chains may change the results of these estimates by a factor of ten or more. This makes it necessary to watch the contamination of natural media carefully.

A comparative estimate of the consequences of operation of ordinary power plants and APP, presented in a Soviet paper [16], is interesting. It is calculated that in the operation of ordinary enterprises even by the year 2000, for the dilution of toxic substances to the admissible level several thousand times larger amount of air is needed than in the operation of APP. The computations were done for large areas: for short-lived substances (or rapidly washed out from the troposphere) up to 10^7 km^2, for long-life isotopes (Kr^{85} and H^3) – for the entire surface of the earth. The possibilities of accidents in APP (up to five cases in a year over the globe) were also taken into consideration. For ordinary electric power plants the calculations were done for sulfur anhydride, ash, and other toxic substances. Furthermore, it was necessary to consider that the total amount of dissipated heat (which may, in the final analysis, cause undesirable climatic changes) per unit usable power of APP is appreciably less than in the operation of ordinary power plants due to the high efficiency. The use of atomic energy does not involve consumption of oxygen and does not lead to continuous increase of carbon dioxide in air. It is true that the amount of heat given off to water in the operation of APP is about 1.5 times larger than in the operation of ordinary power plants (per unit power) [15], which must be taken into consideration. This may cause undesirable heat contamination of water. An American paper [17] was devoted to the thermal effects accompanying the operation of APP.

The growing reaction of the population and the society to the development of nuclear power was noted at the Geneva conference. This problem undoubtedly requires the most careful attention and painstaking analysis.

A meeting of experts on the ecological aspects and public recognition of atomic energy was held during the conference. The representatives of the USSR, India, Spain, Italy, Great Britain, USA, France, Czechoslovakia, Switzerland, Japan, and Argentina participated in the meeting. The experts produced a summarized report of the conclusions in short statements (4-5 min) given by each of them on different problems. The general problems of the effect of APP on the environment were discussed and APP and plants operating with chemical fuel (the representative of the USSR reported on this) were compared; possible ejections from APP into the environment, the problems of safety of the society, and also the possible ways of entrance of isotopes into human organism, the safety standards, thermal effects of APP, possible accident situations in atomic power plants, the reaction of the society to the use of atomic energy in daily life were discussed.

Problems regarding the role of the scientist in the formation of correct public opinion at the epoch of development of nuclear energetics, the fate of accumulating radioactive wastes, the basis of the existing standards for ensuring safety, lowering of these standards, the possibilities of bringing a correspondence between the obtained electrical power and the dose, etc were also touched upon.

The conference stressed that the task of the scientists consists in a careful investigation of the contamination of the environment and an accurate prognosis of the contaminants considering all possible situations. The role of the nuclear energetics in reducing the contamination of the environment by toxic substances from ordinary fuel was noted.

Thus, the development of nuclear energetics can ensure the conservation of adequately clean environment; the replacement of the energy produced from common fuel by atomic energy results in a decrease of the contamination of the environment by toxic substances formed in the combustion of ordinary fuel.

LITERATURE CITED

1. IV Geneva Conference (1971), Paper No. 652 (Voz).
2. Environmental Contamination by Radioactive Materials, Proc. of a Seminar, Vienna (1969).
3. Environmental Aspects of Nuclear Power Stations, Proc. of a Symposium, New York (1970).
4. E. A. Fedorov et al., See [1], paper No. 686 (USSR).
5. F. A. Tikhomirov et al., See [1], Paper No. 685 (USSR).
6. S. Auerbach et al., See [1], Paper No. 085 (USA).
7. P. Kamath, See [1], Paper No. 536 (India).
8. T. Masatoshi et al., See [1], Paper No. 253 (Japan).
9. K. Aurand et al., See [1], Paper No. 399 (France).
10. E. Kunz et al., See [1], Paper No. 550 (Czechoslovakia).
11. V. M. Vdovenko et al., See [1], Paper No. 457 (USSR).
12. A. I. Burnazyan et al., See [1], Paper No. 429 (USSR).
13. B. Kahn et al., See [1], Paper No. 087 (USA).
14. A. Marko et al., See [1], Paper No. 160 (Canada).
15. E. Larson Clarence et al., See [1], Paper No. 723 (USA).
16. Yu. A. Izrael and E. N. Teverovskii, See [1], Paper No. 684 (USSR).
17. R. Foster, See [1], Paper No. 086 (USA).

BOOK REVIEWS

NEW BOOKS

Modelirovanie i Optimizatsiya v Avtomatizirovannykh Sistemakh Upravleniya. [Simulation and optimization in automated control systems], G. N. Balasanov, Atomizdat, Moscow (1972).

The book outlines the basic methods of optimum process control based on computerization (linear and dynamic programming, game theory and Monte Carlo techniques, operations research and queuing theory, pattern recognition, theory of learning and adaptive systems, theory of optimum systems). The requisite mathematical concepts are discussed.

The bulk of the examples cited refer to optimum control, and to mathematical description of technological processes in hydrometallurgy and in chemistry. The methods described in the book are likewise applicable in the chemical, petroleum and petrochemical, metallurgical, and other diverse branches of industry.

The book is intended for students in technical colleges, for graduate students, and also for research workers in planning institutes and industrial plants interested in production control problems.

Rukovodstvo po Vychisleniyu i Obrabotke Rezul'tatov Kolichestvennogo Analiza. [Handbook on computation and processing of quantitative analysis data], R. I. Alekseev and Yu. P. Korovin, Atomizdat, Moscow (1972).

The book discusses the basic problems that workers in analytical laboratories have to confront in the computation and statistical processing of the results of quantitative analysis of the composition of a substance.

The methods for computing and processing the analysis results are presented in "cookbook recipe" format, with numerical examples, so that the techniques recommended can be utilized directly by analytical chemists regardless of their background, or lack of one, in mathematical statistics.

The book is written for analytical chemists working in all branches of the national economy.

Radiatsionnaya Biokhimiya Timusa. [Radiation biology of the thymus], E. F. Romantsev, V. D. Blokhina, Z. I. Zhulanova, N. N. Kashchinko, and I. V. Filippovich, Atomizdat, Moscow (1972).

The book presents modern concepts on the physical and biochemical mechanisms operative in exposure of the thymus, one of the most highly radiosensitive tissues found in the mammalian organism, to ionizing radiations. This lymphoidal tissue is involved in immunological reactions which are of general biological significance. The book goes into the mechanisms at work when the thymus is affected by ionizing radiations and by antiradiation protectants. Information on the structure and function of the thymus is cited; disturbances in nucleic acid and protein metabolism and in the oxidative phosphorylation process in the thymus in response to radiation exposure are described, as well as the way these processes are affected by the presence of chemical radioprotectants.

The book is written for specialists in various lines of work interested in current problems in radiobiology and radiation medicine, for health physicists and medical radiologists, and for senior biology majors in universities and medical institutes.

Svoistva Deformirovannykh Yader s K = 1/2. [Properties of deformed K = 1/2 nuclei], B. S. Dzhelepov, G. F. Dranitsyna, and V. M. Mikhailov, Nauka, Leningrad (1972).

The most frequently encountered deformed atomic nuclei are those whose ground states or excited states have the quantum number K = 1/2. Several interesting features arise in the structure of the rotational

Translated from Atomnaya Énergiya, Vol. 32, No. 4, pp. 278, 286, 292, April, 1972.

bands, in the intensity ratios of the transitions, in the magnetic moments, etc., some to light. The monograph reviews all of the available experimental material on the range of nuclides $150 < A < 190$ and the range $A > 230$, and discusses predictions of theory and inferences that can be drawn from the experimental data. A generalized model and the results of a microscopic approach to the description of the properties of deformed nuclei are utilized in the theoretical analysis.

The book is written for scientific-research workers and for graduate students working on the structure of the nucleus.

Beta-Protsessy. Funktsii dlya Analiza Beta-Spektrov i Élektronnogo Zakhvata. [Beta-decay processes. Functions for analysis of β-ray spectra and electron capture], B. S. Dzhelepov, L. N. Zyryanova, and Yu. P. Suslov, Nauka, Leningrad (1972).

This book is devoted to the functions required for analysis and processing of experimental data on nuclear β-decay and capture of orbital electrons. The self-consistent potential of the atom is utilized in the calculations, and the finite dimensions of the nucleus are taken into account at the same time. The tabular data presented in the book make it possible to analyze the shape of allowed and forbidden β-ray spectra, to determine the value of the product ft, to find the relative probability of capture of electrons from different shells and subshells of the atom.

The book is written for experimental physicists and theoretical physicists working with spectroscopy of the atomic nucleus, and may also prove useful to graduate students specializing in nuclear physics.

Neitron-Neitronnyi i Neitronnyi γ-Metody v Rudnoi Geofizike. [Neutron – neutron and neutron – γ logging techniques in mining geophysics], E. M. Filippov, B. S. Vakhtin, and A. V. Novoselov, Nauka, Novosibirsk (1972).

The book presents general information on neutrons, on neutron sources and neutron detectors, on safety techniques, and provides a classification of relevant techniques, etc. Separate sections of the book deal with laboratory, mine, and borehole modifications of those methods. Extensive material available on these topics is reviewed and generalized systematically. Emphasis is placed on work done by the authors in recent years.

The book will be of interest to staff members of scientific-research institutions, and to workers on the staff of production planning organizations interested in applying nuclear physics techniques or interested in learning about the potentialities of those methods.

Fiziko-Khimiya Redkikh Metallov. [Physical chemistry of rare metals], Nauka, Moscow (1972).

This collection of articles is devoted to the 60th birthday of the major Soviet metals scientist E. M. Savitskii, Corresponding Member of the USSR Academy of Sciences, Disciples and colleagues of the scientist generalize the results of their research in a series of articles and acquaint the reader with the latest achievements in the fields of the production technology of ultrahigh-purity single crystals of rhenium, vanadium, tantalum, yttrium, scandium, gadolinium, ruthenium, and rhodium; production of pure metals and of alloys of tungsten, molybdenum, niobium, etc. Results of the construction of over a hundred "composition vs. property" phase diagrams for those materials are demonstrated. Results of determinations of new chemical compounds and of calculations of the Fermi surface, in order to ascertain the interrelation between the structure and properties of the substances studied, are cited.

This publication is written for a broad range of research personnel: metals scientists, metallurgists, machine designers and instrument designers engaged in the study, winning, processing, and utilization of refractory metals and rare metals in industry, and also for students and instructors in chemical, metallurgical, and machinery design colleges.

Svobodnoradikal'noe Sostoyanie v Khimii. [The free-radical state in chemistry], Nauka, Novosibirsk (1972).

This collection includes articles by leading Soviet scientists and foreign scientists devoted to the most urgent topics in the physics and chemistry of free radicals. The vigorous development of this new branch of chemical physics has made it possible to present convincing and unambiguous proof of the decisive role played by free-radical processes in various radiation-chemical and photochemical reactions, in combustion processes, and so forth. The collection of articles is dedicated to the memory of Academician V. V. Voevodskii, whose work and activities played a decisive role in the development of various research trends

in the physics and chemistry of free radicals. Some of the articles were written by disciples of V. V. Voevodskii.

The book is written for a broad readership of research workers engaged in various branches of physical chemistry, and also for chemists, biologists, and physicists interested in the physics and chemistry of free radicals.

Metallotermicheskie Metody Polucheniya Soedinenii i Splavov. [Metallothermic techniques in the production of compounds and alloys], Nauka, Novosibirsk (1972).

Metallothermic methods for the production of intermetallic compounds and alloys prove to be more convenient, technologically and economically, than methods based on direct fusion of the components, in many instances of practical interest. This collection of articles reports the results and research findings on metallothermic synthesis of intermetallic compounds and alloys in the reduction of oxides, halides, and other substances. The optimum conditions for producing the compounds and alloys are ascertained, as well as the physicochemical characteristics of the substances involved in the reactions; in some instances, attempts are made to lay bare the underlying mechanism and the kinetics of the reduction process.

The book is written for theoretical chemists and for practising chemists.

Élektricheskoe Modelirovanie Yavlenii Teplo- i Massoperenosa. [Electrical simulation of heat-transfer and mass-transfer phenomena], L. A. Kozdoba, Énergiya, Moscow (1972).

This book deals with research on the heat-transfer conditions affecting machine parts, assemblies, facilities, and rooms based on the use of such electrical simulators as resistor networks and combined electrical simulating models. A procedure is presented for electrical simulation of linear and nonlinear problems in nonstationary heat transfer and nonstationary mass transfer. Examples of solutions obtained with electrical simulators are given for direct as well as inverse and inductive problems in heat condition.

The book is intended for engineers and research scientists, and may prove useful to technical college students.

Uspekhi Fiziki Plazmy. Tom 1. Fizika Vysokotemperaturnoi Plazmy. [Translation of: Advances in Plasma Physics. Vol. I. Physics of High-Temperature Plasma, edited by A. Simon and W. Thompson, New York (1968)], Mir, Moscow (1972).

A team of leading American specialists on plasma physics (Dyson, Furth, Kroll, Fowler) decided to undertake a complete review of the advances achieved in plasma physics and applications of plasma physics in various fields. The book includes part of the material appearing in the first volume of the original American edition. Its contents cover a range of key problems in the physics of a high-temperature plasma related to emission, confinement, stability, and thermodynamics of an unstable plasma. The contents reflect the current point of view on those topics, embodying generalizations of the contents of numerous papers published up to 1968 only in the periodical literature.

The book is of considerable interest both to specialists in plasma physics and to research scientists and technicians concerned with the topics discussed, and also to senior undergraduates majoring in related branches of physics.

Magnitnye Poluprovodniki. [Magnetic Semiconductors, S. Methfessel and D. Mattis, translated from the English original in: Handbuch der Physik, Bd. 18/1], Mir, Moscow (1972).

This is the first review to appear in the worldwide literature on the physics of magnetic semiconductors, and sheds light on several topics of theoretical or experimental interest. The quantum mechanism underlying the magnetic and electrical properties of magnetic semiconductor materials is discussed, and a wealth of experimental data is presented.

The book will be useful to research physicists and engineers engaged in theoretical and experimental studies of the properties and applications of magnetic materials, and also to readers interested in the physics of semiconductors, as well as to senior undergraduate students and graduate students in physics and engineering physics technical colleges majoring in solid state physics.

Garmonicheskii Ostsillyator v Sovremennoi Fiziki: ot Atomov do Kvarkov. [Translation of: The Harmonic Oscillator in Modern Physics from Atoms to Quarks, New York (1969)], M. Moshinsky, Mir, Moscow (1972).

M. Moshinskii, a professor at the University of Mexico, is a recognized authority in the field of applications of group-theoretical methods to quantum mechanics. The book, which is based on a lecture course given by this author, is a unique monograph in which a single model is utilized in the investigation of some crucial problems in theoretical physics. Some common vantage points are used to attack what appear to be entirely dissimilar systems (molecules, atoms, molecules). The book is written in a clear and lucid style, so that it is accessible and interesting not only to specialists but also to student physics majors.

Metod Fazovykh Funktsii v Teorii Potentsional'nogo Rasseyaniya. [Translation of : Variable Phase Approach to Potential Scattering], F. Calogero, Mir, Moscow (1972).

F. Calogero is one of the founders of a new and efficacious method for solving problems in quantum mechanics, the method of phase functions. This method, developed in the past 10-15 years, enables scientists to obtain many general results in quantum mechanics in a simple manner. The method is particularly effective in dealing with scattering problems, and also in computer work.

Since this method has not yet filtered down to standard courses given on quantum mechanics, the book will be useful to students specializing in the field of theoretical physics, and to instructors as well. It is also needed by theoretical specialists, since the literature on this topic in the Russian language is meager.

Osnovy Kvantovoi Elektroniki. [Translation of: Fundamentals of Quantum Electronics, New York (1969)], R. Pantell and H. Puthoff, Mir, Moscow (1972).

This is a monograph textbook on the fundamentals of quantum electronics. The book expounds a unique approach to many of the relevant problems, including the latest achievements in the fields of nonlinear optics, semiconductor lasers, and interaction of radiation with matter. The textbook contains problems and exercises.

The book is written for senior undergraduates majoring in engineering physics, radio physics, and electronics, and also for specialists in related areas who are interested in familiarizing themselves with the fundamentals of quantum electronics.

Kataliticheskie Prevrashcheniya Uglevodorodov. [Translation of: Catalytic Conversion of Hydrocarbons, London (1969)], J. Germain, Mir, Moscow (1972).

The book discusses conversions of hydrocarbons belonging to different classes to heterogeneous catalysts, and specifically discusses the oxidation of hydrocarbons, one of the most prominent processes in modern photochemistry. Classification of catalysts (inorganic complexes, metals, acidic homogeneous and heterogeneous catalysts, bifunctional catalysts) is presented, with analysis of the operating mechanisms of the catalysts from the standpoint of modern concepts of physical chemistry and organic chemistry.

The book is of interest to physical chemists, organic chemists, and petroleum chemists working in research institutes and in industrial plants.

Technika Radiacyjna. Podrecznik Akademicki. [Radiation engineering Academic textbook], Wydawnictwa Naukowo-Techniczne, Warszawa (1971) [in Polish].

This text covers ionizing radiations used in radiation engineering, and describes isotope sources and electrical sources of ionizing radiation, industrial radiation facilities, dosimetry, radiation polymerization and irradiation of polymers, radiation conservation of foodstuffs, the use of radiation techniques in chemical process technology, and also radiation effects in inorganic solids.

The book is intended for students majoring in chemistry in technical colleges.

Fizyka dla Inzynierow. Fizyka Wspolczesna. Czesc 2. [Physics for engineers. Modern Physics. Part 2], Wydawnictwa Naukowo-Techniczne, Warszawa (1971) [in Polish].

The book presents general information on atomic physics, solid state physics, and nuclear physics. The material is presented in concise format, and is richly illustrated.

The book is intended for engineers of various specialities, and also for students enrolled in technical colleges.

ANTIMONY, BISMUTH, ARSENIC, AND OTHER ELEMENTS IN ORE BODIES AND HALOES OF A URANIUM – MOLYBDENUM DEPOSIT

G. I. Rossman, N. A. Stepanova,
I. V. Sychev, and G. A. Tarkhanova

UDC 550.8

A geochemical assessment of radiometric anomalies of a uranium mineralization involves determination of the group of indicator elements of this mineralization within the anomalies. Lead and molybdenum are typical indicator elements of many uranium deposits; the sensitivity of their determination by standard analytical methods is fairly high [1]. However, in regions containing lead and molybdenum mineralizations as well as a uranium mineralization, the use of only lead and molybdenum for assessing radiometric anomalies may lead to errors. In such cases one must use other indicator elements of uranium mineralization, such as arsenic, bismuth, antimony, and thallium. However, as the sensitivity of determination of these metals by standard methods is usually inadequate, their value as a criterion for prospecting has never been recognized.

Our paper gives the results of an investigation of the distribution of arsenic, antimony, bismuth, tin, mercury, and thallium in ores and country rocks of a typical uranium – molybdenum deposit. With the exception of mercury, these elements were determined by highly sensitive chemical and chemical – spectral analysis methods [1-5]; mercury was determined by the atomic absorption method.

The sensitivity of these analytical methods is sufficiently high and the errors fairly small (Table 1), which enables one to detect and trace the distribution of the elements in ores and the country rocks. The threshold sensitivity of the analytical methods for arsenic, antimony, bismuth, tin, mercury, and thallium is one order of magnitude higher than that of simple spectral analysis by the "spill" method.

The ore bodies of this uranium – molybdenum deposit are localized in a band of alternating volcanic and sedimentary rocks, in acid tuffs, and occur in blocks bounded by disjunctive dislocations (Fig. 1). These ore bodies, lying in different structural blocks, have been oxidized and leached to different degrees.

Samples were taken from borehole cores and the walls of underground mine workings by the procedure in [1, 6]; replicas of trench samples were investigated within the limits of the ore bodies.

TABLE 1. Sensitivity of the Analytical Methods

Element	Mean content of elements in acid rocks, wt. %		Threshold sensitivity, wt. %		Accuracy of determination, rel. %		Threshold of sensitivity in local geochemical backgrounds	
	according to A. P. Vinogradov (1962)	local geochemical background (1969)	spectral analysis	highly sensitive method	spectral analysis	highly sensitive method	spectral analysis	highly sensitive method
As	$1.5 \cdot 10^{-4}$	$4 \cdot 10^{-4}$	$3 \cdot 10^{-3}$	$1 \cdot 10^{-4}$	120	20	7.5	0.25
Sb	$2.6 \cdot 10^{-5}$	$2 \cdot 10^{-4}$	$5 \cdot 10^{-4}$	$1 \cdot 10^{-4}$	80	32	2.5	0.50
Tl	$1 \cdot 10^{-6}$	$1 \cdot 10^{-5}$	$5 \cdot 10^{-5}$	$1 \cdot 10^{-5}$	80	30	50	1.0
Bi	$3 \cdot 10^{-4}$	$8 \cdot 10^{-4}$	$1 \cdot 10^{-3}$	$2 \cdot 10^{-5}$	85	33	1.25	0.025
Hg	$8 \cdot 10^{-6}$	$5 \cdot 10^{-8}$	$1 \cdot 10^{-2}$	$1 \cdot 10^{-7}$	200	50	$2 \cdot 10^{6}$	2
Sn	$1.5 \cdot 10^{-4}$	$2 \cdot 10^{-5}$	$1 \cdot 10^{-5}$	$1 \cdot 10^{-5}$	120	33	100	0.5

Translated from Atomnaya Énergiya, Vol. 32, No. 4, pp. 279-285, April, 1972. Original article submitted May 6, 1971.

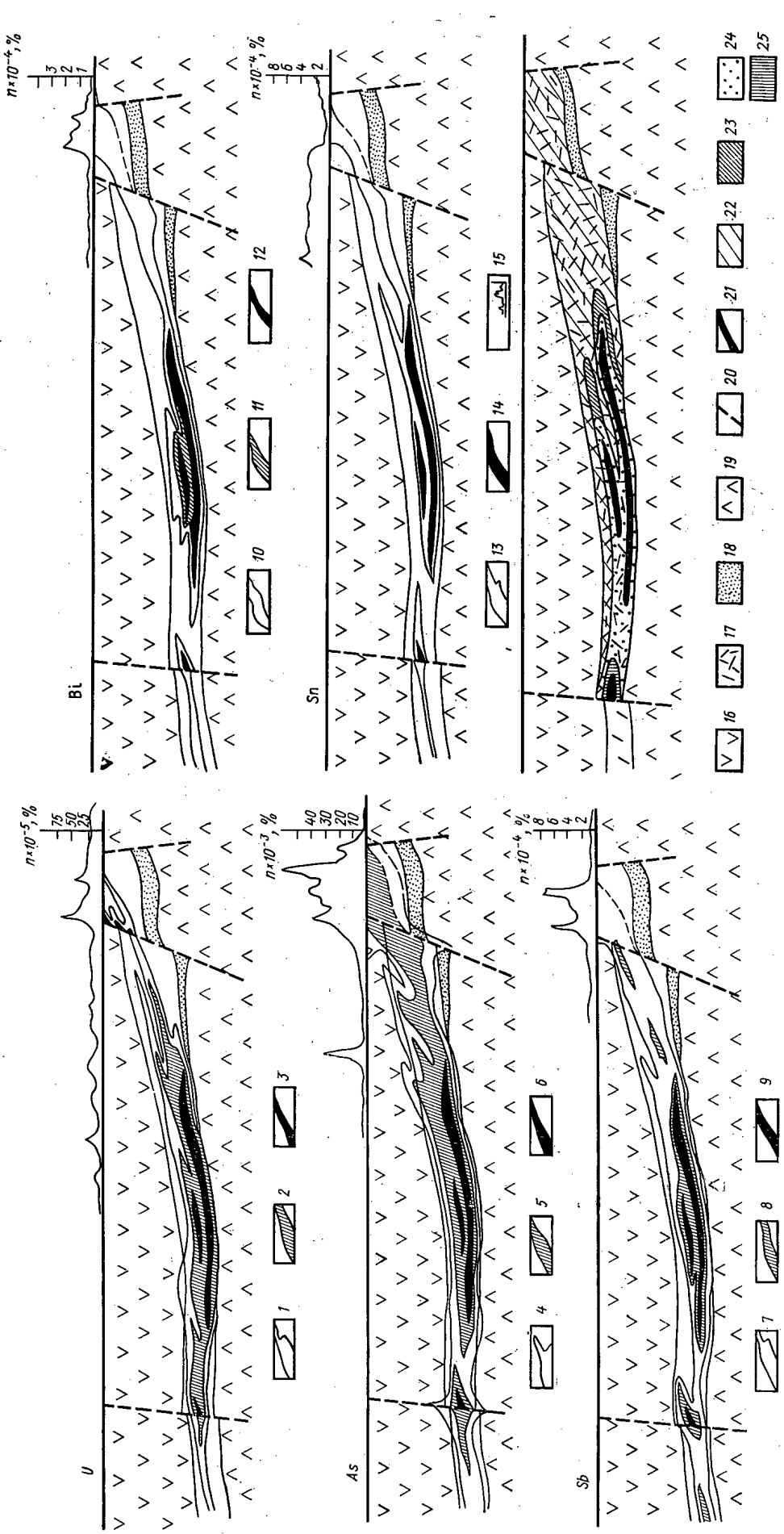

Fig. 1. Geochemical haloes in a vertical cross section of the ore body of a uranium—molybdenum formation. Limits of element contents: 1) 0.0007-0.001; 2) 0.001-0.01; 3) >0.01; 4) 0.001-0.005; 5) 0.005-0.01; 6) >0.01; 7) 0.0006-0.0008; 8) 0.0008-0.001; 9) >0.001; 10) 0.00006-0.0001; 11) 0.0001-<0.0005; 12) >0.0005; 13) 0.0001-0.0002; 14) >0.0002; 15) graphs of contents of elements from surface of erosion section of bedrocks; 16) porphyrites; 17) felsite tuffs; 18) sandstones; 19) crystalline ignimbrites; 20) faults; 21) ore bodies; 22) zone of oxidation and leaching; 23) oxidation zone; 24) regeneration zone; 25) zone of primary pitchblende—hematite mineralization.

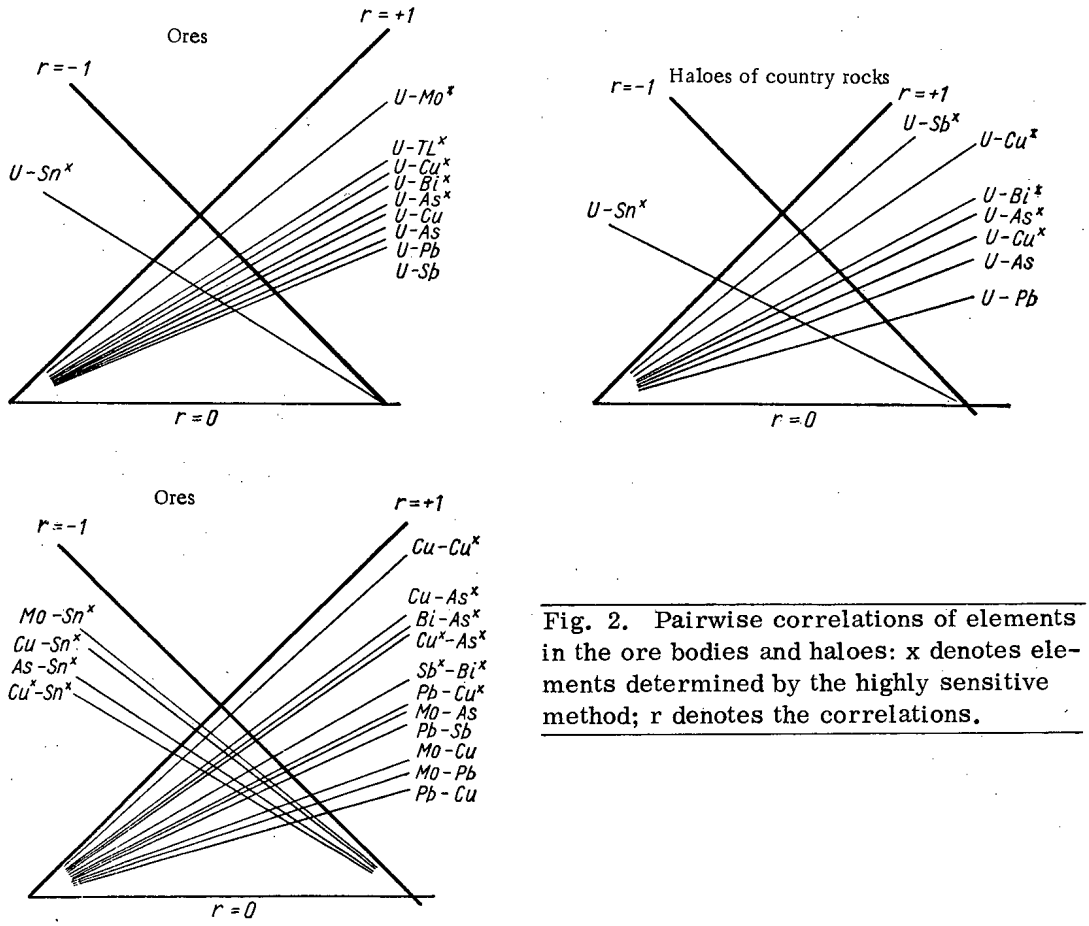

Fig. 2. Pairwise correlations of elements in the ore bodies and haloes: x denotes elements determined by the highly sensitive method; r denotes the correlations.

It was established that simultaneously with uranium, molybdenum, lead, and copper, arsenic (more than 100), antimony (more than 10), bismuth (about 100), mercury (about 80), and thallium (about 100) are concentrated in the ores of the deposit.* However, the ores have low tin contents (0.1).

The data (Fig. 2, Table 2) clearly indicate a close relation between these elements (with the exception of tin) and molybdenum and uranium (their minerals and the minerals present in paragenesis with them). Antimony, arsenic, and bismuth are not only concentrated as admixtures, but form their own minerals, of which the most typical is fahlerz. A much smaller part of the arsenic is also combined with arsenopyrite. Mercury is concentrated as an admixture in fahlerz and is found as occasional segregations of cinnabar. A considerable amount of these elements is present in collomorphic pyrite as an admixture.

These minerals were segregated at about the same time as uraninite. Hence it follows that the bulk of the antimony, arsenic, bismuth, thallium, and mercury is related to the productive stage of the ore-forming process. These elements may be regarded as mineralization indicators which form aggregation haloes; this is confirmed by the data of Fig. 2. On the other hand, tin forms an evacuation (negative) halo.

Haloes of indicator elements are contained mainly in the beds of tuffs adjoining the ores; they are larger than the uranium haloes above the site where the ore bodies taper out (the boundary of the haloes is drawn along the lower anomalous values of the element concentrations, which differ markedly from their background concentrations at a unilateral significance level of 0.05).

Haloes of thallium and mercury are also observed around the ore bodies, but their effective dimensions have not been established. Judging from the existing data, the mercury halo reaches beyond the limits of the bed adjoining the ore and is larger than the uranium, antimony, bismuth, arsenic, molybdenum, lead, and copper haloes. The thallium halo is apparently comparable in size with the bismuth halo.

* The figures in parentheses are the concentration coefficients with respect to the local geochemical background.

TABLE 2. Form of Occurrence of Uranium in Indicator Elements in Ores, the Surrounding Geochemical Haloes, and the Unaltered Rocks

Indicator element	In ores		In haloes		In zone of oxidation and leaching (halo)		In unaltered rocks	
	A	B	A	B	A	B	A	B
U	**Uraninite** **Sooty uraninite** Secondary uranium minerals	?	Sooty uraninite	?	Sooty uraninite **Secondary uranium minerals** (silicates, arsenates, phosphates)	Manganese hydroxides* Gypsum Kaolinite	—	Orthite Monazite **Zircon**
Mo	**Femolite** Molybdenite Molybdenum black	Uraninite Skolite Calcite Hematite	Molybdenum black	Calcite Chlorite	Powellite Wulfenite	In all secondary uranium minerals† Manganese and iron hydroxides Kaolinite	?	**Pyrite**
Tl	—	Femolite Pyrite Marcasite	—	Pyrite	—	Iron hydroxides Manganese hydroxides	—	?
As	**Arsenopyrite** (a little) Fahlerz (a little)	Chalcopyrite Skolite Carbonate Quartz Pyrite	?	»	Uranospinite	Torbenite In all secondary uranium minerals (a little in uranium silicates) Powellite Malachite	—	Pyrite In minerals of the electromagnetic fractions
Sb	Fahlerz	**Uraninite** Hematite Pyrite Femolite	?	»	?	Uranium–molybdenum black Torbenite Malachite Manganese hydroxides	—	Pyrite
Hg	Cinnabar	Fahlerz	?	»	?	?	?	?
Bi	Fahlerz	Uraninite Hematite Tennantite	?	Early pyrite Tennantite Hematite Sooty uraninite	?	Secondary uranium phosphates **Malachite**	?	In minerals of the electromagnetic fractions

Note: A) Intrinsic mineral forms; B) as admixtures in the minerals; the principal form of the minerals is shown in boldface. An asterisk denotes uranium in sorbed form; a dagger denotes an admixture of molybdenum, characteristic of secondary uranium minerals of U–Mo ore bodies; a question mark denotes that the forms of occurrence have not been revealed.

A characteristic feature of these haloes is the zonality of the structure,* which is expressed in a regular variation of the dimensions of the haloes, the correlation coefficients of the indicator elements, their mean contents, and the linear productivities characterizing the different hypsometric levels, which replace one another to the dip of the ore-adjoining structure. The most objective expression of the zonal distribution of the elements is given by the values of the linear productivities (Fig. 3, Table 3).

*It is not our intention to examine the nature of this zonality. A study of this very complex problem is the subject of special investigations of the distribution of a radiogenic admixture of Pb^{206} and uranium in cross section of ore bodies and the surrounding haloes. According to the data of our comparative investigations on isolated ore bodies of deposits with different degrees of oxidation, the primary zonal distribution of the elements developed above the sites where the ore bodies taper out is very similar to that in the zones of oxidation and leaching of ore bodies of similar primary composition [7].

TABLE 3. Change in Values of Linear Productivities of Haloes of Uranium, Its Companion Elements, and Their Ratios

Borehole No.	Depth to the dip of the structure	Linear productivities, M %					Ratios of linear productivities				Geological position of sampling site
		U	As	Sb	Bi	Sn	As/U	Sb/U	Bi/U	Sn/U	
2675	60	0,0375	0,0665	0,035	0,00290	0,0142	8,9	4,7	0,38	1,9	Surface leaching zone
2632	80	0,0117	0,0382	0,028	0,0006	0,0167	3,27	2,4	0,054	1,43	
2656	140	0,0247	0,0393	0,0163	0,0004	0,0065	1,59	0,66	0,016	0,26	Zone of leaching and oxidation of primary ores (upper parts of the ore bodies)
2578	160	0,0240	0,0296	0,0150	0,0010	0,0078	1,23	0,63	0,044	0,32	
2634	180	0,0247	0,0355	0,0147	0,00062	0,0061	1,44	0,59	0,025	0,25	
2533	320	0,0624	0,0236	0,0221	0,00091	0,0053	0,38	0,35	0,015	0,1	Zone of ore body with occurrence of regeneration processes (lower parts of the ore body)
2488	340	0,0103	0,0272	0,0146	0,00022	0,0109	2,64	1,46	0,022	1,0	
2519	400	0,0027	0,0251	—	—	—	9,3	—	—	—	Zone of development of haloes below the boundary of tapering out of the ore body
2517	420	0,0029	0,0079	0,0083	0,00051	0,0056	2,7	2,86	0,19	1,93	
2625	460	0,0015	0,0224	0,0094	0,00106	0,0049	15,0	6,3	0,70	3,28	Zone of influence of underlying ore body
2622	465	0,0048	0,0155	0,0118	0,00119	0,0071	3,23	2,5	0,25	1,5	
2620	480	0,0019	0,0248	0,0530	0,0037	0,0058	13,6	23	1,9	3,2	

It will be seen from the data that prefential deposition of arsenic, antimony, and bismuth is correlated with the upper horizons of the haloes, located above the ore body.

In contrast with this, the linear productivity of uranium in the haloes is maximal for the level of the middle and lower parts of the ore body. The tin content in the region of its "negative" halo is somewhat higher above the upper parts of the ore body.

An analysis of the change in the linear productivity ratios As/U, Sb/U, Bi/U, Sn/U to the dip of the ore-adjoining bed reveals that these ratios regularly decrease as one approaches the ore body. The maximal gradient corresponds to the As/U ratio.

It should be noted that there is a slight change in the sign of the gradient of the values of the linear productivities As/U, Sb/U, Bi/U, and Sn/U in the haloes located below the tapering out of the ore body. Here we again observe an increase of the ratios of the linear productivities of arsenic, antimony, bismuth, and tin to uranium. Such a change in gradient indicates the presence of another, deep ore body, the upper parts of the haloes of which were superimposed on the lower parts of the haloes of the investigated ore body. In fact, a hitherto-unknown blind U – Mo (uraninite – hematite) ore body was discovered 100 m below the point at which the investigated ore body tapers out (see Fig. 1).

The data enable us to infer that arsenic, antimony, and bismuth are accumulated in the zones of oxidation and leaching of the mineralization (see Fig. 3, Table 3). This is confirmed both by their absolute linear productivities and by the ratios of the productivities to those of uranium.

Removal of uranium from the oxidation and leaching zones is proved by comparative investigations of lead isotopes and uranium contents [7].

The place of mercury and thallium in the scheme of zonal structure of the haloes has not been finally established. The existing data indicate that high concentrations of mercury and thallium are characteristic of the upper parts of the haloes developed above the ore bodies. Another characteristic feature is the

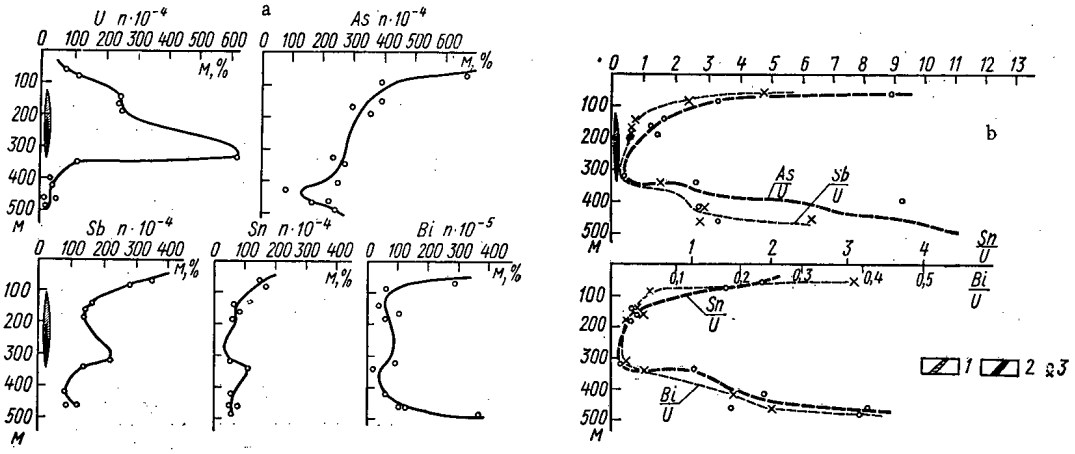

Fig. 3. Change in linear productivities of haloes of uranium, its companion elements (a) and their ratios (b) to the dip of the U–Mo ore body (see Table 3): 1) ore zone exhibiting oxidation and extraction processes; 2) ore zone exhibiting regeneration (cementation) processes; 3) intersection of the central part of the ore zone by the exploratory drill-holes.

asymmetric structure of the haloes of these elements and their extensive occurrence in the strata above the ore body.

Thus the ores and adjoining rocks of this U–Mo deposit, localized in volcanic rocks, contain anomalous concentrations of antimony, arsenic, thallium, and mercury. With respect to uranium, these elements are concentrated in haloes above the point at which the ore bodies taper out to the rise, and persist during weathering of the country rocks.

LITERATURE CITED

1. O. O. Kablukov et al., Use of Dispersion Haloes of Uranium and Its Companion Elements in Prospecting for Hydrothermal Uranium Deposits. Handbook [in Russian], Nedra, Moscow (1964).
2. Symposium: Chemical Analysis of Mineral Raw Material [in Russian], No. 8, Nedra, Moscow (1965), p. 104.
3. Ibid., p. 165.
4. Symposium: Chemical Analysis of Mineral Raw Material [in Russian], No. 11, Nedra, Moscow (1968), p. 43.
5. N. A. Stepanova, L. I. Zemtsova, and T. A. Butkina, Papers of the Seminar "Determination of Microimpurities" [in Russian], Vol. 1, MDIPT im F. É. Dzerzhinskogo, Moscow (1968), p. 3.
6. D. A. Vigdorovich et al., Provisional Instructions for Geochemical Prospecting for Pyrites – Polymetallic Deposits in the Presence of Very Thick Unconsolidated Deposits [in Russian], Seriya Obmena Opytom, No. 34, ONTI VITR (1960).
7. G. I. Rossman et al., Izv. Akad. Nauk SSSR, Seriya Geol., No. 1 (1971).

RADIATION-INDUCED GROWTH OF POLYCRYSTALLINE α-URANIUM

M. A. Vorob'ev, V. F. Zelenskii, É. A. Reznichenko, and A. S. Davidenko

UDC 621.039.548.3

Anisotropic growth of the components of polycrystalline α-uranium crystallites lies at the basis of radiation-induced growth of that uranium phase. Consequently, the problem of what mechanism underlies radiation-induced growth of polycrystalline uranium reduces to ferreting out the relationship between the growth of single-crystal uranium and the growth of polycrystalline uranium, while ignoring the effect of the grain boundaries and of the dislocation structure of the polycrystalline uranium on the growth rate.

This problem arose earlier in calculations of what is termed the growth index, characterizing the dependence of radiation-induced growth of polycrystalline uranium on the degree of definition of the texture [100] or [010] (see references [1, 2]), and also in the discussion of the possible effect impurities might have on radiation-induced growth of uranium single crystals. The problem is that the investigation was carried out on polycrystalline specimens, and the results had to be extrapolated to the case of single crystals in order to reach definitive conclusions [3, 4].

Currently existing methods for calculating the growth index [1, 2] based on the assumed linear relationship between texture and growth rate, fail to take into account interactions between the crystallites, so that they are not of much help in understanding the true relationship between the growth of single-crystal uranium and the growth of polycrystalline uranium. A plausible mechanism underlying radiation growth of polycrystalline uranium, with the interaction between variously oriented crystallites in the irradiated polycrystal taken into account, has been put forth in [5].

It was shown that the interaction between crystallites constituting a polycrystalline aggregate and exposed to radiation is capable of bringing about changes in the initial orientation of the crystallites when adaptive plastic deformation of the crystallites takes place by twinning. It is proposed that this will subsequently bring about the same rate of deformation of all the crystallites in the direction of the overall anisotropy of the material, while at the same time determining the observable rate of radiation-induced growth of the polycrystal as a whole. The change in the initial orientation of the crystals is a necessary prerequisite for radiation-induced growth of polycrystalline uranium, in conformity with such a twinning mechanism accompanying adaptive plastic deformation, and also as a consequence of it.

It is not clear, however, just how radiation-induced growth of uranium must come about in the case where deformation by twinning is hampered, or is absent altogether, at elevated irradiation temperatures and at a low rate of deformation. For example, it has been pointed out [5] that only 10% of the adaptive plastic deformation takes place by twinning even at −196°C, and that the bulk of the deformation occurring does so by gliding. Without completely ruling out the possibility of some reorientation of the crystals in response to irradiation, we can anticipate that this is not the sole cause of the common and identical rate of deformation of all the crystals in the direction of growth of the polycrystal. An alternative mechanism linking the radiation-induced growth of α-uranium single crystals and polycrystals is discussed in the present article.

Mechanism Underlying Radiation-Induced Growth of Polycrystalline α-Uranium. We consider a polycrystalline specimen of uranium exhibiting a certain degree of anisotropy. Under irradiation, the interaction between the growing crystals brings about a state of affairs where the crystals will deform, independently of their orientation, and at the same rate in the direction of the overall anisotropy of the specimen.

Translated from Atomnaya Énergiya, Vol. 32, No. 4, pp. 287-291, April, 1972. Original article submitted April 19, 1971.

Suppose that the external stresses have no effect on the radiation growth processes in the single crystal [5]. Then the rate of growth of the crystallites comprising the polycrystalline aggregate can be assumed equal to the rate of growth of a free single crystal for those irradiation conditions. The effective rate of radiation growth of the polycrystal in the direction of overall anisotropy will be determined by the relationship between the rate of radiation-induced growth of the crystals with preferred orientation and the rate of compensating plastic deformation. In order to determine the rate of the compensating plastic deformation, we consider those factors contributing to that deformation. Clearly, the deformation is brought about by restraining stresses on the part of crystals with other than preferred orientation. These stresses can be determined from the condition

$$\left.\begin{aligned}&(\dot{\varepsilon}_g)_1+(\dot{\varepsilon}_{p.d})_1=(\dot{\varepsilon}_g)_2+(\dot{\varepsilon}_{p.d})_2;\\&\sigma_1+f\sigma_2=0,\end{aligned}\right\}$$

where the subscript 1 refers to crystals with preferred orientation, the subscript 2 refers to the remainder of the crystals; $\dot{\varepsilon}_g$ and $\dot{\varepsilon}_{p.d}$ are the rate of radiation-induced growth and the rate of plastic deformation, respectively; σ_1, σ_2 are the stresses generated in the interaction between crystals 1 and crystals 2; f is the ratio of the transverse cross section area of crystals 2 to the area of transverse cross sections of crystals 1.

If the expression for the dependence of the rate of plastic deformation of crystals 1 and 2 on the stress is known, then we can find the effective rate of radiation-induced growth of the polycrystallite once we have determined σ_1 and σ_2. Irradiation is known to generate appreciable internal stresses in polycrystalline uranium through the interaction between crystals of different orientation. In a completely isotropic material, these stresses bring the material to the familiar "superplasticity" state, when the rate of strain can be described by the Cottrell formula [6]

$$\dot{\varepsilon}=\frac{\sigma}{\sigma_T}\dot{\varepsilon}_g,$$

where σ is the applied stress, and σ_T is the yield limit of the material.

However, in the case of an arbitrary polycrystalline aggregate, the dependence of the rate of plastic deformation of the crystals on stress must be a different one. The reason is that the interaction between crystals 1 and 2 differs from the interaction of crystals in a completely isotropic material. Because of the difficulties associated with attempts to take the interaction of crystallites in an arbitary polycrystal into consideration, we deal here only with the simple case when the expression can be obtained for the rate of plastic deformation, in order to illustrate the actual possibility of achieving radiation-induced growth of the polycrystal in line with the scheme proposed here.

For that purpose, we consider a simplified model of a polycrystalline specimen exhibiting a certain degree of anisotropy in one of the directions. Considering only a stack of identical crystals with three principal orientations [100], [010], and [001], we represent the polycrystalline aggregate in the form of an isotropic matrix with crystals of some one orientation, say [010], "disseminated" in it. In that case, if the density of crystals having the orientation [010] in the selected direction is assigned the value n, then the density of crystals having each of the remaining orientations will be $(1-n)/2$. The area of the transverse cross section of the isotropic matrix will therefore be $3(1-n)S/2$, and that of the "disseminated" crystals will be $(3n-1)S/2$, where S is the transverse cross section area of the entire specimen.

Recalling that the isotropic matrix experiences no growth under irradiation, but does deform at a rate $\dot{\varepsilon}=\sigma\dot{\varepsilon}_g/\sigma_T$ in response to the effect of growth stresses on the part of the "disseminated" crystals, the effective rate of radiation-induced growth experienced by the polycrystal can be found by solving the system:

$$\left.\begin{aligned}&\dot{\varepsilon}_1+\dot{\varepsilon}_g=\frac{\sigma_2}{\sigma_T}\dot{\varepsilon}_g;\\&\sigma_1+\frac{3(1-n)}{3n-1}\sigma_2=0;\\&\sigma_2\leqslant\sigma_T,\end{aligned}\right\}\qquad(1)$$

where subscripts 1 and 2 refer to the "disseminated" crystals and to the isotropic matrix, respectively; $\dot{\varepsilon}_1$ is the rate of the compensating plastic deformation of the "disseminated" crystals in the isotropic matrix under irradiation.

The constraint $\sigma_2 \leq \sigma_T$ means that the rate of plastic deformation of the isotropic matrix under irradiation, at those stresses, can be described only by the equation $\dot{\varepsilon}=\sigma\dot{\varepsilon}_g/\sigma_T$. In the derivation of this

formula and a similar expression for accelerated creep of uranium under irradiation [7], $\sigma \ll \sigma_T$ was assumed. It has been shown [8], however, that acceleration of creep in polycrystalline uranium under irradiation is observed both at low stresses (0.2 kg/mm^2) and at high stresses (15.8 kg/mm^2) when the irradiation temperature was 220°C. For that reason, it is considered possible to extend the Cottrell formula to the case of stresses of any magnitude, but not greater than the yield limit of the material at that temperature.

The dependence of $\dot{\varepsilon}_1$ on σ_1 can be found by relying on the earlier arguments as to the nature of plastic deformation of crystals in a polycrystalline aggregate subjected to irradiation. Since the restraining stresses have no effect on the processes of radiation growth experienced by the crystals, we define the rate of plastic deformation of the "disseminated" crystals as the algebraic sum of the rate of radiation-induced growth $\dot{\varepsilon}_g$ of the single crystal and the rate of the compensating deformation $\dot{\varepsilon}_1'$ due to the restraining of the isotropic matrix. The formula for $\dot{\varepsilon}_1'$ is determined, by analogy with a completely isotropic material, in the form

$$\dot{\varepsilon}_1' = k\sigma_1, \quad \text{i.e} \quad \dot{\varepsilon}_1 = k\sigma_1 + \dot{\varepsilon}_g.$$

It is safe to assume that this stress dependence of the rate of deformation must hold in any case where a crystal experiencing conditions of restrained radiation-induced growth is concerned. The value of the coefficient k will be determined by the restraining pattern.

In order to determine the value of k, we consider deformation under irradiation, of an isotropic polycrystal to which an external stress σ has been applied. In this polycrystal we isolate an isotropic aggregate consisting of three crystals. The rate of deformation of each of those crystals, as well as that of the polycrystal as a whole, is described by the equation $\dot{\varepsilon} = \sigma \dot{\varepsilon}_g / \sigma_T$. At the same time, the deformation of one of the crystals so singled out, say with the orientation [010], can be treated as the result of partial freeing of the strain associated with radiation-induced growth, when $\sigma > 0$. In that case the rate of deformation can be represented as the difference between the rate of deformation $\dot{\varepsilon}_{iso}$ of the crystal in an isotropic medium and the rate of deformation due to restraint by two crystals having the orientations [100] and [001] ($\dot{\varepsilon}_{restr}$):

$$\left.\begin{aligned} \dot{\varepsilon} &= \dot{\varepsilon}_{iso} - \dot{\varepsilon}_{restr}, \\ \dot{\varepsilon}_{restr} &= k'\sigma_{restr} + \dot{\varepsilon}_g. \end{aligned}\right\} \qquad (2)$$

We assume that the coefficient k' is independent of the stress. We find this coefficient from the condition that $\dot{\varepsilon}_{restr} = -\dot{\varepsilon}_g$ in the absence of external applied stress, since the crystal having the orientation [010] is then acted upon by the stress $\sigma_{restr} = -\sigma_T$:

$$-k'\sigma_T + \dot{\varepsilon}_g = -\dot{\varepsilon}_g;$$

$$k' = \frac{2}{\sigma_T}\dot{\varepsilon}_g.$$

Writing Eqs. (2) in expanded form, we get

$$\frac{\sigma}{\sigma_T}\dot{\varepsilon}_g = k\sigma - \frac{2}{\sigma_T}\sigma\dot{\varepsilon}_g,$$

and hence

$$k = \frac{3}{\sigma_T}\dot{\varepsilon}_g.$$

In sum, the dependence of the rate of deformation of a crystal under irradiation and "disseminated" in an isotropic matrix, has the form

$$\dot{\varepsilon}_1 = \frac{3}{\sigma_T}\sigma_1\dot{\varepsilon}_g + \dot{\varepsilon}_g.$$

Using this formula to solve system (1), we get

$$\left.\begin{aligned} &\frac{3}{\sigma_T}\sigma_1\dot{\varepsilon}_g + 2\dot{\varepsilon}_g = \frac{\sigma_2}{\sigma_T}\dot{\varepsilon}_g; \\ &\sigma_1 + \frac{3(1-n)}{3n-1}\sigma_2 = 0; \\ &\sigma_2 \leqslant \sigma_T. \end{aligned}\right\}$$

Hence, the dependence of the effective rate of radiation-induced growth of polycrystalline uranium on the degree of initial anisotropy is $(3n-1)\dot{\varepsilon}_g/(4-3n)$. And since $\dot{\varepsilon}_g = Gi_{sg}\dot{\beta}$ (Gi_{sg} is the radiation growth coefficient of a single crystal, $\dot{\beta}$ is the rate of burnup), the effective radiation growth coefficient of the

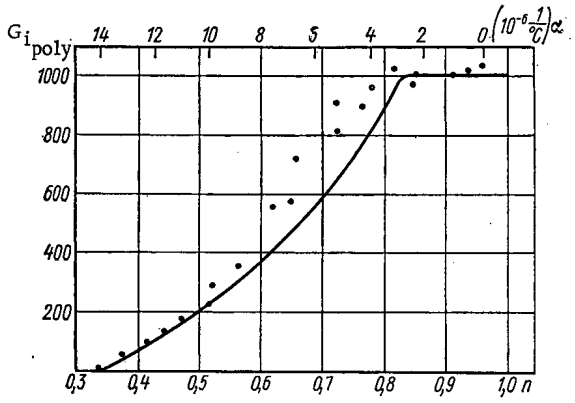

Fig. 1. Dependence of radiation growth coefficient of polycrystalline uranium $G_{i_{poly}}$ on degree of texture definition [010]: continuous curve) predicted curve; ●) experimental data from [5].

polycrystal, as a function of the original texture, has the form $G_{i_{poly}} = (3n-1)G_{i_{sg}}/(4-3n)$. From the constraint $\sigma \leq \sigma_T$, we find that the use of this equation is restricted to the range $n \leq 0.83$. When $n = 0.83$, we have $G_{i_{sg}} = G_{i_{poly}}$. This means, in physical terms, that when $n \geq 0.83$ the isotropic matrix is no longer capable of restraining the radiation-induced growth of the "disseminated" crystals, since the stresses generated by those crystals are sufficient to constrain the isotropic matrix to deform at the same rate at which these crystals themselves deform. In sum

$$G_{i_{poly}} = \begin{cases} \frac{3n-1}{4-3n} G_{i_{sg}} & \text{at} \quad 0.33 \leqslant n \leqslant 0.83; \\ G_{i_{sg}} & \text{at} \quad n \geqslant 0.83. \end{cases} \tag{3}$$

It is interesting to note that if the Cottrell formula is used in the case of rate of deformation of irradiated crystals "disseminated" in an isotropic matrix, the solution of the system of equations (1) for the radiation growth coefficient of the polycrystal will become

$$G_{i_{poly}} = \frac{3n-1}{2} G_{i_{sg}}$$

A similar expression for $G_{i_{poly}}$ can be derived, with this model of a polycrystalline specimen, when we resort to the procedure of calculating the x-ray growth index [1] and the growth index based on combined measurements of the linear expansion coefficient and the electrical resistivity [2]. By relying on a rough approximation which leaves the complicated nature of the interaction of crystals in the polycrystalline specimen out of account, we can derive expressions for the growth indices currently in use.

Figure 1 shows a predicted $G_{i_{poly}}$ curve obtained by using Eq. (3) at $G_{i_{sg}} = 1000$. We make use of measurements results at 80°C borrowed from [5] to afford a comparison between predicted and experimental $\sigma_{i_{poly}}$ values. The texture of the specimens was brought about by different cold deformation of uranium wire previously quenched from the β-phase. In this case, it appears that we can anticipate formations of the simplest texture, one analog of which is the model of a polycrystalline specimen used in the work described here. Experimental values were plotted together with the predicted theoretical curve in Fig. 1. The agreement between predicted and experimental values is reasonably satisfactory. In particular, the predicted growth coefficient in the region of small textures increases to a slighter extent, and in the region of large textures to a greater extent, than the linear dependence indicates. When $n \approx 0.83$, the radiation growth coefficient of the polycrystalline uranium attains values typical of a single crystal.

Consider some of the remarks relating to the proposed mechanism of radiation-induced growth of the polycrystalline α-uranium. The expression for the rate of Cottrell creep was used for the quantitative calculations of $G_{i_{poly}}$ at the irradiation temperature 80°C; Anderson–Bishop analysis [7] can be used in the case of higher temperatures. In both cases the polycrystalline aggregate is treated as an assemblage of distinct crystals whose properties determine the properties of the polycrystal. This explains the need to take that factor into account in the case of irradiation of polycrystalline uranium in the temperature range where intercrystal effects begin to play a role.

An idealized model of a polycrystalline aggregate was selected for quantitative calculations of the radiation growth coefficient of polycrystalline uranium with a different degree of texture definition. Clearly, in a real uranium polycrystal the distribution of the poles of the principal crystallographic directions will differ from the one considered here. The radiation growth coefficient of polycrystalline uranium calculated on the basis of Eq. (3) might consequently differ from the one measured experimentally in the case where a different relationship prevails between the density of the poles [100] and [001]. The theoretical growth coefficient will be somewhat too high, if the density of the [100] poles is greater than the density of the [001] poles, and will be somewhat too low if the density of the [100] poles is lower than the density of the [001] poles. Nevertheless, the discussion of the simple model of a polycrystalline aggregate does prove useful for throwing light on the overall regularities of radiation-induced growth in polycrystalline uranium.

With those remarks in mind, we can draw the following inferences with the aid of the proposed mechanism, in analyzing the possibility that radiation-induced growth of polycrystalline uranium will occur.

1. Radiation-induced growth of polycrystalline uranium must be described without assuming mutual reorientation of the component crystals, and while taking as point of departure the presence of internal stresses generated by the interaction of differently oriented crystals subjected to irradiation. These concepts can then be used subsequently in quantitative calculations of the effective radiation growth coefficient of polycrystalline uranium specimens, in a manner similar to the procedure followed in the simplest case, provided formulas describing deformation of the crystal under conditions where radiation-induced growth is restrained to different extents are derived.

2. The radiation growth coefficient of polycrystalline α-uranium is a nonlinear function of the degree of initial anisotropy of the material. Conclusions on the effect of alloying on radiation-induced growth of uranium single crystals, obtained on the basis of linear extrapolation of the results obtained for weakly textured specimens [3, 4] must not be accepted as sufficiently validated, for that reason.

3. Radiation-induced growth of polycrystalline uranium is associated with the generation of internal stresses, which at the same time constitute the primary cause of accelerated creep in irradiated uranium. Deformation of polycrystalline uranium due to the combined effect of texture and an external applied load cannot be treated, consequently, as the result of a simple superposition of those phenomena.

LITERATURE CITED

1. E. Sturcken and W. McDonnell, J. Nucl. Mat., 7, 85 (1962).
2. J. Stobo and B. Pawelski, J. Nucl. Mat., 4, 109 (1961).
3. W. McDonnell et al., J. Inst. Metals, 97, 26 (1969).
4. J. Lehman et al., Radiation Damage in Reactor Materials, Vol. II, Vienna (1969), p. 413.
5. S. Buckley, Institute of Metals, Symposium on "Uranium and Graphite," Paper No. 6, London (1962).
6. A. Roberts and A. Cottrell, Phil. Mag., 8, 711 (1956).
7. R. Anderson and J. Bishop, Institute of Metals, Symposium on "Uranium and Graphite," Paper No. 3, London (1962).
8. A. S. Zaimovskii et al., 2nd Geneva International Conference on the Peaceful Uses of Atomic Energy, 1958, Report No. 2191 (USSR).

CALIBRATION OF GAMMA – GAMMA DENSITOMETERS

K. Umiastowski

UDC 550.83

The gamma–gamma method, which is one of many geophysical methods of investigating the properties of rocks, is based on measuring the intensity of gamma radiation scattered in the medium. Depending on the relative position of the radiation source, the detector, and the investigated medium, one distinguishes between 2π geometry, 4π geometry, and 2π borehole geometry (Fig. 1). The results of gamma–gamma measurements are used to determine the rock density, the effective atomic number (Z_{eff}), and the content of heavy elements. The gamma – gamma method should be used only for density studies even if the obtained results are usable also for other cases.

Calibration Curve for Gamma–Gamma Densitometers. According to the principle of similitude [1, 2], the radiation intensity I, measured at a distance r from the source, can be written as

$$I(r, \rho, \zeta) = N \frac{f(x, \zeta)}{r^2}, \tag{1}$$

where r is the distance between the source and detector, ρ is the rock density, $x = \rho r$, N is a parameter depending on the source activity and detector efficiency, and ζ is a parameter depending on other conditions of measurement. If the probe length is r_0 and if other conditions of measurement remain unchanged, the recorded radiation intensity depends solely on the density of the material:

$$I(\rho) = \frac{N}{r_0^2} f(r_0, \rho, \zeta) = N' f(\rho), \tag{2}$$

where $N' = N / r_0^2$.

The curve $f(\rho) = N^* r^2 I(x)$ is called the calibration curve. It reflects the dependence of the count rate on the density of the material.

The shape of the calibration curve was calculated with the aid of the Monte Carlo method [3]. The theoretical curves are shown in Fig. 2, where I denotes the number of quanta n through a unit surface S per unit time:

$$I = \frac{n}{S}. \tag{3}$$

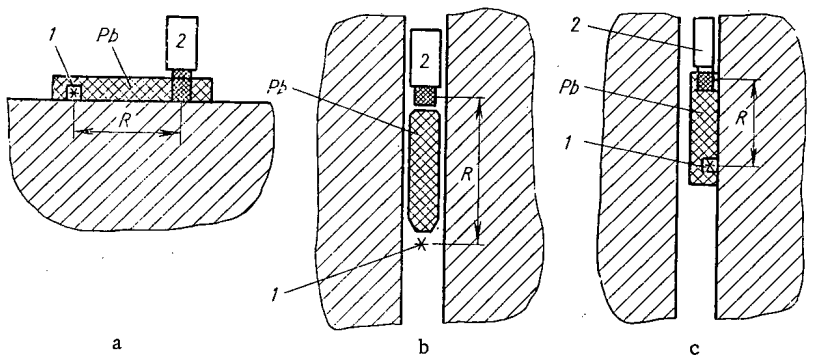

Fig. 1. Schematic representation of 2π geometry (a), 4π geometry (b), and 2π borehole geometry (c).

Institute of Nuclear Physics of the Mining and Metallurgical Academy, Cracow, Poland. Translated from Atomnaya Énergiya, Vol. 32, No. 4, pp. 293-296, April, 1972. Original article submitted October 14, 1971.

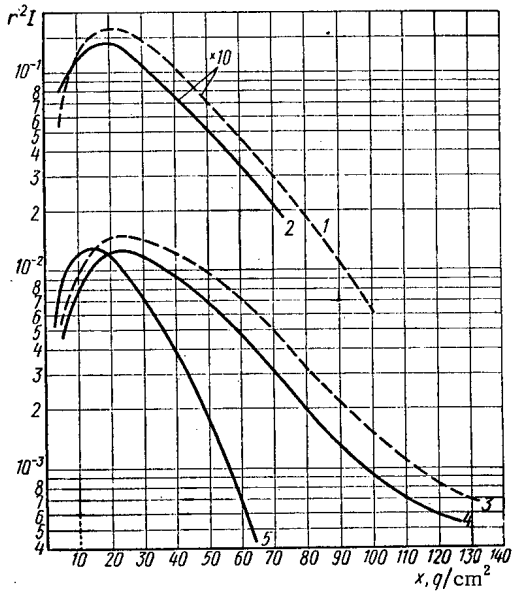

Fig. 2

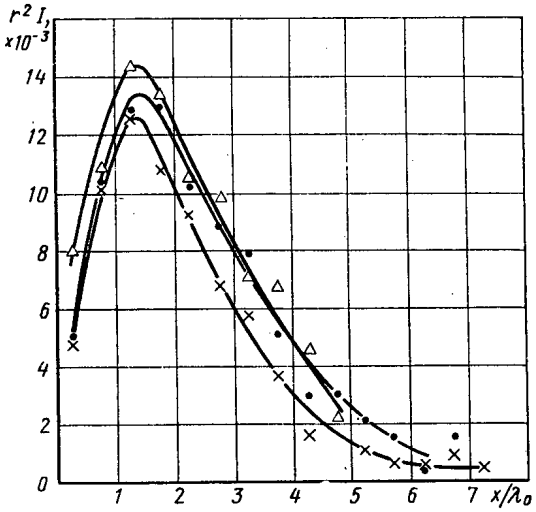

Fig. 3

Fig. 2. Theoretical calibration curve for different materials and source energies: 1) 0.66 MeV, water; 2) 0.66 MeV, aluminum; 3) 1.25 MeV, water; 4) 1.25 MeV aluminum; 5) 0.28 MeV aluminum.

Fig. 3. Theoretical calibration curves for Hg^{203} (●), Cs^{137} (Δ), and Co^{60} (×). x is expressed in quantum free path units (λ_0).

The calculations were made for aluminum (Z = 13) and water (Z_{eff} = 7.4).

By expressing the distance between the source and detector in free path units (λ_0) of a quantum with source energy E_0, the shape of the calibration curve can be made practically independent of the source energy (Fig. 3).

Let us introduce the new quantity $\lambda_p = k\lambda_0$. The probe length is then expressed in dimensionless units $\varkappa = r\rho/\lambda_p$. Expression (1) then becomes

$$I = \frac{N}{r_0^2} f(\varkappa, \zeta), \tag{4}$$

where the function $f(\varkappa, \zeta)$ is independent of the source energy.

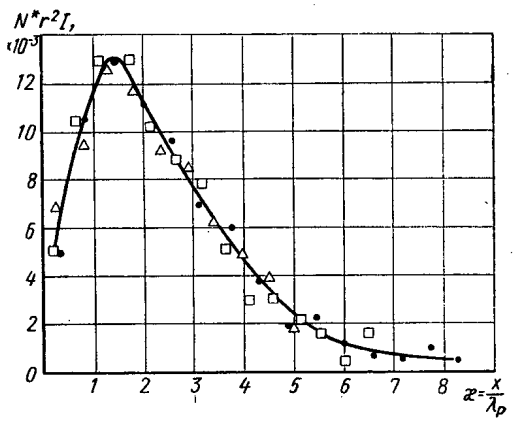

Fig. 4

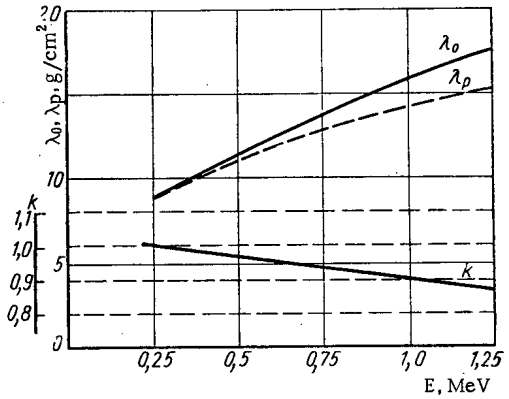

Fig. 5

Fig. 4. Universal calibration curve. x is given in λ_0 units. The factor N* is equal to 1.0 for Hg^{203} (□), 0.87 for Cs^{137} (Δ), and 1.03 for Co^{60} (●).

Fig. 5. Energy dependence of λ_0, λ_p, and k.

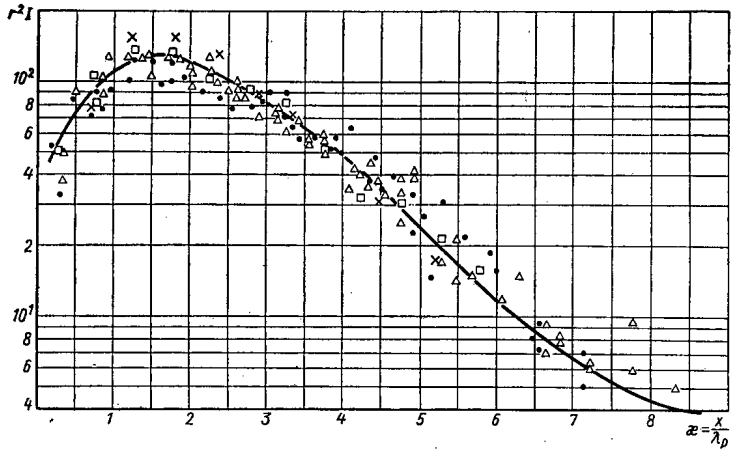

Fig. 6. Universal calibration curve. Experimental data adopted from different sources: Co^{60} (●), Cs^{137} (△), Hg^{203} (□), and Se^{75} (×).

By selecting proper normalization factors N, the curves for radiation sources of different energies can be superposed so that the result is a single universal calibration curve independent of the source energy as shown in Fig. 4.

The dependences of the λ_0, λ_p, and k values on the γ-quantum energy is shown in Table 1 and in Fig. 5.

Comparison with Experimental Data. The function $f(\varkappa)$ can be found experimentally with models of different densities ρ and constant probe length r_0 or with models of a fixed density ρ_0 and probes of different lengths r.

To check their validity the theoretical results were compared with experimental data. The results in [4] were obtained with a graphite model in a 2π geometry. The density of the model material was 1.75 g $/cm^3$. The probe length varied from 20 to 60 cm. The measurements were conducted with a scintillation counter. Cs^{137} and Co^{60} sources were employed. The results of [5-8] were also considered.

With properly selected normalization factors ($\varkappa$ expressed in λ_p units), all experimental points lie on practically the same curve (Fig. 6). The data of Fig. 4 are also plotted on this figure. It is seen that the theoretical and experimental data are in close agreement. The experimental data were obtained in 2π and 2π borehole geometries. The radiation source energy ranged from ~200 keV (Se^{75}) to 1.33 MeV (Co^{60}). Both gas-discharge and scintillation counters were used. The chemical composition of the models differed appreciably. A more detailed comparison of experimental data with expression (4) is given in [10].

Calibration of Gamma–Gamma Densitometers. The shape of the calibration curve depends on the measurement geometry, the discriminator threshold, and on the chemical composition of the medium [9].

For provisional calculations in which an accuracy better than 15% is not required one can use the theoretical calibration curve shown in Fig. 7. This curve was drawn through 80 points. To find the normalization factor, measurements should be made on one model only with a density ρ_0. The factor $\varkappa$ for the given source energy (E_0) and probe length r_0 is then converted into density in accordance with the expression

$$\rho = \varkappa \frac{\lambda_p E_0}{r_0}. \qquad (5)$$

The use of theoretical calibration curves with probes other than those for which the calculations were originally

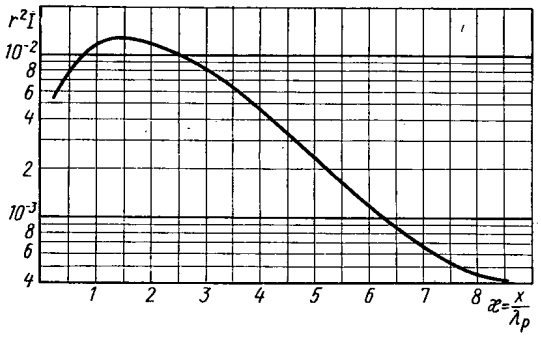

Fig. 7. Universal calibration curve for aluminum.

TABLE 1. Energy Dependence of λ_0, λ_p, and k

E, MeV	λ_0, g/cm³	k	λ_p, g/cm³
1,25	17,8	0,83	14,8
0,66	13,2	0,90	11,9
0,28	9,2	0,96	8,8

made can introduce an error not exceeding 15%. This conclusion is based on the calculation of the relative mean deviation of experimental data from the theoretical ones. The theoretical curve was calculated for the following conditions: 50 keV discrimination threshold, source and detector collimation angle equal to a 2π solid angle about the normal to the surface of the medium, detector efficiency equal to 100% and independent of radiation energy.

If higher accuracy is required for probes of different construction, the calibration curve must be found experimentally. This can be made with a small number of models provided gamma radiation sources of different energies are used. The calibration curve can be plotted for a wider range of densities than those of the models available. The calibration procedure is explained below using a specific example. Let the probe length be r = 20 cm, and let models have densities $\rho = 1.5$, 2.0, and 2.5 g/cm^3. Using these models with a Cs^{137} source ($E_0 = 0.66$ MeV, $\lambda p = 11.9$ g/cm^3) we obtain intensities at points corresponding to $\varkappa_1 = 2.52$, $\varkappa_2 = 3.36$, and $\varkappa_3 = 4.2$ calculated from

$$\varkappa = \frac{r_0 \rho}{\lambda_p (E)}.$$

Then, using a Co^{60} source ($E_0 = 1.25$ MeV, $\lambda p = 14.8$ g/cm^3) and a Hg^{203} source ($\lambda p = 8.8$ g/cm^3), we obtain I at the points $\varkappa_4 = 2.03$, $\varkappa_5 = 2.70$, $\varkappa_6 = 3.38$, $\varkappa_7 = 3.40$, $\varkappa_8 = 4.54$, and $\varkappa_9 = 5.68$. The values of I at the points $\varkappa_2$, $\varkappa_6$, and $\varkappa_7$ are used to normalize the results obtained with three different sources (since it is practically impossible to find sources of the same activity). Converting then $\varkappa$ into densities ρ for a cesium source in accordance with

$$\rho = \frac{\varkappa \lambda_p}{r_0} = \varkappa \frac{11.9\,\text{g/cm}^3}{20\,\text{cm}},$$

we obtain finally $\rho_4 = 1.21$, $\rho_5 = 1.61$, $\rho_6 = 2.01$, $\rho_7 = 2.02$, $\rho_8 = 2.7$, and $\rho_9 = 3.37$ g/cm^3.

Thus, using three models with densities between 1.5 and 2.5 g/cm^3, we obtained seven points on the calibration curve corresponding to densities between 1.21 and 3.37 g/cm^3.

A second densitometer calibration technique follows from the expression [11]:

$$I = \frac{A_b}{r^2} (\rho r)^n e^{-\alpha \rho r - b_1 Z_{eq}^{3,5}}, \tag{6}$$

where A_b, n, α, b_1 are factors that depend on the conditions of measurement. Substituting into this expression

$$\rho r = \lambda_p \frac{\rho r}{\lambda_p} = \lambda_p \varkappa, \tag{7}$$

we have

$$I = \frac{(A_b \lambda_p^n)}{r^2} \varkappa^n e^{-(\alpha \lambda_p)\varkappa - b_1 Z_{eq}^{3,5}}. \tag{8}$$

Denoting $(A_b \lambda_p^n) = A$, $\alpha \lambda p = B$, and equating (8) with (1), we have

$$f(u) = \varkappa^n e^{-B\varkappa - b_1 Z_{eq}^{3,5}}. \tag{9}$$

The factors n and B do not depend on the source energy as the function $f(\varkappa)$ is valid for any source energy. Finally, the intensity of recorded radiation is expressed as

$$I = \frac{A \varkappa^n}{r^2} e^{-B\varkappa - b_1 Z_{eq}^{3,5}}, \tag{10}$$

where the factors n and B depend only on the probe construction and do not depend on the radiation source energy. The factors A and b_1 depend on both the probe construction and the source energy.

Making measurements on N_m models and using N_i sources with different energies we should find $2N_i + 2$ factors in (10) (the two factors B and n, and also the two factors A and b_1 for each source). These factors are found from $N_m N_i$ measurements. Hence follows the condition

$$N_m N_i \geqslant 2N_i + 2 \tag{11}$$

or

$$N_m \geqslant 2 + \frac{2}{N_i}. \tag{11a}$$

Thus, at least four models are required if only a single source is available for the unknown factors. If the calibration is made with two sources, the number of models necessary is reduced to three.

Obviously, the use of several gamma radiation sources with different energies allows a significant improvement of the calibration curve accuracy (provides a greater number of calibration points with the same number of models), and makes it possible to plot the calibration curve for a wider range of densities than that of the models employed.

LITERATURE CITED

1. Sh. A. Guberman, At. Énerg., 10, 369 (1961).
2. J. Czubek, Report CEA-R 3099 (1966).
3. K. Umiastowski, Nukleonika, 15, No. 1, 37; No. 2, 215; No. 3, 259 (1970).
4. K. Umiastowski, Report CEA-R 4028 (1970).
5. J. Tittman and J. Wahl, Formation Density Logging (Proc. Conf. Nuclear Geophysicists), Cracow (1962), p. 339.
6. F. G. Baembitov, I. A. Gulin, and I. G. Dyatchin, Prikl. Yadern. Geofiz., No. 17, 284 (1958).
7. V. A. Artsybashev, Izv. Vuzov; Geol. i Geofiz., No. 9, 102 (1964).
8. E. M. Filippov, Prikl. Geofiz., No. 17, 231 (1958).
9. K. Umiastowski, Nukleonika, 13, No. 4-5, 413 (1968).
10. S. Rychlicki and K. Umiastowski, Nukleonika, 15, No. 1, 47 (1970).
11. J. Czubek, Report INP No. 715/I.

NEUTRON DIFFUSION IN A POLARIZED PROTON MEDIUM

Yu. N. Kazachenkov and V. V. Orlov

UDC 621.039.512.4

Methods have been recently developed for preparation of highly polarized (up to 80%) proton targets. Because of the strong spin–spin dependence of neutron–proton interaction the diffusion of neutrons in such media should differ from diffusion in nonpolarized targets. It suffices to say that the neutron–proton interaction cross section is ~3 b for parallel spins and ~38 b for antiparallel spins, and is independent of energy for neutrons of up to ~60 keV. This difference remains significant up to 4 MeV even if it diminishes with increasing energies. When nonpolarized neutrons are scattered on polarized protons they become partially polarized in the direction of the proton polarization vector thus reducing the scattering cross section for subsequent interactions; this means that the transparency of polarized proton shields is higher than that of similar nonpolarized shields.

Let us now derive equations describing neutron diffusion in a polarized proton medium. First let us find expressions for the scattering cross section and for the neutron polarization after scattering. Before scattering the neutron and proton are described by the density matrix ρ_{in}:

$$\rho_{in} = \rho_1\rho_2 = \frac{1}{4}(1+\mathbf{p}_1\boldsymbol{\sigma}_1)(1+\mathbf{p}_2\boldsymbol{\sigma}_2), \tag{1}$$

where $\mathbf{p}$ is the polarization vector, σ is a vector whose components are the Pauli matrices; the subscripts 1 and 2 refer to the neutron and proton respectively.

It is known that the density matrix of particles after scattering can be expressed in terms of the density matrix before scattering and the interaction amplitude:

$$\rho_{out} = f\rho_{in}f^{+}. \tag{2}$$

For energies up to ~10 MeV the amplitude of neutron scattering on protons has the form [1]

$$f = \left(\frac{3}{4}f_t + \frac{1}{4}f_s\right) + \frac{1}{4}(f_t - f_s)\,\boldsymbol{\sigma}_1\boldsymbol{\sigma}_2, \tag{3}$$

where f_s and f_t is the scattering amplitude in the singlet and triplet states respectively. For neutron energies up to 10 MeV, the only contribution comes from the s wave, and the triplet and singlet scattering amplitudes are written as

$$f_{s,t} = \frac{1}{2ik}(e^{2i\delta_{s,t}} - 1), \tag{4}$$

where k is the wave vector.

The scattering phases obey the equation [2]

$$k\operatorname{ctg}\delta_{s,t} = -\frac{1}{a_{s,t}} + \frac{k^2 r_{s,t}}{2}, \tag{5}$$

where $a_{s,t}$ is the scattering length, and $r_{s,t}$ is the effective interaction radius; their numerical values are given in [3].

The mean value of any operator L acting in the spin space of the exit channel is given by

$$\langle L\rangle = \frac{Sp\,(L\rho_{out})}{Sp\rho_{out}}. \tag{6}$$

Using the expressions (1)-(4), after simple but quite time-consuming manipulations, we obtain expressions for the interaction cross section of polarized neutron and polarized protons, and for the polarization vector of scattered neutrons $\mathbf{p}_1$:

Translated from Atomnaya Énergiya, Vol. 32, No. 4, pp. 297-300, April, 1972. Original article submitted May 6, 1971.

$$\frac{d\sigma}{d\Omega}=\frac{3}{4}|f_t|^2+\frac{1}{4}|f_s|^2+\frac{1}{4}(|f_t|^2-|f_s|^2)(\mathbf{p}_1\mathbf{p}_2); \tag{7a}$$

$$\mathbf{p}_1\frac{d\sigma}{d\Omega}=\frac{1}{2}(|f_t|^2+Ref_tf_s)\,\mathbf{p}_1+\frac{1}{2}(|f_t|^2-Ref_t^*f_s)\,\mathbf{p}_2-\frac{1}{2}Im\,f_t^*f_s\,[\mathbf{p}_1\mathbf{p}_2]. \tag{7b}$$

If the neutrons were not polarized before, then in the course of diffusion they can only acquire a polarization colinear with $\mathbf{p}_2$ (which can be easily verified considering successive collisions) and the last term in (7b) turns identically to zero.

Let us divide all neutrons into those having spins parallel to $\mathbf{p}_2$ and antiparallel to $\mathbf{p}_2$. The probability of scattering with and without the change of neutron polarization can be easily determined from (7):

$$\left.\begin{aligned} w^{++}&=\frac{1}{2}+w_1;\quad w^{+-}=\frac{1}{2}-w_1;\\ w^{--}&=\frac{1}{2}+w_2;\quad w^{-+}=\frac{1}{2}-w_2,\end{aligned}\right\} \tag{8}$$

where

$$\left.\begin{aligned} w_1&=\frac{|f_t|^2+Ref_t^*f_s+(|f_t|^2-Ref_t^*f_s)\,p_2}{3|f_t|^2+|f_s|^2+(|f_t|^2-|f_s|^2)\,p_2};\\ w_2&=\frac{|f_t|^2+Ref_tf_s-(|f_t|^2-Ref_t^*f_s)\,p_2}{3|f_t|^2+|f_s|^2+(|f_t|^2-|f_s|^2)\,p_2}.\end{aligned}\right\} \tag{9}$$

In (8), the first and second upper signs indicate the neutron polarization before and after scattering respectively, $p_2=|\mathbf{p}_2|$.

In addition to protons, practical proton targets also contain nuclei of other elements whose polarization, however, is so negligible [4] that they can be said to be nonpolarized. On being scattered by these nuclei neutrons are depolarized. If the neutron energy is such that the principal contribution into scattering comes from the s wave, the probability of spin reversal by scattering on nonoriented nuclei is [5]

$$Q=\sum_p b_p\frac{2(I_p+1)I_p(a_{p+}-a_{p-})^2}{3(2I_p+1)[(I_p+1)a_{p+}^2-I_pa_{p-}^2]}, \tag{10}$$

where a_{p+} and a_{p-} are scattering lengths of neutrons on the p-th isotope along channels with total spins $I_p+1/2$ and $I_p-1/2$ respectively, $b_p=\Sigma_{sp}/\Sigma_{se}$ is the relative probability of neutron scattering on the p-th isotope nuclei except hydrogen ($\sum_p b_p=1$); the sum is taken over all nonpolarized isotopes in the target, Σ_{sp} is the macroscopic scattering cross section on the p-th isotope, and Σ_{se} is the macroscopic scattering cross section on all isotopes with nonoriented nuclei.

Let us divide all neutrons into two groups: neutrons with spins parallel to the vector $\mathbf{p}_2$ (denoted by a "+" sign) and with spins antiparallel to $\mathbf{p}_2$ (denoted by "-"). Taking the balance of both these groups of neutrons, and allowing for the possibility of neutrons passing from one group to the other as a result of scattering, we obtain the following system of equations (scattering on the nuclei of all isotopes except hydrogen is assumed isotropic):

$$\begin{aligned}(\Omega\nabla)F^+(\mathbf{r},\,\Omega,\,E)+\Sigma^+(\mathbf{r},\,E)F^+(\mathbf{r},\,\Omega,\,E)=\int\int d\Omega'\,dE'\{w_n(E'\to E,\;\Omega'\to\Omega)\\ \times[\Sigma_{sn}^+(\mathbf{r},\,E')F^+(\mathbf{r},\,\Omega',\,E')w^{++}+\Sigma_{sn}^-(\mathbf{r},\,E')F^-(\mathbf{r},\,\Omega',\,E')w^{-+}]\\ +\Sigma_{se}(\mathbf{r},\,E')(1-Q)F^+(\mathbf{r},\,\Omega',\,E')+\Sigma_{se}(\mathbf{r},\,E')QF^-(\mathbf{r},\,\Omega',\,E')\};\end{aligned} \tag{11a}$$

$$\begin{aligned}(\Omega\nabla)F^-(\mathbf{r},\,\Omega,\,E)+\Sigma^-(\mathbf{r},\,E)F^-(\mathbf{r},\,\Omega,\,E)=\int\int d\Omega'\,dE'\{w_n(E'\to E,\;\Omega'\to\Omega)\\ \times[\Sigma_{sn}^-(\mathbf{r},\,E')F^-(\mathbf{r},\,\Omega',\,E)w^{--}+\Sigma_{sn}^+(\mathbf{r},\,E)\,F^+(\mathbf{r},\,\Omega',\,E')w^{+-}]+\Sigma_{se}(\mathbf{r},\,E')(1-Q)\\ \times F^-(\mathbf{r},\,\Omega,\,E')+\Sigma_{se}(\mathbf{r},\,E')QF^-(\mathbf{r},\,\Omega',\,E')\},\end{aligned} \tag{11b}$$

where Σ^+ and Σ^- is the macroscopic interaction cross section of each neutron group respectively, Σ_{sn}^+ and Σ_{sn}^- is the macroscopic scattering cross section of each group of neutrons on oriented protons,

$$\Sigma_{sn}^{\pm}=\Sigma_{sn}\left(1\pm\frac{(f_t)^2-(f_s)^2}{3(f_t)^2+(f_s)^2}-p\right);$$

Σ_{sn} is the macroscopic neutron scattering cross section on nonpolarized protons, $w_n(E'\to E,\;\Omega'\to\Omega)$ is the indicatrix of neutron scattering by protons.

Generally speaking, in considering the diffusion of fission neutrons in the upper energy groups one must take into account the change in polarization resulting from spin – orbit interaction. However, as shown in [6], the corresponding corrections are quadratic with respect to the spin – orbit interaction parameters which, in turn, are much smaller than the parameters of spin – spin neutron – proton interaction. It can be thus assumed in the first approximation that spin – orbit interaction does not affect the neutron transport in polarized neutron shields.

As already noted before, the albedo of a polarized proton shield should be lower than that of a similar nonpolarized shield. As an example of calculating this effect we have determined the change in K_{eff} of a plutonium slab reactor caused by polarization of a water reflector (existing polarized proton targets contain many crystallization molecules of water). Since the lifetime of one generation increases with reflector thickness, and since the effect is small in thin reflectors, we have selected a reflector 6 cm thick. After considering various concentrations of nuclei and different core dimensions, we have accepted the following reactor dimensions and element concentrations:

$$d_{core} = 1.715 \text{ cm},$$

$$\rho_{Pu^{239}} = 0.5 \cdot 10^{24} \text{ nuclei/cm}^3,$$

$$\rho_{B^{10}} = 0.149 \cdot 10^{24} \text{ nuclei/cm}^3,$$

$$d_{ref} = 6 \text{ cm},$$

$$\rho_{O^{16}} = 0.0335 \cdot 10^{24} \text{ nuclei/cm}^3,$$

$$\rho_{H^1} = 0.067 \cdot 10^{24} \text{ nuclei/cm}^3,$$

The first three lines refer to the core, the last three to the reflector. The calculations were made in a 26-group P_2 approximation for a reactor with polarized and nonpolarized reflectors. The results indicate that K_{eff} of the reactor with a polarized reflector is 2.7% less than with a nonpolarized reflector. The lifetime of one generation l was found to be $\sim 2 \cdot 10^{-8}$ sec.

If the reactor is used in a pulse mode, the minimum halfwidth of a neutron pulse Δt is 1 μsec. The numerical calculations were made by Yu. G. Kaufman.

The reactivity of a reactor with a polarized proton reflector can be rapidly increased by applying a magnetic field normal to the direction of proton polarization. In such a case the spins of protons and neutrons will start to precess in opposite directions and the nucleons will "forget" their former polarization. Let us estimate the dependence of this effect on the magnetic field. The change of the average particle momentum in the beam, and thus of the polarization $\mathbf{p}$ in a domain of magnetic induction $\mathbf{B}$, obeys the equation of motion (see, e.g., [7])

$$\frac{d\mathbf{p}}{dt} = \gamma [\mathbf{pB}], \tag{12}$$

where γ is the gyromagnetic ratio of the particle. From (12) follows that the change of the scalar product of neutron and proton polarization, $\mathbf{p_n}$ and $\mathbf{p_p}$, in time is described by

$$\frac{d(\mathbf{p}_n\mathbf{p}_p)}{dt} = (\gamma_n - \gamma_p)\, \mathbf{B}[\mathbf{p}_n\mathbf{p}_p], \tag{13}$$

where γ_n and γ_p are the gyromagnetic ratios of the neutron and proton.

As mentioned above, before the field is applied $\mathbf{p_n}$ and $\mathbf{p_p}$ are colinear; when the magnetic field is applied their precession will take place in the same plane.

Thus

$$\mathbf{p}_n\mathbf{p}_p = |\mathbf{p}_n|\,|\mathbf{p}_p| \cos\theta; \tag{14a}$$

$$\mathbf{B}[\mathbf{p}_n\mathbf{p}_p] = B\,|\mathbf{p}_n|\,|\mathbf{p}_p| \sin\theta \tag{14b}$$

(the field is assumed to be normal to the plane of rotation of the polarization vectors).

Solving equation (13) under the conditions (14), for neutrons polarized at the instant t = 0 along $\mathbf{P_p}$ we have the expression

$$\mathbf{p}_n\mathbf{p}_p = |\mathbf{p}_n|\,|\mathbf{p}_p| \cos(\gamma_n - \gamma_p) Bt. \tag{15}$$

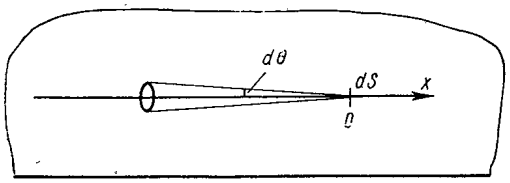

Fig. 1. Calculation of neutron polarization.

As before, let us divide all neutrons into two groups: those that at the instant t = 0 were polarized along or against the direction of polarization of protons. Expression (15) then becomes

$$\mathbf{p}_n\mathbf{p}_p = \frac{1}{2}|\mathbf{p}_p|[(1+|\mathbf{p}_n|)\cos(\gamma_n-\gamma_p)Bt - (1-|\mathbf{p}_n|)\cos(\gamma_n-\gamma_p)Bt]. \quad (16)$$

The scalar product of neutron and proton polarization of the beam at a given point of space can be represented as the average scalar product of all neutrons arriving at this point and proceeding in the given direction. This circumstance makes it possible to evaluate the change in the scalar product of polarizations due to the magnetic field.

Consider an infinite homogeneous polarized medium in which there acts a magnetic field normal to the direction of polarization. Let neutrons diffuse along the x axis with a velocity v (see Fig. 1). The scalar product of neutron and proton polarization can then be written as

$$\mathbf{p}_n\mathbf{p}_p = \frac{|\mathbf{p}_p|\sum_{m=0}^{1}[1+(-1)^m|\mathbf{p}_n|]\int_0^\infty dt\cos\varkappa x\exp\left[-\Sigma\int_0^x dx'\{1+(-1)^m\alpha[\mathbf{p}_p|\cos\varkappa x'\}\right]}{\sum_{m=0}^{1}[1+(-1)^m|\mathbf{p}_n|]\int_0^\infty dt\exp\left[-\Sigma\int_0^x dx'\{1+(-1)^m\alpha\cos\varkappa x'\}\right]}, \quad (17)$$

where $x = tv$, $\varkappa = (\gamma_n - \gamma_p)B/v$, $\beta = \alpha\Sigma v|\mathbf{p}_p|/(\gamma_n - \gamma_p)B$, $\alpha = \Sigma_p/\Sigma$, and Σ_p is the macroscopic polarization cross section.

Solving the integrals in (17) and considering strong magnetic fields only ($\beta \ll 1$), we have

$$\overline{\mathbf{p}_n\mathbf{p}_p} \approx \frac{1}{1+\frac{(\gamma_n-\gamma_p)^2B^2}{v^2\Sigma^2}}|\mathbf{p}_n||\mathbf{p}_p| - \frac{\alpha}{1+\frac{4(\gamma_n-\gamma_p)^2B^2}{v^2\Sigma^2}}|\mathbf{p}_p|^2. \quad (18)$$

It should be noted that the scalar neutron and proton polarization product will decrease with increasing magnetic fields faster than follows from Eq. (18) since the absolute value of neutron polarization $|\mathbf{p}_n|$ also decreases. The reduction of polarization effects with an increasing magnetic field as given by Eq. (18) can be thus regarded as an upper bound. This is particularly rapid in magnetic fields for which

$$\left|\frac{(\gamma_n-\gamma_p)B}{v\Sigma}\right| \gg 1.$$

In the case of a water reflector, for example, this quantity equals unity for a magnetic induction of 13,000 G and a neutron energy of ~1 MeV.

The design of reactors with polarized proton reflectors will certainly meet with technical difficulties (construction of large polarized targets (~1 liter), application of cryogenic techniques, use of very strong pulsed magnets). These difficulties are however not fundamental, and the parameters of a pulsed reactor should be considerably much more attractive than those of conventional reactors.

LITERATURE CITED

1. V. F. Turchin, Slow Neutrons [in Russian], Gosatomizdat, Moscow (1963).
2. L. D. Landau and Ya. A. Smorodinskii, Zh. Éksp. Teor. Fiz., 14, 269 (1944).
3. V. S. Barashenkov, Interaction Cross Sections of Elementary Particles [in Russian], Nauka, Moscow (1966).
4. V. I. Lushikov, Yu. V. Taran, and F. L. Shapiro, Yadern. Fiz., 10, 1178 (1969).
5. O. Halpern and M. Tohnson, Phys. Rev., 55, 898 (1939).
6. Yu. N. Kazachenkov, Yadern. Fiz., 1, 763 (1965).
7. Yu. G. Abov, A. D. Gul'ko, and P. A. Krupchitskii, Polarized Slow Neutrons [in Russian], Atomizdat, Moscow (1966).

THE ENERGY LIFETIME AND DIFFUSION OF PARTICLES IN "TOKAMAK" SYSTEMS

Yu. N. Dnestrovskii, D. P. Kostomarov, and N. L. Pavlova

UDC 621.039.643

In our previous papers [1-3] we studied the energy balance in a plasma on the basis of the neoclassical thermal conductivity for ions [4, 5] and a phenomenological description of the anomalous conductivity and thermal conductivity of the electrons. The results of the calculations of the ion and electron temperatures and the current-diffusion time in the plasma are found to be in good agreement with experiments. At the same time the experimentally measured energy lifetime τ_E turns out to be several times smaller than the calculated value. This means that an additional departure of energy from the plasma exists which was not taken into account in [1-3].

The present paper considers two models which allow the results of the theory and experiment to be reconciled. According to the first model the additional departure of heat takes place due to the elevated thermal conductivity of the electrons. Since in [2, 3] the thermal conductivity of the electrons was already anomalous, such a still further elevated thermal conductivity is naturally called "superanomalous." The calculations showed that for a fixed superabnormality factor (equal to 7) the experimental and calculated values of τ_E coincide in a wide range of variation of plasma currents and density.

According to the second model the additional energy losses take place via the ions. Whereas in [1-3] the heat exchange between ions and electrons and the thermal conductivity of the ions were considered to be classical, they are now assumed to be anomalous having the same abnormality as the plasma resistance and electron thermal conductivity. The results of calculations according to this model are also in fairly

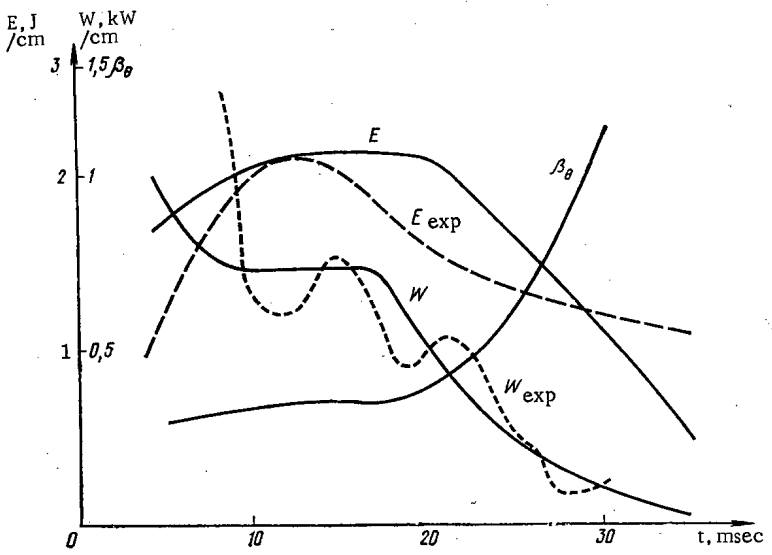

Fig. 1. Dependence of the total plasma energy E, the Joule heat W, and β_θ on time for a discharge having the parameters (9).

Translated from Atomnaya Énergiya, Vol. 32, No. 4, pp. 301-305, April, 1972. Original article submitted July 21, 1971.

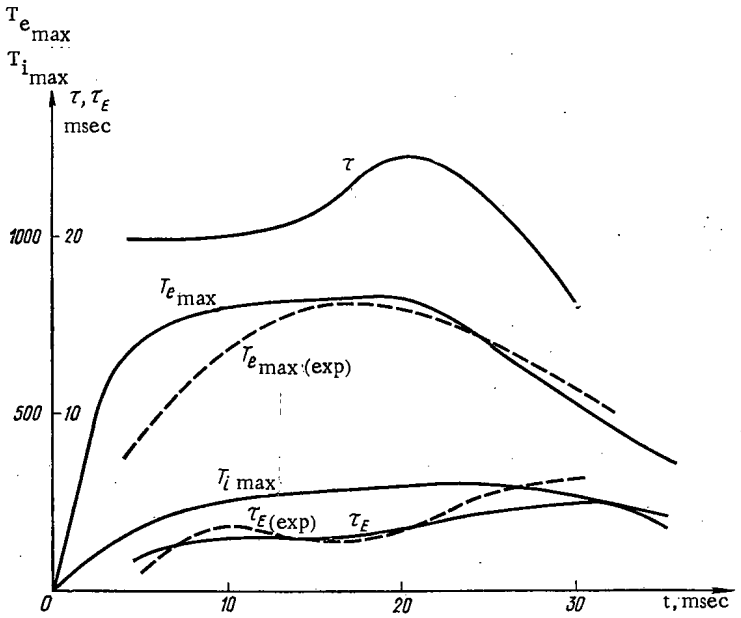

Fig. 2. Dependence of the maximum ion and electron temperatures $T_{i\,max}$ and $T_{e\,max}$, the energy lifetime τ_E, and the particle lifetime τ on time for a discharge having the parameters (9).

good agreement with experiment, although the ion temperature and the diffusion time of the current in the plasma turn out to be somewhat too high.

Within the framework of a phenomenological description one cannot give preference to any one model, and very sophisticated experiments are required to determine the channel of energy extraction from the plasma.

Measurements of the dependence of the plasma density on time indicate that the ionization of neutrals plays a substantial role in the particle balance. In order to consider the role of neutrals the system of thermal balance equations is augmented by the equation for the neutrals in this present paper. It is shown that available experimental data on plasma density and the flux of neutrals from the walls may be reconciled with calculated data on the assumption that the nature of the diffusion of the plasma particles is neoclassical.

Principal Equations

In order to describe the behavior of the plasma we shall use the following system of equations in the plasma density n(x, t), a function proportional to the magnetic field of the current $\mu(x, t) = RH_\theta/RH$, and the ion and electron temperatures $T_i(x, t)$ and $T_e(x, t)$:

$$\frac{dn}{dt} = \frac{1}{x} \cdot \frac{d}{dx}(x\gamma_2 DS) + P; \tag{1}$$

$$\frac{d\mu}{dt} = \frac{A}{x} \cdot \frac{d}{dx}\left[\frac{\gamma}{T_e^{3/2}} \cdot \frac{1}{x} \cdot \frac{d}{dx}(x^2\mu)\right]; \tag{2}$$

$$\frac{dT_i}{dt} = \frac{1}{nx} \cdot \frac{d}{dx}\left(xn\chi_i\gamma_3 \frac{dT_i}{dx}\right) + \frac{Cn}{T_e^{3/2}}(T_e - T_i)\gamma_3 + Q_i; \tag{3}$$

$$\frac{dT_e}{dt} = \frac{1}{nx} \cdot \frac{d}{dx}\left(xn\chi_e\gamma\gamma_1 \frac{dT_e}{dx}\right) - \frac{Cn}{T_e^{3/2}}\gamma_3(T_e - T_i) + \frac{B\gamma}{nT_e^{3/2}}\left[\frac{1}{x} \cdot \frac{d}{dx}(x^2\mu)\right]^2 + Q_e. \tag{4}$$

Here $x = r/a$; $A = 6.1 \cdot 10^3/a^2$; $B = 2 \cdot 10^7 H^2/R^2$; $C = 470$; H is the longitudinal magnetic field in kilooersteds; R and a are the major and minor radii of the plasma torus in centimeters. D, DS, χ_i and χ_e denote the neoclassical expressions for the diffusion coefficient, the particle flux, and the ion and electron thermal conductivity coefficients [4, 5]. The time is measured in milliseconds, the temperature is measured in electron volts, and the density is measured in 10^{13} cm^{-3}.

The multipliers γ, γ_1, γ_2, and γ_3 in Eqs. (1)-(4) allow a phenomenological description of the anomalous increase in the transport coefficients. In calculations for the abnormality of the resistance γ the local

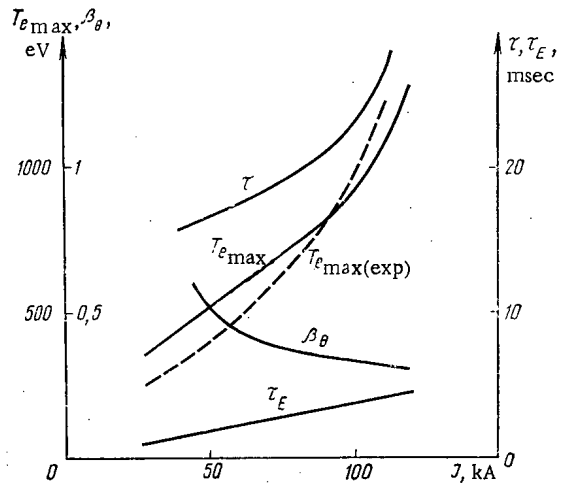

Fig. 3

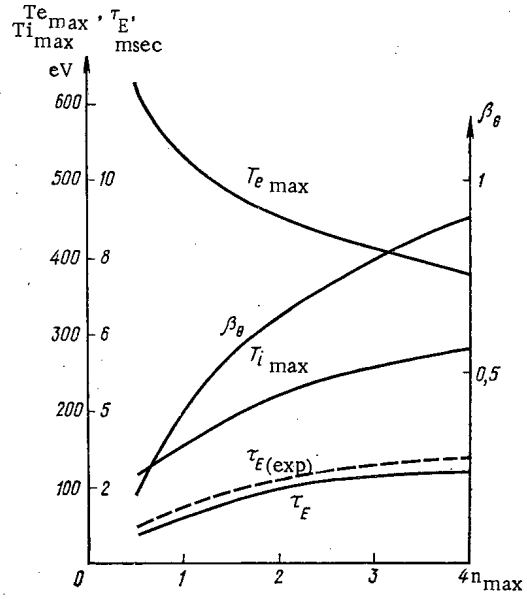

Fig. 4

Fig. 3. Dependence of the stationary values of $T_{e\max}$, β_θ, τ_E, and τ on current for H = 25 kOe, n(0, 0) = 2.

Fig. 4. Dependence of the stationary values of $T_{e\max}$, $T_{i\max}$, β_θ, and τ_E on the plasma density for H = 25 kOe, I = 45 kA.

model described in [2, 3] was used. The significance of the remaining anomalous corrections is discussed below.

The quantities P, Q_i, and Q_e in Eqs. (1), (3), (4) describe the variations of the plasma density and of the temperature of the plasma components as a result of the ionization and charge-exchange processes:

$$P = 60nN\sqrt{T_e}\,\sigma_e; \quad Q_e = -60N(T_e - T_n)\sqrt{T_e}\,\sigma_e;$$
$$Q_i = -56N(T_i - T_n)(\sqrt{T_i}\,\sigma_p + 1{,}07\sqrt{T_e}\,\sigma_e).$$

Here N(x, t) and T_n(x, t) are the density and temperature of neutral hydrogen atoms in 10^{13} cm^{-3} units and electron volts; $10^{-16}\sigma_e$ cm^2 is the cross section for the ionization of atomic hydrogen by electrons; $4 \cdot 10^{-15}$ σ_p cm^2 is the charge-exchange cross section.

The system (1)-(4) was augmented by the necessary initial and boundary conditions. In particular, the boundary condition for Eq. (2) has the form $\mu(1, t) = 0.2RI(t)/a^2H$, where I(t) is the total current which was assumed to be a stipulated time function.

The Distribution of Neutrals in the Plasma

The complete problem involving the distribution function of neutrals in a plasma cylinder leads to a very cumbersome equation. Since, however, neutrals do not play a noticeable role in the energy balance of the plasma, a reasonable simplification of the problem must not lead to a radical alteration of the physical picture of the process. Starting from these notions, let us consider the problem of neutrals in planar geometry rather than in cylindrical geometry. Under these conditions the solutions of these two problems on the periphery of the plasma differ little, while in the center of the plasma where the difference is substantial the density of neutrals is low for a sufficiently high plasma density. Moreover, we shall assume that for charge exchange at point x at time t a neutral atom is produced having an energy equal to the ion temperature at this point and equiprobable forward and backward velocity directions. In this case we shall have the following problem for determining the distribution function of neutrals f(x, v) in the layer $-a < x < a$:

$$v\frac{df}{dx} + sf = FN\frac{1}{2v_0}\left[\delta\left(\frac{v - v_i}{v_0}\right) + \delta\left(\frac{v + v_i}{v_0}\right)\right]; \tag{5}$$

$$f(\pm a, v) = \frac{N0}{v_0}\delta\left(\frac{v \pm v_0}{v_0}\right) \quad \text{for} \quad v \gtrless 0, \tag{6}$$

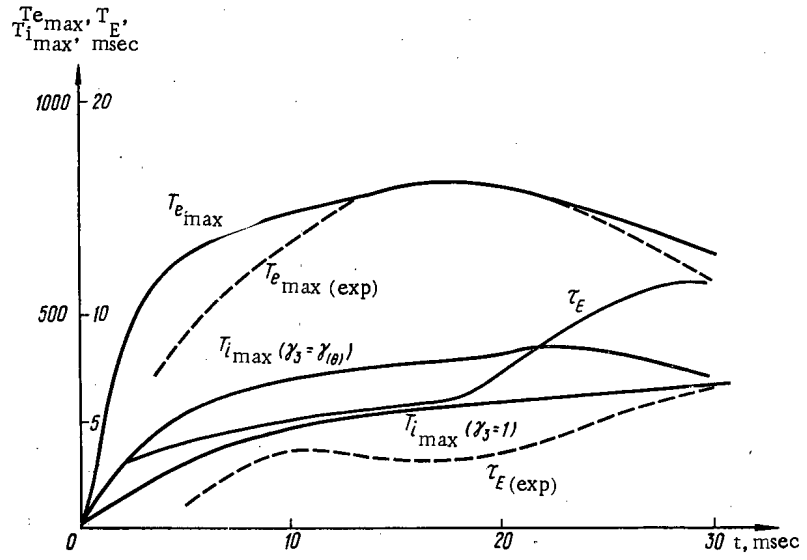

Fig. 5. Dependence of $T_{i\,max}$, $T_{e\,max}$, and τ_E on time in the model of anomalous ionic processes for a discharge having the parameters (9). The $T_{i\,max}$ curve for $\gamma_3 = 1$ corresponds to classical ionic processes.

where $s = s(x) = F + 10^{-3}\sigma_e n v_e$; $F = F(x) = 0.04\sigma_p n v_i$; $v_i = v_i(x) = 1.4 \cdot 10^6\sqrt{T_i}$; $v_e = v_e(x) = 0.6 \cdot 10^8\sqrt{T_e}$; $mv_0^2/2$ is the energy of the entering neutral. From Eqs. (5), (6) one can easily derive the integral equation for the density of the neutrals N(x):

$$N(x) = N_0(x) + \int_0^a K(x, \xi) N(\xi)\, d\xi, \tag{7}$$

where

$$K(x, \xi) = \frac{1}{2} \cdot \frac{F(\xi)}{v_i(\xi)} \{\Phi(\xi, x, v_i(\xi)\,\mathrm{sign}(x - \xi)) + \Phi(0, \xi, v_i(\xi))\,\Phi(0, x, v_i(x))\};$$

$$N_0(x) = N^0 \{\Phi(x, a, v_0) + \Phi(0, a, v_0)\,\Phi(0, x, v_0)\};$$

$$\Phi(\xi, x, v) = \exp\left[-\frac{1}{v}\int_\xi^x s\, dx'\right].$$

Equation (7) was solved numerically by means of the method of successive approximations:

$$N(x) = \sum_{k=0}^{\infty} N_k(x); \quad N_{k+1}(x) = \int_0^a K(x, \xi) N_k(\xi)\, d\xi. \tag{8}$$

The zero term $N_0(x)$ of this series corresponds to the density of neutrals without allowance for secondary charge-exchange neutrals, while each subsequent term yields neutrals which appear as a result of k-fold charge exchange.

The density N(x) of the neutrals depends parametrically on time via the functions F, v_i, s, N^0. In experimental measurements of the density of the neutrals in a vacuum it was established that this quantity decreases with time during the discharge process. Therefore, the dependence of N^0 on time was chosen in the form $N^0(t) = N_{in}(1 + t/\tau_n)^{-1}$, where N_{in} and τ_n are constants which are determined from the agreement between the experimental and calculated values of the density of the plasma and the neutrals. From the density N(x) one can establish the space distribution $T_n(x)$ of the temperature of the neutrals by means of (7).

The calculations carried out for Eq. (7) showed that for a plasma having a density $n < 0.5$ the neutrals penetrate fairly freely into the central portion: $N(0) \approx 1/2N(1)$. For a denser plasma ($n > 2$) the principal portion of the neutrals is ionized in the peripheral layer: $N(0) < 0.1N(1)$. The temperature of the ions and electrons has only a weak effect on the profile of the density of the neutrals N(x).

Superanomalous Thermal Conductivity of the Electrons

Let us investigate the possibility of reconciling the theoretical and experimental results for the energy lifetime using the proposition that there is an additional heat flux via the electrons and assuming in Eq. (4) that the coefficient $\gamma_1 > 1$. The calculations show that the best results are obtained for $\gamma_1 = 7$. In this case one can reconcile theory and experiment over a wide strip of values of plasma density and current.

Figures 1 and 2 show the results of calculations for the parameters

$$R = 100,\ a = 15,\ H = 25\ \text{kOe},\qquad I_{\max} = 90\ \text{kA}. \tag{9}$$

The rise time of the current is 4 msec. Beginning at time t = 17 msec, the current decreases and vanishes at t = 38 msec. In the calculations the local model of plasma-resistance abnormality [2, 3] was used for $\theta_1 = 1$, $\Delta\theta = 2$, $\gamma = 15$. The flux of neutrals from the walls was determined by the parameters: $N_{in} = 0.0003$, $\tau_n = 10$, $mv_0^2/2 = 10$.

Figure 1 shows the experimental [6] and calculated dependences of the total plasma energy E, the Joule heat W, and $\beta_\theta = \langle nT\rangle/(1/8\pi)H_\theta^2 = 1330E/I^2$ on time. The falloff of the current for t > 17 msec leads to an abrupt decrease in W, and then to a decrease in the total energy as well. The quantity β_θ increases rapidly under these conditions, which likewise corresponds to experiment [6]. Figure 2 shows plots of the time dependence of the maximal temperatures $T_{e\,max}$, $T_{i\,max}$, the energy lifetime τ_E, and the particle lifetime τ. The diffusion of the particles was assumed to be neoclassical ($\gamma_2 = 1$). Note that the principal portion of the particle flux to the wall is associated with the term proportional to $\partial T_e/\partial x$ in the expression for the flux DS (thermal diffusion).

As a consequence of the strong nonlinear dependence of the conductivity on T_e, an increase by a factor of seven in the thermal conductivity (superanomalous thermal conductivity) reduces the electron temperature by only 25-30%. Under these conditions the ion temperature changes insignificantly (by 3-5%). The high thermal conductivity of the electrons determines the rapid spreading of the skin-layer and the diffusion of current into the interior of the plasma during the initial stage of the process. At t = 5 msec the current density already depends monotonically on the quantity x. For t > 20 msec a current in the backward direction appears in the surface layer of the plasma; however the magnitude of this current does not exceed 10-15% of the total current. Scanning of the electron temperature likewise is not observed.

An analysis of the dependence of the plasma density on time shows that the neutrals play a noticeable role in the particle balance for $N^0 > 2\cdot 10^9\ \text{cm}^{-3}$. At lower values of N^0 the ionization is comparable with the diffusion only in the surface layer of the plasma.

The curves displayed in Figs. 1 and 2 show that at times t ≈ 10-15 msec a stationary mode is established in the discharge. During this stage the abnormality in the resistance γ is practically constant over the cross section. For t ≈ 10-15 msec, $\gamma \approx 12$, which is in good agreement with the experimental value $\gamma \approx 10$.

Figure 3 shows the dependences of the stationary values τ_E, τ, $T_{e\,max}$, and β_θ on the current I for H = 25, n(0, 0) = 2. In [7] it was established experimentally that τ_E increases along with the current according to a linear law. The curve for τ_E in Fig. 3 provides good substantiation of this dependence. The experimental results for $T_{e\,max}$ from the laser measurements performed in [8] (the dashed curve in Fig. 3) are likewise in agreement with our calculations. The falloff of β_θ with increasing current was observed in a number of experiments.

Figure 4 displays the dependences of τ_E, $T_{e\,max}$, $T_{i\,max}$, and β_θ on the plasma density n for I = 45, H = 25. It is evident that the theoretical values of τ_E are in good agreement with experiments. The behavior of $T_{e\,max}$, $T_{i\,max}$ and the increase in β_θ along with the plasma density likewise reflect the dependences of the experimental data.

Anomalous Ionic Processes

We shall now assume that the energy transfer from electrons to ions and the thermal conductivities of the ions are anomalous with the same abnormality coefficient γ as that associated with the plasma resistance. For this purpose we place $\gamma_1 = 1$, $\gamma_2 = 1$, $\gamma_3 = \gamma = \gamma(\theta)$ in the system (1)-(4). Figure 5 shows the dependences of $T_{e\,max}$, $T_{i\,max}$, and τ_E on time for a discharge having the parameters (9). The experimental

results are plotted by the dashed curves. For comparison purposes the curve $T_{i\,max}$ for the previous model with classical ionic processes and a superanomalous electronic thermal conductivity is given. Let us note first of all the good agreement between theory and experiment for $T_{e\,max}$ and τ_E. The weak spot of the model is the excessively high (approximately by 100 eV) ion temperature. Moreover, the diffusion of the current in the plasma turns out to be retarded, and right up to $t \sim 7$ msec the current distribution is nonmonotonic along the radius. The weak nonmonotonicity at this stage of the discharge is likewise observed in the radial distribution of the electron temperature. Thus, the results of calculations according to the two models differ little. Very detailed experiments are required in order to have a basis for discarding one of the models used and preferring the other model to it.

The authors express deep thanks to L. A. Artsimovich for stating the problem and discussing the results, and likewise to I. N. Golovin, V. S. Strelkov, K. A. Razumova, V. S. Mukhovatov, E. P. Gorbunov, and S. V. Mirnov for numerous counsels and useful discussions.

LITERATURE CITED

1. Yu. N. Dnestrovskii and D. P. Kostomarov, At. Énerg., 29, 434 (1970).
2. Yu. N. Dnestrovskii, D. P. Kostomarov, and N. L. Pavlova, "Energy balance and current diffusion in toroidal plasma installations," Trudy VTs MGU, Moscow (1970).
3. Yu. Dnestrovskii, D. Kostomarov, and N. Pavlova, Fourth European Conference on Thermonuclear Reaction and Plasma Physics, Rome (1970), p. 17.
4. A. A. Galeev and R. Z. Sagdeev, Zh. Éksperim. i Teor. Fiz., 53, 348 (1967).
5. L. M. Kovrizhnykh, Zh. Éksperim. i Teor. Fiz., 56, 877 (1969).
6. L. A. Artsimovich et al., International Conference on Closed Systems [in Russian], Dubna (1969).
7. L. A. Artsimovich et al., Plasma Physics and Controlled Nuclear Fusion Research, Vol. 1, Vienna, IAEA (1969), p. 157.
8. H. Peacock et al., Nature, 224, 448 (1969).

NEUTRON SLOWING-DOWN THEORY IN P_2-APPROXIMATION OF THE METHOD OF SPHERICAL HARMONICS

I. A. Kozachok and V. V. Kulik

UDC 539.125.523

The P_2-approximation has been used to derive a differential equation describing the space-energy distribution of slowed-down neutrons. Boundary conditions are derived in the same approximation.

The following assumptions are assumed valid:

1) the contribution of the third moments and higher-order moments of spherical harmonics in the angular distribution can be neglected;

2) the distribution function varies smoothly with the lethargy u; over an interval of the same order of magnitude as the average logarithmic decrement of the energy ξ, this variation is practically linear, and the relative value is much smaller than unity;

3) cross sections with varying lethargy vary smoothly, and the relative change over an interval of the order of ξ is much smaller than unity. These assumptions are less rigid than similar conditions imposed in neutron-age theory. All of the remaining assumptions entertained in the derivation of the equation are the same as in the neutron-age theory [1].

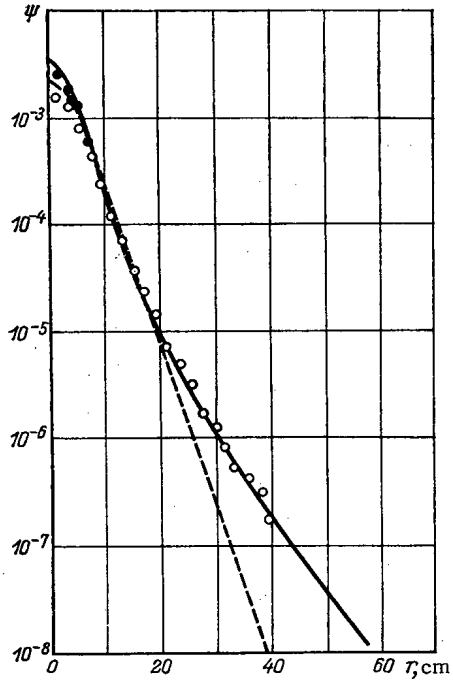

Fig. 1. Experimental data on distribution of U^{235} fission neutrons in water, in the case of a thick converter (○) and thin converter (●): ———) theoretically predicted curve; - - - -) curve plotted in age approximation.

The form of the resulting equation is:

$$\frac{\partial X}{\partial \tau} - \lambda_s^2 \frac{\partial^2 X}{\partial \tau^2} - \Delta X = S(\mathbf{r}, \tau). \tag{1}$$

Here $X(\mathbf{r}, u) = \xi\psi(\mathbf{r}, u)$; ψ is the neutron collision density; τ is the modified age; λ_s^2 is a constant; S is the source function; u is the lethargy.

The boundary conditions on the interface separating media with different slowing-down properties have, in the P_2-approximation, the form

$$\Phi(\mathbf{r}_0, u) + \frac{2}{5}\frac{l_s}{1-f_2^{(0)}}[\operatorname{div}\mathbf{J}(\mathbf{r}, u) - 3\operatorname{grad}_n J_n(\mathbf{r}, u)]_{\mathbf{r}=\mathbf{r}_0} - \text{continuous}$$
$$J_n(\mathbf{r}_0, u) - \text{continuous} \tag{2}$$

Here Φ is the neutron flux; $\mathbf{J}$ is the neutron current; $\mathbf{r} = \mathbf{r}_0$ defines the interface surface; l_s is the neutron free path length; $f_2^{(0)}$ is the zero energy moment of the second harmonic of the scattering function; the subscript n indicates the component of the vector directed normal to the surface.

On the free surface of the medium, we have the boundary condition

$$\Phi(\mathbf{r}_0, u) - 2J_n(\mathbf{r}_0, u) + \frac{1}{4}\frac{l_s}{1-f_2^{(0)}}[\operatorname{div}\mathbf{J}(\mathbf{r}, u) - 3\operatorname{grad}_n J_n(\mathbf{r}, u)]_{\mathbf{r}=\mathbf{r}_0} = 0, \tag{3}$$

where J_n is the component of $\mathbf{J}$ along the external normal.

Translated from Atomnaya Énergiya, Vol. 32, No. 4, pp. 307-308, April, 1972. Original article submitted July 22, 1971; abstract submitted October 5, 1971.

It is shown that the range of validity of Eq. (1) is much broader than that of the age equation. In particular, it constitutes an excellent approximation for the case of hydrogen-containing media.

The results obtained with the aid of Eq. (1) are in excellent agreement with the experimental data.

One illustration of the above is the distribution of neutron collision density plotted in Fig. 1 for a point source of U^{235} fission neutrons slowed-down in water to indium resonance energy, as well as the square of the slowing-down length of the fission neutrons calculated for the same case (26.2 cm^2), for a Po – Be source (57.2 cm^2), and for a Na – Be source (13.0 cm^2).

LITERATURE CITED

1. B. Davison, Neutron Transport Theory [Russian translation], Atomizdat, Moscow (1960).
2. L. N. Yurova, A. A. Polyakov, and A. A. Ignatov, At. Énerg., 12, 151 (1962).

MULTIPARAMETER OPTIMIZATION OF NUCLEAR POWER STATION WITH FLASH DESALINATION FACILITIES

Yu. D. Arsen'ev, Yu. S. Bereza, S. V. Radchenko, and V. A. Chernyaev

UDC 621.039.516.338.4

The advantages of engineering cost optimization in a dimensionless ratio form have been discussed in relation to complex multiparameter problems [1-3]. Two operating programs coded for input to a Minsk-22M (Minsk-32) computer are cited.

The physical interrelations in the controlled plant are approximated by Brandon's method [1, 2] in the first program, which has the following data: maximum number of parameters to be maximized, 10; maximum number of original data points in one parameter, 20; maximum degree of expansion polynomial with respect to parameter, 3.

As a result of computing with this program, all of the physical relations $F_0 \ldots F_m$ can be expressed in matrix form as the product of the Vandermonde's determinant set up from the parameters $|D|$ and the determinant $|B_i|$ set up from the expansion coefficients F_i of the function in question:

$$F_i = j_i c_i |B_i| \cdot |D|,$$

where j_i is the dimensionality index; c_i is the Brandon dimensionless correlation coefficient.

The data obtained with this program are realized as early as in the second engineering costs optimization program, which presents the following data: maximum number of cost components, 10; maximum dimension of matrix of polynomial expansion coefficients, 400.

The overall program utilizes the method of descent by coordinates with several iterations providing the required computational accuracy. The program makes it possible to calculate and print out the base values of dimensionless complexes of the specified structure at intermediary stages in the calculations.

The final formulas for the computations exhibit a rather simple form, are uniform for all the parameters involved, and are written as the minors of the diagonal determinants obtained by multiplying the two determinants $|D| \cdot |B_i|$.

A concrete example of optimization of a dual-purpose nuclear power station with a flash desalination plant is presented in the article. Variables optimized include: the number of evaporator effects (stages),

Translated from Atomnaya Énergiya, Vol. 32, No. 4, p. 308, April, 1972. Abstract submitted June 28, 1971.

the number of brine recycling steps, the temperature of the heating steam, the temperature difference in the condensors of the evaporator effects.

It must be emphasized that the initial salt content of sea water is treated in these calculations in a similar manner as the parameters to be optimized, in a matrix of coefficients for physical relationships. This approach greatly expanded the potentialities of the procedure proposed.

LITERATURE CITED

1. Yu. D. Arsen'ev, S. V. Radchenko, and V. A. Chernyaev, At. Énerg., 28, 418 (1970).
2. Yu. D. Arsen'ev and G. A. Moskvicheva, Teploénergetika, No. 428 (1971).
3. O. O. Kazachkovskii et al., At. Énerg., 27, 183 (1969).

PSEUDOBLIND STARTUP OF NUCLEAR REACTOR

B. G. Volik, T. A. Gladkova, and G. L. Polyak

UDC 621.039.514.2

Methods for starting up a reactor automatically [1] are based on the fact that information on reactor power level and period are available continuously from the instant the startup commences. Under real conditions, however, a power drop to below the level corresponding to the sensitivity of the measuring equipment is possible in a shutdown reactor by the time the startup is initiated, and this is equivalent to a break in the startup controls feedback loop. That brings up the question of how to determine the parameters of the controller so that the reactor can be started up from any initial state without activating the reator protection system. The startup process may consist of startup stages with and without feedback. Such a process is classified as a pseudoblind startup process [2-4]. The article centers its attention on investigation of the first stage,* where the problem reduces to minimizing the allowable rate of continuous rod travel which will bring the sensitivity of equipment up to rated level, with period T_{sens}, which will not be greater than the setting of the reactor protection system (or the total reactivity ρ_{sens}) when the depth of subcriticality ρ_0, the differential weight of the rods $d\rho/dx$, and the intensity of extraneous neutron sources S are all unknown.

The article also analyzes the process taking place at the instant the feedback loop of the startup controller closes. The results of the investigation are as follows.

1. The reactor subcriticality ρ_0 at constant reactivity insertion rate has practically no effect on the value of T_{sens} and ρ_{sens}; only the startup time depends on the subcriticality.
2. The rate of reactivity insertion $d\rho/d\tau$ exerts a substantial influence on the values of T_{sens} and ρ_{sens}. When the reactivity is used as the controlled variable, the probability that the process will be resumed when the feedback loop is restored becomes much greater.
3. The intensity of the neutron sources exerts a great influence on the first stage, so that forecasting the minimum value of S before each startup operation is an important contribution to increasing the probability that the process will be resumed.

We can draw the following inferences from the above.

1. The automatic startup controller can be used, with continuous advance of the control rods, to bring about reactor startup from any initial state (including when the initial power level is below the level

*The second stage has been studied quite exhaustively in references [1, 5, 6].

Translated from Atomnaya Energiya, Vol. 32, No. 4, pp. 308-309, April, 1972. Original article submitted June 1, 1971; abstract submitted December 2, 1971.

corresponding to the sensitivity of the measuring equipment) when the signal at the controller output is limited in some manner to determine the reactivity insertion rate.

2. The reactivity should be used as the controlled variable and the reactor protection parameter, in preference to the reactor period.

3. The probability that the process will be resumed when the level is crossed can be enhanced by using the rate of positive reactivity insertion.

LITERATURE CITED

1. M. Schultz, Control of Nuclear Reactors and Power Plants [Russian translation], IL, Moscow (1957).
2. I. Furet and I. Pupponi, Report P-80 (France) submitted to III Geneva Conference, 1964.
3. N. Filipczak et al., "Report of blind experiments of the Cabri Reactor on July 4-8, 1966," ORNL-tr-1938, CEA-R3341.
4. W. Filipczak and N. Filipczak, "Structure of 'Maxtrel' nuclear reactor protection and control system," Conference on Reactor Physics and Engineering, Prague (1963).
5. P. I. Popov, "Analysis of some automatic nuclear reactor startup systems," in: Automatic Control and Telemechanics, No. 1 [in Russian], Gosatomizdat, Moscow (1960).
6. B. G. Volik, N. A. Dolginova, and M. M. Solov'ev, At. Énerg., 23, 223 (1967).

REDISTRIBUTION OF FUEL IN IRRADIATED DISPERSION TYPE FUEL ELEMENTS

L. M. Tuchnin and E. F. Davydov

UDC 621.039.548

Dispersion type fuel elements constitute multicomponent systems whose components usually contrast noticeably in their physical properties, which can become, under irradiation, a cause of redistribution of the components of the fuel meat [1] resulting in critical changes in the heat-transfer characteristics of the fuel elements.

The article describes the observed post-irradiation fuel redistribution over the transverse cross section of dispersion type fuel elements. Three plate fuel elements clad with zirconium alloy and UO_2 dispersed in a zirconium matrix as meat, with virtually zero porosity, were irradiated in an SM-2 reactor at a maximum cladding temperature ~300°C. One of the fuel elements failed at burnup 0.09 g·fragments/cm^3.

Investigation of the structure revealed that appreciable redistribution of the fuel core components had occurred at the site of failure and in the immediate vicinity. Fuel particles at the center of the fuel element had become fused into a solid mass with infrequent inclusions of matrix material; separate particles of fuel located some distance from the center were found combined into small conglomerates with appreciable sticking of fused particles to each other. A zone consisting practically of matrix alone formed alongside the cladding, particularly at the side ribs of the fuel-element plate.

Clearly, it is possible for fuel particles to become displaced relative to one another and to move toward the center of the fuel element, in the case of a solid-state dispersion system, as a result of appreciable thermal stresses existing around the fuel particles, and in the presence of temperature gradients, resulting in local changes in the plastic properties of the fuel-element matrix [2].

Translated from Atomnaya Énergiya, Vol. 32, No. 4, p. 309, April, 1972. Original article submitted February 16, 1971; abstract submitted August 19, 1971.

LITERATURE CITED

1. O. O'Royle and F. Brown, J. Nucl. Materials, 29, 27 (1969).
2. A. G. Samoilov et al., Dispersion Type Fuel Elements [in Russian], Atomizdat, Moscow (1965).

THE NEUTRON RADIATION OF $Pu^{238}O_2$ CONTAINING DIFFERENT AMOUNTS OF O^{18}

V. A. Arkhipov, G. V. Gorshkov,
B. S. Grebenskii, B. A. Mikhailov,
V. V. Fedorov, S. P. Khormushko,
and A. A. Chaikhorskii

UDC 539.125.5.164.03:546.799.4

In this study the authors investigated the yield and spectral composition of the neutron radiation of $Pu^{238}O_2$ sources containing different amounts of the isotope O^{18}. The neutron yield was determined by means of an all-wave counter. Measurement of the yields for higher and lower O^{18} content in the $Pu^{238}O_2$ showed that the main contribution to the yield is made by the neutrons formed in the $O^{18}(\alpha, n)Ne^{21}$ reaction. The total neutron yield from the investigated $Pu^{238}O_2$ specimen containing oxygen isotopes in natural proportions was $(2.0 \pm 0.1) \cdot 10^4$ neutrons/sec per gram of Pu^{238}, and the yield of neutrons from the (α, n) reaction involving O^{18} is $1.4 \cdot 10^4$ neutrons/sec per gram of Pu^{238}.

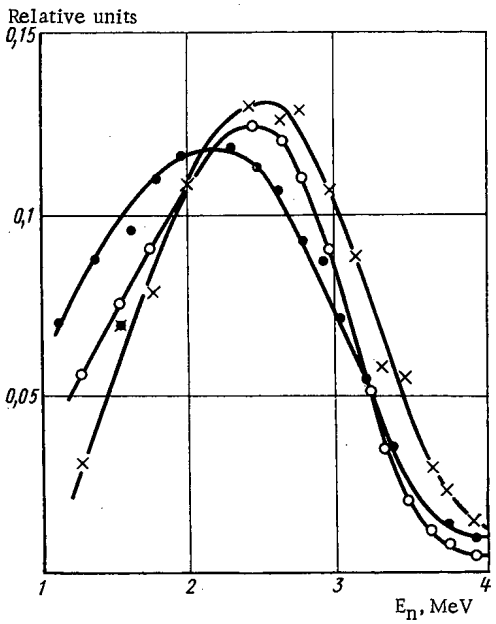

Fig. 1. Spectra of neutrons from $Pu^{238}O_2$ containing different amounts of O^{18}: ○) natural oxygen composition; ×) O^{18} enrichment; ●) O^{18} depletion.

The total neutron yield consists of the neutrons formed in the (α, n) reaction involving O^{18}, the neutrons resulting from spontaneous fission of Pu^{238} ($2.8 \cdot 10^3$ neutrons/sec per gram of Pu^{238}), and the neutrons formed in (α, n) reactions involving light impurity elements (for the specimen under investigation the value was $3.2 \cdot 10^3$ neutrons/sec per gram of Pu^{238}).

The fast-neutron spectra were measured with a single-crystal scintillation spectrometer using a stilbene crystal with discrimination of γ-quanta on the basis of their release time. Figure 1 shows the spectra of neutrons from a $Pu^{238}O_2$ source with a natural O^{18} content, a source which had been enriched in O^{18} to a value of 1%, and a source in which the O^{18} had been depleted to 0.02%. The spectra from the source with a natural O^{18} content and from the enriched source differ only slightly, with the neutrons from the enriched source displaced toward higher energies. The maxima of the spectra occur at approximately 2.5 MeV. The fact that the neutron radiation is more intense in the low-energy range for the source with a natural O^{18} content is attributable to the contribution made to its yield by neutrons from the spontaneous fission of Pu^{238} and by the "impurity" neutrons (for the enriched source this is very low).

Translated from Atomnaya Énergiya, Vol. 32, No. 4, p. 310, April, 1972. Original article submitted July 19, 1971; abstract submitted November 22, 1971.

Both of the spectra are in satisfactory agreement with the data of [1, 2]. The spectrum of the depleted source differs considerably from the other two spectra (especially in the low-energy region) because of the contribution made to the total neutron yield by the spontaneous-fission neutrons and by the neutrons formed in the (α, n) reaction involving the impurities. This contribution will be greater than the contribution made by the neutrons from the (α, n) reaction involving the O^{18}. The spectrum of the depleted source has a maximum at an energy of 2.3 MeV.

LITERATURE CITED

1. T. Herold, Nucl. Applications, 4, 19 (1968).
2. M. Anderson, Trans. Amer. Nucl. Soc., 9, 600 (1966).

MAGNETIC SYSTEMS FOR THE TRANSPORT AND ACCUMULATION OF SLOW NEUTRONS

I. M. Matora and O. A. Strelina

UDC 539.125.5.172

Vladimirskii [1] considered the motion of slow neutrons in the magnetic fields of multipole devices and indicated that cold neutrons could be transported and stored in magnetic systems of this type. A more detailed study of such systems shows that the most interesting among them are the neutron-optical systems using six pole magnets. These have the important characteristic that the neutrons with a given energy that are focused at the same time in both transverse directions have the same period of oscillation for all amplitudes.

In a straight horizontal neutron guide with a six-pole magnetic arrangement and in an annular horizontal accumulator using a six-pole magnet there is a single horizontal equilibrium plane for the neutrons being focused. It is displaced from the horizontal plane of symmetry of the six-pole device downward by a distance independent of the neutron energy and equal to $h = mg/2A\mu$ (using the notation of [2]). The equilibrium trajectory of the neutrons being focused in a straight horizontal neutron guide is a straight line lying at the intersection of the aforementioned plane and a vertical plane passing through the axis of symmetry of the field. In the case of an annular accumulator the circular equilibrium orbits are situated only on the outside of a cylinder whose circular base has a radius of R, equal to the distance from the center of the annulus to the center of symmetry of the cross section of the magnet, and accumulation for neutrons is possible in the energy range $0 \leq W \leq A\mu(R + a)a$, where a is the semiaperture of the magnet.

The study gives the formulas necessary for calculating the motion and intensity of the neutrons.

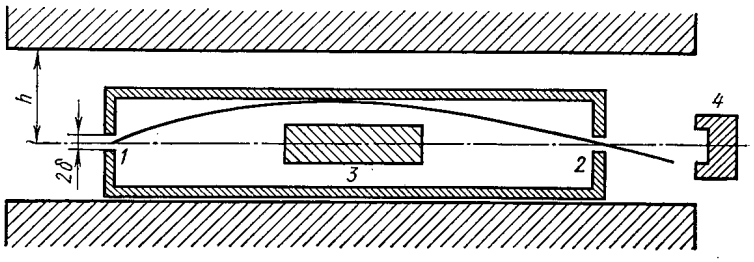

Fig. 1. Diagram of magnetic neutron guide.

Translated from Atomnaya Énergiya, Vol. 32, No. 4, pp. 310-311, April, 1972. Original article submitted July 5, 1971; abstract submitted December 2, 1971.

The article also proposes an experiment for determining the gravitational acceleration of a neutron polarized along the vertical and conversely, with an accuracy at least one order of magnitude better than in [3]. The idea of the experiment is the following. Suppose that in a straight horizontal magnetic neutron guide (see Fig. 1) with six-pole field symmetry, we make two slits 1 and 2, each having a total width of 2δ, near the inlet and outlet ends of the guide. Suppose also that the plane of symmetry passing through the middle of the slits is horizontal, i.e., that its distance from the axis of the six-pole device is constant. Furthermore, let us place between these slits a shield 3, which is not penetrable to any radiation (including neutrons) rectilinearly propagated from slit 1. Then a slow-neutron detector 4 placed at the exit from slit 2 will fix a sharp counting maximum at the unique value of the magnet excitation current when the said plane of symmetry of the slits is an optical plane, and the vertical component of the gradient of the field is equal [2] to

$$G_y = 2Ah = \frac{mg}{\mu} = G_{\text{equiv}} \simeq 170 \text{ e/cm}.$$

It can be seen from this that both G_y and $g_{\downarrow\uparrow}$ can be measured with a relative accuracy of $\delta/2h$.

LITERATURE CITED

1. V. V. Vladimirskii, Zh. Éksp. Teor. Fiz., 39, 1062 (1960).
2. I. M. Matora, At. Énerg., 27, 71 (1969).
3. J. Dabbs et al., Phys. Rev., 139b, 756 (1965).

THERMODYNAMICS OF FORMATION OF PLUTONIUM TRICHLORIDE IN A FUSED POTASSIUM CHLORIDE MEDIUM

M. V. Smirnov, V. I. Silin, and O. S. Skiba

UDC 541.135:546.799.4

The equations for the isotherms of a plutonium electrode potential with respect to the chloride electrode in a fused KCl medium at temperatures of 810, 844, and 870°C in the concentration range 0.64-15.2 wt. % are obtained from the measurements of equilibrium emf of the galvanic cell $Pu_l | PuCl_3 - KCl_{fus} | KCl_l | Cl_{2(g)}, C_s$. The temperature dependence of the apparent standard potential of the plutonium electrode is deduced from these equations: $E^*_{Pu^{3+}/Pu} = -3.765 + 10.8 \cdot 10^{-4} T$, V.

The change in the partial Gibbs molar free energy during the formation of plutonium trichloride in sodium chloride according to the reaction $Pu_l + 3/2Cl_{2(g)} = PuCl_{3fus}$ is of the form

$$\Delta\bar{G}^*_{PuCl_3(fus)} = 3F \cdot E^*_{Pu^{3+}/Pu} = -260500 + 74.7 \cdot T, \text{cal/mol}.$$

Thus the partial molar enthalpy of formation of $PuCl_3$ in a fused KCl medium in the temperature range 1083-1143°K is $\Delta\bar{H}^*_{PuCl_3} = -260.5$ kcal/mole, and the apparent partial entropy of the reaction is $\Delta\bar{S}^*_{PuCl_3(fus)} = -74.7$ cal/deg · mole.

The heat and the entropy of the interaction of $PuCl_3$ in a mixture with fused sodium chloride are estimated; these are found to be equal to: $\Delta H_{PuCl_3} = -48.3$ kcal/mole, $\Delta S_{PuCl_3} = -40.7$ cal/deg · mole.

It is shown that the partial enthalpy of formation of $PuCl_3$ in chlorides of alkali metals increases in proportion to the increase in the radius of the salt-solvent cation.

Translated from Atomnaya Énergiya, Vol. 32, No. 4, p. 311, April, 1972. Original article submitted August 24, 1971.

EFFECT OF OXIDATION ON STRENGTH CHARACTERISTICS OF GRAPHITE

E. I. Kurolenkin, N. S. Burdakov,
Yu. S. Virgil'ev, V. S. Ostrovskii,
V. N. Turdakov, and Yu. S. Churilov

UDC 621.039.53

The graphite stack of nuclear reactors is subjected to inevitable corrosion and erosion disintegration, which affects the period of its service [1].

The rate of oxidation is determined by a number of factors (the nature of the raw material used and its granulometric composition, thermal treatment, etc.), and during its use in nuclear reactors by the conditions of irradiation, i.e., the dose and the temperature. The pore structure of the graphite [2], its strength [3], electrical and thermal conductivities [4], gas permeability, etc. undergo changes.

In the present work the effect of the degree of oxidation on the change in the limiting compressive strength and on the change of the volumetric weight characterizing the strength is investigated for two industrial marks of construction graphite, GMZ and MPG types.

The investigations have been carried out on cylindrical ($\phi 8 \times 80$ mm) graphite samples which get oxidized in tubular electric furnace at 700°C in atmospheric air. The degree of oxidation is determined from the loss in the weight of the sample. The nature of the effect of oxidation on the change of the strength and volume weight for both original and irradiated graphite materials is illustrated in Fig. 1.

The decrease in the yield point and the volume weight of graphite with the change in the degree of oxidation occurs due to the development of porosity; in fine-grain materials of type MPG the process of oxidation occurs more intensely. The change in the pore structure of graphite due to oxidation is studied by the method of small-angle scattering [5]. It is shown that the change in the specific surface of the pores is at first due to burning up of the couplings, and later (for more than 10% oxidation), when the filtration coefficient increases sharply, also due to burning up of the fillings.

It is found that at oxidation temperature of 600-800°C the decrease in the volumetric weight occurs mainly in the surface layer. This agrees with the two-stage mechanism of oxidation of graphite [6], showing in this temperature range the process is intermediate between the kinetic (volume oxidation) and the diffusion processes.

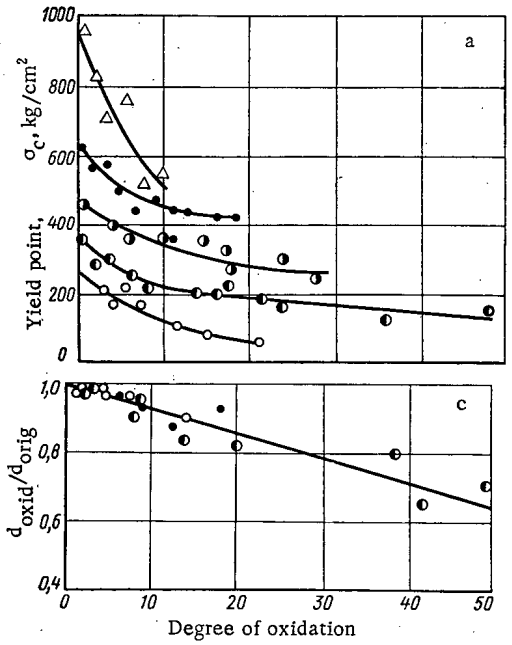

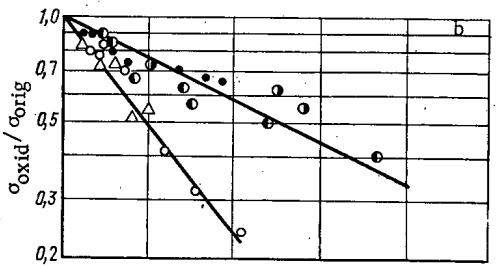

Fig. 1. Dependence of strength (a, b) and volumetric weight (c) of graphite GMZ on degree of oxidation (in air at 700°C) before (○) and after (●) irradiation at 300°C by an integral flux of 10^{21} neutron/cm^2; MPG graphite (△); for natural graphite (○).

Translated from Atomnaya Energiya, Vol. 32, No. 4, p. 312, April, 1972. Original article submitted April 12, 1971.

Empirical relationships, connecting the change in the compressive strength of the graphite and the volumetric weight with the degree of oxidation, are given.

LITERATURE CITED

1. R. V. Moore, H. Kronberger, and L. Grainger, II Geneva Conference (1958), Paper No. 312.
2. I. Watt and R. Franklin, 1st Geneva Conference on Ind. Carbon and Graphite, Pergamon Press, New York (1956), p. 321.
3. A. Collins et al., J. Nucl. Mater., 15, 135 (1965).
4. J. Rounthwaite, G. Lyons, and R. Snowdon, 2nd Conference on Ind. Carbon and Graphite, Pergamon Press, New York (1956), p. 299.
5. E. I. Kurolenkin, Yu. S. Virgil'ev, and Yu. S. Churilov, Zh. Neorgan. Mater., 8, 80 (1972).
6. G. M. Volkov and T. V. Kotova, in: Graphite Constructional Materials, No. 4, Metallurgiya, Moscow (1969), p. 80.

THE EQUATION OF STATE OF URANIUM HEXAFLUORIDE OVER A WIDE RANGE OF PARAMETERS

V. V. Malyshev

UDC 533.12

A method using a constant-volume piezometer was applied to the experimental investigation of the compressibility of uranium hexafluoride (UF_6) with the density varying up to 3.417 g/cm^3 at intervals of ~0.1 g/cm^3 and the temperature varying from 364 to 592.2°K with intervals of ~10°K for the gas and ~5°K for the liquid, with the pressure varying up to 242 bar. The errors in measurement were less than 0.1-0.2% for the pressure, 0.05-0.13% for the density, and 0.07°K for the temperature. A special method was applied to remove the hydrogen fluoride from the uranium hexafluoride, and as a result the hydrogen fluoride content of the product investigated was less than 0.002%.

The liquid – vapor equilibrium region was investigated. The experimental data for the pressure of the saturated vapor P_s, the equilibrium density of the vapor ρ_v, and the equilibrium density of the liquid ρ_{liq} were approximated, respectively, by the following equations:

$$\lg P_s\,(\text{bar}) = 10.5488 - 2344.4/T - 0.013624T + 1.0347\cdot 10^{-5}T^2; \quad (1)$$

$$\rho_v\,(\text{g/cm}^3) = 1.369 - 0.2826\Theta - 0.0211\Theta^2 + 0.0503\Theta^3; \quad (2)$$

$$\rho_{liq}\,(\text{g/cm}^3) = 1.369 + 0.0616\Theta + 0.2757\Theta^2 + 0.09975\Theta^3 + 0.01677\Theta^4 - 0.00102\Theta^5, \quad (3)$$

where

TABLE 1. Values of the Coefficients b_{mk}

Value of m	Value of k				
	0	1	2	3	4
1	18,295	−53,108	50,313	−16,690	
2	−41,084	92,104	−34,541	−39,884	2,368
3	133,936	−400,153	394,801	−127,996	
4	−101,408	308,826	−311,388	103,431	
5	25,155	−74,139	75,528	−25,397	

TABLE 2. Values of the Coefficient B

$T°$, K	$-B$, cm^3/g	$T°$, K	$-B$, cm^3/g	$T°$, K	$-B$, cm^3/g
463,3	1,036	507,9	0,841	552,5	0,675
473,2	0,983	512,9	0,832	562,5	0,626
483,2	0,939	522,8	0,794	572,4	0,608
493,0	0,892	532,8	0,763	582,3	0,561
502,9	0,862	542,6	0,724	592,2	0,533

Translated from Atomnaya Énergiya, Vol. 32, No. 4, p. 313, April, 1972. Original article submitted June 1, 1971; abstract submitted October 25, 1971.

$$\Theta = (504.5 - T)^{1/3}.$$

Equation (1) describes the experimental data with an error of less than 0.3% in the 364.0-504.5°K temperature range, Eq. (2) with an error of 0.5% in the 403.7-504.5°K range, and Eq. (3) with an error of 0.2% in the 372.6-504.5°K range.

The critical parameters of UF_6, as determined from the expressions (1)-(3), take on the following values: $\rho_c = 1.369 \pm 0.005$ g/cm^3, $T_c = 504.5 \pm 0.2$°K, $P_c = 46.0 \pm 0.1$ bar, $S_c = \rho_c T_c R_\mu / P_c = 3.55 \pm 0.02$, where $R_\mu = R/\mu$.

The values of the heat of vaporization, calculated from the Clapeyron – Clausius equation by using the relations (1) and (3), were approximated by Tiezen's formula $r(kJ/kg) = 128(1-\tau)^{0.406}$ with an error of 1.1%, where $\tau = T/T_c$.

An analytical expression was obtained for the equation of state of UF_6 in the form of a fifth-degree interpolation polynomial which had the following form for the parameters mentioned:

$$\frac{\pi\varphi}{\tau} = 3.55\left[1 + \sum_c \sum_m b_{mc}/\tau^c \varphi^m\right], \quad (4)$$

where $\pi = P/P_c$, $\tau = T/T_c$, $\varphi = \rho_c/\rho$, and the values of the 21 coefficients b_{mk} are given in Table 1.

Equation (4) describes the experimental data with an error of 0.2-0.3% over the entire range of existence of the superheated vapor ($\rho \leq 1.4$ g/cm^3) and not more than 1% for UF_6 densities of up to 2.8 g/cm^3.

The values of the second virial coefficient B for UF_6 as a function of temperature are given in Table 2.

The intermolecular parameters of UF_6, as calculated from the force constants of the Lennard – Jones potential (12-6), have the following values: $\varepsilon/k = 258 \pm 6$°K, $b_0 = 452 \pm 14$ cm^3/mole, $\sigma = 7.10 \pm 0.06$ Å.

EXPERIMENTAL STUDY OF THE PERFORMANCE OF THE RG-1M GEOLOGICAL RESEARCH REACTOR

V. I. Alekseev, A. M. Benevolenskii,
V. V. Kovalenko, O. E. Kolyaskin,
L. V. Konstantinov, V. A. Nikolaev
V. F. Sachkov, and A. M. Shchetinin

UDC 621.039.524.44

The RG-1M geological research reactor, with a thermal power rating of 30 kW, was started up in April, 1970. The fuel was 10% enriched uranium dioxide, with desalinated water as moderator and coolant.

Ten vertical experimental channels are inserted in the reactor, one of them equipped with a pneumatic shuttle. In contrast to the RG-1 reactor of similar design and 5 kW rating [1], the thermal power rating of the RG-1M reactor was brought up to 30 kW, which necessitated a change in the coolant temperature control system.

TABLE 1. Thermal Flux and γ-Radiation Dose Rate in Experimental Devices

Experimental device	TsEK	VÉK-1	VÉK-2	VÉK-3	VÉK-4	VÉK-5	VÉK-6	VÉK-7	VÉK-8	Channel in
Thermal flux, $\phi \cdot 10^{-11}$, neutrons/cm^2·sec	8,0	5,5	2,6	2,6	2,8	2,6	—	3,0	1,2	5,8
γ-Radiation dose rate, $P \cdot 10^{-6}$, r/h	10	2,5	1,8	1,8	—	1,8	—	2,2	0,7	—

Heat is extracted from the core of the RG-1M reactor with the aid of a heat exchanger presenting a heat removal surface area of 2.5 m^2, installed in parallel with the distillate purification system. Coolant flow through the heat exchanger is 8 m^3.

The results of experiments characterizing the experimental capabilities of the reactor system, obtained during the startup and initial period of operation of the reactor, are cited below.

Figure 1 shows a diagram of the core fueling and arrangement of the reactor experimental devices. The

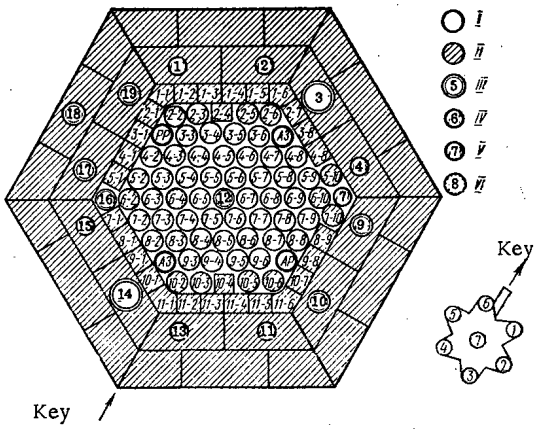

Fig. 1. Core loading diagram: I) fuel assembly; II) graphite; III) vertical experimental channel; IV) ionization chamber channel; V) pneumatic shuttle channel; VI) photoneutron source; 1) NK-1; 2) IK-2; 3) V-4; 4) IK-3; 5) V; 6) IK; 7) PP; 8) B-4; 9) V-5; 10) V-6; 11) IK-4; 12) TsEK; 13) IK-5; 14) V-7; 15) IK-6; 16) V-1; 17) V-2; 18) V-8; 19) V-3.

Translated from Atomnaya Energiya, Vol. 32, No. 4, pp. 315-316, April, 1962. Original article submitted May 11, 1971.

fuel charge consists of 40 fuel assemblies (2.37 kg U^{235}), 40 graphite push rods, and a single beryllium unit for the photoneutron source. The controlled reactivity margin of the system, with experimental devices not filled up, is 0.7 β_{eff}.

The total effectiveness of the two scram rods is 1.9 β_{eff}. System subcriticality with the two scram rods fully inserted into the core, and other control components fully inserted into the core, is 3.2 β_{eff}. Filling the other experimental devices with water has practically no effect on system reactivity.

Table 1 indicates values of the thermal flux and γ-radiation dose rate in the reactor experimental devices at the level of the core center, referred to the reactor power rating (30 kW).

In the experimental arrangements of the reactor, the thermal neutron fluxes were determied by measuring the absolute activity of gold indicators (to a relative error of 8%) by the $\beta-\gamma$ coincidence method; the dose rate of the γ-radiation was measured to a relative error of 10%.

The biological shielding of the RG-1M reactor, when the reactor is operating at 30 kW output, makes for a safe radiation environment in the reactor hall and in all the rooms adjacent to the reactor room.

The unclad fuel assemblies [2] and graphite push rods used in the RG-1M reactor make it possible to set up different core and reflector configurations while the reactor is in operation. It should also be noted that, if necessary, the number of experimental channels provided with a pneumatic shuttle system for feeding specimens to the core and reflector can be increased. This does not mean any basic design limitations, nor any limitations from the standpoint of nuclear and radiation safety in the RG-1M reactor and environs.

Operating experience has shown that the cooling system of the RG-1M reactor has important reserves, which can be utilized in principle to increase the reactor power output to 100-120 kW with no essential changes in the working core loading.

LITERATURE CITED

1. Yu. M. Bulkin et al., At. Énerg., 21, 319 (1966).
2. Yu. M. Bulkin et al., Nuclear Research Reactor [in Russian], Avt. Svid. No. 227939, July 12, 1968.

SURFACE CONTAMINATION OF VVR-M FUEL ELEMENTS BY FISSIONABLE MATERIAL AND ITS CONTRIBUTION TO THE FRAGMENT ACTIVITY OF THE COOLANT

N. G. Badanina, K. A. Konoplev, and Yu. P. Saikov

UDC 621.039.548.535

One of the possible sources of the fission fragment activity of a reactor coolant is the contamination of the fuel element cladding by nuclear fuel during the manufacturing process. Under ordinary conditions of fuel element fabrication a contamination of up to 10^{-8} g U/cm^2 is tolerated [1]. A VVR-M fuel assembly consists of three fuel elements in the form of concentric tubes (the outer being hexagonal) clad with 0.9 mm of aluminum for a total tube thickness of 2.5 mm.

The surface contamination of the fuel elements for the reactor at the A. F. Ioffe Physicotechnical Institute of the Academy of Sciences of the USSR was studied by using track detectors to record the fission fragments formed under neutron bombardment [2]. By varying the integrated neutron flux this method can be used to determine surface concentrations of uranium from trace amounts in clean structural materials to pure nuclear fuel. By using an integrated neutron flux at $\sim 10^{12}$ neutrons/cm^2 surface concentrations of 10^{-11}-10^{-6} g U^{235}/cm^2 can be measured, with the error reaching ±70% at the limits of the interval. This method of studying surface contamination has the great advantage of permitting the determination of the spatial distribution of uranium. This can be useful in revealing the causes of contamination in the fuel element fabrication process.

The recording of fission fragments by track detectors is based on the fact that a fission fragment leaves a defective region (track) which under selective etching becomes visible under a microscope. Dacron was chosen as a detector material since it is convenient to use on surfaces of complicated configuration and the technology of its manufacture eliminates the presence of heavy elements; i.e., it is a detector practically free of background [3].

The outer surfaces of the hexagonal fuel elements were examined for surface contamination.

A standard with a known amount of U^{235} uniformly spread over an area 1 × 1 cm was attached to each face of a fuel element. The surface of the fuel element was then covered tightly with dacron 30 μ thick. The fuel element was then irradiated in a horizontal channel of the VVR-M reactor in a special device which permitted vertical displacements of the fuel element to achieve uniform irradiation over its whole height.

The fuel element was irradiated for 12-16 h in a thermal neutron flux of $(1\text{-}2) \cdot 10^7$ neutrons/cm^2·sec. After irradiation the dacron film was etched in a 40% solution of KOH at t = 60°C for 2.5 h and then washed in water and dried. This etching procedure eliminates the recording of α-particles, as was confirmed by irradiation with 5 MeV α-particles.

Tracks were counted with a 90 power microscope. The U^{235} surface contamination was computed from

$$\rho = \frac{N \cdot m}{N_1} \text{ g } U^{235}/\text{cm}^2,$$

where N and N_1 are respectively the number of tracks on the detector taken from the fuel element area of interest and the standard; m is the U^{235} content of the standard. The standard usually employed has a U^{235} content of $\sim 10^{-10}$ g/cm^2.

The experimental error in determining the U^{235} surface contamination of a fuel element from the results of a two-stage irradiation of a single fuel element was 40%. The error is made up mainly of the

Translated from Atomnaya Énergiya, Vol. 32, No. 4, pp. 316-318, April, 1972. Original article submitted May 18, 1971; revision submitted July 21, 1971.

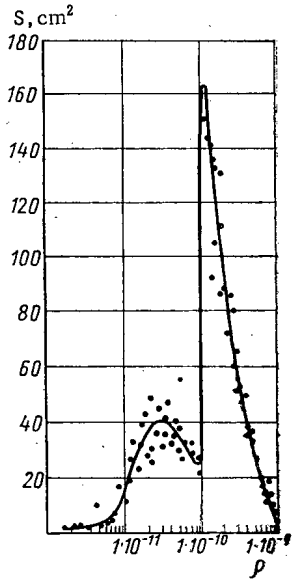

Fig. 1

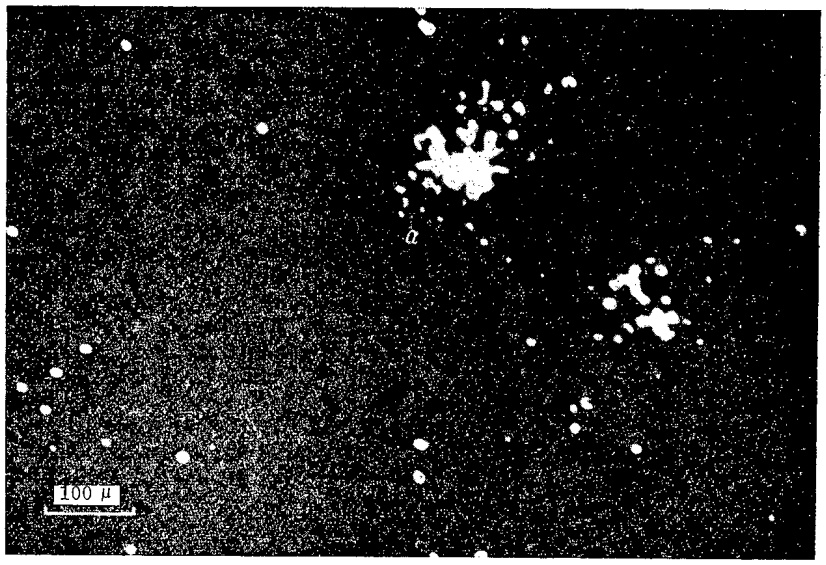

Fig. 2

Fig. 1. Surface area S having a contamination of ρ g U^{235}/cm^2.

Fig. 2. View of a portion of a contaminated fuel element appearing on the detector in the field of view of the microscope (a is an anomalous part).

subjective error in counting tracks, the error due to the nonuniformity of the neutron flux, the statistical error, and the error in determining U^{235} in disseminations.

After all the interesting area of the detector film (5923 cm^2) was counted, a graph was plotted (Fig. 1) showing the area having a given contamination. A surface concentration of uranium in the 10^{-11}–10^{-10} g U^{235}/cm^2 range is explained by the presence of uranium in the cladding material.

The U^{235} surface contamination found in a specimen of the aluminum alloy going into the manufacture of fuel elements was $2.7 \cdot 10^{-11}$ g/cm^2, which corresponds to a natural uranium content in structural materials of 10^{-6} g/g [1].

Sixty-five percent of the fuel element area examined had a rather uniform contamination over the 10^{-10}–10^{-9} g U^{235}/cm^2 range.

The portions with a U^{235} content of more than 10^{-9} g/cm^2 were considered anomalous and apparently arose from microdisseminations of uranium in aluminum. The α-spectrum of one such portion showed that the microdisseminations involved uranium enriched in U^{235}. On the average 20% of the U^{235} on the fuel element surfaces examined was on these anomalous parts, although they occupy an area of only 3.74 cm^2, which is 0.072% of the total area examined. The frequency of occurrence of disseminations, defined as the ratio of the number of anomalous portions observed to the whole fuel element area examined, is 0.05 cm^{-2}. This implies that on the average there is one dissemination for each 20 cm^2 of area. Figure 2 shows one contaminated portion of a fuel element appearing on the detector in the field of view of the microscope.

To determine how strongly the contamination was fixed to the surface we rubbed the fuel assembly with a piece of wet cloth. Measurements of the surface contamination before and after rubbing showed that on the average 70% of the U^{235} in the dissemination was smeared over the surface. This was particularly clear on the parts with a large U^{235} content (over 10^{-7} g/cm^2).

In spite of the fact that smearing out and transport of contamination were observed, the change in surface contamination produced by rubbing the fuel elements was within the limits of experimental error.

The average value of the surface contamination was determined from the histograms in Fig. 1 by

$$\bar{\rho} = \sum_{i=1}^{n} \rho_i \frac{S_i}{S_n},$$

where S_i is the area occupied by the contamination ρ_i, and S_n is the total area examined. The average value of the surface contamination of the fuel elements was $(3.3 \pm 1) \cdot 10^{-10}$ g U^{235}/cm^2, where the deviation is mean square.

The contribution of the surface contamination of the fuel elements to the fragment activity of the coolant was calculated by determining the equivalent U^{235} content (P_{eq}, g/cm^2) by the relation

$$B = \frac{a\rho}{P_{eq}},$$

where the coefficient $a = 0.5 - 1$ takes account of the fact that some of the fragments may enter the fuel elements rather than the coolant. The quantity P_{eq} is used to characterize the fragment activity of the water in the primary loop and is determined from its rate of increase, which is a quantity equivalent to the U^{235} content on the fuel element surface when all the fragments enter the coolant [4].

The quantity P_{eq} was determined from the radiochemical analysis of the VVR-M primary loop water for the sum of the isotopes of iodine, strontium, and barium during 1970; it varied from $9 \cdot 10^{-9}$ to $2 \cdot 10^{-9}$ g U^{235}/cm^2 from run to run. The average value of the equivalent U^{235} content during the year was $6 \cdot 10^{-9}$ g U^{235}/cm^2.

The contribution of surface contamination to the fragment activity of the coolant, determined from the average value of the equivalent U^{235} content during 1970, was $3 \pm 1\%$ for $a = 0.5$.

In conclusion the authors thank D. M. Kaminker, I. G. Berzina, G. Ya. Vasil'ev, and V. A. Perelygin for their support and assistance in the work.

LITERATURE CITED

1. V. I. Polikarpov et al., Checking the Tightness of Fuel Elements [in Russian], Gosatomizdat, Moscow (1962).
2. P. Price and R. Walker, Appl. Phys. Lett., 2, 23 (1963).
3. I. G. Berzina et al., At. Énerg., 23, 520 (1967).
4. N. G. Badanina and Yu. P. Saikov, ibid., 24, 429 (1968).

EQUIPMENT FOR STUDY OF MIGRATION OF RADIOACTIVE PRODUCTS ALONG THE CROSS SECTION OF FUEL ELEMENT

A. V. Sukhikh, V. K. Shashurin,
E. F. Davydov, and M. I. Krapivin

UDC 621.039.548

The methods of γ-spectrometry using semiconductor detectors are well adapted to the investigation of fuel elements after irradiation. A further development of these methods is γ-scanning of the diameter of the fuel element [1-2].

The study of migration of fusion fragments in thermal compositions at different thermal loads, the distribution of the fissionable isotopes along the diameter of the fuel element, experiments for detection of probable transfer of elements of the shell into the fuel, determination of the boundary of the fused zone from the distribution of high-melting fission fragments in ceramic fuel elements are some of the problems that can be solved with the use of spectrometric scanning of a section of the fuel element.

The equipment for the investigation of the processes of migration of radioactive isotopes along the radius of the fuel elements consists of a mechanism for shifting a section of the fuel element in front of the aperture of the collimator and a γ-spectrometer.

The mechanism for the displacement of the section (Fig. 1) is a coordinate stand in a B-50 type box. The displacements along the horizontal and vertical planes is read with indicators with 0.01 mm divisions. The section is displaced relative to a changeable lead collimator 300 mm in length. The diameter of the collimator aperture can be changed from 0.25 to 1 mm.

A semiconductor γ-spectrometer with Ge(Li)-detector is placed on the side of the front wall of the box around the collimator. In order to reduce the γ-background the detector is surrounded by a 50 mm thick layer of lead.

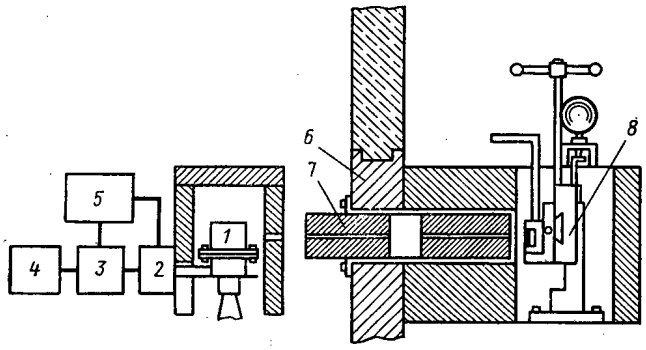

Fig. 1. Block diagram of the equipment for γ-scanning of the fuel element along the diameter: 1) semiconductor Ge(Li)-detector in cryostat; 2) preamplifier; 3) amplifier-expander; 4) AI-128 analyzer; 5) power supply block; 6) protective wall of the box; 7) collimator; 8) mechanism for the displacement of the sample.

Translated from Atomnaya Énergiya, Vol. 32, No. 4, pp. 318-319, April, 1972. Original article submitted June 1, 1971.

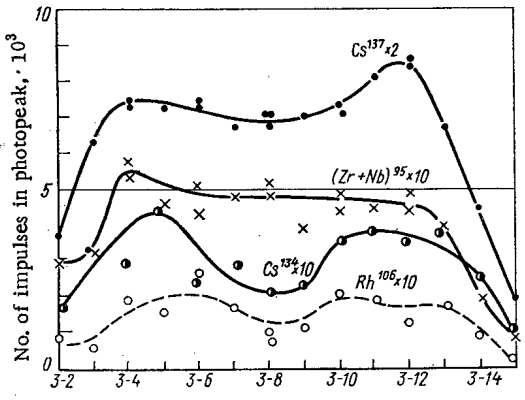

Fig. 2

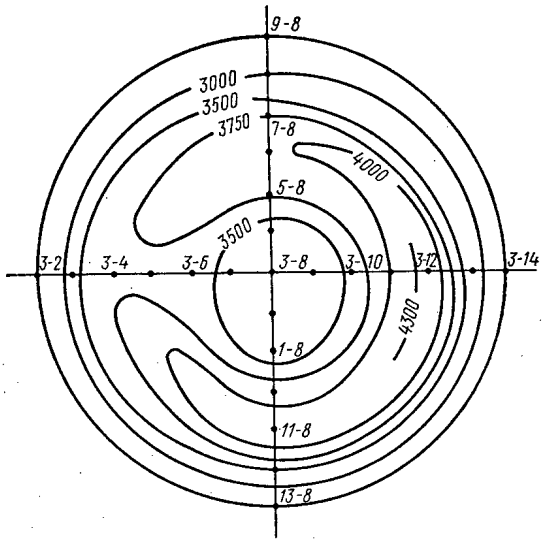

Fig. 3

Fig. 2. Distribution of fission fragments along the diameter of the sample. (Double points on the figure are control measurements.)

Fig. 3. Distribution of Cs^{137} over the area of the sample.

The sample of the investigated fuel element, which is in the form of a cylinder with a height of 1-2 mm and with two plane parallel surfaces, is placed on a backing and is set in the displacement mechanism (the sample is prepared in a hot chamber and is led into the box along a conveyer). The distribution of fission fragments is measured by the coordinate method along the entire area of the section. The results of measurements are processed by the usual method, i.e., the distribution curves of given radioactive isotopes along the diameter of the fuel element are constructed.

In order to illustrate the potentialities of the procedure we present the data obtained for a fuel element of 6 mm diameter with stainless steel shell and the fuel in the form of UC tablets. The thickness of the sample is 1 mm. The temperature at the center of the fuel element in the process of irradiation reached up to 1200°C, and in the shell up to 600°C. The fuel element is irradiated up to ~6% burn-up; the delay between the end of irradiation and the time of measurement is ~1 year.

The sample under investigation is scanned along its entire area with 0.5 mm step by a cylindrical collimator of 1 mm diameter. The γ-spectrum of the fission fragments is measured in the energy range 400-800 keV. In Fig. 2, which shows the distribution of fission fragments along the diameter of the sample, there is a tendency for joining of the center of the element by Cs^{137} and Cs^{134} isotopes. An asymmetry of distribution of Cs^{137} is observed over the area of the section (Fig. 3).

The obtained results confirm the efficiency of the equipment: the exposure time is about 15 min and a good reproducibility of the results is seen with an acceptable accuracy of the mechanism of the displacement. A further improvement of the equipment consists in the reduction of the input aperture of the conical collimator to 0.1 mm and the use of coaxial Ge(Li)-detectors with large efficiency for recording γ-radiation.

LITERATURE CITED

1. Report AERE, R-5149 (1966).
2. H. Kamogama et al. (Japan), III Geneva Conference (1964), Paper No. P/430.

VACUUM-CATHODE ETCHING OF URANIUM IN VUP-2K EQUIPMENT

D. M. Skorov, A. I. Dashkovskii, V. V. Volkov, and B. A. Kalin

UDC 621.039.542.32

The use of vacuum-cathode etching for revealing the structure of materials is due to certain advantages over chemical and electrolytic etching; using this method it is possible to etch any metal and multiphase alloys in a wide range of temperatures and also after irradiation. The form of the inclusions is retained in etching, which is important, for example, in electron-microscope investigation of alloys; false phases etc., do not appear in the structure revealed in etching [1-9]. Native equipment of types UVR, ITR, VUP, etc. are in serial production, which permit vacuum-cathode etching of metals including uranium. However, the use of these equipment, for example, of VUP-2K for etching uranium is beset with some difficulties of constructional and procedural nature. In particular, we have found that the construction of the discharge chamber does not permit to choose the regime of operation with small current density: the discharge was extremely unstable and was not focussed accurately on the sample and the samples got heated in the process of etching. The oxidation of the samples is observed and etching holes appear at the surface. Intense pulverization of the material of the stand of the sample also occurs.

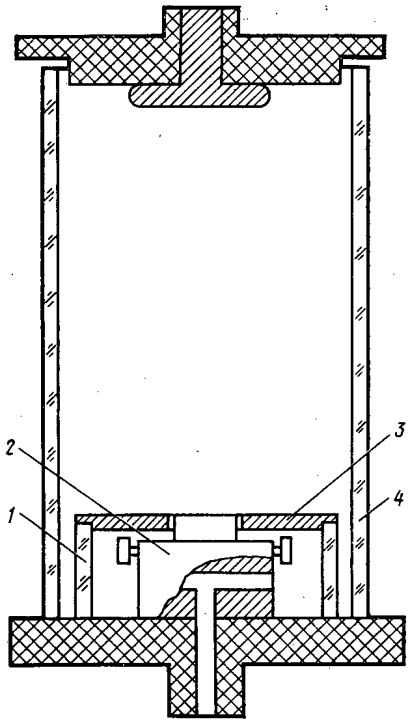

Fig. 1. Schematic diagram of the discharge chamber.

In order to eliminate these drawbacks an additional inner glass cylinder 1 was placed in the discharge chamber concentric to the main cylinder (Fig. 1): the cylinder is 66 mm in diameter and 28 mm in length. As a result it is possible to obtain a stable regime of vacuum-cathode etching of uranium by argon or krypton; the voltage is 5.0 kV, current 1-3 mA, etching time 30-60 min, and the pressure in the volume of the dome about 10^{-4} mm Hg. For the purpose of decreasing the pulverization of the aluminum stand 2 a Teflon disk 3 with an aperture under the sample is placed or the stand is covered by niobium foil. The temperature of the stand is maintained below 0°C by cooling by liquid nitrogen, which excludes noticeable heating of the sample and shortens the etching time by several times. The termination of etching is determined from the darkening of the outer glass cylinder 4 of the discharge chamber. The hermetic sealing of the assembled system, the feed of the gas from a standard container to the inlet at a pressure of 1.5-2.5 atm, and a careful degassing of the dome and the discharge chamber of the equipment made it possible to eliminate oxidation of uranium in the process of etching. A typical form of the microstructure of uranium after optimum vacuum-cathode etching is shown in Fig. 2. A longer-duration etching of the samples does not reveal any new details of the structure and is accompanied by unetching of the boundaries of the grains, duplicates, etc.

The advantage of vacuum-cathode etching is seen especially clearly in electron-microscope investigation of the structure of

Translated from Atomnaya Énergiya, Vol. 32, No. 4, pp. 319-320, April, 1972. Original article submitted June 7, 1971; revision submitted December 2, 1971.

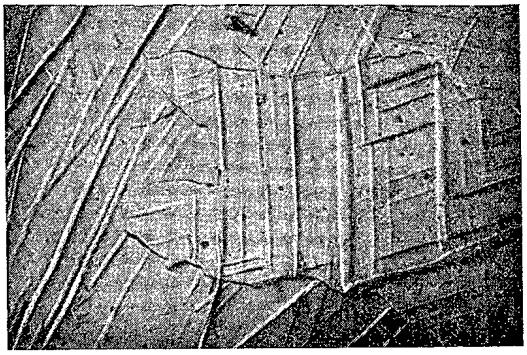

Fig. 2

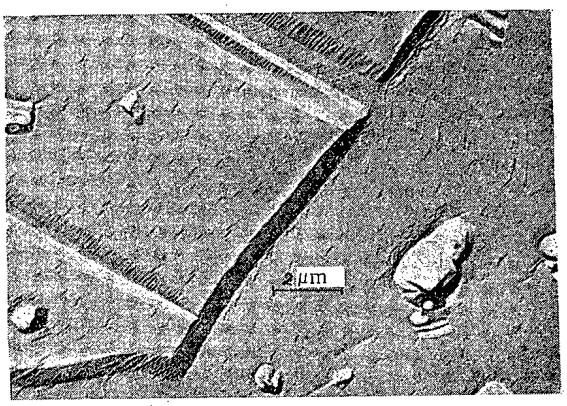

Fig. 3

Fig. 2. Structure of uranium after vacuum-cathode etching (slant light, ×440).

Fig. 3. Electron-microscope photograph of angular replica taken from the surface of etched uranium.

uranium (Fig. 3). The procedural and constructional recommendations given here for vacuum-cathode etching on VUP-2K equipment are appropriate even for certain alloys of uranium.

LITERATURE CITED

1. N. V. Pleshivtsev, Cathode Pulverization [in Russian], Atomizdat, Moscow (1968).
2. D. Armstrong, P. Madsen, and E. Sykes, J. Nucl. Mat., 2, 127 (1959).
3. T. Padden and F. Cain, USAEC Report WAPD-83 (Del.), Westinghouse Atomic Power Division (1953).
4. T. Padden and F. Cain, Metal Progress, 66, 108 (1954).
5. T. Bierlein, USAEC Report HW-32676, Hanford Atomic Products Operation (1954).
6. T. Bierlein, ibid., Report HW-34390 (1955).
7. T. Bierlein, J. Morgan, and G. Mallet, ibid., Report HW-42184 (Rev.) (1956).
8. J. Newkirk and W. Martin, G. E. Research Lab., Memo MC-24 (1957).
9. T. Bierlein and B. Mastel (USA), II Geneva Conference (1958), Paper No. 1855.

CHANGE IN THE STRUCTURE AND PROPERTIES OF TITANIUM CARBIDE UNDER THE ACTION OF IRRADIATION

M. S. Koval'chenko, Yu. I. Rogovoi, and V. D. Kelim

UDC 669.018.4:539.2:669.01

Extremely few studies have been devoted to the effects of irradiation on carbides [1-3].

In view of this, an experimental investigation was made of the change in the microstructure, lattice parameter, electric resistance, and microhardness of titanium carbide with the composition $TiC_{0.94}$ under the action of neutron irradiation with integral doses of $1.0 \cdot 10^{19}$, $3.7 \cdot 10^{19}$, $7.5 \cdot 10^{19}$, and $1.5 \cdot 10^{20}$ thermal neutrons/cm^2 (the ratio of the thermal neutron flux to the flux of fast neutrons is equal to 8 : 1) on a VVR-M reactor at a temperature of ~50°C, as well as with subsequent annealing.

Annealing of irradiated samples was conducted under a vacuum of 10^{-4} mm Hg at temperatures of 100-1000°C at 100°C intervals for a period of 1 h. The samples were prepared for the investigation from a powder of technically pure titanium carbide by the method of hot pressing at a temperature of 2300°C under a pressure of 240 kg/cm^2, followed by electric spark cutting. Four prismatic samples with dimensions 2.5 × 2.5 × 10 mm, possessing the same initial state for the four selected doses of irradiation, were cut out of the hot-pressed cylindrical bullets 8 mm in diameter and 10-12 mm high. The porosity of the samples did not exceed 5%, while the average grain size was approximately 14 μ. The microhardness was

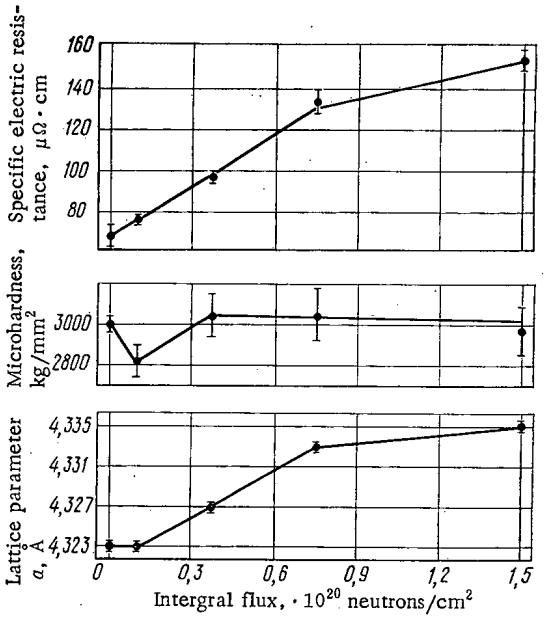

Fig. 1

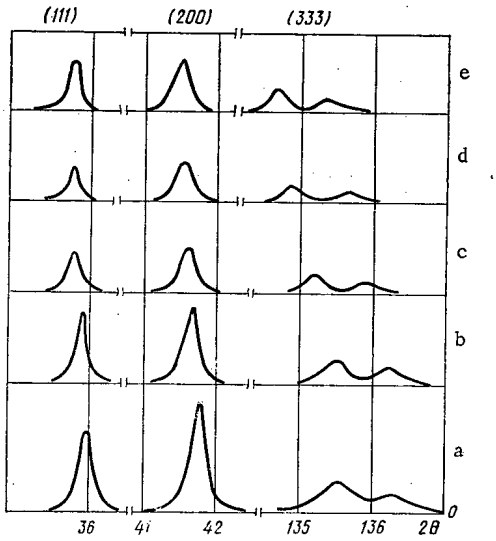

Fig. 2

Fig. 1. Change in the lattice parameter and properties of the carbide $TiC_{0.94}$ during neutron irradiation.

Fig. 2. Diffraction effects in the carbide $TiC_{0.94}$: a) before irradiation, after irradiation with doses (neutrons/cm^2); b) $1.0 \cdot 10^{19}$; c) $3.7 \cdot 10^{19}$; d) $7.5 \cdot 10^{19}$; e) $1.5 \cdot 10^{20}$.

Translated from Atomnaya Énergiya, Vol. 32, No. 4, pp. 321-323, April, 1972. Original article submitted June 3, 1971; revision submitted October 3, 1971.

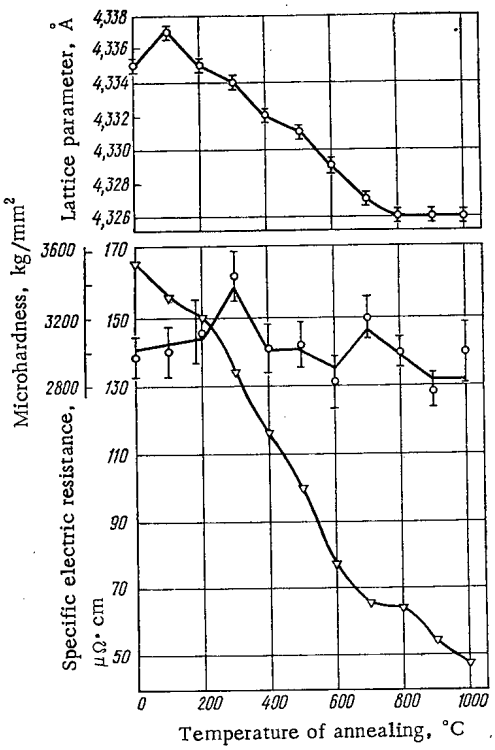

Fig. 3. Isochronous recovery of the lattice parameter and properties of the carbide $TiC_{0.94}$, irradiated with a dose of $1.5 \cdot 10^{20}$ neutrons/cm^2 at a temperature of ~50°C.

TABLE 1. Activation Energy and Kinetic Parameters in the Annealing of Irradiated Titanium Carbide

T, °C	Homologous temperature	E, eV	K_0, sec^{-1}	γ
350	0,18	0,26	$7{,}7 \cdot 10^{-3}$	1
600	0,25	0,40	$2{,}0 \cdot 10^{-2}$	1

measured on a PMT-3 instrument according to 50-100 imprints. Metallographic investigation was conducted on an MIM-8M microscope, and x-ray diffraction study on a URS-50-IM diffractometer. The specific electric resistance was measured by a compensation method according to a two-probe circuit.

Metallographic investigation did not show any change in the average grain size of the samples after irradiation, as well as subsequent annealing.

After irradiation with a dose of $1.5 \cdot 10^{20}$ neutrons/cm^2, an increase of 0.3-0.5% in the volume of the sample was observed. Irradiation led to a substantial increase in the electric resistance of the lattice parameter of the carbide (Fig. 1); after a dose of $7.5 \cdot 10^{19}$ neutrons/cm^2 this increase was sharply reduced. A regular shift of the diffraction peaks in the direction of smaller angles with a simultaneous decrease in their intensity is observed (Fig. 2), along with an improvement of the degree of resolution of the α-doublet on the line (333).

After annealing at 100°C (Fig. 3) there was an increase in the lattice parameter, accompanied by a decrease in the intensity of the line (111) and especially for (200). At temperatures of annealing 200-800°C, the lattice parameter systematically decreased. The intensity and resolution of the α-doublet of the line (333) was unchanged after all stages of annealing of $TiC_{0.94}$, remaining rather high. The lines (111) and (200) were distinguished by a substantial and almost unchanged intensity after annealing of the samples at temperatures above 100°C. Other than a 15% increase after annealing of the samples at 300°C, the microhardness did not undergo any significant changes (Fig. 3). A complete recovery of the supplementary electric resistance induced by irradiation occurred at 650°C.

According to the data of annealing, we can distinguish two stages of recovery – at the temperatures 350 and 600°C, whereas the expected temperature of the beginning of migration of vacancies in titanium carbide according to a composition close to stoichiometric is ~750°C [2]. Qualitatively close data were obtained in the annealing of uranium carbide [1], where two stages of recovery were established: around 200°C and between 400 and 600°C.

A quantitative evaluation of the results of annealing (see Table 1) was performed according to the data of the recovery of electric resistance using the kinetic equation:

$$-\frac{dC}{dt} = C^{\gamma} K_0 e^{-E/kT},$$

where C is the concentration of defects; E is the activation energy; γ is the order of the reaction; K_0 is the kinetic coefficient [4].

A substantial increase in the lattice parameter with a simultaneous decrease in the intensities of the lines without any appreciable broadening of them, as well as the linear variation of the electric resistance of the carbide up to a dose of $7.5 \cdot 10^{19}$ neutrons/cm^2, permit us to assume that after irradiation, chiefly point defects remain in $TiC_{0.94}$. The diffraction effects in the samples, due to a dose of $1.5 \cdot 10^{20}$ neutrons/cm^2 (see Fig. 2e) as well as the absence of appreciable strengthening (according to the data of microhardness),

permit us to assume the occurrence of a process of annihilation of defects, since a strengthening of the material and a broadening of the x-ray reflections would be observed if accumulations of defects were formed.

The increase noted in the lattice parameter of titanium carbide after annealing at 100°C may evidently be associated with a "recovery" of the dynamic crowdions during thermal activation [5]. We may also assume a relaxing shift of the carbon atoms, leading to a more substantial change in the contour of the line (200) in comparison with the line (111). Such a conclusion is based on the fact that the plane (100) in TiC is a cleavage plane [6, 7], with a tendency to decoration by carbon [7]. The relaxing movement of the interstitial atoms, scattered close to dislocations, with deposition on the latter, may explain the increase in the microhardness when the temperature of annealing is increased to 300°C. The stage of recovery at 350°C is also evidently associated with the movement of carbon atoms, i.e., with recombination of the interstitial carbon atoms with vacancies. It may be assumed that this recombination occurs according to a mechanism of transition of carbon atoms from tetrahedral vacancies to octahedral vacancies, as a result of which there is a decrease in the lattice parameter. The decrease in the microhardness at this stage may be caused by a liberation of point defects from dislocations. The stage of annealing at 600°C should evidently be ascribed to recombination of the interstitial titanium atoms with vacancies. At this stage the lattice parameter is changed to a greater degree (see Fig. 3).

The similarity of the mechanisms of annealing at both stages is confirmed by the closeness of the kinetic coefficients and the values of the activation energy (see Table 1). The first order of the reaction, due to recombination of interstitial atoms chiefly with the closest vacancies [8, 9] also does not contradict the mechanism noted.

The improvement of the degree of resolution of the α-doublet on the line (333) after irradiation of the carbide is evidence of a decrease in the microstresses, apparently as a result of capture of interstitial atoms in the disturbed regions of the lattice and in submicropores, present in hot-pressed samples of titanium carbide [2]. This agrees with the nature of the change in the microhardness, as well as with the decrease in the microhardness and with the lag in the change in the lattice parameter in the carbide after irradiation with a dose of 10^{19} neutrons/cm^2.

LITERATURE CITED

1. B. Childs and J. Ruckman, New Nucl. Materials Including Nonmetallic Fuels, Vol. 2, Vienna, IAEA (1963).
2. M. S. Koval'chenko and V. V. Ogorodnikov, Poroshkovaya Metallurgiya, No. 10, 48 (1966).
3. G. Keilholtz, R. Moore, and M. Osborne, Nucl. Applications, 4, 330 (1968).
4. M. Balarin, R. Rattke, and A. Zetsche, Auswertungsmethoden für Erholungsvorgänge, Zentralinstitut für Kernforschung Dresden (1966).
5. S. T. Konobeevskii, Effects of Irradiation on Materials [in Russian], Atomizdat, Moscow (1967).
6. W. Williams, J. Appl. Phys., 32, 552 (1961).
7. S. E. Brooks, Special Ceramics (Transactions of the Symposium of the British Ceramic Society) [Russian translation], Metallurgiya, Moscow (1968), p. 90.
8. A. Damask and J. Deans, Point Defects in Metals [Russian translation], Mir, Moscow (1966).
9. M. Thompson, Defects and Radiation Damages in Metals [Russian translation], Mir, Moscow (1971).

CHANGE IN THE DENSITY OF SINGLE-CRYSTAL TUNGSTEN DURING NEUTRON IRRADIATION

V. N. Bykov, G. A. Birzhevoi, and M. I. Zakharova

UDC 621.039.531:669.27

The investigations were conducted on single-crystal samples of tungsten, produced by electron beam zone melting [1]. The quality and perfection of the single crystals were monitored by an x-ray method and by selective etching. The dislocation density was $5 \cdot 10^5$ cm^{-2}, angles of disorientations from 30" to 30'. The samples for irradiation were cut out from the middle portion of a single-crystal rod.

The results of spectrochemical analysis are cited in Table 1. To remove the cold-hardened layer the samples were treated electrolytically in a 2% solution of KOH under a voltage of 14 V and a current of 5 A. The removal of the cold-hardened layer was monitored according to the width of the x-ray diffraction line; the depth of the removed layer was 200 μ. The finished samples had a length of 25 mm, and a diameter of 2.5 mm.

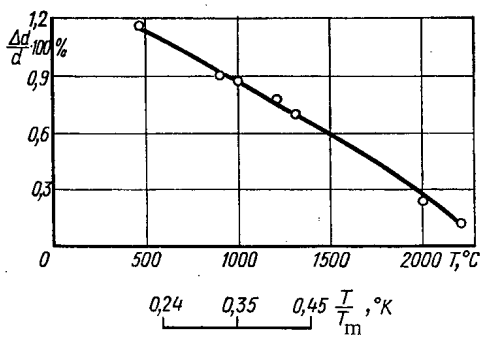

Fig. 1. Curve of restoration of density in isochronal annealing of tungsten single crystals, irradiated with a dose of $1.4 \cdot 10^{22}$ neutrons/cm^2 at 0.20-0.21 T_m.

Irradiation was conducted in hermetically welded ampoules at the temperature 450-500°C (0.20-0.21 T_m) with an integral flux of $1.4 \cdot 10^{22}$ neutrons/cm^2 ($4 \cdot 10^{21}$ neutrons/cm^2, E > 1 MeV). After irradiation the samples were washed in a mixture of hydrofluoric and nitric acids, then electrolytically polished. As a result of such treatment the surface layer, contaminated by radioactivity during the finishing of the ampoules, was removed.

The samples were annealed in a vacuum furnace in the temperature range 500-2200°C for 1 h at a residual pressure of no more than $5 \cdot 10^{-5}$ mm Hg.

The density was determined by a hydrostatic method [2]; calculation was performed according to the formula

$$d = \frac{P}{P-Q}(\delta - \lambda) + \lambda,$$

TABLE 1. Results of Spectrochemical Analysis

Element	Zr	Nb	Ta	Ti	Mo	Fe	Mg	Mn	Pb	Cr	Ni
Amount, % by weight	$<1\cdot10^{-3}$	$<1\cdot10^{-2}$	$<3\cdot10^{-2}$	$<1\cdot10^{-3}$	$8\cdot10^{-3}$	$<1\cdot10^{-3}$	$\leqslant1\cdot10^{-4}$	$<1\cdot10^{-4}$	$<1\cdot10^{-3}$	$2{,}8\cdot10^{-3}$	$<3\cdot10^{-3}$
Element	Al	Bi	Cu	Ca	Cd	Sb	Ba	Co	Zn	Sn	Ag
Amount, % by weight	$\leqslant1\cdot10^{-3}$	$\leqslant3\cdot10^{-4}$	$<1\cdot10^{-4}$	$<1\cdot10^{-3}$	$<1\cdot10^{-4}$	$<1\cdot10^{-3}$	$<1\cdot10^{-3}$	$<3\cdot10^{-3}$	$<3\cdot10^{-3}$	$<3\cdot10^{-4}$	$<1\cdot10^{-4}$

Translated from Atomnaya Énergiya, Vol. 32, No. 4, pp. 323-324, April, 1972. Original article submitted May 7, 1971.

where P is the weight of the sample in air; Q is the weight of the sample in liquid (in our case distilled water); δ is the density of the liquid at the temperature of measurement; λ is the density of air. The weight of the samples was determined with an absolute error of $1 \cdot 10^{-4}$ g. The mean square error in the determination of the density according to 25 measurements was 0.01%.

As a result of the investigation, we found a 1.17% decrease in the density of the irradiated samples in comparison with the initial values. Figure 1 presents the curve of the dependence of the relative change in the density ($\Delta d/d$) on the temperature of annealing. As can be seen from the figure, the restoration of density occurs in the entire investigated temperature range. After annealing at the temperature 2200°C, the densities of the nonirradiated and irradiated samples differ by 0.12%.

There is not yet an unambiguous interpretation of the decrease in the density of the metal as a result of irradiation. Our investigations of the stages of annealing of irradiation defects, conducted on the same samples according to the curves of the specific electric resistance, show that in tungsten during irradiation three types of radiation defects are accumulated, with activation energies 0.70 ± 0.03 eV, 3.2 ± 0.3 eV, and 6.4 ± 0.5 eV, the maxima of the rate of annealing of which lie at 0.24, 0.35, and 0.45 T_m. The restoration of the density in the temperature intervals of stability of these defects comprises: 28% in the temperature range 500-800°C; 15% in the range 960-1200°C; 57% in the range 1200-2200°C, i.e., chiefly complex defects, which are annealed with the activation energy of self-diffusion, are responsible for the decrease in the density: pores, dislocation loops. As a rule, the change in the density of the metals and formation of pores are observed after irradiation at a temperature of 0.3 T_m or more [3-5]. In our case the temperature of irradiation was 0.21 T_m; however, the dose of irradiation was an order of magnitude greater than the dose of irradiation in the known experiments on polycrystalline samples. This, as well as the absence of grain boundaries in the single crystals, may lead to the formation of complex defects of the type of pores at temperatures lower than 0.3 T_m.

Thus, the data of this work indicate that a decrease in the density of metals may arise during neutron irradiation at a temperature below 0.3 T_m.

LITERATURE CITED

1. V. N. Bykov and M. I. Zakharova, in: Physicochemical Bases of Crystallization Processes of Profound Purification of Metals [in Russian], Nauka, Moscow (1970), p. 128.
2. V. G. Livshits, Physical Properties of Metals and Alloys [in Russian], Mashgiz, Moscow (1959), p. 276.
3. R. Rau, F. Secco, D. Aragona, R. Ladd, Philos, Mag., 21, 441 (1970).
4. R. Rau, R. Ladd, and J. M'oteff, Nucl. Mat., 33, 324 (1969).
5. J. Calligan and T. Oku, Phys. Stat. Sol., 36, K79 (1969).

SOME PRINCIPLES OF THE OXIDATION OF REACTIVE GRAPHITE

N. S. Burdakov and V. N. Turdakov

UDC 621.039.524.2

In the development of more economical systems of operation of atomic electric power plants with graphite coolants, the problem of protecting the lining from oxidative breakdown arises.

Investigations of oxidation have been conducted on domestic reactor graphite, possessing a density of 1.6-1.7 g/cm^3, a porosity of 15-20%, and a total content of impurities of $3 \cdot 10^{-3}$% [1].

Special attention was paid to investigations of the oxidative characteristics of graphite in the presence of microconcentrations of O_2. The rate of oxidation was determined according to the concentration of oxidation products ($CO + CO_2$) or according to the loss of weight. In the first case (Fig. 1) a graphite bushing 1 m long and 84 × 70 mm in diameter was placed in a tubular electric furnace 13. The temperature of the graphite was measured with a chromel – alumel thermocouple. A nitrogen – oxygen mixture was delivered to the furnace in an amount of 1-5 liters/min (7-40 cm/sec). The gas mixture was prepared by a dynamic method in two mixers 5 and 8. The gas pressure was stabilized with monostats 1, 2, 9. The gas flow was measured with capillary rheometers 3, 4, 6, 7, 16. The CO_2 content was measured with automatic gas analyzers 11 and 12 of the OA-2211 type (scale 0-0.01% CO_2) and GIP-7 type (scale 0-0.1% CO_2), operating on a principle of selective absorption of infrared radiation [2]. The O_2 content was measured with automatic gas analyzers 15, 17 of the GL5108 (scale 0-0.01% O_2), and DPG-5A-52 (scale 0-1.0% O_2) types,

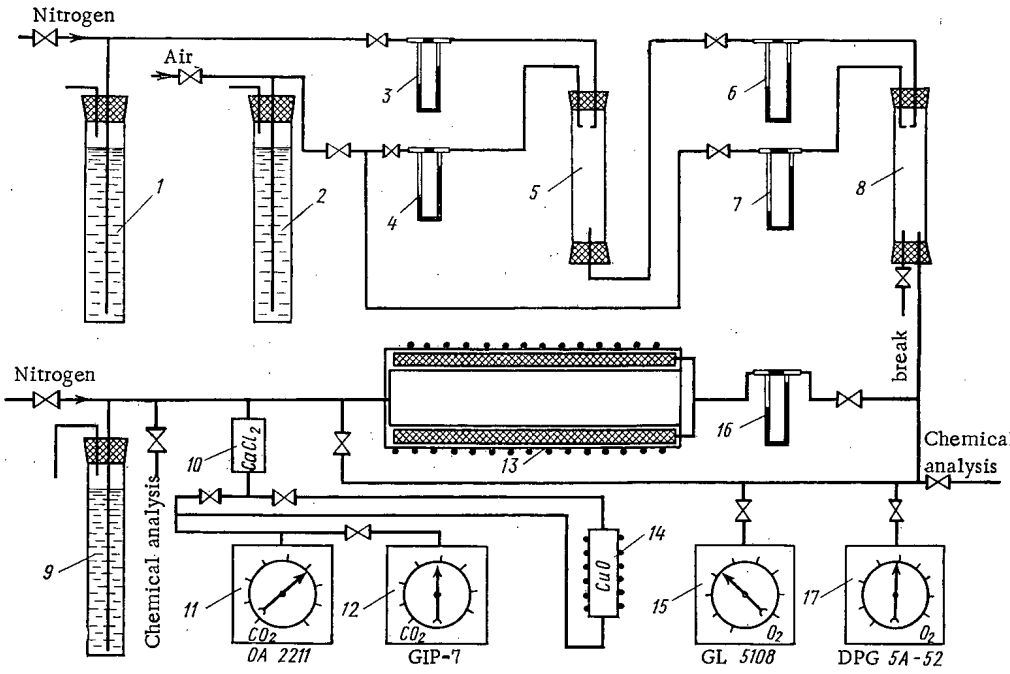

Fig. 1. Scheme of apparatus for investigating the oxidation of graphite using the method of gas analysis.

Translated from Atomnaya Énergiya, Vol. 32, No. 4, pp. 324-326, April, 1972. Original article submitted June 14, 1971.

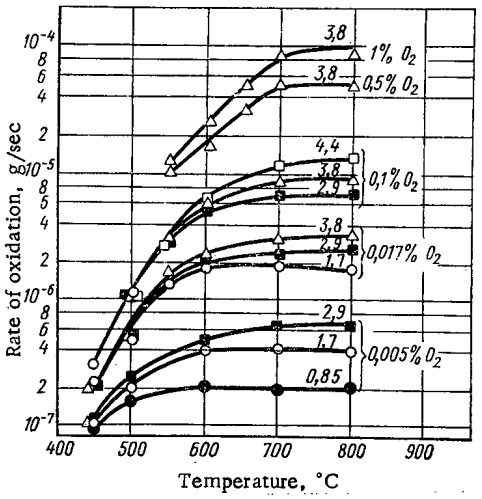

Fig. 2

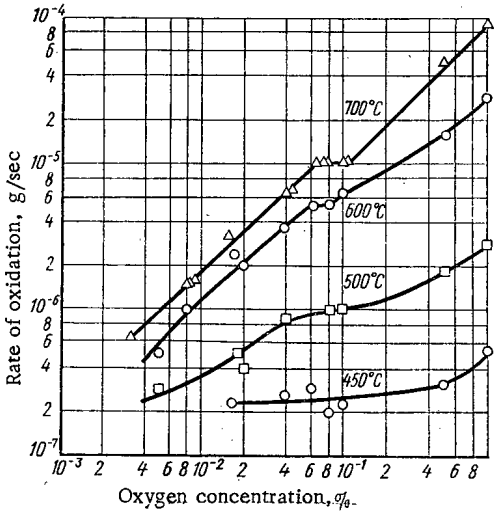

Fig. 3

Fig. 2. Temperature dependence of the oxidation of graphite at various rates of flow of gas (ϑ) and O_2 concentrations, obtained by the method of gas analysis. Reaction surface 4850 cm^2.

Fig. 3. Influence of the oxygen concentration on the rate of oxidation of graphite in the temperature interval 450-700°C.

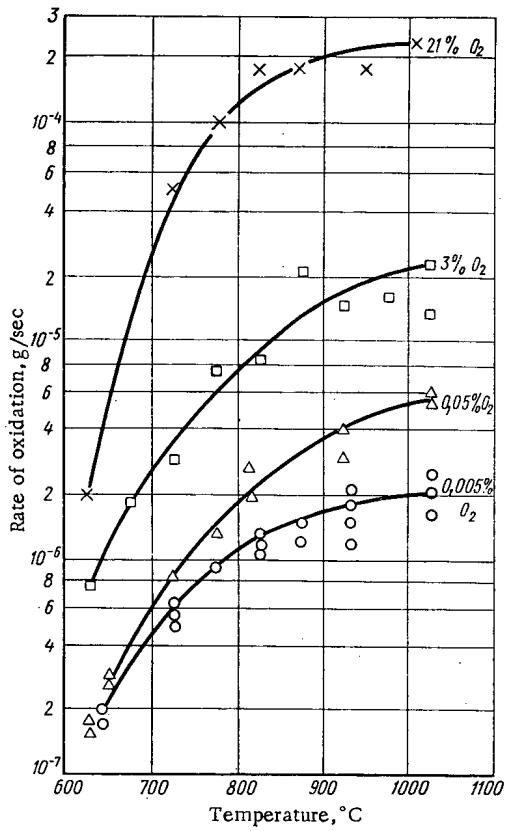

Fig. 4. Temperature dependence of the oxidation of graphite at various O_2 concentrations, obtained with an electronic microbalance.

operating according to an electrochemical principle. The CO partially formed in the reaction was oxidized to the formation of CO_2 in a furnace 14 at 300°C on granulated copper oxide. A moisture absorber 10 was set up in front of the gas analyzers 11, 12.

A second method of measuring the rate of oxidation was used in work on small samples, weighing 2-3 g. The change in weight in this case was registered with an electronic microbalance of the ÉM-1-3MP type, mounted above a tubular electric furnace, in which the samples were suspended. Stabilization of the temperature at the set level was accomplished with a photoelectric positional regulating device, connected to an MR-1-02 millivoltmeter and a relay of the P6-121 type. The sensitivity of the balance was 0.1 mg. The error in the determination of the rate of oxidation in both cases was ±10%, but the values for different samples differed by 200-300%. This is probably due to nonuniformity of the distribution of the properties of graphite along the billet (porosity, impurities, texture, etc.).

With increasing temperature, the process of diffusion of oxygen to the active centers on the graphite centers begins to compete with the purely chemical process of oxidation. As a result of this, the temperature curve of oxidation has a characteristic S-shape. From Fig. 2, obtained on the apparatus using methods of gas analysis, it is evident that lowering the O_2 concentration from 1 to 0.005% leads to an expansion of the diffusion step of oxidation in the direction of lower temperatures. At the same time, increasing the rate of flow of the gas

leads to a broadening of the kinetic step and to a restoration of the absolute value of the oxidation rate.

Analogous results were obtained in an investigation of the rate of oxidation on an electronic microbalance (Fig. 4) at a gas velocity of 3 cm/sec. The only difference lies in the fact that here the diffusion region begins almost 100°C lower than on the preceding figures. Possibly the fact that not only the chemical oxidation, but also erosion of graphite are registered on the oxidation curve has an influence. The apparent activation energy E, determined according to the slope from Figs. 2 and 4, varies from 0 to 30 kcal/mole. The nature of the change in the value of E is in good agreement with the known data [3, 4].

The reaction order, determined for the temperatures 450-700°C from graphs of log v versus log C (Fig. 3), proved variable. Moreover, the interval of O_2 concentrations corresponding to zero order of the reaction decreases with increasing temperature.

The experimental results obtained can be used to predict the period of service of a graphite lining in accord with the set system of gas purging.

LITERATURE CITED

1. V. V. Goncharov, At. Énerg., 3, 398 (1957).
2. V. A. Pavlenko, Gas Analyzers [in Russian], Mashinostroenie, Moscow – Leningrad (1965).
3. A. S. Predvoditelev et al., Combustion of Carbon [in Russian], Izd-vo AN SSSR, Moscow (1949).
4. E. S. Golovina (editor), Reactions of Carbon with Gases [Russian translation], IL, Moscow (1963).

HOW INORGANIC ELECTRICAL INSULATING MATERIALS ARE USED IN REACTORS

N. A. Aseev

UDC 621.039.553:621.315.6

The information available on the conductivity [1-3] and peculiar aspects of the behavior [4, 5] of inorganic insulators exposed to radiation are inadequate for the design of measuring systems in in-channel experiments, or for estimating the accuracy of various sensors installed in the reactor system. This has led to an investigation of the behavior of certain inorganic dielectrics in the channels of the SM-2 reactor.

The conductivity of solid dielectrics was measured with the aid of a circuit featuring a guard electrode on disk-shaped specimens 32 to 35 mm in diameter and 1 to 2.5 mm thick. These wafer specimens were placed in special measuring cells. The conductivity of glass fiber was measured on a cable with 1.5 mm thick insulation. This work disclosed the dependences of the conductivity (σ_V) of ceramics on the intensity of reactor radiation, on the temperature at constant radiation intensity, and on the integral fast dose (Figs. 1-3), as well as the dependence of the resistance of glass fiber insulation on the temperature at constant radiation intensity (Fig. 4).

The conductivity of all the dielectrics investigated increases more or less linearly with increasing intensity of reactor radiation [1, 3], and there exists a region within which the conductivity is only slightly affected by the temperature and is determined completely by ionization. The size and the position of that region on the temperature scale depends on the energy of activation of the carriers in thermal ionization. As the temperature is increased, the contribution made by the ionization diminishes. The nature of the dependence of the ceramics MgO and MG-2 on the integral fast dose acts to confirm the effect of neutron irradiation on conductivity [2].

One additional feature of the in-pile behavior of dielectrics is related to the appearance of space charge as a result of the escape of electrons in β-decay [4, 5]. The conditions governing compensation of space

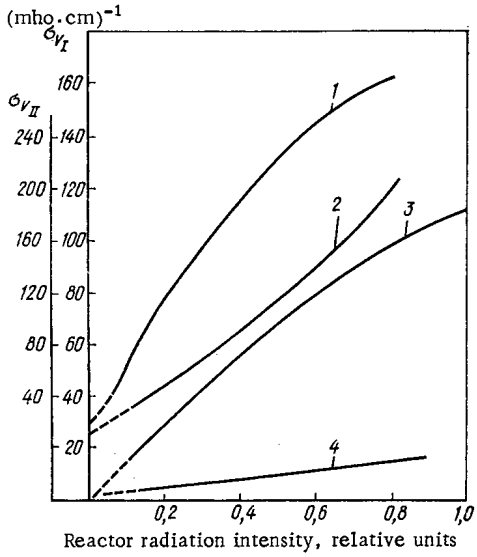

Fig. 1. Dependences of conductivity of ceramics on radiation intensity: 1, 3, 4) ceramics MG-2, MgO, M-23 respectively [t_{irrad} = 35-85°C; one relative unit corresponds to γ-ray dose rate 10^5 R/sec, to fast flux $5.5 \cdot 10^{12}$ neutrons/cm^2·sec, and to thermal flux $4 \cdot 10^{13}$ neutrons/cm^2·sec]; 2) Al_2O_3 [t_{irrad} = 40-200°C; one relative unit corresponds to γ-ray dose rate $6.5 \cdot 10^5$ R/sec, to fast flux $3.2 \cdot 10^{14}$ neutrons/cm^2·sec, and to thermal flux $3.2 \cdot 10^{14}$ neutrons/cm^2·sec]. Ordinate scale σ_{V_I}) for curves 1, 3, 4 ($\sigma_{V_I} \cdot 10^{-14}$, $\sigma_{V_I} \cdot 10^{-12}$, $\sigma_{V_I} \cdot 10^{-12}$, respectively); ordinate scale $\sigma_{V_{II}}$) for curve 2 ($\sigma_{V_{II}} \cdot 10^{-12}$).

Translated from Atomnaya Énergiya, Vol. 32, No. 4, pp. 326-328, April, 1972. Original article submitted May 14, 1971.

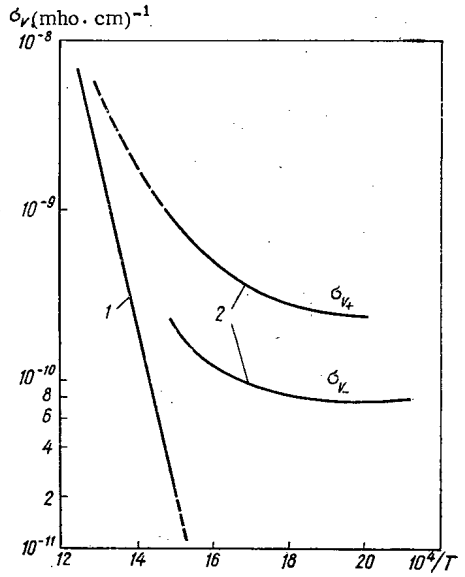

Fig. 2

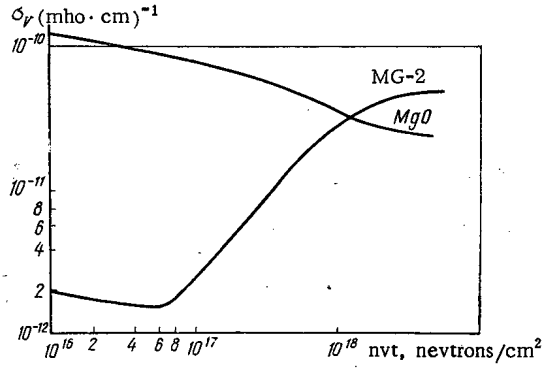

Fig. 3

Fig. 2. Dependence of conductivity of Al_2O_3 on temperature: 1) under laboratory conditions; 2) in reactor at constant radiation intensity [$6.5 \cdot 10^5$ R/sec, $3.2 \cdot 10^{14}$ (fast) neutrons/cm^2 · sec, $3.2 \cdot 10^{14}$ (thermal) neutrons/cm^2 · sec]. σ_{V+}) conductivity when polarity of high-voltage electrode is positive; σ_{V-}) conductivity when polarity of high-voltage electrode is negative.

Fig. 3. Dependence of conductivity on integrated dose nvt of fast neutrons (t_{irrad} = 100°C).

charge depend on the electrophysical characteristics of the dielectric and of the surroundings. Appreciable space charge is generated in a ceramic containing oxides of elements susceptible of activation, when the ceramic is exposed to high-intensity thermal flux. The current compensating that charge can flow through the circuit elements of the sensor and of the measuring circuit, thereby introducing additional error into the measurements. The presence of space charge establishing impressive potentials across the electrodes affects the conductivity measurements of dielectrics because the conductivity then depends on the polarity of the applied voltage (see Fig. 3).

Figure 5 displays dependences of the potential of cable cores insulated with M-23 grade porcelain and stabilized by polyethylene on the temperature at constant reactor radiation intensity. The appearance of potential must be taken into account when using measuring circuits with a high input impedance.

The results of the tests run on the inorganic dielectrics allow us to draw the following inferences.

1. The ionization-derived conductivity is fairly low even when the specimens were irradiated by high-intensity reactor flux [the γ-radiation dose rate is $6.5 \cdot 10^5$ R/sec, the fast flux and the thermal flux are both $3.2 \cdot 10^{14}$ neutrons/cm^2 · sec]. Any sites where the insulator joints are not sound, and any microcracks in insulating layers fabricated by sputtering methods, will therefore have a decisive effect on the performance of insulation on sensors. The conductivity of the gas clearances may reach 10^{-4} to 10^{-6} $\Omega \cdot cm^{-1}$.
2. As the integrated dose increases, the conductivity of the dielectrics varies, but not necessarily with the same sign.
3. At elevated temperatures, the conductivity of dielectrics is affected primarily by thermal ionization.
4. The possible effect of factors associated with generation of charges must be taken into cognizance when selecting insulating materials. The use of insulators and measuring cable cores containing isotopes likely to be activated must be avoided in weak-current sensors.

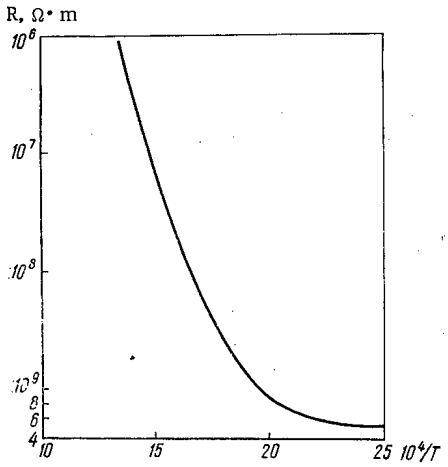

Fig. 4

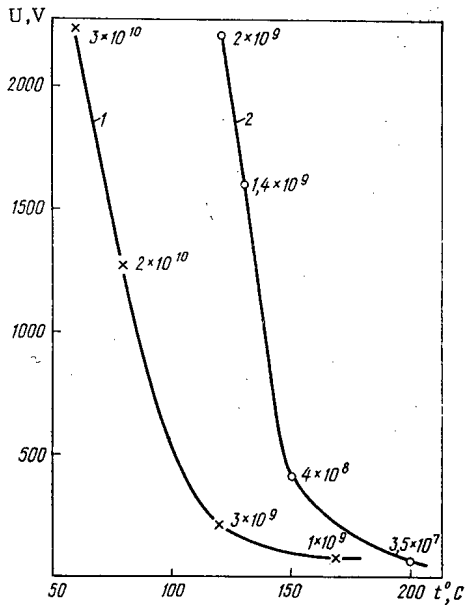

Fig. 5

Fig. 4. Temperature dependence of resistance presented by insulation of meter length of cable insulated with glass fiber, at constant radiation intensity: gammas $3 \cdot 10^5$ R/sec, fast flux $3 \cdot 10^{13}$ neutrons/cm^2·sec, thermal flux $2 \cdot 10^{13}$ neutrons/cm^2·sec.

Fig. 5. Temperature dependences of cable core potential: 1) polyethylene, intensities 10^5 R/sec (gammas), $5.5 \cdot 10^{12}$ (fast) neutrons/cm^2·sec, $4 \cdot 10^{13}$ (thermal) neutrons/cm^2·sec; 2) porcelain, intensities $5 \cdot 10^5$ R/sec (gammas), $2.5 \cdot 10^{14}$ (fast) neutrons/cm^2·sec, $2.5 \cdot 10^{14}$ (thermal) neutrons/cm^2·sec. Numerical data at data points correspond to level of insulation, in ohms.

The author expresses his thanks to V. A. Tsykanov, B. V. Samsonov, and N. S. Kostyukov, for their kind assistance in carrying out the experiments and discussing the results.

LITERATURE CITED

1. B. M. Bul, Fiz. Tverd. Tela, 3, 2264 (1961).
2. Yu. K. Gus'kov and V. F. Sachkov, At. Énerg., 6, 204 (1959).
3. I. Cary and M. Devis, Nucl. Sci. and Engng., 21, 30 (1965).
4. V. V. Gromov, At. Énerg., 26, 250 (1969).
5. V. G. Baru and F. F. Vol'kenshtein, Izv. Akad. Nauk SSSR, Seriya Khim., No. 11, 1936 (1964).

NEUTRON DIFFUSION IN A MEDIUM WITH CHANNELS

N. I. Laletin

UDC 539.125.52

Coefficient of Diffusion Cooling with Anisotropic Diffusion. One can write the neutron balance in a nonbreeder slug with the absence of sources in the form

$$-\frac{d\bar{n}}{dt}=\Pi+Y,$$

where $\bar{n}=\int n(\mathbf{r}, \mathbf{v}, t)d\mathbf{r}d\mathbf{v}/V$, $n(\mathbf{r}, v, t)$ is the neutron flux with velocity v; V is the slug volume; Π is the neutron absorption per unit volume per unit time; Y is the neutron leakage per unit time per unit volume. After establishment of the fundamental harmonic, and separation of space, energy, and time variables $\Pi=(v\Sigma_a)_0\bar{n}$, where Σ_a is the macroscopic absorption cross section for the slug material, we have $Y=y\bar{n}$;

$$-\frac{d\bar{n}}{dt}=[(v\Sigma_a)_0+y]\bar{n},\ n=n_0e^{-\alpha_0 t},\ \alpha_0=(v\Sigma_a)_0+y.$$

We shall consider the leakage probability y. It is known that in the diffusion approach $y=DB^2$, where $D=\int\lambda_{tr}(v)vf(v)dv/3$. The neutron distribution f(v) differs from that of Maxwell M(v) only because of the leakage, and to a first approximation, one is able to write in the form

$$f(v)=M(v)-D_0B^2\psi(v).$$

Here $D_0=\int\lambda_{tr}(v)vM(v)d\mathbf{v}/3$; $\psi(v)$ is a function dependent only on the microscopic cross section for the interaction of the neutrons with the slug material. As a result, we obtain the well-known equation [1]

$$y=D_0B^2-C_0B^4, \tag{1}$$

where $C_0=\int\lambda_{tr}(v)vD_0\psi(v)dv/3$ is the coefficient of diffusion cooling.

For the case of a slug with a regular array of hollow channels in which, due to its structure, the neutron diffusion is anisotropic, the corrections are discussed using the above reasoning with one difference – the substitution D_0B^2 by $D_\perp^2B_\perp^2+D_\parallel B_\parallel^2$.* Consequently, one is able to write

$$y=D_\perp B_\perp^2+D_\parallel B_\parallel^2-C_0\left(\frac{D_\perp}{D_0}\right)^2B_\perp^4-C_0\left(\frac{D_\parallel}{D_0}\right)^2B_\parallel^4-2C_0\frac{D_\perp D_\parallel}{D_0^2}B_\perp^2B_\parallel^2. \tag{2}$$

Comparing Eq. (2) with formula (3) from [3], we obtain

$$C_\perp=C_0\left(\frac{D_\perp}{D_0}\right)^2=C_0S_\perp^2,\ C_\parallel=C_0\left(\frac{D_\parallel}{D_0}\right)^2=C_0S_\parallel^2,\ C_x=2C_0\frac{D_\perp D_\parallel}{D_0^2}=2C_0S_\perp S_\parallel. \tag{3}$$

Hence, there follows the relation $C_\parallel/C_\perp(D_\parallel/D_\perp)^2$, obtained in [4]. Furthermore, if one writes $D_\parallel/D_\perp-1=\beta$, then, except for terms linear in β, we have

$$C_x=C_0S_\perp^2\frac{S_\parallel}{S_\perp}+C_0S_\parallel^2\frac{S_\perp}{S_\parallel}=C_\perp(1+\beta)+C_\parallel(1-\beta)^{-1}=C_\perp+C_\parallel,$$

i.e., to this approximation, the formula agrees with the corresponding expression in [4]. The discrepancy in the higher order terms in β is, apparently, a consequence of the approximation made with the result of this relation in [4].

*The question of anisotropic diffusion coefficients is considered in the monograph [2], which also has an extensive bibliography.

Translated from Atomnaya Énergiya, Vol. 32, No. 4, pp. 328-330. Original article submitted May 6, 1971.

Equations (1), (2) are obtained in the diffusion approximation. Transport corrections for the case of a solid slug are proportional to B^4, but with numerical coefficients which are far smaller than C_0 [5]. In the case when the anisotropic diffusion is assumed due to the presence of hollow channels in the slug, the transport corrections appear to be more significant. The most significant correction to the longitudinal diffusion is associated with calculation of variations in the neutron distribution along the channel and its finite length [6]. Due to this, the following terms must appear in Eq. (2)

$$-\frac{\varepsilon}{2\pi}\cdot\frac{p}{1+p}\cdot\frac{3}{2}QD_0\frac{R^2}{\lambda_{tr}}B_{||}^3\equiv -GB_{||}^3,$$

where $\varepsilon = 3\pi^2/4 - 3/2 + 3\pi \mathrm{Si}(\pi)/2$; $\varepsilon/2\pi \approx 1.15$; $p = V_c/(V - V_c)$; V_c is the volume of the hollow channels; R is the radius of the channel; and Q is a number characterizing the geometric form of the channels. Apart from this, the necessary corrections are associated with $B_{||}^4$, dependent on the channel radius R, which for sufficiently large R can be compared with the coefficient of diffusion cooling. It is somewhat difficult to calculate them, but is hardly necessary. In reality, the significant contribution in the terms with $B_{||}^4$, will necessitate taking into account the sharp drop in the flux at the channel boundary, and the large value of this term will indicate breakdown of the assumption regarding the separation of variables. Therefore, it is necessary to achieve this in order that the corresponding correction proves to be negligible in an experiment. Apparently, this can be achieved with fulfilment of the condition

$$G \leqslant C_{||}B_{||}. \tag{5}$$

In the same way, in the preparation of experiments with hollow slugs, one can recommend the formula

$$\alpha = v\Sigma_a + D_\perp B_\perp^2 + D_{||}B_{||}^2 - C_0\left(\frac{D_\perp B_\perp^2 + D_{||}B_{||}^2}{D_0}\right)^2 - GB_{||}^3, \tag{6}$$

with which one must bear in mind condition (5).

Neutron Momentum Loss in a Slug with a Single Central Channel

The damping constant α for neutron momenta in a slug with a single channel can be determined using elementary reasoning. From consideration of the neutron balance in the slug, we obtain in this case the absorption probability

$$v\Sigma_a = \frac{1}{1+p}(v\Sigma_m + pv\Sigma_B\eta), \tag{7}$$

where Σ_m and Σ_B are the macroscopic cross sections for the material and air; η is the ratio of the neutron flux, averaged over the channel, to that averaged over the material.

For η in the case for a slug with rectangular cross section $a \times b$, the zeroth-order approximation is sufficient, and we obtain

$$\eta \approx \frac{a}{\int\limits_{-\frac{a}{2}}^{\frac{a}{2}}\cos\frac{\pi x}{a}\,dx}\cdot\frac{b}{\int\limits_{-\frac{b}{2}}^{\frac{b}{2}}\cos\frac{\pi y}{b}\,dy} = \frac{\pi^2}{4}. \tag{8}$$

From the diffusion approach, we obtain the transverse leakage probability as follows:

$$y_\perp \approx D_0B_\perp^2\left(1+\frac{2\Delta B_\perp}{B_\perp}\right) \approx D_0B_\perp^2(1+0.5p) \equiv D_0B_\perp^2\delta. \tag{9}$$

Here $B_\perp$ is the transverse buckling of the slug without a channel; $\Delta B_\perp$ is the change due to the channel.

In order to obtain an expression for the probability of prolonged leakage, we consider the analogous expression for the case of a slug with a lattice of channels. The latter can be written in the form

$$y_{||} = D_{||}B_{||}^2 = D_0B_{||}^2 + (D_{||} - D_0)B_{||}^2.$$

The second term on the right side, which describes the increase in the leakage resulting from the channel, must be proportional to the neutron flux in the neighborhood of the channel, whereas the first term on the right is proportional to the average over a unit flux. For the case of a slug with a large number of channels, this flux ratio equals one. Clearly, for a slug with a single channel, the probability for transverse leakage is determined by the expression

$$y_{\parallel} = D_0 B_{\parallel}^2 [1 + \eta (S_{\parallel} - 1)]. \quad (10)$$

Finally, the formula for the damping constant with calculation of the terms for diffusion cooling and the transport corrections, which are obtained by arguments analogous to those discussed in connection with consideration of a slug containing a channel lattice, assumes the characteristic form

$$\alpha = v\Sigma_a + D_0 B_{\perp}^2 \delta + D_0 B_{\parallel}^2 [1 + \eta (S_{\parallel} - 1)] - GB_{\parallel}^3 - C_0 B_{\perp}^4 \delta^2 - C_0 B_{\parallel}^4 [1 + \eta (S_{\parallel} - 1)]^2 - 2C_0 \delta B_{\perp}^2 B_{\parallel}^2 [1 + \eta (S_{\parallel} - 1)].$$

LITERATURE CITED

1. G. Dardell, Trans. Roy. Inst. Technol., 1, No. 75 (1954).
2. I. S. Grigor'ev and V. M. Novikov, Neutron Diffusion in Heterogeneous Media [in Russian], Atomizdat, Moscow (1968).
3. I. F. Zhezherun, At. Énerg., 32, 143 (1972).
4. A. V. Stepanov, "Dispersion law for the control of neutron transport in heterogeneous media," Preprint No. 10, P. N. Lebedev Institute of Physics of the Academy of Sciences of the USSR, Moscow (1969).
5. M. V. Kazarnovskii and F. L. Shapiro, in: Neutron Physics [in Russian], Atomizdat, Moscow (1961).
6. N. I. Laletin, At. Énerg., 7, 18 (1959).

RECORDING OF ACOUSTIC-EMISSION SIGNALS IN CONSTRUCTION ELEMENTS

Yu. V. Miloserdin, V. M. Baranov, and K. I. Molodtsov

UDC 621.039.564:534.8

The phenomenon of generation of sonic and ultrasonic waves in materials during their deformation (acoustic emission) is finding broader application in science and technology, in particular, in nuclear power engineering [1, 2]. The use of methods using acoustic emission are well known in the investigation of reactor materials [3, 4], flaw detection of design elements, and also in the operational control of nuclear power plants [5].

Acoustic emission occurs throughout the deformation of a material, beginning with the stage of motion and emergence on the surface of dislocations, and ending with the complete fracture of the sample or manufactured product under investigation. This fact enhances the possibility of predicting fracture in materials and construction elements, since the emitted sound signal can be detected during microcrack formation, due to the local concentration of stresses, even when the construction element on the whole still continues to perform its function. The basic simplicity of the recording of the process, accomplished in the simplest case using a piezoelectric transducer, electronic amplifier, and detector (oscillograph, recorder, electronic counter), has favored the wide introduction of the method of acoustic emission into various areas of new technology. The basic difficulty in the realization of this method is evidently the need to eliminate acoustic and electrical background noise, which is always present under industrial and laboratory conditions. Overcoming the indicated difficulty by means of creating acoustically and electrically shielded rooms considerably restricts the area of applicability of the method.

In the operational control of nuclear power plants, the source of background noise is the technological equipment, which creates vibrations and shocks, which may be received by the transducer of the instrument, and also noises connected with the motion and boiling of the coolant. The latter factor can be used for detecting the boiling of a liquid-metal coolant in fast reactors [6]; for predicting the fracture of important elements by the method of acoustic emission, however, it presents a handicap because of the very broad frequency spectrum of the noise of boiling [7].

Two instruments have been developed for recording processes of crack formation using the acoustic emission of incipient and moving cracks. The instruments are made portable by the use of transistors and integrated circuits; the transducers of the instruments are suitable for operation in a broad temperature range.

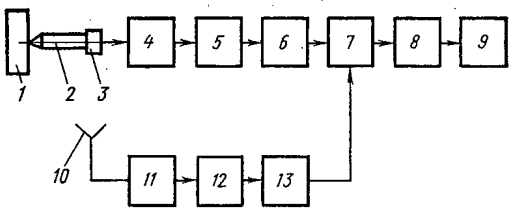

Fig. 1. Block diagram of the ultrasonic instrument for recording microcracks.

The first instrument (the acoustic-emission recorder of cracks) was developed for recording processes of crack formation in construction elements in contact with an intensely boiling liquid [8]. Solution of the indicated problem is hindered by the high temperature of the object under investigation and the intense noise of the boiling liquid, which drowns out the signals from the cracks that are formed.

Elimination of the low-frequency components of the incoming signals allows us to simultaneously eliminate the

Translated from Atomnaya Énergiya, Vol. 32, No. 4, pp. 330-331, April, 1972. Original article submitted September 28, 1971.

spurious signals connected with the ambient noise, which have comparatively narrow frequency spectrum (up to 50-100 kHz). The instrument was designed in the form of a portable electronic block with a self-contained power supply, having an external piezoelectric probe with a preamplifier. To transmit the oscillations from the heated object to the piezotransducer, we use a stainless-steel bar 3 mm in diameter. One end of the bar is fastened to a clamp attachment of the external probe of the instrument, which ensures a reliable contact between it and the piezotransducer; the second end, with the use of a protective device, is brought into contact with the object. Such a design ensures normal operation of the piezotransducer at temperatures up to 700-800°C, high sensitivity owing to the direct contact between the piezotransducer and the amplifier without having to use a high-frequency cable, and the complete elimination of industrial electrical noises.

When a crack forms, the instrument generates a sonic warning signal. Furthermore, a connection is provided for external recording devices (recorder, loop oscillograph or electronic oscillograph, or electronic pulse counter). Testing of the instrument showed that it reliably records the formation of cracks of size 0.5-0.8 mm and above, and also the supercritical growth and branching of similar cracks. The intensity of the noise of boiling can exceed the magnitude of the signal being recorded by 200-250%. Signals resulting from crack formation in zirconium carbide are reliably recorded for rapid cooling of samples in water from 500-700°C, accompanied by vigorous boiling of the water. The minimum recordable magnitude of elastic stress of the effective signal acting on the transducer was 3-5 g/mm^2.

The second instrument (for recording microcracks) differs from that already described by the presence of an electromagnetic-noise blocking circuit, thanks to which it proves to be possible to increase the sensitivity of the instrument and ensure that it can obtain its power supply from a commercial electrical line. A block diagram of the instrument is shown in Fig. 1. The acoustic signal from the sample (or the construction element) 1 through the acoustic line 2 proceeds to the piezotransducer 3, positioned together with the preamplifier 4 of the transducer signals in the body of the external probe. After passing through the preamplifier, the signal passes to the main amplifier 5, which has a gain of about 50,000 and a pass band of 500 kHz-3 MHz. After the signal is detected by the detector 6, it passes to the input of the suppression circuit 7. The function of the latter is to filter the signals that result from the passage of the electrical noise into the amplifier channel (blocks 4-6). To carry out the filtering, an additional channel (blocks 10-13) is provided; this records the electrical noises. For the indicated purpose, we connect the transducer with the main amplifier to the cable; the positioned wire conductor plays the role of the antenna 10, the signal from which is amplified by the amplifier 11, detected by the detector 12, and shaped by the shaper 13. The shaped signal is controlled by the operation of the circuit 7, which blocks the signal when there is electromagnetic noise. The signals that are transmitted to the output of the circuit 7 are, in addition, amplified by the amplifier 8, and fed to the input of the compatible cascade 9, with which the output jack of the instrument is connected. A recording device can be connected to the output of the instrument.

Thanks to the noise-shielding circuitry of the instrument, we are assured high sensitivity with the absence of spurious signals at the output of the sources of acoustic and electrical noise. Preliminary testing of the instrument showed that it is possible to record the initial formation of cracks 0.1-0.2 mm in length for object temperatures limited only by the melting point of the material of the acoustic line. The instrument was used for the investigation of vibrational fatigue of separate materials under various operational conditions, including corrosive action and high test temperatures. In particular, it was established that it is possible to predict the fatigue fracture of certain brittle materials, e.g., graphite.

In materials-research laboratories dealing with the development of reactor materials, the instruments described can be used to investigate strength characteristics, corrosion cracking, hydridization radiation, and thermocyclic effects on materials, and in the solution of other research problems.

LITERATURE CITED

1. R. Liptai and D. Harris, Mater. Research and Standards, 11, 8 (1971).
2. A. Green, Nucl. Safety, 10, 4 (1969).
3. K. Gilchrist and D. Wells, Carbon, 627 (1969).
4. D. Romrell and L. Bunnell, Mater. Evaluation, 28, 267 (1970).
5. J. Vetrano and D. Joll, Mater. Evaluation, 29, 23A (1971).
6. R. Saxe, IEEE Trans., NS-18, Pt. 1, No. 1, 337 (1971).
7. M. Osborne and F. Holland, J. Acoust. Soc. Am., 19, 13 (1947).
8. V. M. Baranov and V. A. Luk'yanenko, VII All-Union Acoustics Conf. (Summary of Papers) [in Russian], Leningrad (1971), p. 104.

DETERMINATION OF THE INDIVIDUAL FLUXES OF γ-QUANTA AND NEUTRONS BY MEANS OF A THERMOLUMINESCENT LiF CRYSTAL

K. M. Kudelin

UDC 539.1.07:539.12.08

The thermoluminescence curve of a lithium fluoride crystal used in detectors for measuring γ-ray and x-ray doses [1, 2] in the 20-200°C temperature range has two clearly separated thermal peaks, one at 140 and one at 180°C. On irradiation with γ-quanta (up to 100 R) the value of the first thermal peak is three to four times that of the second thermal peak. The ratio of the amplitudes of the thermal peaks changes sharply when the crystal is irradiated with heavy particles (n, α) [3].

Figure 1 shows the curves of the thermoluminescence of the same specimen of LiF upon irradiation with γ-quanta (a Co^{60} source) and neutrons (a Pu – Be source). The numerical values of the ratio of the amplitudes of the two thermal peaks ($\delta = I_2/I_1$, where I_1 and I_2 are the amplitudes of the thermal peaks at 140 and 180°C, respectively) are $\delta_\gamma = 0.43$ and $\delta_n = 1.45$. The inequality $\delta_\gamma < \delta_n$ was satisfied for all the LiF crystal specimens investigated (more than 100 specimens). A variation in the neutron flux of three to four decimal orders of magnitude from the lower threshold of sensitivity of the crystal ($\sim 10^6$ neutrons/cm^2) does not affect the value of the ratio δ_n. The variation (i.e., the increase) of δ_γ begins at a γ-ray dose of the order of 250 R [3]. The difference between the δ_γ and δ_n values was used in determining how much of the amplitudes of the thermal peaks was caused by the neutron and γ-components of the Pu – Be source. After irradiation, the crystals were de-excited by means of the instrument described in [2] with a heating rate of ~4°C/sec. The rate of heating was kept constant to within ±5%.

Using the notation $\delta_n = I_{2n}/I_{1n}$ and $\delta_\gamma = I_{2\gamma}/I_{1\gamma}$, where I_{1n}, I_{2n}, $I_{1\gamma}$, and $I_{2\gamma}$ are the amplitudes of the first and second thermal peaks, respectively, upon irradiation with neutrons alone and with γ-quanta alone, we can write

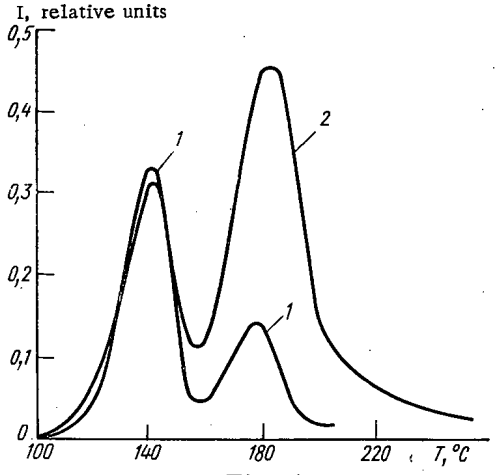

Fig. 1

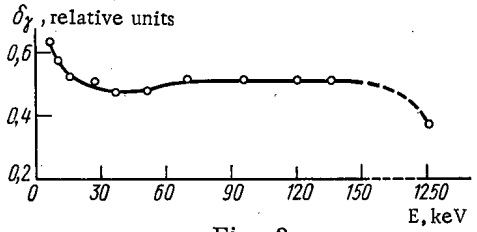

Fig. 2

Fig. 1. Curve of thermoluminescence of an LiF crystal on irradiation with γ-quanta (0.4 R) and neutrons ($\sim 5 \cdot 10^7$ neutrons/cm^2) (curves 1 and 2, respectively).

Fig. 2. Variation of δ_γ as a function of γ-ray energy.

Translated from Atomnaya Énergiya, Vol. 32, No. 4, pp. 331-333, April, 1972. Original article submitted March 9, 1971; revision submitted October 18, 1971.

TABLE 1. Results of Experiments to Determine the Contribution of Neutrons and γ-Quanta from a Pu – Be Source

No. of crystal	δ_n	δ_γ	$\delta_{n+\gamma}$	k_n	$\delta'_{n+\gamma}$	k'_n	$\delta''_{n+\gamma}$	k''_n
1	1,58	0,414	1,19	0,666	0,850	0,375	0,780	0,314
2	1,83	0,426	1,25	0,586	1,00	0,408	0,860	0,309
3	1,98	0,462	1,51	0,663	1,05	0,389	0,950	0,321
4	2,45	0,660	1,87	0,676	1,38	0,401	1,22	0,313
5	2,51	0,615	1,89	0,673	1,43	0,430	1,27	0,316
Average values	2,09	0,515	1,57	0,655	1,14	0,401	1,02	0,315

$$\delta_{n+\gamma} = k_n\delta_n + k_\gamma\delta_\gamma, \tag{1}$$

where $\delta n + \gamma = I_{2(n+\gamma)}/I_{1(n+\gamma)}$; $I_{1(n+\gamma)}$ and $I_{2(n+\gamma)}$ are the amplitudes of the first and second thermal peaks on irradiation with a mixed flux of $n + \gamma$; k_n and k_γ are the relative contributions of the neutron and γ-components to the amplitude of the first thermal peak, and

$$k_n = \frac{1}{1+\Delta}, \quad k_\gamma = \frac{\Delta}{1+\Delta}, \tag{2}$$

where $\Delta = I_{1\gamma}/I_{1n}$.

For known values of δn and $\delta\gamma$ and for a given (measured) value of $\delta n + \gamma$, we immediately obtain the values of k_n and k_γ from the expression (1):

$$k_n = \frac{\delta_{n+\gamma} - \delta_\gamma}{\delta_n - \delta_\gamma}; \tag{3}$$

$$k_\gamma = \frac{\delta_n - \delta_{n+\gamma}}{\delta_n - \delta_\gamma}. \tag{4}$$

Using the values of the contributions of the separate components to the amplitude of the first thermal peak, we can determine the signals of thermoluminescence from the neutrons and the γ-quanta of a given source and thereby determine the exposure dose of each of the components:

$$I_{1n} = k_n I_{1(n+\gamma)}; \tag{5}$$

$$I_{1\gamma} = (1 - k_n)\, I_{1(n+\gamma)}. \tag{6}$$

Thus, a thermoluminescent detector with two clearly distinct thermal peaks can be used, in principle, for determining the amounts contributed by the different sources in the $n + \gamma$ flux without using any additional means for separating one of the components. However, since the values of δn and $\delta\gamma$ depend on the energy of the neutrons [3] and the γ-quanta (Fig. 2), respectively, the determination of k_n or k_γ by formula (3) or formula (4) is possible only in the case when δn and $\delta\gamma$ are known for radiation of a given spectral composition present in the flux being measured.

The validity of the relation (1) was verified experimentally by varying the relative contribution of neutrons and γ-quanta to the amplitudes of the thermal peaks. The ratio δn (see Table 1) was determined by using a Pu – Be source with the crystals shielded with lead 5 mm thick. The ratio $\delta\gamma$ was determined by means of an x-ray apparatus at an effective x-ray energy of 35 keV and a dose of 400 mR. The crystals were then irradiated without any shield, using a Pu – Be source with a neutron flux of $4.1 \cdot 10^7$ neutrons/cm^2. In this case the thermoluminescence signal for the first thermal peak (the average value obtained from five crystals) was equal to the signal produced by irradiation with a dose of 350 mR. The table shows the experimental values of $\delta n + \gamma$ and k_n. Using the values of $\langle k_n \rangle$ (see Table 1), we find from the expressions (5) and (6) the contribution made by neutrons and γ-quanta to the amplitude of the first thermal peak: I_{1n} = 230 mR and $I_{1\gamma}$ = 120 mR.

After irradiation of the crystals with a Pu – Be source ($4.1 \cdot 10^7$ neutrons/cm^2) and, in addition, with an x-ray apparatus (effective energy of 35 keV, dose 200 mR), we measured the values of $\delta'_n + \gamma$ (see Table 1) and determined the contributions k'_n, where $\langle k'_n \rangle = 0.401$, and the calculated value of the contribution determined from formula (2) is 0.418. The eighth and ninth columns of Table 1 show analogous results for additional irradiation of the crystals with a dose of 400 mR. For this case we have: $\langle k''_n \rangle = 0.321$, whereas

the value found from formula (2) for the neutron contribution is 0.307. In each case, for the additional irradiation, the discrepancy between the experimental and calculated values of k_n does not exceed ±5%.

In conclusion, we must point out that a determination of the contributions of the different components by the method discussed above is possible only when the thermoluminescence signal values caused by the neutron component and the γ-component are comparable in magnitude.

LITERATURE CITED

1. K. M. Kudelin, V. B. Bulgakov, and G. N. Popov, At. Énerg., 26, 385 (1969).
2. K. M. Kudelin, V. B. Bulgakov, and A. A. Lebedev, Pribory i Tekh. Éksperim., No. 1, 69 (1968).
3. E. N. Brandes, K. M. Kudelin, and A. M. Shalagin, Trudy Metrolog. Inst. SSSR, No. 124 (184), Standartov (1970), p. 224.

EXPERIMENTAL DETERMINATION OF SENSITIVITY OF DIRECT CHARGE DETECTORS IN THERMAL AND EPITHERMAL REGION

N. D. Rozenblyum, E. N. Babulevich,
A. E. Alekseev, V. A. Zagadkin,
V. S. Kirsanov, É. M. Kuznetsov,
A. A. Kononovich, and M. G. Mitel'man

UDC 539.1.074.88

The present article is devoted to the calibration of direct charge detectors (DCD) with rhodium, silver, and vanadium emitters in the thermal and epithermal regions.

The sensitivity in the epithermal region was determined for DCD with rhodium emitter of 0.5 ± 0.01 mm diameter and 100 mm length. A quartz capillary with 0.15 mm thick wall served as the insulator of the emitter. A 200 mm long cadmium sheath with 0.76 mm thick wall was put on the DCD as filter. The DCD current was measured by a PÉMU-1 amplifier with an overall error of 5%. The neutron flux was determined by the gold foil method [1].

The calibrated detector and the gold foil were alternately placed at the same point in the reactor. The activity of the gold foil due to the capture of epithermal neutrons was determined by the expression

$$A = N_{Au}(1 - e^{-\lambda t_1})\, e^{-\lambda t_2} \Phi_e I F_{Cd}, \quad (1)$$

where NAu is the number of gold atoms in the foil, λ is the radioactive decay constant of gold, t_1 is the irradiation time, t_2 is the time elapsed from the end of the irradiation to the measurement of the activity, Φ_e is the flux of epithermal neutrons, I = 1533 ± 40 barn is the resonance integral for gold [2], and F_{Cd} is the coefficient of cadmium correction [2].

The maximum admissible relative error in the determination of the flux of epithermal neutrons was determined from the formula

$$\delta\Phi = \delta A + \delta N_{Au} + \delta(1 - e^{-\lambda t_1}) + \delta e^{-\lambda t_2} + \delta I; \quad (2)$$

it comprised ±7.7%.

TABLE 1. Calibrated Detectors

Number of DCD	Emitter				Insulator		Filter	
	material	diameter, mm	length, mm	weight, g	material	thickness, mm	material	thickness, mm
733	Rhodium	0.8	150	0.888	Quartz	0.2	—	—
734	Vanadium	1.0	150	0.678	"	0.2	—	—
735	Silver	1.0	150	1.177	"	0.2	—	—
471	"	1.0	150	1.175	"	0.2	Cadmium	0.75
472	Rhodium	0.8	150	0.888	"	0.2	"	0.75

Translated from Atomnaya Énergiya, Vol. 32, No. 4, pp. 333-335, April, 1972. Original article submitted February 23, 1971; revision submitted July 15, 1971.

TABLE 2. Results of Experiment

Depth of insertion into active zone, cm	i_T^{Rh}, μA	i_e^{Rh}, μA	i_T^{Ag}, μA	i_{Ag}^e, μA	i_V, μA	$\frac{i_T^{Ag}}{i_T^{Rh}}$	$\frac{i_e^{Ag}}{i_e^{Rh}}$	$\frac{i_V}{i_T^{Rh}}$
0	1,34±0,21	0,19±0,037	0,87±0,08	0,88±0,016	0,083±0,003	0,61±0,155	0,42±0,16	0,062±0,12
10	1,86±0,23	0,44±0,022	1,3±0,19	0,23±0,025	0,1±0,005	0,7±0,19	0,52±0,083	0,054±0,094
20	2,73±0,23	0,59±0,027	1,7±0,17	0,34±0,021	0,16±0,018	0,62±0,114	0,58±0,063	0,058±0,11
30	3,41±0,2	0,78±0,022	1,98±0,17	0,42±0,021	0,21±0,015	0,58±0,083	0,54±0,042	0,061±0,08
40	3,8±0,18	1,0±0,022	2,22±0,16	0,53±0,02	0,23±0,014	0,58±0,07 *	0,53±0,03 *	0,06±0,065*

*Values used in calculations.

The flux of epithermal neutrons, measured from the activation of gold foil, is $(1.9 \pm 0.15) \cdot 10^{11}$ neutrons/cm^2·sec; the DCD current screened by the cadmium filter was 0.0062 ± 0.0005 μA and the sensitivity of the DCD to epithermal neutrons was $\varphi = (3.3 \pm 0.6) \cdot 10^{-19}$ A·cm^2·sec/neutron·m. The error in the determination of the sensitivity is given taking account of the identical nature of the DCD (±2%).

In order to calibrate the detectors with rhodium and silver emitters their readings were compared with those of the DCD with rhodium emitter of 0.8 mm diameter, which served as the standard. According to the data of [1] its sensitivity to thermal neutrons is $(2.1 \pm 0.2) \cdot 10^{-19}$ A·cm^3·sec/neutron·m. The intercalibration of the detectors was done on the reactor MR of the I. V. Kurchatov Atomic Energy Institute.

In order to take account of the background currents of the connecting line of the detector a two-core cable of type KTMS-2 with magnesium insulation was used. One of the cores was used as the current-carrying core and the other, placed in conditions identical to those of the first, was used as the background core. The detector current was taken as the algebraic difference of the two currents. The magnitude of the background current was proportional to the depth of insertion of the cable into the active zone of the reactor. In order to reduce the error due to the background current the measurements were made in the upper part of the active zone.

Five DCD were prepared; the data for these are given in Table 1.

The calibration error is determined from the formula

$$\delta\varphi = \delta\varphi_{Rh} + \delta i_{Rh} + \delta i_{cal} \tag{3}$$

Here $\delta\varphi_{Rh}$ is the maximum admissible error in the determination of the sensitivity of the standard rhodium detector; δi_{Rh}, δi_{cal} are respectively the maximum admissible error in the measurement of the currents of the standard and the calibrated detectors:

$$\delta i = \delta i_{ins} + \delta i_{pos}, \tag{4}$$

where δi_{ins} is determined by the accuracy class of the measuring instrument and δi_{pos} is determined by the error in fixing the position of the detector (±1 cm).

The results of the measurements, with the currents in the connecting line taken into consideration, are given in Table 2; the volume of the detector currents, caused by thermal and epithermal neutrons, and also their ratio to the current of the standard detector are given.

Table 2 shows that the scatter of the data is within the limits of accuracy of the experiment; the error for the point corresponding to insertion depths of 30 and 40 cm is the minimum. Just these points were used in the computations.

The current due to thermal neutrons is

$$\begin{aligned} i_T^{Ag} &= \varphi_T^{Ag}\Phi_T, \\ i_T^{Rh} &= \varphi_T^{Rh}\Phi_T, \end{aligned} \tag{5}$$

where i_T^{Ag}, i_T^{Rh} are respectively the current due to thermal neutrons for rhodium and silver detectors; φ_T^{Ag}, φ_T^{Rh} are the sensitivities of the detector to thermal neutrons; and Φ_T is the flux of thermal neutrons.

It follows from (1) that

$$\frac{\varphi_T^{Ag}}{\varphi_T^{Rh}} = \frac{i_T^{Ag}}{i_T^{Rh}}, \tag{6}$$

i.e., the ratio of the sensitivities of the detectors in the thermal region is equal to the ratio of their currents caused by thermal neutrons.

Similarly for the epithermal region we have

$$\frac{\varphi_e^{Ag}}{\varphi_e^{Rh}} = \frac{i_e^{Ag}}{i_e^{Rh}}, \tag{7}$$

where φ_T^{Ag}, φ_e^{Rh} are the sensitivities of the DCD in the epithermal region; i_e^{Ag}, i_e^{Rh} are the DCD currents caused by epithermal neutrons.

Knowing the sensitivity of a DCD with rhodium emitter in the thermal region we find the sensitivity for a DCD with silver emitter of 1 mm diameter:

$$\varphi_T^{Ag} = (1.2 \pm 0.26) \cdot 10^{-19} \text{ A} \cdot \text{cm}^2 \cdot \text{sec/neutron} \cdot \text{m}.$$

It follows from Table 2 that the contribution of epithermal neutrons in the readings of the rhodium DCD is not more than 12% for zero insertion depth and reaches 21% for insertion of the DCD to 40 cm.

It is well known that

$$\frac{I^{Rh}}{\sigma_T^{Rh}} \gg \frac{I^V}{\sigma_T^V}, \tag{8}$$

where I^{Rh}, I^V are the resonance integrals for rhodium and vanadium [2]; σ_T^{Rh}, σ_T^V are the activation cross sections for rhodium and vanadium respectively.

It follows from (8) that the relative contribution of epithermal neutrons in the readings of a vanadium DCD is much smaller than for rhodium DCD and it can be assumed with 2-4% accuracy that the readings are only due to thermal neutrons. Knowing the sensitivity of the standard DCD in the thermal region and the ratio of the currents of the vanadium and the standard DCD we find the sensitivity of the vanadium DCD with an emitter of 1 mm diameter:

$$\varphi_T^V = (1.2 \pm 0.26) \cdot 10^{-20} \text{ A} \cdot \text{cm}^2 \cdot \text{sec/neutron} \cdot \text{m}.$$

LITERATURE CITED

1. A. E. Alekseev et al., At. Énerg., 28, 139 (1970).
2. K. Bekurts and K. Virts, Neutron Physics [in Russian], Atomizdat, Moscow (1968).

GAMMA-RAY DETECTORS FROM i-CONDUCTIVITY GERMANIUM

V. S. Vavilov, L. A. Goncharov,
T. I. Pavlova, Ya. Khurin,
and M. V. Chukichev

UDC 539.1.074.55

At the present time germanium detectors for γ-ray spectrometry are usually fabricated by introducing lithium ions into p-type material [Ge(Li)-detectors] or by compensating n-type germanium by means of radiation-induced defects (radiation detectors). A disadvantage of Ge(Li)-detectors, associated with the behavior of lithium at room temperatures in the lattice of germanium, is that they require permanent cooling.

Compensation of germanium by radiation-induced defects has the advantage that the detectors are stable at room temperatures. The technology of making detectors suitable for spectrometry is, however, far from easy.

The construction of a detector based on hyperpure germanium with a conductivity close to intrinsic [1] marks a new stage in the development of semiconductor γ-ray spectrometry. As there is so far no universally accepted terminology for this sort of device, we propose to call it an i-germanium γ-detector.

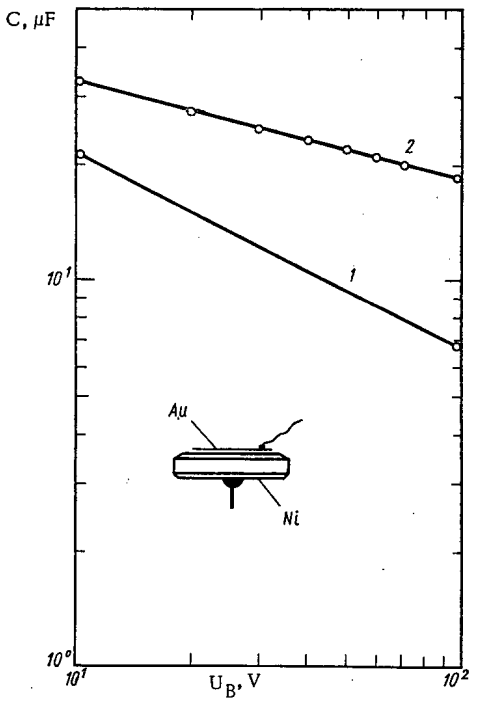

Fig. 1

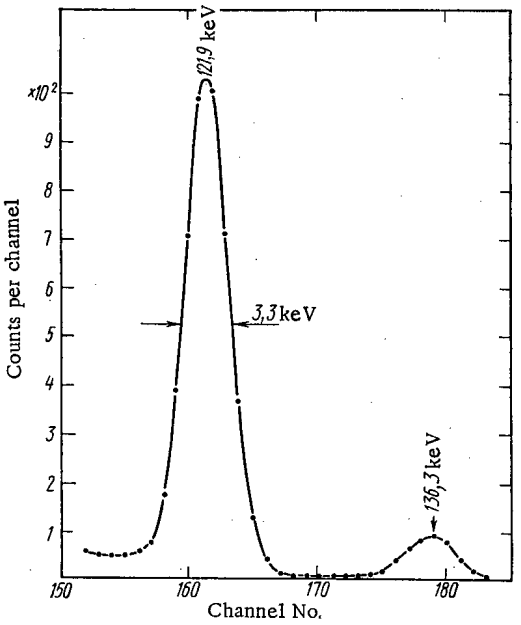

Fig. 2

Fig. 1. Voltage–capacitance characteristic of i-germanium γ-detector: 1) detector capacitance; 2) capacitance of detector and cryostat.

Fig. 2. Co^{57} spectrum obtained with investigated detector (U_B = 48 V, S = 20 mm^2, T = 77°K).

Translated from Atomnaya Énergiya, Vol. 32, No. 4, pp. 335-336, April, 1972. Original article submitted July 30, 1971.

Thanks to the work of Hall [2] on the purification of germanium it is now possible to obtain single crystals with $N_D - N_A$ as low as $2 \cdot 10^{10}$ cm^{-3}. Theoretically, if there are no deep recombination centers or trapping centers this permits of a sensing layer of thickness more than 10 mm and of good energy resolution. However, in his estimate of the required degree of purity (residual impurity concentration), Hall concerns himself only with the difference in the concentrations of the electrically active impurities. He thus connects subsequent progress in the use of i-germanium for γ-ray detectors only with purification which reduces the difference $N_D - N_A$, and he does not consider the influence of the net impurity concentration.

It does not follow that "purity" in the strict sense should be understood to mean only a low value of $N_D - N_A$.

It is shown in [3] that for $N_D - N_A \approx 10^{12}$-$10^{11}$ cm^{-3} the net impurity concentration ($N_D + N_A$) can be as much as $\sim 10^{13}$ cm^{-3}, which characterizes a high level of compensation. At high compensation levels there is an increase in the scattering of carriers by charge centers and in the volume inhomogeneity of the material, which will degrade the resolution of the detector even if there are no trapping effects. It is thus highly desirable to investigate how the characteristics of i-detectors are influenced by the degree of compensation.

In our experiment we used germanium with $N_D - N_A = 1.5 \cdot 10^{12}$ cm^{-3} and $\mu = 3.8 \cdot 10^4$ cm^2/V $\cdot$ sec at 77°K. The measured net concentration $N_D + N_A = 1.35 \cdot 10^{14}$ cm^{-3}. The values of ($N_D - N_A$), μ, and ($N_D + N_A$) were measured in samples cut from the crystal immediately adjacent to the slab used as the detector. The crystal was grown in the $\langle 111 \rangle$ direction. Its diameter was 28 mm and the dislocation density was $2 \cdot 10^3$ cm^{-2}.

The sample was nickel plated after the usual mechanical treatment. The bottom surface of the sample was then masked and the nickel removed from the rest of the surface by nitric acid. The sample was thereupon etched in CP4A (three times at 1 min each) and washed with deionized water. After this it was etched for 2 min in a 1 : 1 mixture of HF and H_2O_2. The sample was then carefully washed with deionized water. A gold electrode was then evaporated onto the etched surface and a lead attached by means of FSP-49 silver adhesive. The resulting surface-barrier detector was placed in a cryostat for the subsequent measurements.

The voltage – capacitance characteristic of the detector was plotted (Fig. 1). The slope of this curve is around 0.5, a result typical for a sharp p – n junction. This detector was used at a bias of 50 V to record the spectrum of Co^{57}. The result is shown in Fig. 2. The intrinsic noise level of the electronics is ~1.6 keV. As can be seen from the figure, the total resolution equals 3.3 keV.

Our results show that a homogeneity of the initial material acceptable for spectrometry detectors can be attained even at a large compensation level and that, consequently, the spectrometry properties of the detectors can be improved by reducing the net impurity concentration. Our results also indicate the feasibility of employing highly compensated material in the fabrication of detectors for certain physical problems.

LITERATURE CITED

1. A. Tavendale, Nucl. Instrum. and Methods, 84, 314 (1970).
2. R. Hall, Semiconductor Nuclear-Particle Detectors and Circuits, Publ. No. 1593, National Academy of Sciences, Washington (1969), p. 171.
3. B. A. Sakharov et al., Tsvetnye Metally, No. 7, 52 (1970).

GERMANIUM RADIATION COUNTERS AS CHARGED-PARTICLE SPECTROMETERS

S. M. Ryvkin, V. V. Peller,
N. B. Strokan, V. P. Subashieva,
N. I. Tisnek, and V. K. Eremin

UDC 539.1.074.55

The usual application of germanium counters is in γ-ray spectrometry. Ge(Li)-counters have been used with success, however, in charged-particle spectrometery [1]. In comparison with silicon, germanium has a greater retarding capability and a smaller mean energy of formation of electron–hole pairs.

In the present note we communicate the results of some experiments in which germanium radiation counters were used to determine the energy of charged particles [2-4]. Such counters, as opposed to Ge(Li)-detectors, can function stably at room temperature and do not require to be permanently cooled. The resolution R of radiation detectors depends on the donor impurity concentration N_D in the initial germanium. For presently attainable values of $N_D \approx 5 \cdot 10^{12}$ cm^{-3} it is possible to achieve for γ-quanta a resolution $R \leqslant 1\%$ in a working region d = 5 mm [4].* However, if ionization occurs near the p contact and the holes have to move through a distance less than 1 mm, the resolution can be expected to improve greatly (in comparison with $R \approx 1\%$).

*The resolution R can, of course, be improved or the working region extended by raising the purity of the germanium. A working region $d \approx 1$ cm can be achieved with hyperpure germanium (concentration of uncompensated impurities $\sim 10^{10}$ cm^{-3} [5]).

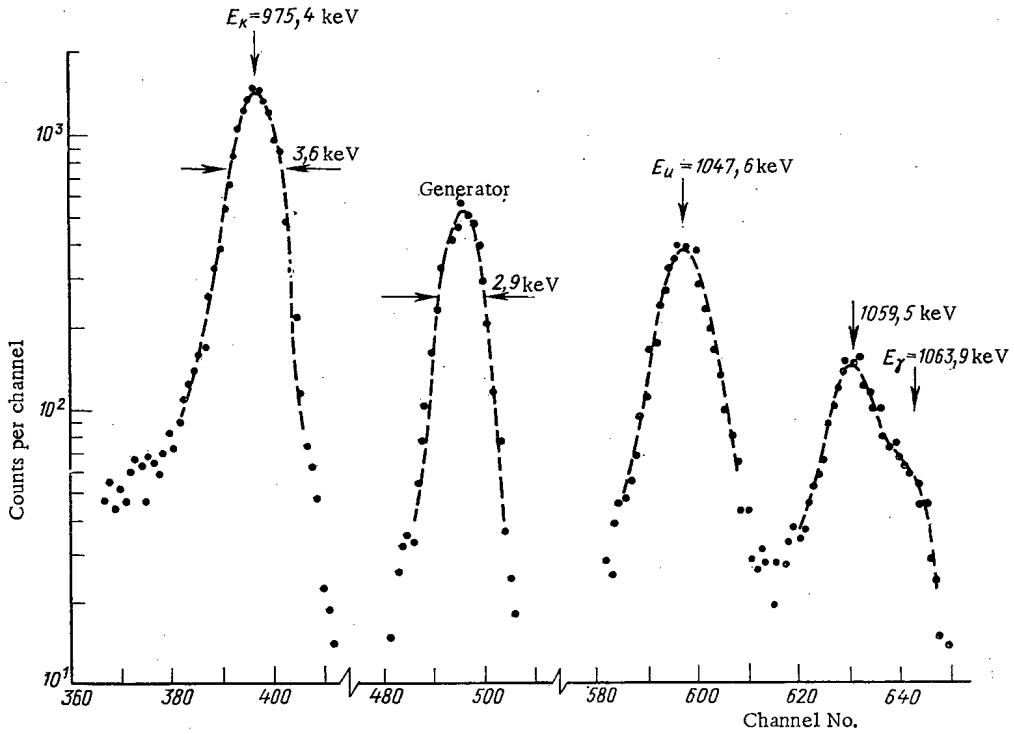

Fig. 1. High-energy portion of Bi^{207} spectrum obtained with detector sample No. 1.

Translated from Atomnaya Énergiya, Vol. 32, No. 4, pp. 336-338, April, 1972. Original article submitted May 3, 1971.

TABLE 1. Spectrometry Characteristics of Counters

Sample No.	S, cm^2	W, mm	R, for Cs^{137}, %	Ratio photopeak/compton	R_β for Bi^{207}, %	R_α for Pu^{238}, %
1	2,5	3,5	0,96	2,7	0,23	0,36
2	2,5	3,5	0,63	2,5	0,19	0,40
3	2,5	3,2	0,88	2,2	0,21	—
4	2,5	3,2	0,88	1,5	0,42	0,29
5	2,5	4,5	0,70	2,5	0,60	0,35
6	1,1	3,5	0,68	2,2	—	0,25

Another way of improving R is to utilize the anisotropy of the electron drift velocity. It is known [6] that the ultimate drift velocity in the [100] direction is 1.6 times greater than in the [111] direction normally used in the growth of germanium crystals. Indeed, observation of current pulses directly in the counter confirmed the greater velocity in the [100] direction. In the spectrometry of shortlived particles it is thus advantageous to use counters made from germanium grown in the [100] direction and irradiate the counter through the p contact.

The counters used in our measurements were made from germanium with an initial impurity concentration $\sim 5 \cdot 10^{12}$ cm^{-3} and grown in the [111] as well as the [100] direction. The detectors were mounted in sectional capsules and were irradiated with Pu^{238} α-particles and Bi^{207} electrons (see Fig. 1). Despite the considerable noise from the electronics, the lines associated with the γ- and β-radiation, separated by 4.4 keV, were almost resolved. The gold film forming the p contact also served as the "input window." During irradiation the sample, which was soldered to the base of the capsule, and the radiation source were located in a chamber evacuated by a sorption pump to $\sim 10^{-4}$ mm.

The electrical circuit contained a preamplifier with a noise level of 1.6 keV + 0.03 keV/μF (time constant of shaping circuits 1 μsec) and a Didax-800 analyzer. The experimental data on the resolution after deduction of the noise are listed in Table 1. It follows from Table 1 that the resolution of the counters for Cs^{137} γ-quanta equals 1%. The resolution for α- and β-particles is even greater.* The fact that r_β is greater than r_α for samples 4 and 5 is reasonable bearing in mind that less holes are trapped in α-particle spectrometry. The opposite result, $R_\alpha > R_\beta$, for samples 1 and 2 and also the constancy of R_α ($\sim$0.35%) can be ascribed to energy losses in the "input window." In this connection the resolution of sample 2 exhibits a very weak dependence on the bias voltage. Thus, reducing the bias from 500 to 50 V degrades the resolution in all to 26.5 keV, i.e., incomplete collection of charge has only a slight effect. The resolution for electrons, equal to 2 keV at the 1 MeV line, is only twice the ultimate value set by ionization fluctuations.

The properties of the counters were unaffected by storage under normal conditions or by repeated opening of the capsule (when changing the radiation source, mounting the counter in the chamber, and so on).

LITERATURE CITED

1. C. Gruhn et al., IEEE Trans. Nucl. Sci., 15, 337 (1968).
2. S. M. Ryvkin et al., Dokl. Akad. Nauk SSSR, 165, 548 (1965).
3. S. M. Ryvkin et al., IEEE Trans. Nucl. Sci., 15, 226 (1968).
4. S. M. Ryvkin et al., Fiz. i Tekh. Poluprov., 4, 1303 (1970).
5. R. Baertsch and R. Hall, IEEE Trans. Nucl. Sci., 17, 235 (1970).
6. M. Nathan, Phys. Rev., 130, 2201 (1963).
7. A. Kh. Khusainov, Dissertation [in Russian], Leningrad (1970).

*We note that $R_\alpha \approx 0.3\%$ was observed using radiation counters, and also in [7] for an area of 2 cm^2 and d = 2 mm.

NEUTRON RADIATION STANDARDIZATION

V. G. Zolotukhin, I. B. Keirim-Markus,
O. A. Kochetkov, V. I. Tsvetkov,
and O. V. Cherkashina

UDC 539.12.08

The recommendations of the International Commission of Radiological Protection [1] and domestic standards [2] regarding maximum permissible fluxes (MPF) of neutrons are based on calculations of the maximal equivalent dose created by monoenergetic neutrons in the human body. Such calculations were performed by Snyder and Noifeld [3] for a model of the body in the form of an infinite slab of a tissue-equivalent substance, 30 cm thick, upon which a neutron flux is directed along the normal. Obviously, this model is extremely schematic in reflecting the actual conditions under which a human being is irradiated. By our method, Monte-Carlo calculations [4] are applied to intense doses of monoenergetic neutrons which are incident on an infinite, elliptical cylinder, with axes of 24 and 36 cm, of tissue-equivalent material along eight different directions.

In Fig. 1, the energy dependence of the maximal specific equivalent dose relative to the volume of the body [3] and at the surface [4] is shown. The neutrons are incident normally (along the minor axis of the body). From a comparison of the curves, it follows that for intermediate neutrons the data in [3] are shown to be overstated as much as 80% (when E_n = 5 keV), which corresponds to the difference in the equivalent doses at the surface of the body and at maximum, which for the given E_n occurs deep within the body.

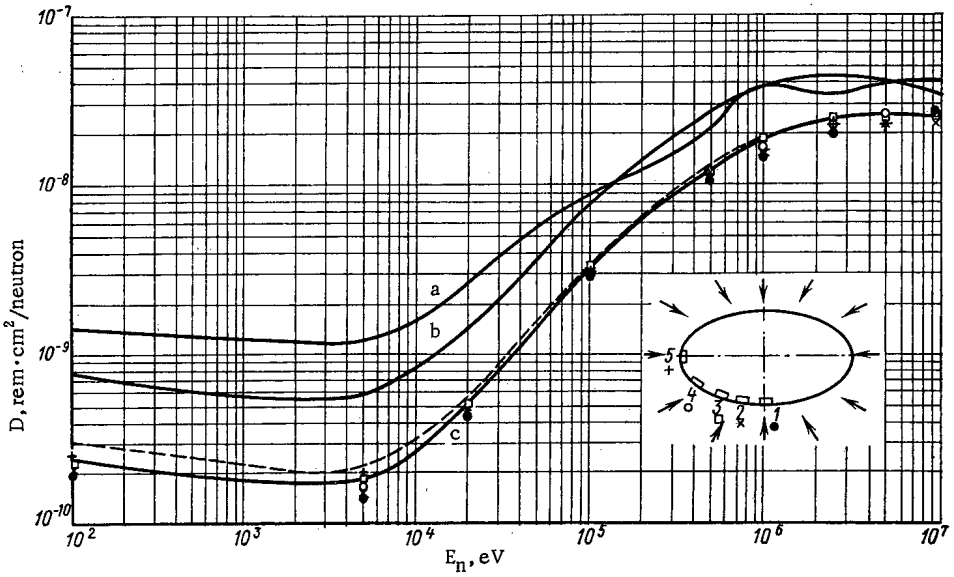

Fig. 1. Specific equivalent dose D of monoenergetic neutrons: a) maximal in the human body at normal incidence [3]; b) on the surface of the body at normal incidence [4]; c) maximal on the surface of the body with isotropic irradiation; the points show the values at corresponding regions of the surface of the body; the broken line is the recommended value.

Translated from Atomnaya Énergiya, Vol. 32, No. 4, pp. 338-339, April, 1972. Original article submitted June 3, 1971.

TABLE 1. Monoenergetic Neutron Flux Density (Neutron $\cdot cm^{-2} \cdot sec^{-1}$), Creating a Maximal Strength Equivalent Dose of 0.1 rem/week

Irradiation criterion	Neutron energy										
	thermal	100 eV	5 keV	20 keV	100 keV	500 keV	1 MeV	2,5 MeV	5 MeV	10 MeV	Literature
Maximum for the body at normal incidence of radiation "from the front"	730	550	670	280	80	37	19	23	19	17	[1, 3]
Same as above	694	771	926	434	109	35	27	20	17	14	[7]
Maximum for the body's surface for unidirectional radiation	—	1000	1290	520	95	30	20	18	18	17	Authors' data
Maximum on the surface for radiation isotropic in the horizontal plane	—	2250	2880	1320	220	65	43	31	28	28	The same
Maximum on the surface for radiation, isotropic in space	—	3100	4100	1470	230	65	42	32	30	30	" "
Recommended values	4000	2500	3500	1400	230	65	40	30	30	30	" "
Recommended coefficient of isotropy	6,0	5,0	6,1	5,0	2,9	2,2	2,2	1,5	1,6	1,7	" "

Man is almost always exposed to the influence, not of monoenergetic neutrons, but those with a broad energy spectrum [5]. For this case, the neutron dose is maximal at the surface of the body, decreasing with depth, while for monoenergetic neutrons the maximum can be found at a depth of the body, and at different depths for various neutron energies. Therefore, under actual conditions, it is necessary to control the maximal equivalent dose at the surface of the body, but not present on the Snyder curve which describes the energy dependence of the maximal equivalent dose relative to the volume of the body in the case of monoenergetic neutrons.

Apart from this, under actual conditions during work, man is not exposed to unidirectional, but enveloping neutron irradiation. Even if the neutron radiation acting on man is not isotropic, the angular distribution of radiation relative to his body remains symmetrical relative to the vertical direction with his motion during the course of work.

Using our own data [4], we calculated the specific equivalent dose of monoenergetic neutrons on the surface of a man's body at the points shown in Fig. 1, for the case where the neutron directions are isotropically distributed in space. The results obtained are shown in Fig. 1 as points; curve b almost coincides with that for the maximal value.

As is seen from Fig. 1, the doses at the surface of the body are not equal. For small E_n, the maximal values for the equivalent doses at the surface are displaced from the middle of the body to the sides. However, the difference in the surface doses does not exceed 25%. The doses at the surface of the body with isotropic irradiation are four times lower than with the normally incident radiation, while compared to the data in [3] and the standardized values in [1, 2], it is seven times lower. This is explained by the fact that in the human body neutrons of all energies, aside from the very highest, are absorbed almost completely. Correspondingly, radiation acts on the surface of the body through approximately half of the full bodily angle. (In order to consider this fact, we recommended [5] that one introduce the coefficient of isotropy K which is equal to two for the majority of cases.) Aside from this, with neutrons incident at an angle to the normal, doses are found to be significantly lower than at normal because of an increase in the albedo of the neutrons [6]. Due to this, K is significantly larger than two when $E_n < 500$ keV.

In Table 1, values for the MPF of neutrons are shown, corresponding to 0.1 rem for a 36-hour work week, calculated with the data in [3], [7], and [4] in the case of normally incident radiation and, for our data [4], where the radiation is isotropic in the horizontal plane as well as space. From Table 1, it is seen that the MPF of neutrons, at the present time, have been received with considerable hesitation. Therefore, it follows either to reconsider the MPF of the neutrons, extending them by consideration of the data obtained or, with their practical application, to take into account the coefficient of isotropy K for the radiation, which one is able to take as 2.5, and to define more precisely the neutron spectra involved, as well as the angular distribution of the radiation incident on a human body.

The actual conditions of irradiation for a person during work, within a neutron field without protection, are intermediate between those mentioned in lines four and five of Table 1 in the majority of cases. The

radiation is usually not entirely isotropic in space. At the same time, it is not all concentrated in the horizontal directions, but falls also at angles to the body, resulting in a decrease in the dosage. On the basis of these considerations, the recommended values for the MPF of monoenergetic neutrons are presented in line six of Table 1, and the values of the coefficient of isotropy K corresponding to them are presented in line seven. It is necessary to multiply the values for the MPF of the neutrons by the coefficient K, if they are calculated for normally incident radiation (line one of Table 1), and to divide the values of equivalent doses for the neutrons, as well as their fluxes, measured by dosimetric devices, having isotropically sensitive detectors, "in air" (in the absence of screening by a human body).

LITERATURE CITED

1. Radiation Protection (Recommendations of the International Commission of Radiological Protection, Sixth Edition) [Russian translation], Atomizdat, Moscow (1967).
2. Radiation Hazards Standards [in Russian], Atomizdat, Moscow (1969).
3. Protection against Neutron Radiation up to 30 MeV, Handbook 63, National Bureau of Standards USA, Washington (1957).
4. V. G. Zolotukhin et al., Tissue Neutron Doses in the Human Body [in Russian], Atomizdat, Moscow (1972).
5. I. B. Keirim-Markus and O. A. Kochetkov, in: Problems of Dosimetry and Radiation Protection [in Russian], V. I. Ivanova (editor), Atomizdat, Moscow (1969), p. 15.

CALCULATION OF THE CONCENTRATION OF β-ACTIVE GASES RADIOMETRICALLY MEASURED WITH A CYLINDRICAL COUNTER

A. A. Gusev

UDC 539.1.074.2

Radiometric measurement of β-active gases is frequently carried out by means of cylindrical gas-discharge counters mounted in flowthrough cylindrical chambers or in cylindrical chambers designed for a single specimen [1-3]. Sometimes the counter is placed directly in the air of the room, this is typical for ventilation studies carried out by the method of radioactive indicators [4, 5]. The concentration q of the gas in the space surrounding the detector can be determined from the pulse counting rate N by means of the formula

$$N = Kq, \tag{1}$$

where K is a coefficient which depends on the geometry, on the disintegration scheme of the radiation source, and on the maximum energy of its β-spectrum.

Ordinarily K is found experimentally by various methods [1]. However, all of these methods are cumbersome, and their accuracy is not very high, owing to the associated errors in the measurement of the activity of the standard gas, in the placement of the solid source (the simulation method), in the absorption and reactions of vapors at the chamber and counter walls (the method of vaporization of volatile liquids), etc.

It is therefore desirable to make a theoretical calculation of K. Since it is difficult to allow for all the diverse factors affecting the recording of the β-particles, no suitable equation is yet known for this purpose.* Approximate calculations use the formulas for γ-active gases [2] or make allowance for the absorption of γ-rays in the counter walls, disregarding the attenuation in air and the fact that the path length

*Some calculated data are given in [5]; since the initial equation was not published, it has been impossible to appraise its usefulness.

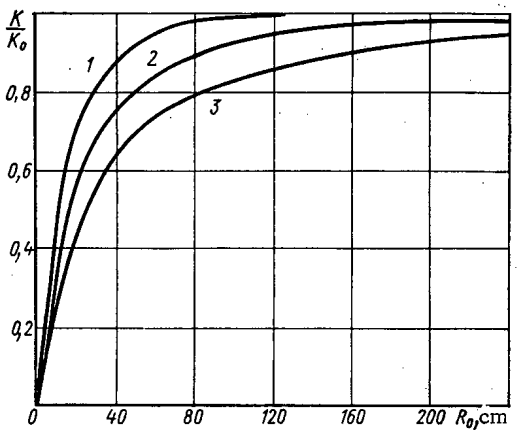

Fig. 1. Graphs of $K = K(R_0)$ for the STS-6 counter: 1) E = 0.67 MeV; 2) E = 1.2 MeV; 3) E = 2.48 MeV.

TABLE 1. Values of K for Kr^{85} and Ar^{41} (STS-6 counter)*

R_0, cm	H_0, cm			R_0, cm	H_0, cm		
	7,2	10	16		7,2	10	20
	Kr^{85}				Ar^{41}		
3	6,38	6,90	7,00	5	35,4	37,8	40,6
5	11,9	12,4	12,9	10	67,8	75,6	81,8
10	23,0	25,2	25,7	20	110	128	135
20	36,0	39,2	40,1	40	151	180	186
50	48,9	54,0	54,1	80	182	216	222
∞	53,0	58,6	58,8	∞	200	242	250

*For values of H_0 greater than those on the extreme right, the value of K is practically constant.

Translated from Atomnaya Énergiya, Vol. 32, No. 4, pp. 340-342, April, 1972. Original article submitted June 1, 1971.

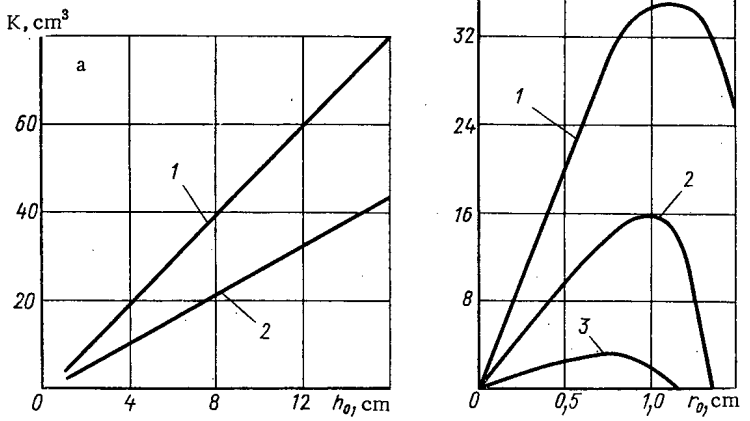

Fig. 2

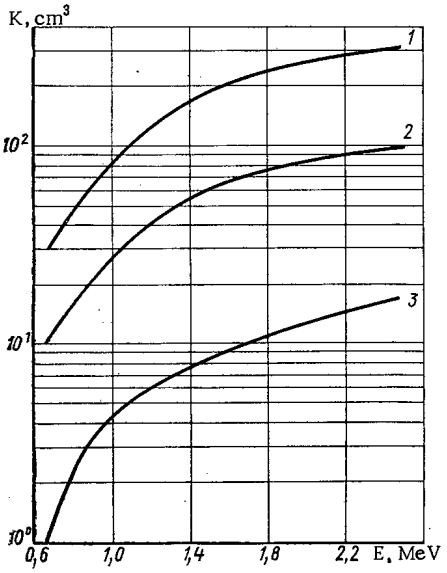

Fig. 3

Fig. 2. Graphs showing K as a function of the geometric dimensions of the counter (Kr^{85}, R_0 = 15 cm, H_0 = 20 cm, ρ_1 = 7,800 mg/cm², $c = 7 \cdot 10^{-3}$ cm): a) $K = K(h_0)$, 1) r_0 = 0.9 cm, 2) r_0 = 0.45 cm; b) $K = K(r_0)$, 1) h_0 = 7.2 cm, 2) h_0 = 3.7 cm, 3) h_0 = 1 cm.

Fig. 3. Graph of K = K(E) as $R_0 \to \infty$ and $H_0 \to \infty$: 1) STS-6; 2) STS-5; 3) SBM-10.

of the β-particles is limited [3]. In both cases, the softer the β-radiation and the larger the dimensions of the air space surrounding the radiation detector, the more significant the inaccuracies will be.

The author has derived a general equation which takes account of the β-particle path length and of the absorption of β-particles in air and in the detector walls; the derivation is given in [6]. The equation (applicable to an arrangement analogous to that of Fig. 1 of [7]) has the following form:

$$K = \varepsilon\lambda \int_{r_0-c}^{r_0} \int_{R_2}^{R_2} \int_{Z_1}^{Z_2} \int_{h_1}^{h_2} \frac{RG(R,r) \exp\left\{-G(R,Z,h,r)\left[\sigma + \frac{\sigma_1 G_1(r)}{G(R,r)}\right]\right\} dr\,dR\,dZ\,dh}{G^{3/2}(R,Z,h,r)}, \quad (2)$$

where r_0 is the outer radius of the counter; R and r are the radii vectors for an elementary volume dV of gas and an elementary area dS of the cross section of the counter; Z and h are vertical coordinates which define dV and dS; σ and σ_1 are the linear coefficients of the absorption of β-particles in air and in the counter walls; ε is the efficiency of the counter; λ is the yield of β-particles per disintegration;

$$G(R,r) = \sqrt{R^2 - r^2};\ G(R,Z,h,r) = \sqrt{R^2 + (Z-h)^2 - r^2};$$
$$G_1(r) = \sqrt{r_0^2 - r^2} - \sqrt{(r_0 - c)^2 - r^2}.$$

The limits of integration with respect to h, Z, and R take account of the goemetry and also of the possibility of recording β-particles in the case when their total path length in the gas and the walls does not exceed a maximum P. The "geometric" limits are:

$$h_1 = h_{g1} = -h_0 - \frac{(Z+h_0)G_2(r)}{G(R,r) - G_2(r)};\ h_2 = h_{g2} = h_0 - \frac{(Z-h_0)G_2(r)}{G(R,r) - G_2(r)};\ Z_1 = Z_{g1} = -H_1;\ Z_2 = Z_{g2} = H_2; \quad (3)$$
$$R_2 = R_{g2} = R_0,$$

where h_0 is half the height of the counter; H_1 and H_2 are the distances from the center of the counter to the top and bottom of the chamber; R_0 is the radius of the chamber; $G_2(r) = \sqrt{(r_0 - c)^2 - r^2}$.

The "physical" limits are expressed by the formulas

$$h_1 = h_{p1} = Z - \sqrt{\frac{P^2}{\left[\rho + \frac{\rho_1 G_1(r)}{G(R,r)}\right]^2} - G^2(R,r)};$$

$$h_2 = h_{p2} = Z + \sqrt{\frac{P^2}{\left[\rho + \frac{\rho_1 G_1(r)}{G(R,r)}\right]^2} - G^2(R,r)};$$

$$Z_1 = Z_{p1} = -h_0 - \frac{[G(R, r) - G_2(r)]}{G(R, r)} \sqrt{\frac{P^2}{\left[\rho + \frac{\rho_1 G_1(r)}{G(R, r)}\right]^2} - G^2(R, r)}; \quad (4)$$

$$Z_2 = Z_{p2} = h_0 + \frac{[G(R, r) - G_2(r)]}{G(R, r)} \sqrt{\frac{P^2}{\left[\rho + \frac{\rho_1 G_1(r)}{G(R, r)}\right]^2} - G^2(R, r)};$$

$$R_2 = R_{p2} = \frac{\sqrt{\rho^2 r^2 + [P - \rho_1 G_1(r)]^2}}{\rho},$$

where ρ and ρ_1 are the density of the air and of the counter-wall material.

The integration is carried out for whichever limit (h_g or h_p, Z_g or Z_p, R_g or R_p) is smaller in absolute value.

Equation (2) was solved numerically on an electronic computer. We give below some results of this solution for counters placed at the center of a chamber with a half-height of H_0. Table 1, for example, gives data on K for the STS-6 counter used in measurements of Kr^{85} and Ar^{41}.

The height of the measuring chamber has little effect on K, particularly for small values of E and R_0. For example, in the case of the STS-6 and the STS-5, the values of K for Ar^{41} as $H_0 \to \infty$ will be only 1.25 and 1.5 times the corresponding values of K for $H_0 = h_0$. It does not seem practical, therefore, to try to increase K by making the chamber higher.

The value of K is more strongly affected by the radius of the chamber. This fact is illustrated by the curves of Fig. 1, constructed on the basis of averaged data for different values of $H_0 \geq h_0$ corresponding to the same value of R_0 (the averaging error is of the order of 3%). The vast majority of the β-particles hitting the detector come from a volume constituting only a small percent of the volume bounded by the maximum path length. If we take as our "effective" radius of the cylinder, R_{eff}, the value at which K reaches 90% of the maximum value K_0, we can find R_{eff} approximately from the formula recommended for use in selecting the optimum volume for the measuring chamber

$$R_{eff} = 69E^{0,87}, \quad (5)$$

where R_{eff} is expressed in centimeters and E in MeV.

Figure 2 illustrates how K is affected by the dimensions of the counter. The function $K = K(r_0)$ is of interest because there is an extremum value $r_0 = r_k$. As R_0 increases, r_k will increase slightly, reaching values of 1-1.2 cm (Kr^{85}, Ar^{41}) for counters with $\rho_1 c = 40$-60 mg/cm^2 and $h_0 = 3.5$-7.5 cm in various chambers. As E increases, the coefficient K will increase, as is to be expected (Fig. 3).

The value of K is strongly affected by c, the thickness of the counter walls. Thus, as the c value of the STS-6 increases to 30% more than the average (certified) value, the value of K for Kr^{85} is reduced by a factor of 1.7. The decrease in K as the surface density of the walls is increased by $\Delta(\rho_1 c)$ can be evaluated as $\exp[-s\Delta(\rho_1 c)]$, where s is 0.033 cm^2/mg for Kr^{85} and 0.022 cm^2/mg for Ar^{41}.

The experimental verification of the calculated data was carried out by two methods. In the first case the calculated values of K were compared with the values found in measurements of the pulse counting rate: the air from a box in which ampoules containing Kr^{85} of known activity were uncovered was pumped through cylindrical chambers containing STS-5 and STS-6 counters. In the second case the $K = K(R_0)$ curve was plotted on the basis of data obtained in direct measurements using Kr^{85} and in the simulation of this gas by a Te^{127m} point source (the E values for these isotopes differ by 1.5%). The results of the comparison agreed within the limits of experimental error.

It is useful to give the approximate formulas obtained from Eq. (2), for example, for $H_1 = H_2 = H_0$ in particular cases:

1) if $R \gg r$, $Z \gg h$, $r \gg c$, $P \to \infty$, and the exponent is $n = 0$ (a "point" detector and a γ-active gas), we obtain the expression proposed in [7]:

$$K = 4\varepsilon\lambda r_0 h_0 H_0 \ln\left(\frac{R_0 + \sqrt{R_0^2 + H_0^2}}{r_0 + \sqrt{r_0^2 + H_0^2}}\right); \quad (6)$$

2) if $R \gg r$, $Z \gg h$, $r \gg c$, $P \to \infty$, and $n \ll 1$ (a "point" detector and a β-active gas with $E \geq 2$ MeV), then

$$K = 4\varepsilon\lambda r_0 h_0 \left\{ H_0 \ln\left(\frac{R_0+\sqrt{R_0^2+H_0^2}}{r_0+\sqrt{r_0^2+H_0^2}}\right) - \frac{\sigma_1 c H_0}{2} \ln\left(\frac{R_0^2+H_0^2}{r_0^2+H_0^2}\right) \right.$$

$$\left. - \operatorname{arctg}\frac{H_0}{R_0}\left[\frac{\sigma}{2}(R_0^2+H_0^2)+\sigma_1 c R_0\right] + \operatorname{arctg}\frac{H_0}{r_0}\left[\frac{\sigma}{2}(r_0^2+H_0^2)+\sigma_1 c r_0\right] - \frac{\sigma R_0 H_0}{2} \right\}.$$

LITERATURE CITED

1. L. V. Artemenkova et al., in: "Assessment of airborne radioactivity" (Proc. Symposium), IAEA, Vienna (1967), p. 561.
2. V. V. Bochkarev and V. A. Bazhenov, in: "Metrology of ionizing radiation" [in Russian] (K. K. Aglintsev and G. A. Dorofeev, editors), Gosatomizdat, Moscow (1962), p. 241.
3. V. I. Zadontsev et al., Dosimetry of Radioactive Gases and Aerosols on Board Ship [in Russian], Sudostroenie, Leningrad (1965).
4. A. Howland et al., J. Instn. Heat. and Ventilat. Engrs., 28, 57 (1960).
5. M. Beer et al., Dtsch. Agrartechn., 15, 166 (1965).
6. A. A. Gusev, in: "Physics" (Proceedings of the 29th Scientific Conference of the Leningrad Institute of Engineering and Construction) [in Russian] (L. A. Oborin, editor), LISI, Leningrad (1970), p. 24.
7. A. A. Gusev, At. Energ., 30, 314 (1971).

BACKSCATTERING COEFFICIENTS FOR 12-25 MeV ELECTRONS INCIDENT OBLIQUELY ON METALLIC SURFACES

V. P. Kovalev, V. P. Kharin,
V. V. Gordeev, and V. I. Isaev

UDC 539.171.2

In order to obtain the information necessary for the shaping of broad beams of electrons we measured the relative backscattering coefficients for 12-25 MeV electrons incident obliquely on lead, copper, iron, and aluminum surfaces.

A beam of electrons 1 cm in diameter emerging from the exit window of a linear accelerator fell on the metal samples attached to an insulating rod and placed 10 cm from the exit window in air. The beam was monitored by a secondary emission detector. During the measurements the beam current was 3-5 μA. The samples were polycrystalline disks whose dimensions were chosen so that their thicknesses were not less than two mean free paths and their diameters not less than the diameter of the beam at the location of the sample plus two mean free paths for 25 MeV electrons in the sample material. The target current was measured for various angles of incidence of the electron beam. The samples were rotated by remote control.

If J_0 is the current incident on the sample, $J_t(\alpha)$ the target current, $J_b(\alpha)$ the backscattered current, and $J_s(\alpha)$ the secondary emission current, then obviously

$$J_0 = J_t(\alpha) + J_b(\alpha) + J_s(\alpha). \quad (1)$$

By definition the backscattering coefficient for a beam incident on a surface at an angle α is

$$\eta(\alpha) = \frac{J_b(\alpha)}{J_0}. \quad (2)$$

From Eq. (1) and (2) it is easy to obtain the relation

$$\frac{1-\eta(\alpha)}{1-\eta_0} = \frac{J_t(\alpha)+J_s(\alpha)}{J_{t0}+J_{s0}}. \quad (3)$$

TABLE 1. Backscattering Coefficients for Electrons (%)

α, deg	15 MeV		25 MeV		
	Fe	Cu	Al	Fe	Cu
90	1,9	2,9	0,5	1,2	1,3
96	2,2	3,0	0,7	1,3	1,5
102	2,3	3,5	1,2	1,7	1,8
108	2,4	3,6	1,5	1,9	2,2
114	3,6	4,4	1,9	2,8	3,2
120	4,3	6,1	2,5	3,8	4,1
126	6,1	7,4	3,5	4,5	5,0
132	8,4	10,0	4,9	6,4	6,9
138	12,5	13,5	7,6	8,6	9,5
144	16,8	19,2	11,4	12,8	13,0
150	24,4	25,3	17,8	18,1	19,1
156	32,6	34,5	25,8	27,0	28,3
162	—	46,4	39,1	—	39,9
168	—	62,0	57,3	—	58,4

Translated from Atomnaya Énergiya, Vol. 32, No. 4, pp. 342-344, April, 1972. Original article submitted May 21, 1971.

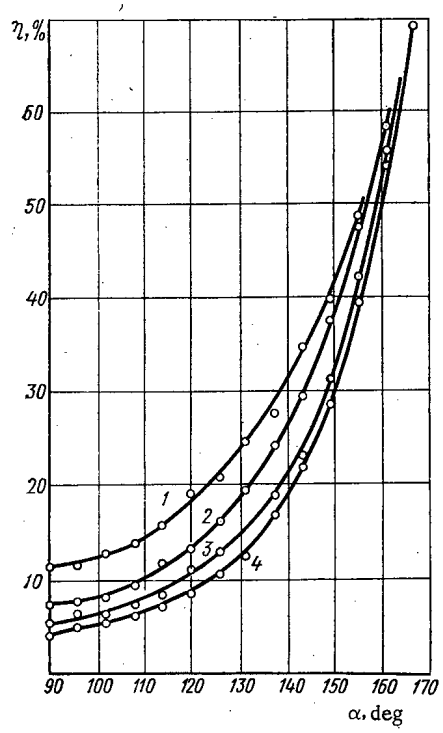

Fig. 1

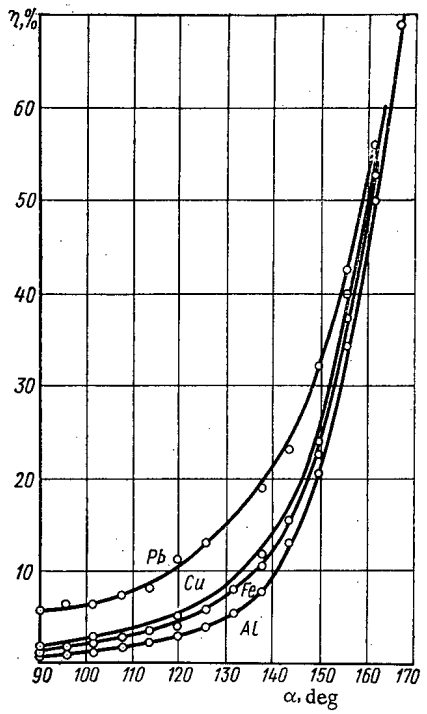

Fig. 2

Fig. 1. Backscattering coefficient as a function of the angle of incidence on lead for various initial electron energies: 1) 12.8 MeV; 2) 15 MeV; 3) 20 MeV; 4) 25 MeV.

Fig. 2. Backscattering coefficient as a function of the angle of incidence of 20 MeV electrons on targets of Al, Fe, Cu, and Pb.

Here η_0, J_{t0}, and J_{s0} are respectively the backscattering coefficient, the target current, and the secondary emission current for normal incidence of electrons on the sample. Equation (3) was used to calculate $\eta(\alpha)$. We measured J_{t0} and $J_t(\alpha)$; the values of η_0 were taken from [1] and averaged over the spectrum of the incident electron beam [2]. The experimental data on J_s as a function of α are very sparse [3]. In calculating $\eta(\alpha)$ we used two forms of $J_s(\alpha)$. The first form, based on theoretical reasoning in [4], was

$$J_s(\alpha) = J_{s0} \sec\theta, \tag{4}$$

where $\theta = \alpha - \pi/2$. The second form, in accord with [5], was

$$J_s(\alpha) = \delta_0 [1 + \beta\eta(\alpha)]. \tag{5}$$

Here δ_0 is the secondary emission coefficient for the incident beam and β is the efficiency of backscattered electrons in forming secondary electrons. β was taken as unity in the range of electron energies studied. The values of δ_0 are given in [1] as 2.1, 2.5, 2.8, and 4% for aluminum, iron, copper, and lead respectively. In the range of electron energies investigated the energy dependence of δ_0 is weak and was neglected in the calculations. The calculations with the two forms of $J_s(\alpha)$ did not differ by more than 2% for 25 MeV electrons on Fe. Most of the results were obtained with (5). It should be noted that since δ_0 = 2-4%, neglecting secondary emission from a sample does not change the value of $\eta(\alpha)$ obtained by using $J_s(\alpha)$ by more than 10%.

Typical curves of $\eta(\alpha)$ are shown in Figs. 1 and 2. The remaining results are given in Table 1. The error in the relative measurements is determined mainly by the accuracy of the microammeter; for $J_t(\alpha)/J_{t0}$ it is ±3%. The error in measuring η_0 is no more than ±10% according to the data in [1]. Since δ_0 is so small the error in its determination has no significant effect on the error in measuring $\eta(\alpha)$.

LITERATURE CITED

1. T. Tabata, Phys. Rev., 162, 336 (1967); K. Wright and I Trump, J. Appl. Phys., 33, 687 (1962); D. Harder and H. Ferbert, Phys. Lett., 9, 233 (1964); S. Okabe et al., Ann. Rep. of the Rad. Center of Osaka, Pref., No. 4 (1963).

2. V. I. Ermakov et al., At. Énerg., 29, 206 (1970).
3. A. Schulz and M. Pomerantz, Phys. Rev., 130, 2135 (1963).
4. E. Sternglass, Phys. Rev., 108, 1 (1957).
5. L. N. Dobretsov and T. L. Matskevich, Zh. Tekh. Fiz., 27, 734 (1957).

SEARCHES FOR TRACKS OF FRAGMENTS FROM THE SPONTANEOUS FISSION OF FAR TRANSURANIUM ELEMENTS IN NATURAL MINERALS

O. Otgonsurén, V. P. Perelygin,
S. P. Tret'yakova, and Yu. A. Vinogradov

UDC 546.799

The problem of determining whether there are any relatively stable transuranium elements with atomic numbers $Z \approx 114$ (~126) and $N = 184$ is attracting the attention of increasing numbers of investigators. In recent years, experiments have been carried out with a view to discovering far transuranium elements in primary cosmic rays [1, 2], to synthesizing them in nuclear reactions [3], and to finding such elements in minerals containing gold, platinum, and lead [4-7], in various types of glass containing heavy elements [8-10], and in iron-manganese concretions [11]. A selective survey of previous investigations can be found in an article by Flerov and Karamyan [4]. In a number of cases dielectric detectors and proportional counters were used to observe an effect which may be due to the spontaneous fission of nuclei of an unknown element [8-11].

The present article is a continuation of investigations aimed at finding far transuranium elements in natural minerals and various types of glass by the method of dielectric detectors. A necessary condition for detecting an effect caused by the spontaneous fission of unknown elements is that the age found on the basis of the density of spontaneous-fission tracks must be greater than the values obtained by other methods. However, this condition is not sufficient.

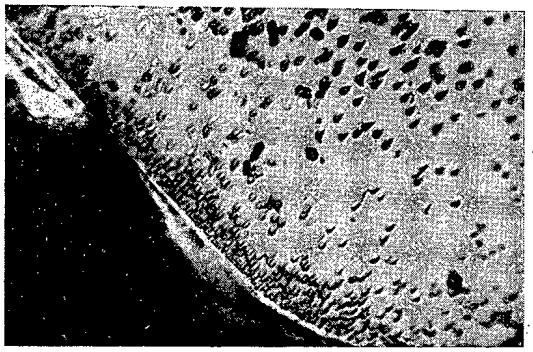

Fig. 1

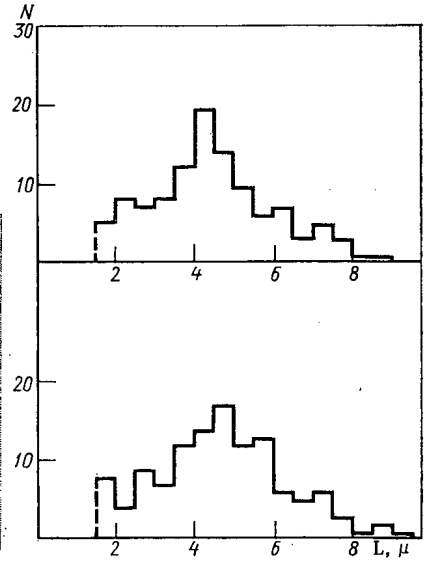

Fig. 2

Fig. 1. Tracks of fission fragments in a cavity on the surface of quartz.

Fig. 2. Distribution of lengths of tracks of spontaneous-fission and induced-fission fragment tracks in quartz: a) spontaneous fission; b) U + n.

Translated from Atomnaya Énergiya, Vol. 32, No. 4, pp. 344-347, April, 1972. Original article submitted May 18, 1971; revision submitted June 28, 1971.

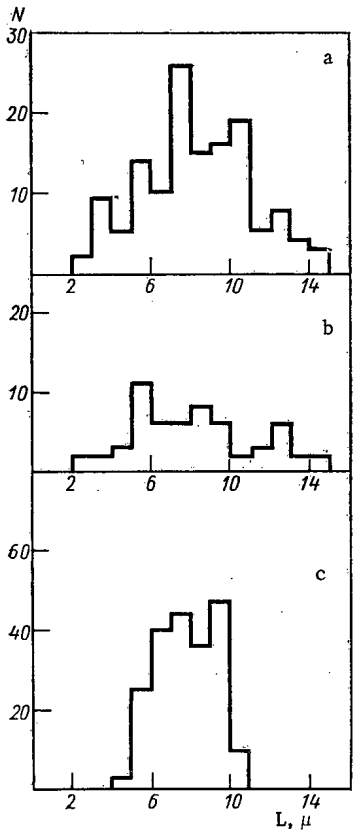

Fig. 3. Distribution of the lengths of tracks of fragments from the fission of nuclei formed in the U + 300 MeV Ca^{40} reaction (a), the U + 380 MeV Ar^{40} reaction (b), and the spontaneous fission of Cm^{244} (c). The conditions for the annealing and etching of the mica are the same for all specimens: a) $\theta_{lab} = 75\text{-}90°$; b) $\theta_{lab} = 90 \pm 5°$.

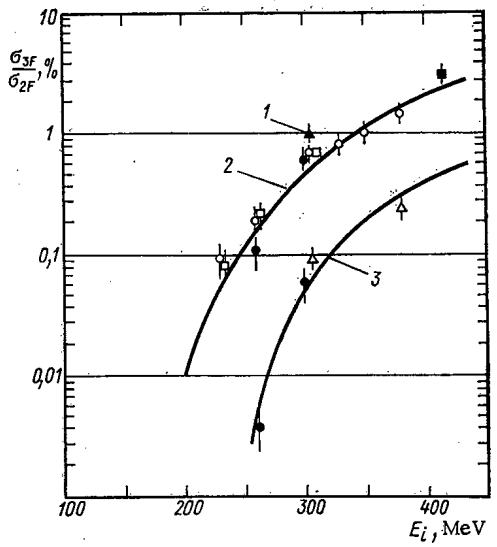

Fig. 4. Variation of the probability of three fission fragments in relation to that of two fission fragments, as a function of the energy of the bombarding particles: 1) $Z^2/A = 45$; 2) $Z^2/A = 43.5$; 3) $Z^2/A = 41$.

In the first place, a high density of fragment traces may be due to the migration of uranium from the specimen. In the second place, some minerals exhibit a background caused by defects in crystal structure – dislocations and hollow channels (capillaries). In the third place, the fission of heavy-element nuclei may be caused by particles generated by primary cosmic rays [12, 13] or by the neutron background produced by terrestrial radiation [14].

We selected minerals from different hydrothermal formations – pegmatite deposits, quartz veins, and sulfide ore manifestations. We investigated minerals containing lead or found in contact with lead compounds, as well as minerals in which there was a possibility of isomorphic intrusion of lead, bismuth, thallium, platinum – indium group elements, or rare-earth elements.*

The ages of these specimens were determined with high reliability by other methods; for most of the minerals the age was measured by the potassium – argon method at the Absolute-Age Laboratory of the Institute of Ore-Deposit Geology, Petrography, Mineralogy, and Geochemistry by L. L. Shanin and co-workers.

The first group of minerals used were micas – lithium muscovite, biotites, and phlogopites from various deposits. For most of the micas the age we found was considerably less than the age obtained by the potassium – argon method. This result is due to a thermal regression of the fragment tracks to early geologic times. However, for one of the specimens – a phlogopite – the age was found to be 5.5 ± 1.7 million years, whereas according to the measurements made by the potassium – argon method the age was 1.7 million years.

Experiments with specimens of pollucite, microcline, and amazonite (the lead content of the amazonites was 10^{-1}-10^{-2}%) from various deposits showed that the age measured on the basis of fragment-track density was only a small fraction of the absolute age.

* The authors express deep gratitude to G. N. Goncharov for his valuable advice and his careful verification of the experimental setups used in searching for far transuranium elements in primary minerals.

Somewhat better agreement was found between the ages found for the mineral wulfenite (~100 million years) by the track method, in a deposit 200 million years old, and auripigment (~60 million years) in a deposit 100 million years old.

We investigated a large number of contacts of lead-bearing and bismuth – lead minerals with crystals of rock crystal. In most cases the surface of the quartz exhibited a considerable number of tracks caused by crystal-structure defects ($\gtrsim 10^2$ cm^{-2}). In one of the specimens – rock crystal from a deposit 250 million years old – we found crystals of iron pyrites both on the surface and in the interior of the quartz.

Crystals found near the surface of rock crystal had been destroyed by the action of moisture, and cavities having the shape of pyrites crystals had been filled with a powdery mass consisting of iron oxides and hydroxides. The measurements the density of spontaneous-fission fragment tracks in the cavities yielded a value between $(3\text{-}5)\cdot 10^4$ and $(1\text{-}3)\cdot 10^5$ cm^{-2} (Fig. 1). The spectra of the lengths of the tracks detected in the quartz practically coincide with the tracks of fragments from the fission of U^{235} by thermal neutrons (Fig. 2). We measured the uranium content of the substance which filled these cavities. From a cavity measuring 2 × 2 mm we succeeded in extracting an undamaged layer of the filler substance. This substance was brought into contact with a polyethylene terephthalate surface and irradiated with thermal neutrons. Its uranium content was found to be $(1.2 \pm 0.2)\cdot 10^{-6}$ g/g. On the basis of our measurement of the density of spontaneous-fission fragment tracks in this cavity – $(2.0 \pm 0.2)\cdot 10^5$ cm^{-2} – we determined the age of the contact, which was 1.0 ± 0.2 million years, a figure substantially in excess of the 250-million-year age of the rock-crystal deposit. The results obtained for the crystals of rock-crystal quartz and phlogopite may be due to the migration of uranium from the specimens under investigation as a result of the action of water on the uranium compounds, which are contained in the stratification planes of the mica or in the finely dispersed filler substance obtained from cavities in the quartz.

Another possible explanation of the observed anomaly is the hypothesis that there is spontaneous fission of an unknown element contained in the crystal lattice of the mica or absorbed by the finely dispersed substance replacing the pyrites in the rock crystal.

The literature contains data on cases in which the age measured by the dielectric-detector method considerably exceeded the values determined by other methods. Thus, in Miller's studies [15], conducted as early as 1967, information was published on measurements of the age of micas from various regions of North America. Miller discovered that the age of some pegmatites, determined by the track method, is 600 to 1700 million years, whereas the age of these micas as determined from the results of investigations by the potassium – argon and rubidium – strontium methods is only 255 million years. Miller emphasized that this discrepancy called for further research, and he assumed that the discrepancy is attributable to the migration of uranium from the mica specimens.

Fleischer et al. [16] published data on the excess density of heavy-particle tracks in minerals extracted from the interior of meteorites. They concluded that the observed effect was attributable to the spontaneous fission of Pu^{244} synthesized during the formation of the solar system. However, in this case also it is necessary to consider other hypotheses in more detail, particularly so long as it is not possible to exclude the effect of fission of heavy-element nuclei contained in these minerals – U, Th, Bi, Pb, and others – by fast particles generated by primary cosmic rays. Another hypothesis, which was recently discussed in detail in [6], is one which attributes the observed effect to the spontaneous fission of far transuranium elements. The authors concluded that since the average track length in these minerals does not exceed the average total path length of two fragments from the fission of uranium by neutrons, and also since the probability of three fission fragments is less than 10^{-4} times that of two fission fragments, the effect of the spontaneous fission of far transuranium elements may be disregarded.

In their calculations the authors of [6] assumed that the total kinetic energy of the fragments from the fission of nuclei in the Z = 110-114 region is 216-235 MeV. However, experimental measurements of the energy of fragments from the fission of nuclei formed in the U^{238} + 300 MeV Ar^{40} reaction (Z = 110) showed that the average total energy of the two fragments does not exceed 200 MeV [17]. We made direct measurements of the lengths of tracks produced by fragments from the fission of uranium nuclei by argon and calcium ions in muscovite [18].

Figure 3 shows the distributions of the lengths of the tracks of fission fragments from the U + 380 MeV Ar^{40} reaction, and from the U + 300 MeV Ca^{40} reaction (at an angle of ~90° to the ion beam) and fission fragments produced by the spontaneous fission of Cm^{244} in mica in various specimens of muscovite (annealing and etching conditions were the same for all the detectors [18, 19]).

As can be concluded from Fig. 3, the average track length for the fission fragments is about 8 μ for all the spectra, even though the fragments generated in reactions with heavy ions exhibit a broader distribution of lengths than the spectrum from Cm^{244}.

In their discussion of the question of the probability of the fission of far transuranium elements into three fragments of comparable mass, Price and Fleischer [6] disregard the fact that this probability decreases rapidly as the excitation energy of the compound nucleus decreases. Our investigations show that as the energy of the bombarding particles decreases from 300 to 230 MeV (the $U^{238} + Ar^{40}$ reaction), the ratio of the probability of three fission fragments to that of two fission fragments decreases by a factor of 10.

A simple extrapolation shows that for nuclei of far transuranium elements ($Z \approx 110$-114) which are in the ground state, this probability will be of the order of $P_{3f}/P_{2f} < 10^{-3}$-10^{-4} (Fig. 4). Thus, both arguments cited in Price and Fleischer's study [6] are found to have insufficient experimental support, at least for the $Z = 110$-114 region, and the question of the origin of the excess density of tracks in minerals taken from meteorites will have to be studied further.

In spite of the high sensitivity and simplicity of the dielectric-detector method, it is very difficult to draw any definitive conclusions concerning the nature of the observed effect. However, the data obtained by this method may serve as a starting point for further investigations using other methods.

In conclusion, the authors wish to express their deep gratitude to G. N. Flerov for his statement of the problem and his valuable comments.

The authors are deeply grateful to G. P. Barsanov, L. L. Shanin, Yu. P. Dikov, and G. N. Goncharov for placing many mineral specimens at our disposal, as well as to I. A. Smol'nikova, G. Sung-Ch'yn-Yang, and A. I. Kalinin for the chemical analysis of some of the minerals.

LITERATURE CITED

1. P. Fowler et al., Proc. Roy. Soc. Letters, 318A, 1 (1970).
2. P. Price et al., Acta Physiol. Hung., 29, 417 (1970).
3. S. Thompson, Report at APS Meeting (Miami, 1968).
4. G. N. Flerov and S. A. Karamyan, OIYaI Preprint R6-4902 (1970).
5. A. Wyttenbach, Z. Naturforsch., 25a, 307 (1970).
6. P. Price and R. Fleischer, Phys. Rev. Letters, 30B, 246 (1970).
7. P. Price, R. Fleischer, and R. Woods, Phys. Rev., 1, 1819 (1970).
8. G. N. Flerov and V. P. Perelygin, At. Énerg., 26, 520 (1969).
9. G. N. Flerov et al., OIYaI Preprint D6-4554 (1969).
10. E. Tseslyak, OIYaI Preprint R-15-4738 (1969).
11. O. Otgonsuren, V. P. Perelygin, and G. N. Flerov, Dokl. AN SSSR, 189, 1200 (1969).
12. A. V. Podgurskaya et al., Zh. Éksp. i Teor. Fiz., 28, 503 (1955).
13. Kh. Abdullaev, Dissertation [in Russian], OIYaI (1969).
14. Yu. A. Shukolyukov, Uranium Fission in Nature [in Russian], Atomizdat, Moscow (1970).
15. D. Miller, Earth and Planetary Sci. Letters, 4, 379 (1968).
16. R. Fleischer, P. Price, and R. Walker, Geochim. et Cosmochim. Acta, 32, 21 (1968).
17. S. A. Karamyan et al., Yadern. Fiz., 6, 494 (1967).
18. V. Perelygin et al., Nucl. Phys., A127, 577 (1969).
19. V. Perelygin et al., Proc. Intern. Conf. on Nuclear Track Registration (Clermont-Ferrand, 1969). Ed. by Faculte des Sciences, Universite de Clermont, Vol. 1 (1969), p. 28.

CESIUM DISTRIBUTION IN THE SURFACE LAYER OF THE PACIFIC OCEAN

O. S. Zudin, B. A. Nelepo,
A. N. Spiring, and A. G. Trusov

UDC 551.46:539.16

As a result of the testing of thermonuclear weapons, the oceans have been contaminated with radioactive products. This is primarily true of the Pacific Ocean, where most of the tests have been carried out.

Measurements of the fragment (Cs^{137}, Sr^{90}) radioactivity in the Pacific Ocean were begun in 1954, and the radioactivity distribution was determined [1-4]. However, the relative paucity of experimental information hindered analysis. Recent years have seen improvements in the measurement procedures and efficiency, so a large store of experimental information has been accumulated and reported [5-8]. Irregularities and nonuniformities in the radioactivity measurements in the ocean required the development of a special theory for best determining the radioactivity distribution [9].

The basic assumptions underlying an objective analysis of the radioactivity distribution were checked experimentally for the Atlantic Ocean. It was found possible to convert from actual measurements carried out irregularly over the ocean to Sr^{90} concentrations at points on a regular grid, through the use of the method of optimum interpolation. The deviation of the concentration C_0' at a grid point from the average value found from all measurements in the region is calculated from

$$C_0' = \sum_{i=1}^{N} P_i C_i'.$$

Here C_i' are the corresponding concentration deviations from the average value for each measurement point, P_i are weighting factors found from the condition for minimum reconstruction error, and $\sum_{j=1}^{N} \mu_{ij} P_j = \mu_{0i}$, where μ_{ij} are the normalized correlation coefficients for points i and j. The normalized correlation function is found through a special analysis of the experimental data, on the basis of the equation

$$\mu_{lk} = \frac{1}{2N_{lk}\sigma_{lk}^2} \sum_{j,\, i=1}^{N_{lk}} C_i' C_j',$$

where N_{lk} is the number of products $C_i' C_j'$ at points separated by a distance between ρ_k and $\rho_k + \Delta\rho$ ($\Delta\rho$ = 111 km). This function can be approximated by an exponential function (Fig. 1).

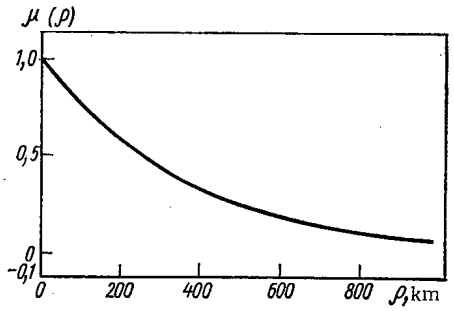

Fig. 1. Normalized correlation function for Sr^{90} in the Atlantic Ocean.

Computer calculations ultimately led to the Sr^{90} radioactivity distribution in the surface layer of the Atlantic Ocean [10].

Analysis of data on the Cs^{137} concentration in the Pacific Ocean [5] yielded information about its statistical structure and significantly extended the knowledge available about the radioactivity of the Pacific Ocean as a whole.

The effects of various factors on the accuracy with which the statistical characteristics are reconstructed were analyzed in [11-13]. The results of an analysis of the raw data, the average

Translated from Atomnaya Énergiya, Vol. 32, No. 4, pp. 347-350, April, 1972. Original article submitted January 7, 1972.

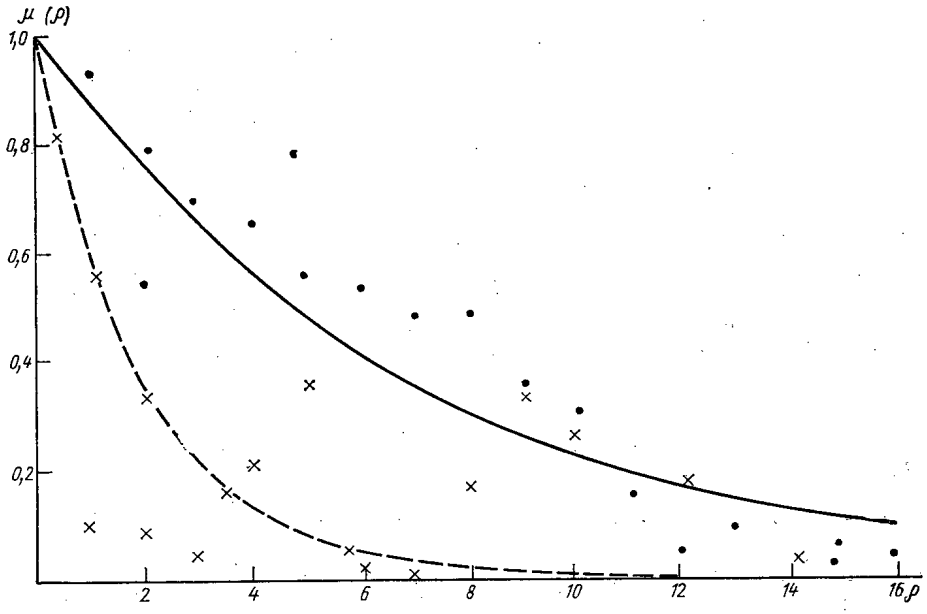

Fig. 2. Normalized correlation functions for Cs^{137} in the Pacific Ocean (1966): ●, ——) $\exp(-0.15\rho)$, long. 118-160° W, lat. 20-33° N, N = 80, $\overline{C} = 0.67$, $\sigma^2 = 0.089$, and $\sigma^2_{smo} = 0.0068$; ×, - - - -) $\exp(-0.5\rho)$, long. 120-140° W, lat. 30-50° N, N = 42, $\overline{C} = 0.91$, $\sigma^2 = 0.093$, and $\sigma^2_{smo} = 0.044$.

concentration values found, their dispersions, and their normalized correlation functions were reported subsequently. A preliminary comparison of the results of the Cs^{137} measurements carried out in different seasons and even different years shows that the cesium concentration has remained relatively stable. It is therefore legitimate to combine the results obtained at different times.

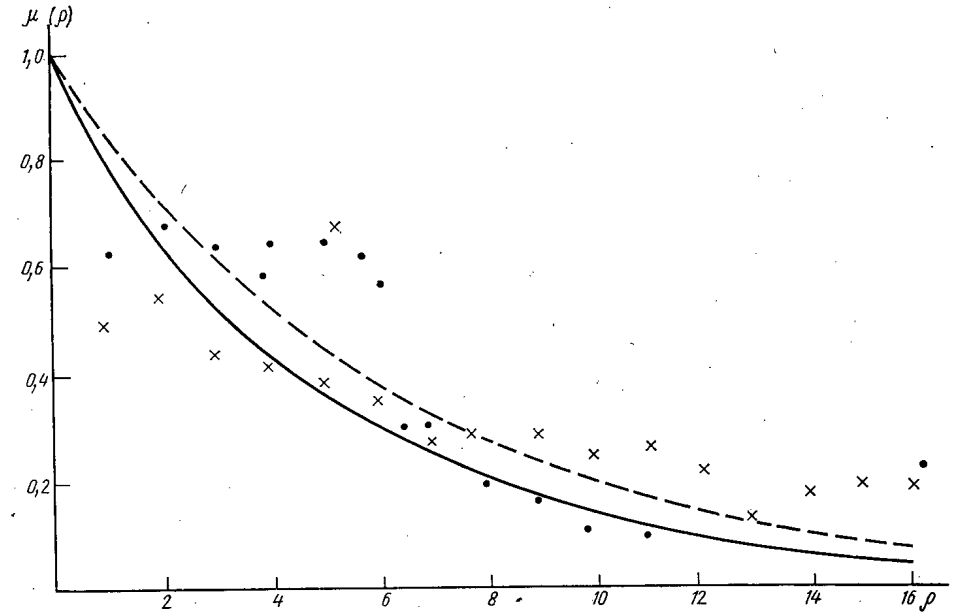

Fig. 3. Normalized correlation functions for Cs^{137} in the Pacific Ocean (1967): ●, - - - -) $\exp(-0.175\rho)$, long. 105-140° W, lat. 20° S to 50° N, N = 341, $\overline{C} = 0.386$, $\sigma^2 = 0.081$, and $\sigma^2_{smo} = 0.0118$; ×, ———) $\exp(-0.2\rho)$, long. 104-126° W, lat. 20° S to 30° N, N = 195, $\overline{C} = 0.222$, $\sigma^2 = 0.033$, and $\sigma^2_{smo} = 0.019$.

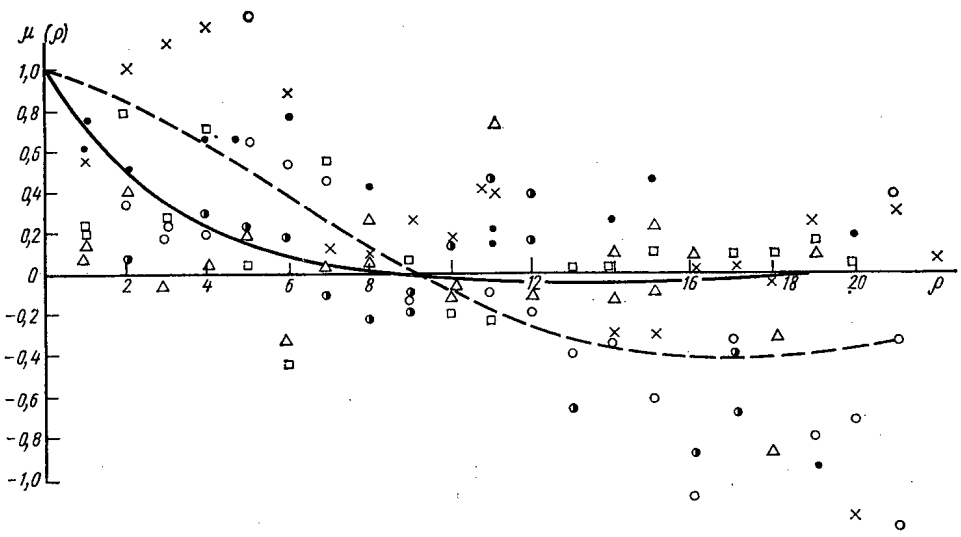

Fig. 4. Normalized correlation functions for Cs^{137} for the Pacific Ocean: - - - -) $\exp(-0.05\rho)$, long. 104-126° W, lat. 20° S to 30° N, $\sigma^2_{smo} = 0.05$ (●, ×, ○); ———) $\exp(-0.3\rho)$, long. 104-126° W, lat. 20° S to 18° N, $\sigma^2_{smo} = 0.06$ (●, Δ for $0° \leq \theta < 60°$; ×, □ for $-60° \leq \theta < 120°$; ○, ◐ for $120° \leq \theta < 180°$).

Analysis leads to a physical interpretation of the experimental results. For example, for a nonuniform distribution of samples over the region between long. 100° W and 140° W and between lat. 10° N and 40° N, with N = 365 samples, $C_{max} = 1.89$ pCi/liter, and $C_{min} = 0.05$ pCi/liter (where C is the cesium concentration), i.e., with a 40-fold concentration range, the errors involved in a determination of the arithmetic mean from all the sample is much larger than for a uniform distribution. The extent to which this error is larger depends on the distribution of sampling points and the elementary averaging form, reaching 100% in the worst case. The dispersion may be many times greater than in the case of a uniform distribution of sampling points.

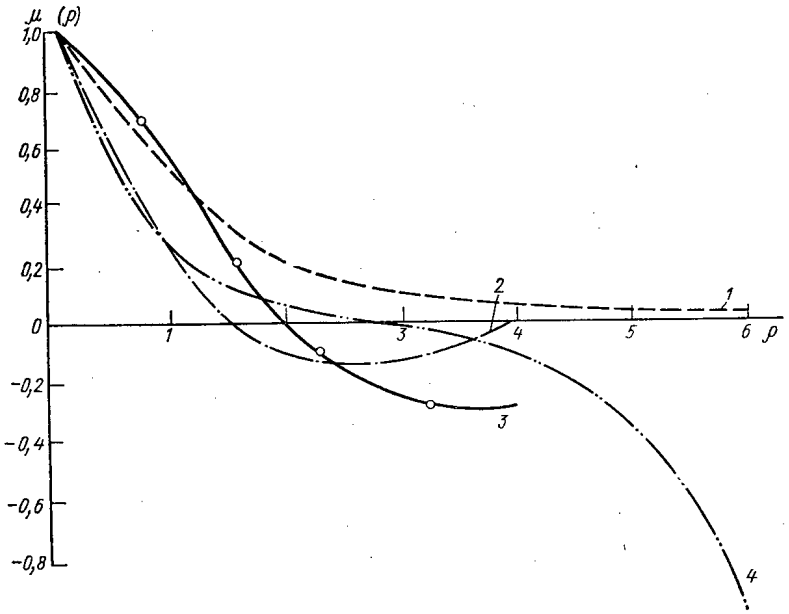

Fig. 5. Normalized correlation functions for Cs^{137} for the region of the Pacific Ocean between long. 105° W and 140° W and between lat. 20° N and 50° N: 1) $0 \leq \theta < 45°$, $\exp(-0.75\rho)$, $\sigma^2_{smo} = 0.013$; 2) $45° \leq \theta < 90°$, $\exp(-0.75\rho)$, $\sigma^2_{smo} = 0.023$; 3) $90° \leq \theta < 135°$, $\exp(-0.3\rho)$, $\sigma^2_{smo} = 0.027$; 4) $135° \leq \theta < 180°$, $\exp(-1.3\rho)$, $-\exp(\rho - 6)$, and $\sigma^2_{smo} = 0.005$.

Near the west Coast of the United States (long. 110-120° W and lat. 32-36° N) the average concentration is 0.8-0.9 pCi/liter and the dispersion is $\sigma^2 = 0.05$-0.1, while in the open ocean (long. 104-126° W and between lat. 20° S and lat. 30° N, the average value is 0.1-0.15 pCi/liter and the dispersion is $\sigma^2 = 0.008$-0.01. This discrepany between the average radioactivities is due not only to the nonuniform distribution of sampling points near the United States, but also to differences in the nature of the fields. In analyzing the Cs^{137} distribution over the Pacific Ocean, particular attention must be paid to the fact that the formation and structure of this distribution differ in nature from those for the Sr^{90} distribution [6] in the Atlantic and Indian Oceans.

Figures 2-5 show normalized correlation functions calculated from the experimental data [5] obtained at various times in various parts of the Pacific Ocean. Over the period 1966-1967, the curves are essentially the same. The curves in Fig. 2 correspond to different regions of the Pacific Ocean (1966). The curves in Fig. 3 correspond to regions having similar statistic characteristics. The rapid decay (lower curve in Fig. 3) for the open ocean seems to be due to anomalous individual measurements against a background of a stabilization toward the equator.

A comparison of these curves shows that the average value and dispersion decrease, the scatter in the ordinates of the normalized correlation functions increases, and the smoothing error becomes comparable to the dispersion (N decreases) in the transition from the west coast of the United States (long. 105-140° W, lat. 20° S to 30° N) to the open ocean (long. 104-126° W, lat. 20° S to 30° N). The distribution becomes much more stable.

A comparison of the normalized correlation functions for the water to the west of the United States (near the coast and in the open ocean) and the curves calculated on the basis of the correlation directions (Figs. 4 and 5) shows them to undergo similar changes. Differences are due primarily to a decrease in the amount of experimental information available and thus to an increase in the role of random errors. The decrease in the correlation radius from 8-10° to 2-3° is due to random errors in the determination of the deviations from the average.

These correlation functions thus show that the formation of the concentration distribution in the Pacific Ocean is affected by such factors as the discharge of radioactive waste from atomic industries and the burial of this waste as well as by the worldwide radioactive contamination.

Information about the statistical structure of the radioactivity distribution in the Pacific Ocean can thus be used to predict the distribution of Sr^{90} and Cs^{137} radioactivity.

LITERATURE CITED

1. Y. Miyake et al., Res. Oceanogr. Works Japan., 2, No. 1, 18 (1955).
2. V. I. Baranov et al. (USSR), Report No. 384 to the III Geneva Conference (1964).
3. N. I. Popov et al., Tr. In-ta Okeanologii AN SSSR, 82 (1966).
4. T. Folsom et al., Nature, 187, No. 4736 (1963).
5. Fallout Program. HASL-197 (1968).
6. V. M. Vdovenko et al. (USSR), Report No. 457 to the IV Geneva Conference (1971).
7. Fallout Program. HASL-217 (1970).
8. Fallout Program. HASL-227 (1971).
9. V. I. Belyaev et al., Izv. AN SSSR. Ser. Fizika Atmosfery i Okeana, 5, No. 8, 860 (1969).
10. B. A. Nelepo, Nuclear Hydrophysics [in Russian], Atomizdat, Moscow (1970).
11. V. I. Dmitriev et al., "Determination of the error involved in calculating the normalized calculation function in the case of a limited amount of experimental information," Tr. GGO, No. 286 (1972).
12. O. S. Zudin and B. A. Nelepo, "Error in interpolation and in choosing the interval for discrete measurements in a hydrophysical field," Tr. AANII, 301, 80 (1972).
13. O. S. Zudin and B. A. Nelepo, "Detecting statistical structures," Report of the 4th Symposium on Automating Oceanological Research, Marine Hydrophysical Institute, Sevastopol' (1971).

SEASONAL EXTREMES OF CONCENTRATION OF NUCLEAR FISSION PRODUCTS IN THE ATMOSPHERE

A. É. Shem'i-zade

UDC 551.578

During the period when nuclear tests are not conducted in the atmosphere, the seasonal extremes in the concentration of radioactive products in the atmospheric ground layer are caused by the inversion of air masses between the stratosphere and the troposphere. The mechanism of this inversion is not completely clear, since none of the current theories can explain the diversity of the observed effects.

Investigating the pattern of alternate maxima and minima in the concentration of radioactive products in the atmospheric ground layer, one can come to some conclusions concerning the intensity of the transition of the stratospheric air masses, contaminated by fission products, to the troposphere.

According to published data, the contamination maximum in the atmospheric ground layer by radioactive aerosols is observed during the spring, while the minimum occurs during the autumn. Investigations conducted by the author showed that in Tashkent the successive maxima appeared in June, while the minima appear in December to January (see Fig. 1). In some work carried out by researchers at various stations on the earth, the seasonal maximum is recorded during the spring, April to May [1-4]. From the data in [4], which generalizes the results of observations at nine stations, one can see that the maxima in the radioactive fission products during 1963-1964 for the German Democratic Republic were observed in May. As the analysis shows, the annual variation in the concentration of fission products in the lower troposphere of such diverse regions of the planet as Western Europe (German Democratic Republic) and Central Asia (Uzbek SSR) is shown to a significant degree to be the same.

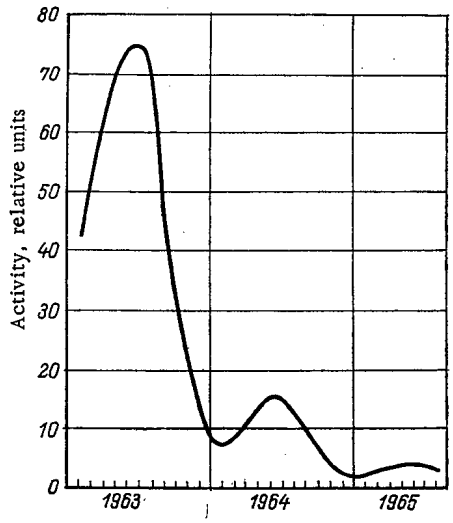

Fig. 1. Concentration of fission products in the atmospheric ground layer of the troposphere at Tashkent.

During the year immediately following intense injections of radioactive products into the stratosphere, seasonal extremes develop very sharply. Subsequently, as a result of the smaller activity of the fission products in the atmosphere as a whole, the seasonal extremes appear to be less sharp. With some sufficiently low value of the resultant activity the seasonal extremes cannot, in general, develop as was the case in Tashkent in 1961. The absence of seasonal extremes is, apparently, not evidence of a breakdown or disappearance in the mechanism causing them (the stratosphere – troposphere inversion), and is evidenced by the coincidence in the extremes of variation in the radioactive contamination level of the stratosphere with those taking place under the influence of processes in the lower troposphere.

It is interesting to consider the question of the rate of decrease in the concentration of radioactive products in the troposphere after a seasonal maximum. This rate is easy to evaluate relative to the significant period T for the concentration to decrease by half during the interval from maximum to minimum in the seasonal level. If ρ_0 is the concentration at a maximum, and ρ_t is the concentration at time t, then the period for the concentration to decrease by half is given by:

Translated from Atomnaya Énergiya, Vol. 32, No. 4, pp. 350-352, April, 1972. Original article submitted April 13, 1971.

$$T = 0.693 \frac{t}{\ln \frac{\rho_Q}{\rho_t}}. \quad (1)$$

A similar evaluation was conducted for Tashkent, the German Democratic Republic (data averaged over nine stations) [4], and Budapest [1]. A month was taken as the unit for the time scale; correspondingly ρ_t denotes the average monthly concentration of nuclear fission products. The following values for the periods in which the concentration of fission products in the troposphere decreased by half in the designated regions were obtained:

	1963	1964
Tashkent	53 ± 5 days	52 ± 5 days
GDR	69 ± 9 days	60 ± 6 days
Budapest	72 ± 3 days	60 ± 6 days

In the same manner, the values for the periods in which the concentration of fission products decreased by half in various regions of the earth after the spring – summer maximum exhibit to a sufficient degree a similarity among themselves.

It is interesting to compare the values of T calculated from Eq. (1) with those of this same quantity obtained by an independent method. In [5] there is proposed for the calculation of the period for semidecontamination of the troposphere from nuclear fission products the following equation:

$$T = \frac{0.693}{H/(H-h)}, \quad (2)$$

where H is the height of the troposphere; h is the height of the tropospheric layer decontaminated after one day.

In our calculations, the value of H was assumed equal to 10,000 m, the value of h was identified with the turbulent rate of fallout [6], which is defined as the ratio of the density of the fission products fallout on the earth's surface a to their volume concentration ρ. If one takes the average over a year for the quantity $h = a/\rho$ in the calculation of T by Eq. (2), then the period during which the concentration of fission products decreases to half will be 35 days. This value differs significantly from the value of T obtained by Eq. (1). However, a comparison of the values for the semidecontamination periods of the troposphere is necessary to make the correct calculations. More precisely, one calculates the value of T, using a value of h pertaining to a month relative to which the semidecontamination period after maximum is calculated. Utilizing this type of calculation with Eq. (2), one obtained the following values for the semidecontamination period of the troposphere: 53 ± 24 days in 1963 and 62 ± 28 days in 1964.

However, final conclusions concerning the agreement for the values of T determined by the two independent methods corresponding to Eq. (1) and (2) are not permitted by the investigation of a limited number of cases. It is desirable to conduct a corresponding calculation with data obtained in other regions of the earth. Clearly, carrying out this kind of calculation requires one to know the value of h for a day without fallout, which is a condition excluding abrupt changes in the values of decontamination rate of the troposphere in a near contaminated layer. This condition is essential for the identification of h with the turbulent rate of fallout.

The results obtained by us do not contradict the assumption that, during the time interval from minimum to maximum of the seasonal level in the troposphere, a significant quantity of radioactive products enter from the stratosphere. In other months, the emission from the stratospheric region is insignificant during which time there results a basically purified troposphere, which occurs at a rate dependent also on causes associated with the location and the altitude at which the radioactive products are injected into the atmosphere.

In the same way, and irrespective of the dependence on the mechanism determining the seasonal extremes, the assumption that the magnitude of the seasonal maximum is determined by the reserve of radioactive products in the stratosphere appears plausible. Hence, it follows that during the period when powerful nuclear tests, which can significantly influence the reserves of fission products in the stratosphere, conforming to a change in the magnitude of the seasonal maxima, are not produced, one can estimate the purification rate in the stratosphere, if the period during which it is purified halfway is calculated:

$$T_{start} = 0.693 \frac{t'' - t'}{\ln \frac{\rho_0'}{\rho_0''}}, \quad (3)$$

where ρ_0' and ρ_0'' are average monthly concentrations of radioactive products at a maximum at time t' and t" respectively.

At Tashkent in 1963 $\rho_0' = 218 \cdot 10^{-16}$ Ci/liter, in 1964 $\rho_0'' = 51 \cdot 10^{-16}$ Ci/liter, $t'' - t' = 12$ months. $T_{strat} = 5.7$ months was obtained by this calculation. The same value of T_{strat} was obtained, if the average monthly concentrations of radioactive products at the seasonal minimum were assumed for ρ_0' and ρ_0''.

The calculation of T_{strat} with respect to the average monthly concentration of fission products at a seasonal maximum was carried out with the data in [1, 4] for Budapest and GDR, respectively (at nine observation stations): for Budapest $T_{strat} = 5.9$ months for GDR $T_{strat} = 5.7$ months.

In the same way, the rate of purification of the stratosphere from radioactive products, calculated by the proposed method with respect to the value of the average monthly concentration at the time of seasonal maxima (or minima), is characterized by $T_{strat} = 5.7 \pm 0.1$ months.

LITERATURE CITED

1. A. Shimon, Jdojaras, Szam 151 (1963/4).
2. H. Volchok, Nature, 206, No. 4988, 1031 (1965).
3. S. G. Malakhov, E. N. Davydov, and M. P. Nekhorosheva, in: Radioactive Isotopes in the Atmosphere and Their Utilization in Meteorology [in Russian], Atomizdat, Moscow (1965), p. 323.
4. M. Zier, Kernenergie, 10, No. 2, 59 (1967).
5. V. P. Shvedov and L. I. Gedeonov, in: Soviet Studies on the Danger of Nuclear Weapons Tests [in Russian], Atomizdat, Moscow (1959), p. 45.
6. V. N. Lavrenchik, Global Fallout of the Products of Nuclear Explosions [in Russian], Atomizdat, Moscow (1965), p. 133.

AGREEMENT ON SETTING UP THE INTERATOMINSTRUMENT SOCIETY

Yu. Yurasov

A multilateral intergovernmental agreement on setting up the international sociopolitical association for nuclear instrumentation, "Interatominstrument," the first multilateral economic organization in the socialist countries, was signed in Warsaw on February 22 of this year. The authorized signatories of the respective governments were: Kh. Khristov, Academician and Director of the Physics Institute of the Academy of Sciences of the Peoples Republic of Bulgaria, D. Osztrowszki, chairman of State Atomic Energy Committee of the Hungarian Peoples Republic, R. Becker, deputy minister in charge of electrical engineering and electronics of the German Democratic Republic, S. Andrzejewski, authorized representative of the government of the Polish Peoples Republic on peaceful uses of atomic energy, A. M. Petros'yants, chairman of the USSR State Committee on the Peaceful Uses of Atomic Energy [GKIAÉ], and J. Neumann, chairman of the Czechoslovak Atomic Energy Commission.

The problem of elaborating new forms of collaboration in the field of nuclear instrument design was first posed, as a further development of the decisions taken at the XXIII (special) session of COMECON, in October 1969, at an extraordinary session of the PK IAÉ SÉV [Permanent Committee on the Peaceful Uses of Atomic Energy Attached to the Council for Mutual Economic Aid (COMECON)]. After this question had been studied by a provisional work team under the Commission's jurisdiction, a recommendation on the feasibility of setting up an international economic association dealing with nuclear instrumentation, to be termed Interatominstrument (IAI), was adopted in June 1970. A preparatory committee of authorized representatives of the interested nations was organized in October 1970 for the purpose of preparing drafts of IAI constitutional documents and other necessary documents, such as the test of the Agreement, statutes, specific statements on personnel and staffing, basic scientific-technical and economic problems, justification of the size of the statutory capital outlay, rules of procedures governing deliberations of the IAI Council, and so forth. Participating in the work of this preparatory committee were the authorized representatives and expert consultants of Bulgaria, Hungary, the German Democratic Republic, Poland, Rumania, the USSR, and Czechoslovakia. This work was completed in 1971.

The basic purpose of the IAI is to satisfy the needs of the nations signatory to the Agreement more fully in terms of devices and instruments for atomic industry which will be commensurate in quality with the worldwide scientific and engineering levels of excellence. To achieve that goal, IAI will carry out scientific research work, experimentation, design, drafting, and production activities in the field of nuclear instrument design and fabrication, and will organize scientific-technical, production, and commerical collaboration between the economic organizations of the signatory nations, in addition to aiding in the expansion of trade along those lines with still other nations.

The sphere of IAI activities is extended to include collaboration in the field of designing dosimetric, radiometric, and nuclear physics research equipment, including multidimensional and multichannel systems for nuclear research and nuclear power; radioisotope and nuclear medical equipment and devices; detectors of ionizing radiations; special devices for use in radioisotope laboratories, nondestructive testing equipment, and so forth. In line with decisions of the IAI council, the activities can be extended to other types of instruments and devices employed in nuclear industry and in nuclear engineering.

With the agreement of the respective governments, IAI is authorized to set up its representative agencies and subdivisions on the territories of the nations signatories to the Agreement and other consenting nations, and also to set up production-oriented branches, design and planning organizations, and other bodies.

Translated from Atomnaya Énergiya, Vol. 32, No. 4, pp. 353-354, April, 1972.

The tasks and the functions of the IAI will be to:

1. Develop scientific and technical forecasts and draw up future plans of coordination and joint scientific research and planning and design work in the field of nuclear instrument design and fabrication, and to study market conjunctures, plus engage in exchange of data and exchanges of experience on these topics.
2. Coordinate and execute scientific research and planning and design work in the development of new lines of instruments and devices for nuclear engineering, as well as to plan, develop, and carry through jointly agreed-upon measures on improving the product quality of nuclear instrumentation.
3. Elaborate engineering costs justifications and measures to be taken in specialization and cooperation in production and in planning and design work on the basis of contracts concluded between the interested parties.
4. Coordinate the production, development, and execution of plans for using free production capacities, and studies of production costs and production technology in the field of nuclear instrument design and fabrication.
5. Organize mutually beneficial exchanges of technical documentation and scientific-technical achievements.
6. Develop proposals on unified standards, engineering specifications, and methods for testing nuclear engineering instruments and devices.
7. Coordinate mutual deliveries of instruments and devices, collaborate in the development of trade, through mediating bodies, upon the concluding of contracts between the organizations or agencies and the purchasing enterprises which are licensed under the laws of their respective nations to conclude foreign trade arrangements.
8. Develop proposals on joint or agreed-upon purchases and sales of licenses on the markets of interested third parties, and develop plans for joint utilization of licenses and know-how in the field of nuclear instrumentation, on the basis of contractual stipulations.
9. Provide for technical servicing of instruments and devices used in nuclear engineering, in the countries whose economic organizations are members of the association, and in other countries as well.
10. Act jointly in expediting the routine use of nuclear engineering devices and instruments in the various branches of the national economy.
11. Organize and compile scientific-technical and economic information on nuclear instrumentation.

The first members adhering to IAI were the State Economic Association Resprom (Bulgaria), Kombinat Gamma and the foreign-trade organization Migert (Hungary), VÉB RFT Messelektronik Otto Schon and the foreign-trade organization Élektrotechnik Export – Import (East Germany), the United Nuclear Instrument Enterprises Polon (Poland), the V/O Izotop Agency and the All-Union Export–Import Agency Tekhsnabeksport (USSR), and the production costs agency Tesla and foreign-trade organization Kovo (Czechoslovakia).

The seat of the IAI is located in Warsaw.

The Agreement does not touch upon the legal status of the economic organizations belonging to IAI in their countries. These economic organizations retain their full economic and juridic independence.

IAI activities are based on the principles of economic accounting. A basic capital outlay totaling 2,100,000 convertible rubles has been laid aside to back up IAI activities. Dues and fees paid in to the basic capital fund by the members are set so that the total contributions by the economic organizations of each country will be equal. The basic capital fund can be increased when so proposed by the IAI Council. Another provision is that IAI members will forward additional contributions to cover costs of maintaining the association apparatus during the initial period of IAI activities, before the transition to the status where IAI will be able to pay its own way (that is expected to last for the first two to three years of activity).

The highest governing body of IAI is the Council, made up of representatives appointed by member-organizations of IAI, each one having one permanent representative. On basic questions involving IAI

activities, the Council will arrive at decisions by unanimous agreement, and on other questions decisions can be taken by a qualified majority of not less than 3/4 of the votes, or by a simple majority.

The director and assisting directors appointed by the Council from among citizens of those countries whose economic organizations function as IAI members, will be in charge of the day-by-day activities of IAI. An auditing commission appointed by the Council will keep track of financial and economic activities.

Annual plans and long-range plans approved by the Council lie at the basis of IAI activities. These plans are coordinated with national-economic plans of the various countries, to the extent necessary for the upkeep of normal IAI activities. IAI logistics will be handled in accordance with procedures set up in Poland.

The IAI can obtain credits from the appropriate banking institutions in the country where it is located, or from the International Economic Collaboration Bank or the International Investment Bank, according to the statutes and regulations of those banks, or also from its members under conditions made explicit in the understanding between IAI and its members.

The work done by IAI in meeting orders forwarded by IAI members and other organizations and enterprises will be carried out under conditions stipulated in the appropriate contractual agreements and pacts.

Profits accrued as a result of IAI activities will be distributed among its members in proportion to the dues paid, except for the part earmarked for further developments or for setting up certain special funds.

IAI will maintain liaison with the appropriate COMECON bodies, and can also establish business relations with international and other economic organizations on questions pertaining to IAI activities and concerns.

With the explicit agreement of all of the governments of the countries signatory to the Agreement on the founding of IAI, governments of other nations sharing the goals and principles of IAI and willing to assume the obligations stipulated in the Agreement will be able to adhere to IAI in the future.

COLLABORATION LOGBOOK

The second session of the Coordination Scientific-Technical Council (KNTS) of COMECON member-nations on radiation engineering and radiation technology was held November 1-4, 1971 in Moscow. Reports on the most pressing trends in this field were heard: "On the organization of full-scale industrial production of radiation-grafted materials and products" by V. B. Osipov, and "Engineering costs fundamentals of industrial applications of high-level sources of ionizing radiations," by V. M. Kodyukov.

V. B. Osipov emphasized the point that irradiation of polymers, and specifically polyethylene, greatly improves the physicomechanical and electrophysical properties of the material. The method yields its greatest effect when additives hindering oxidation and enhancing the radiation stability of the polymer are introduced into the composition of the initial polymeric composition beforehand. In that case grafting of the polymer is achieved successfully, i.e., new crossbonding between chains of molecules is effected, bringing about a three-dimensional network somewhat reminiscent of crystalline structure. The strength of the polymer, its dielectric qualities, and other properties and characteristics undergo essential improvements. Radiation grafting of polymers on an industrial scale has been achieved successfully in the United States, Britain, Japan, and some other capitalist countries.

Close attention is being given to this production technique in COMECON member-nations. A broad assortment of cableware with insulation made of radiation-grafted polyethylene has been manufactured in the Soviet Union for the past four years; high-voltage cable with radiation-grafted insulation is being fabricated in the German Democratic Republic, and thermosetting polyethylene tubing is being fabricated in Hungary. Polymers are irradiated directly to form the finished products. The basic equipment in all these countries is electron accelerators of various types. One of the sections of the report deals with the process of radiation vulcanization of rubbers, including the process designed to produce self-adhering strip with siloxane rubber bases.

The report by V. M. Kodyukov presented methodological aspects of cost estimates of the effectiveness of radiation technique and equipment, and cited comparative calculations of cost savings when different radiation sources are used, and also presented recommendations on how to use them most profitably in production.

The two reports stimulated great interest in the session audience, and were followed by intense and general discussion. KNTS set forth concrete measures to take toward expediting the industrial scale-up of radiation-grafting processes and radiation-vulcanization processes in the interested countries, and adopted a resolution on the development of a procedure for engineering cost estimates of the effectiveness of radiation techniques and equipment to be followed by all the COMECON member-nations.

The KNTS work plans for 1972-1975 call for discussion of other processes which hold forth promise for the industries of COMECON member-nations, such as radiation sterilization of medical wares, radiation processing of foodstuffs and agricultural products, radiation production of wood and plastic materials, etc.

The Council at the same time adopted a resolution on scheduling symposia of specialists of COMECON member-nations over the 1972-1975 period on the following topics:

radiation sterilization of medical materials and wares (1973);

copolymerization and graft-polymerization of monomers to natural and synthetic materials (1974);

radiation processing of foodstuffs and agricultural products (1975).

Translated from Atomnaya Énergiya, Vol. 32, No. 4, pp. 354-355, April, 1972

Proposals on the agenda of a forthcoming conference on implementation of radiation processes and equipment in production, to be held in Hungary in October 1972, were discussed before the Council.

The KNTS resolutions were approved at the XXI session of the PKIAÉ SÉV. The fulfillment of these resolutions will contribute to further deepening of economic and scientific-technical ties between the COMECON member-nations, to combining the scientific-technical potential of the interested nations in the solution of various problems confronting the national economies.

* * *

A conference of specialists of COMECON member-nations on scientific and technical collaboration in the field of water-cooled water-moderated reactors was held in Moscow in January 1972.

The purpose of this conference was to go into greater detail on the scope and timing of work, forms of completion of the work and of collaboration called for in the program of collaboration on VVÉR type reactors adopted by PKIAÉ, including the plans for building a VVÉR type reactor power facility of unit electrical output 1000 MW.

Specialists in the field of reactor science and reactor engineering, and in the nuclear power industry of COMECON member-nations took part in the conference; specialists were from Bulgaria, Hungary, East Germany, Poland, Rumania, the USSR, and Czechoslovakia. A work plan on realization of the previously adopted program was worked out and approved, and proposals relating to the application of new and more effective forms of collaboration were discussed.

The work plan will contribute to a deeper scientific-technical groundwork for various important decisions envisaged in the technical project for the 1000 MW VVÉR reactor facility, and the development of more sophisticated design solutions for individual equipment components and subassemblies, including instrumentation and computer system equipment. For example, the work plan calls for research on the physical parameters and water management parameters of the reactor system in boron control; investigation of critical heat flux under stationary and nonstationary heat transfer conditions, and devising instruments and sensors for that work; development of unitized standard mathematical programs for computer calculations of reactor physical characteristics; development of bantam-size and high-efficiency sensors for measuring energy release and temperatures in the reactor core.

At the present time nuclear power is being employed most extensively in order to develop electrical power in large nuclear power stations incorporating a VVÉR type reactor unit with specific electric powers of 440 MW, already existing or in the course of construction in the COMECON countries.

The conference was an important step in the work of carrying out the measures flowing from the comprehensive program, adopted at the XXV session, on combining the efforts of COMECON member-nations in efforts to achieve the scientific-technical and production prerequisites for accelerated development and more effective acceptance of nuclear power on an industrial scale in the national economies. Collaboration of COMECON member-nations in the building of more powerful reactor facilities designed to serve future nuclear power stations is therefore being expedited within the framework of PKIAÉ [COMECON Permanent Commission on the Peaceful Uses of Atomic Energy].

THE MOSCOW ENGINEERING AND PHYSICS INSTITUTE SCIENTIFIC CONFERENCE

V. Frolov

The regularly scheduled scientific conference of instructors and students of the Moscow Order of the Labor Red Banner Engineering and Physics Institute (MIFI) was held in October 1971. This session with 23 panel sessions scheduled provided a forum for 418 reports and communications.

The panel on experimental nuclear physics was host to a report by S. A. Volobuev et al., on detection of the first extra-galactic source of γ-photons, which was greeted with great interest.

A paper presented by V. V. Borog dealt with an application of the ionization calorimeter method to the study of the nuclear interaction between cosmic muons of energies above 10^{11} eV. Three series of measurements with a total exposure time of 11,300 h were carried out. The events were classified on the basis of the experimental data in terms of the form of cascades in an iron absorber, nuclear-cascade average curves were plotted for different energies, and the average fraction of energy transferred to π^0-mesons in inelastic $\mu - N$ interactions was estimated.

Of the many reports delivered at the panel on experimental techniques in nuclear physics, we have to single out one by V. A. Grigor'ev and colleagues on the mechanism underlying low-temperature (exciton) luminescence of unactivated alkali halides. Original findings from an investigation of the temperature variation of luminescence supported the inference of a mechanism of high-temperature quenching of exciton luminescence in those crystals, and inferences as to the structure of luminescence centers.

A combined report submitted by ITÉF (Institute of Theoretical and Experimental Physics) and MIFI colleagues on a system processing plates taken by the two-meter liquid-hydrogen bubble chamber met with keen interest. This system incorporates four scanning measuring projectors, a buffer memory bank, and an interfacing system linking up with a Razdan-3 computer.

S. S. Karavaev et al. discussed methods of recording single pulse signals ~1 sec long with a leading-edge growth time of 10^{-8}–10^{-7} sec under the influence of noise, when the initial instant of the signal was not known in advance.

A report by B. A. Dolgoshein et al. on liquid electronic radiation detectors was greated with great interest. New results from an experimental study made on different techniques for recording ionizing radiations in liquid argon, and based on the phenomenon of electrostatic emission of electrons from the liquid phase into the vapor phase, were cited in the report.

The panel on nuclear reactor physics entertained a large number of papers on developement of reactor design calculation techniques, and computational studies of static and dynamic reactor performance characteristics. Reactor optimization and reactor transients were discussed, as well as techniques for experimental study of reactor characteristics. There was keen interest in reports by A. M. Pavlovichev and L. K. Shishkov on a method of speeding up the convergence of a process of external iterations in the solution of the stationary reactor equation; by V. B. Troyanskii and M. P. Zaitsev on calculations of an asymmetric neutron field by the wave method; by N. N. Khrennikov and V. I. Naumov on computational procedures and programs for calculating the space – energy distribution of neutrons in polylattices; by A. P. Rudik on the optimum spatial distribution of nuclear fuel in a reactor; by A. V. Bushuev et al. on determinations of initial physical characteristics of a reactor through the investigation of the γ-ray spectra of the reactor fuel elements by nondestructive means.

The panel on physics of elementary processes was addressed by colleagues of Tomsk Polytechnic Institute, I. A. Tikhomirov et al., who outlined a theory of probe and microwave measurements applied to

Translated from Atomnaya Énergiya, Vol. 32, No. 4, pp. 357-358, April, 1972.

the plasma of radiofrequency torch discharges, and cited research findings on the physics and diagnostics of such a plasma.

The panel on the physics of separation processes heard reports on the theory and practice of separation of stable isotopes, and on special topics in mass spectrometry and in molecular physics. A lively discussion was stimulated by the presentation of N. A. Kolokol'tsov's paper on design and optimization of two-component and many-component separatory stages, and the associated difficulties.

A report by M. S. Chupakhin on the present status of isotope mass spectrometry and analytical mass spectroscopy focused special attention on ways to determine trace impurities in such modern engineering materials as silicon, germanium, and the like.

The plasma physics panel heard an interesting report by V. M. Smirnov on simulation of the process of implosion of an infinite plasma pinch by an external magnetic field with straight lines of force extending parallel to the axis of the pinch, and a report by B. A. Trubnikov on a new model of ball lightning, in the form of an autonomous plasma-shielded bunch of submillimetric radio waves.

A paper by L. B. Begrambekov et al. covered a theoretical and experimental study of diffusion and release of gas by light particles when targets are heated after ion bombardment of the targets has ceased. A report by D. M. Skorov et al. was devoted to a study of the properties of materials for future thermonuclear reactors.

Several review papers were presented at the panel on solid state physics. I. I. Ashmarin et al. reported out the results of their work on holography and coherent optics. Coherence of laser radiation, effect of scattering on coherence, coherence of emission of semiconductor lasers and their applications in the holography of three-dimensional objects, were topics covered. The interaction between powerful laser radiation and matter was investigated by pulse holography techniques, and investigations were carried out on holographic pattern recognition and applications to automatic translation, decoding of optical spectra, and processing of results of physical experiments.

A report by A. N. Oraevskii presented a review of the state of the art in chemical lasers, in the USSR and elsewhere. A report by O. B. Anan'in et al. was devoted to various aspects of the interaction of laser radiation and condensed-phase media at different flux densities. A new mechanism to account for failure of material by cratering was proposed on the basis of experimental data, for the range of flux densities $\sim 10^6$ to 10^8 W/cm^2. Development of an injector of multiply charged ions, based on the use of a high-power optical maser in multiple ionization of atoms, is also reported. Physicotechnical data on the injector, and results of tests demonstrating the basic advantages of a laser injector over several types of competing injection devices, are cited.

The panel on radiation physics heard results, in a report by V. I. Ivanov and G. V. Kulakov, of an investigation of direct-charging detectors for dosimetry of high-intensity γ-ray flux. The physical and dosimetric characteristics of such detectors were reported. Some interesting findings were presented in a paper by E. L. Stolyarova et al. on the design of a shower spectrometer. A function describing statistical processes occurring in such a spectrometer was derived. Under the assumption that the fluctuation in the number of charged particles at different levels of development of a cascade is described by a Poisson distribution, a computer program for calculating line shapes was compiled.

V. S. Endovitskii et al. presented a series of papers on computation methods in the study of a nucleon-meson cascade developing in dense media and initiated by high-energy hadrons. The distribution function of the cascade particles and various functionals taken of it were obtained. The results of the calculations are in excellent agreement with experimental data.

At the panel on electrophysical equipment, the most interesting paper heard was one by P. N. Chistyakov on MIFI research in the area of exoelectronic (post-discharge) emission excited by a current pulse in a gas. It was found that purification of metallic surfaces in a vacuum or in an inert gas medium leads, at the terminal stage, to a gradual fall-off in emission to the point of complete disappearance. A method for inspecting the surface of metals in vacuum and in gases through the use of post-discharge emission, which would make it possible to ascertain the presence of films or of local inclusions of dielectric and semiconducting materials, was proposed.

A report by V. A. Volodin and A. V. Shal'nov dealt with the properties of waveguide sections as accelerating elements in linear and cyclic accelerators. A procedure was developed for studying a broad class of accelerating sections with virtually arbitrary degree of nonuniformity.

V. P. Kozlov discussed the shaping of the electron beam over different portions of a linear accelerator. A procedure for calculating transverse motion and focusing of particles in such an accelerator was presented. Basic results of calculations and recommendations on the choice of focusing fields were reported.

At the session on heat physics, G. P. Dubrovskii and L. S. Kokorev reported on a physical model of burnout in boiling of liquid in a large volume, in a paper on limiting conditions in heat transfer. The concepts developed were used to generalize experimental measurements of the growth rate of a steam bubble in a large volume, and the initial stage of disruption of water films flowing freely over a heated rod.

L. S. Kokorev et al. presented research findings on turbulent flow of an incompressible fluid through parallel interconnected channels. The calculations were verified experimentally in a simulated aerodynamic channel with two interconnected cells, at $s/d \approx 1.05$.

A report by L. R. Fokin et al. dealt with a procedure for jointly processing experimental data on the speed of sound and on the density of superheated cesium vapor. This procedure makes it possible to provide a complete description of the nonideal behavior of superheated cesium vapor at temperatures up to 1280°K and at pressures up to 5 atm.

A report by Yu. F. Babikova on techniques using isotope tracers and their applications in science and industry was heard with great interest at the panel on applied nuclear physics. A classification of techniques accompanied a description of special procedures in use in industry.

P. L. Gruzin et al. cited results of the use of the nuclear γ-resonance method in investigating properties of two types of ferridielectrics: garnets and spinels, as well as data on the dynamics of the ferrite crystal lattice over a broad temperature range. A method for rapid analysis of the process variables of ferrite charges for content of free ferric α-oxide was developed. A paper by A. M. Somonov et al. dealt with optimization of time-of-flight instrumental techniques in activation analysis of biomedia. E. D. Kokhov et al. discussed the present status and developmental outlook of x-radiometric methods of analyzing the composition of matter. The advantages of the method are rapidity, compact equipment, easy operation, and comparatively low cost.

Many of the reports presented at the conference will be published in topical scientific symposia of articles by the Institute.

SEVENTH ALL UNION CONFERENCE OF REPRESENTATIVES OF FOUR NUCLEAR DATA CENTERS

A. Abramov and V. Popov

The VII conference of four nuclear data centers was held at Brookhaven (USA), October, 25-29, 1971, with the present authors representing the Soviet Union.

The basic problem confronted by the conference was to discuss experience in the exchange of experimental nuclear data within the framework of the EXFOR system (special format for display of nuclear data on computer magnetic tapes). As reported earlier, EXFOR was developed through the joint efforts of staff at four centers. The decision to exchange nuclear data in that format was taken at a conference of representatives of the four data centers in Moscow in late 1969. The exchange of data commenced in practice in late 1970. During that time, our center obtained several magnetic tapes from the Western centers with results of many experiments on measuring neutron cross sections, the parameters ν and α, and several other nuclear constants written in. In turn, the USSR turned over two tapes to Vienna with records of research results obtained by Soviet physicists. Particular inaccuracies in the rules for presenting and encoding that data turned up in the exchange process, as well as ambiguous concepts and definitions, and shortcomings on the organizational end. Analysis of the drawbacks and inaccuracies by the participants at this conference will make it possible to enhance the effectiveness of collaborative efforts in this field appreciably.

Incompatibilities of the computer magnetic tapes in use at these data centers was until recently a major obstacle to the expansion of data exchange between our center and Western centers. In order to read the tapes obtained and to transcribe the Soviet data onto IBM computer tapes, our center staffmembers had to get in touch with institutes located in other cities. At present, our center is putting into service its own M-222 digital computer with a Western-designed magnetic tape system hooked up to it. This will greatly facilitate and speed up the process of data exchanges with various centers. A set of special programs was compiled at Obninsk to facilitate this work. Extremely useful in this connection was the conference discussion on the programs of other centers (especially test programs) and also conversations relating to the exchange of these.

In addition to EXFOR, the conference also discussed topics pertaining to other international information-handling systems. Specifically, the discussion of the systematized catalog of bibliographic references (SINDA) brought out the fact that this catalog can be used as a sort of "table of contents" for the EXFOR system. In order to make that suggestion a reality, however, some technical problems involving the SINDA and EXFOR systems will have to be solved. The conference assigned to the Saclay data center the task of preparing further proposals on this topic.

The SINDA catalog is rapidly expanding: in 1969 it contained about 55,000 entries, while the number of entries had grown to 75,000 in 1971. Already, the SINDA-71 issue will have to use a new and more compact notation system, and the SINDA-72 catalog may even have to be split into two volumes.

A lot of work has been in recent years in solving some practical problems on handling inquiries on nuclear data. The systematized inquiry forms (RENDA) issued by the Vienna data center are now being used in the elaboration of work plans for defining the most urgent research trends. References to the corresponding experimental works are being cited, with experimental error indicated, to facilitate comparisons between the level of inquiries and the level of accuracy attained in RENDA materials. But this method of handling demands and possibilities suffers from the disadvantage that there is always the possibility of systematic errors unattended to and cropping up. This means that the errors computed by the respective authors of papers cannot be treated as a criterion of the level of knowledge attained on any particular

Translated from Atomnaya Énergiya, Vol. 32, No. 4, pp. 359-360, April, 1972.

parameter. From that point of departure, the conference responded to our suggestion by adopting a recommendation to indicate the uncertainties of constants in RENDA materials not in terms of the experimental papers and their data, but rather on the basis of work done specifically to estimate those constants. This will of course require that estimated errors also figure in the results of work on estimates of nuclear data. The corresponding proposal was also introduced by our representatives and acknowledged to be quite useful. It was pointed out, however, that carrying out such a proposal will be no easy task. In particular, not a single one of the presently available formats for estimated data was designed for inclusion of information on errors, so that much further study will be required. Since each of the four centers uses its own format for estimated data at the present time, and data are not always transferred with ease from one such format to another, it would be convenient in the future to agree upon some unified format for all the data centers (similar to the way EXFOR was devised for experimental data). It is impossible to work out such a format at the present time, however, for a number of reasons, and the conference met the challenge only by agreeing to not introduce any new formats.

Close attention was given to the organization of exchange of what was termed "non-neutron" data (information on nuclear-levels, decay schemata, moments, masses, half-lives of radioactive nuclides, etc.). Information of that type is sorely needed for both applied research (e.g., activation analysis and dosimetry), and the development of theoretical methods of estimating neutron constants.

Intensive work is underway in the USSR, USA, and several other countries on collection of non-neutron data, but regularized international exchange of the data had not been smoothed out as of recently. The principal difficulties standing in the way concern the great discrepancies in the data and the enormous quantities of data. But that is precisely why it is virtually impossible to utilize conventional forms for disseminating those data in the form of articles, reports, etc., and why special computerized techniques have to be developed. Experience accumulated by the four data centers in exchange of neutron data will be highly useful, of course. The basic aspects of this problem were discussed at the conference. A more detailed discussion of the problem is scheduled for March 1972, at the first conference of the new IAEA-sponsored international work group on compilation, evaluation, and dissemination of data on the structure of the nucleus and on nuclear reactions.

The VII conference of representatives of four data centers was well organized and took place in a businesslike atmosphere, and proved most helpful to further development of international collaboration in the area of nuclear data.

THE ALL-UNION CONFERENCE ON PLASMA THEORY

I. P. Yakimenko

The All-Union Conference on Plasma Theory, organized by the Theoretical Physcis Institute of the Academy of Sciences of the Ukrainian SSR acting jointly with the Scientific Council of the Academy of Sciences of the USSR on the problem of "Plasma Physics," was held in Kiev from October 19 to 23, 1971. About 250 Soviet theoretical physicists and mathematicians, as well as 50 foreign scientists from 14 countries, participated in the Conference. As Academician N. N. Bogolyubov, Chairman of the Organizing Committee, remarked in his opening statement, this was the first time such a conference on plasma theory had been convened, not only in the Soviet Union but in the entire world.

Among the plasma-theory questions discussed at the Conference, most of those relating to practical applications were concerned with the problem of controlled thermonuclear synthesis. As is known, the best results in the long-term maintenance of high-temperature plasma are being obtained nowadays with the "tokamak" type of toroidal installation proposed by Soviet scientists. Naturally, the participants in the Conference displayed the greatest interest in the theoretical papers on the study of transfer processes in toroidal systems. A survey report was presented by A. A. Galeev, one of the authors of the neoclassical theory of transfer processes; he explained the results obtained for a number of practically feasible cases, from the hydrodynamic to the so-called "banana" type of operation. The applicability of the neoclassical theory to the explanation of energy loses due to ionic thermal conductivity was checked on a tokamak by Academician L. A. Artsimovich and co-workers. M. Rosenbluth (United States) gave a survey report characterizing the neoclassical theory as the most successful theoretical development of recent years but emphasized that even this theory does not explain all the known facts. Thus, for example, whereas the transfer of heat by ions is neoclassical, the transfer of heat by electrons is better explained by a pseudoclassical formula. Rosenbluth described the theory of pseudoclassical diffusion as the first problem of the tokamak. The second problem is the anomalously rapid penetration of the toroidal current into the plasma, which may be explained by postulating that the transfer process is more powerful than the pseudoclassical diffusion process. The third puzzle of tokamaks is the nature of the severe instabilities which frequently lead to the disruption of a discharge; this was partly solved in a report by P. Rutherford and H. Furth (United States), who considered the mechanisms of tiring instability. A fourth problem, according to Rosenbluth, is related to the possibility that in the transition to a reactor regime there may be a dangerous instability caused by trapped particles, as predicted by B. B. Kadomtsev and O. P. Pogutse. The possible solutions of these problems and the structure of the future theory of transfer processes were discussed in a survey report by H. Grad (United States), who, after a critical analysis of the existing theories, formulated the requirements that must be satisfied by a diffusion theory: it must abandon the assumption that the electrical field is a potential field, it must take account of the transient conditions of operation, and it must take into consideration the actual geometry of the systems involved.

The Conference showed that, in addition to successful investigations of toroidal thermonuclear systems, other types of reactors are also being investigated today and there is a continuing search for new ideas on how controlled thermonuclear synthesis can be achieved. A report by G. I. Budker, V. V. Mirnov, and D. D. Ryutov noted a number of important advantages of straight systems, such as the simplicity of manufacturing technology, the convenience of heating the plasma, and the utilization of the energy liberated during the reaction. The theory discussed in the report leads to estimates which indicate that a straight reactor with dense plasma is feasible in practice if a change is made from a homogeneous longitudinal magnetic field to an undulating field. The participants took great interest in A. A. Rukhadze's report, which gave a comparative analysis of the efficiency and economy of various thermonuclear reactor designs. The cost of a thermonuclear reactor for research purposes runs to 2-4 billion rubles if the

Translated from Atomnaya Énergiya, Vol. 32, No. 4, pp. 360-362, April, 1972.

calculation is based on the diffusion-coefficient values obtained on today's best toroidal installations. This cost can be reduced (by a sharp reduction in the cost of the reactor magnetic system). About the same amount would be required for a reactor based on the use of the laser thermonuclear synthesis method proposed by N. G. Basov and O. N. Krokhin, if account is taken of the fact that the power lasers existing today have low efficiencies. Since the efficiency of the conversion of stored energy into beam energy is very high (70-80%), an idea that comes to mind is that of using high-current electron beams for heating the plasma. A successful practical implementation of this idea depends on the solution of two central problems: the focusing of high-power electron beams on a 0.3-0.6 cm^2 area, and the dissipation of the energy of the electron beam and the heating of the plasma. Rukhadze's report showed that these problems can be solved by having the beam pass through a dense plasma.

A. A. Rukhadze also gave a survey of the prospects for using electron beams in accelerator technology, plasma electronics, ionospheric research, electronic technology, etc. Further development of plasma electronics, the foundations for which were laid as early as 1949 by A. I. Akhiezer and Ya. B. Fainberg (USSR) and by D. Bohm and E. Gross (United States), depends on satisfying two opposite requirements: high efficiency and narrow generation spectrum. In order to solve this problem, we can use relativistic and nonrelativistic modulated beams. An interesting possibility for using the interaction of the modulated beam with the plasma in order to increase the power of diffraction-radiation generators was discussed in a report by V. P. Shestopalov et al.

Extensive discussion at the Conference was devoted to papers on the study of various instabilities in plasma and the physical phenomena connected with them. The present state of plasma stability theory was presented in a survey report by A. B. Mikhailovskii. The principal trend in the development of this theory at the present time is that theoreticians are shifting their interest from one class of instabilities (the "force" type) to another class (thermal instability). This trend is related to the increased interest being taken in the instabilities of an inhomogeneous colliding plasma. The crucial influence of instabilities is confirmed, for example, by the sharp increase in plasma resistance when the electrical field becomes greater than some critical value. A complete theory of this anomalous resistance of plasma was given in a report by Academician R. Z. Sagdeev. He discussed the successive stages of development of various instabilities and the corresponding effective collision frequencies, analyzed the assumptions made, and pointed out possible lines for the further development of the theory. In recent years a great deal of attention has been devoted to the study of solid-state plasma instabilities. As is known, almost all instabilities in semiconductors can be utilized for the development of new radioelectronics instruments. Furthermore, the study of oscillations and instabilities in semiconductors contributes to a better understanding of the problem of instability in plasma and helps in verifying the correctness of the theory. The various aspects of the theory of instability in semiconductors and its application were discussed in reports by M. Glicksman (United States) and V. V. Vladimirov. Much interest was aroused by L. M. Gorbunov's report, which dealt essentially with the problem of parametric instabilities in plasma. A number of questions relating to the theory of stability were discussed in reports by A. Simon (United States), H. Wilhelmsson (Sweden), A. Legatowicz (Poland), and G. Laval (France).

It is impossible to construct a consistent theory of stability without the theory of nonlinear processes in plasma. H. Grad (United States), in particular, made some critical remarks concerning the standard methods for estimating the increments of dissipative instabilities, pointing out that a correct approach would require solving a nonlinear problem with initial conditions rather than looking for normal modes and increments. Nonlinear effects play an equally important role in the theory of transfer processes, turbulence processes, etc. This explains the consistent interest in the theory of nonlinear processes at every plasma-physics conference held in recent years. Naturally, this problem was also given an important place at the Conference on Plasma Theory. A survey of the present state of the theory of propagation and stability of finite-amplitude waves was presented in a report by V. N. Oraevskii. Collision-free shock waves of large amplitude were also discussed in a report by A. D. Pataray. A number of problems of nonlinear theory – the effect produced by the capture of particles on their resonance interaction with waves, the effect of self-stress in the propagation of strong electromagnetic waves in plasma, and nonlinear Landau attenuation – were discussed in a review by W. D. Shapiro.

In addition to the nonlinear theory, rapid progress is being made today in the linear theory of wave processes in plasma, primarily the theory of oscillations and waves in an inhomogeneous unbounded plasma. This was reflected in reviews presented by S. S. Moiseev and the author of this article. The theory of wave propagation in media with one-dimensional inhomogeneity in a hydrodynamic approximation is still far

from complete, but the agenda already includes problems in which it is necessary to take into account inhomogeneity in more than one dimension, imbalances in an inhomogeneous medium, and kinetic effects. A characteristic feature of a consistent theory of bounded plasma must be that it takes account simultaneously of three-dimensional dispersion and of plasma inhomogeneity. The need for such a theory is dictated by the fact that the boundaries may have a strong (often decisive) influence on wave processes in plasma, and therefore also on transfer processes, stability, turbulence spectra, etc. At present, studies are also intensively being conducted on the influence of relativistic effects on wave processes in plasma, which is important in problems involving strong external high-frequency fields. The latest results of such investigations were presented in a review by N. L. Tsintsadze.

Of great interest in present-day plasma theory is the problem of turbulence, the solution of which is equally important for applications (controlled thermonuclear synthesis, radioelectronics, plasma-cosmic experiments, etc.), and for the further development of all of plasma theory. An exhaustive analysis of the fundamentals of the theory of weak turbulence and the prospects for its future use was given in a survey report by B. B. Kadomtsev, and a number of new aspects of the theory of strong turbulence were discussed in a survey presented by S. Ishimaru (Japan). Kadomtsev's report emphasized that the weak-turbulence theory developed today has a fairly broad field of application, even though it is not always exact in the part relating to the details of turbulence spectra. Subtle effects of this kind will be described better by using new concepts and approaches close to the theory of strong turbulence than by using a higher order of infinitesimals. In S. Ishimaru's study the theory of strong turbulence is developed on the basis of a chain of Bogolyubov equations. The point of departure of the theory is the study of states with strong correlations. This leads to an important physical property, since the theory explicitly takes account of the fact that the interaction between the particles may change radically as a result of strong correlations in the turbulent plasma. A report by I. A. Akhiezer et al. discussed an original method for the stochastic heating of plasma, based on the use of an effect consisting in the increase of plasmon energy when the external magnetic fields are slowly modulated. A report by V. N. Tsytovich was devoted to a nonlinear effect in turbulent plasma. New results in the theory of weak turbulence, obtained in Khar'kov and Moscow, were presented in a review by A. I. Akhiezer.

A special meeting was held for the benefit of physicists and mathematicians working on numerical methods of plasma theory. The role and importance of these methods is immeasurably greater today because the available analytical devices are frequently inadequate for the investigation of physical phenomena taking place in natural plasmas and in laboratory installations. Moreover, as was pointed out in a survey report by A. A. Samarskii, a numerical experiment can sometimes be successfully substituted for a complicated, time-consuming, and expensive physical experiment. Samarskii gave a survey of the existing numerical methods and used an investigation of low-temperature plasma as an example to illustrate their importance. Concrete applications of numerical methods in plasma theory were cited in reviews by a large group of workers at the Applied Mathematics Institute of the Academy of Sciences of the USSR. In a survey report, Yu. N. Dnestrovskii and D. P. Kostomarov discussed methods for the numerical simulation of kinetic processes in plasma. B. Fried (United States), in a survey report, gave a detailed description of the popular "on-line" mathematical systems designed for theoreticians who want to use the computer as an analytical tool but are not familiar with programming.

Electromagnetic phenomena in interstellar and circumterrestrial plasma were the subject of survey reports by Ter Haar (England) and B. A. Tversky. Ter Haar pointed out the interrelationship between plasma physics and the problem of the study of pulsars, discussing two fundamental problems in detail: the plasma aspects of the theory of pulsar radiation and the influence of interstellar plasma on this radiation. B. A. Tversky's report showed that the magnetohydrodynamic mechanism of interaction between the solar wind and the geomagnetic field is in satisfactory agreement with the processes observed in the earth's magnetosphere.

As can be seen from this brief summary, the Conference on Plasma Theory afforded an excellent opportunity for physicists from many countries to discuss practically all of the current problems of modern plasma theory. In his closing statement, R. Z. Sagdeev expressed the firm conviction that such representative meetings of theoreticians must continue to be held in the future and thanked the staff of the Theoretical Physics Institute of the Academy of Sciences of the Ukrainian SSR, who had done everything possible to make the Conference a success.

The proceedings of the All-Union Conference on Plasma Theory will be published in mid-1972.

THE TENTH INTERNATIONAL CONFERENCE ON PHENOMENA IN IONIZED GASES

P. P. Kulik

The International Conferences on Phenomena in Ionized Gases have traditionally been held every two years beginning in 1953. In addition to information on important scientific achievements, such conferences also provide an opportunity for bringing out the basic trends in the development of individual lines of this broad field of science, comparing studies conducted in the various parts of the world, and also as a rule, discovering and appraising new directions as they arise. It is therefore quite understandable that this physicists' forum attracts a great deal of attention.

The first such conference was held at Oxford at the initiative of A. von Engel. The Tenth Jubilee Conference was again held at Oxford. About 650 participants from 28 countries attended the Conference. It included representatives of many large foreign firms and scientific research laboratories engaged in the investigation of technical and technological problems related to the use of plasma.

The work of the Conference was organized as follows: the morning plenary meetings heard and discussed survey reports on outstanding fundamental problems; the evening sectional meetings, held by five parallel sections, discussed reviews giving surveys of original reports. Altogether, the Conference heard 14 survey reports and 75 reviews on 440 individual reports. The author's reports were published in a special collection issued before the start of the Conference. The main subjects of the reports presented in individual sections were: collision of particles, surface phenomena, electrical discharges, plasma physics, and general experimental techniques.

The Conference indicated a trend toward the development of a number of subdivisions of plasma and gas-discharge physics and their applications. Table 1 gives the statistical data on the relative numbers of reports on various subjects presented at such conferences in recent years.

Three subjects were consistently represented by large numbers of reports at each conference: discharges at low and high pressures and the interaction of waves with plasma. At the last conference the number of articles on low-pressure discharges was somewhat less than the number dealing with high-pressure discharges. This trend is attributable to the increasing interest in dense-plasma physics and has, in turn, led to an increase in the number of studies on dense-plasma radiation. This is natural, since the subjects are closely related.

The number of studies on particle collisions had increased sharply. The reason for this is probably the increased interest in plasmochemical processes and in the study of the interaction of laser radiation with gas atoms and molecules.

There was a substantial decrease in the number of studies devoted to surface phenomena. This decrease is apparently due to the occurrence of many problems in this field that are closely related to the specific nature of plasma itself, so that the reports on these problems were assigned to sections on gas-discharge processes and not to the section on surface phenomena. It should be noted that almost simultaneously with this Conference a number of special international forums were held on the problems of interaction between plasma and surfaces (in particular, the Fifth International Congress on Vacuum Problems Boston, October 11-15, 1971). The number of reports on shock waves was also reduced, probably for analogous reasons.*

* An International Conference on Shock Waves was held in London on July 4-13, 1971, shortly before the Oxford Conference.

Translated from Atomnaya Énergiya, Vol. 32, No. 4, pp. 362-364, April, 1964.

It is somewhat surprising that there has been a sharp drop in the number of studies on thermodynamics, kinetic theory, and transfer phenomena in plasma. The decrease in the number of studies on plasma-beam interaction – one of the prominent topics in plasma physics – is attributable to the nature of the Conference itself and to the work of special conferences on plasma-beam interaction, not to any loss of interest in this subject.

Mathematical simulation methods, which are widely being developed today in many countries, have not yet become "naturalized" at these conferences.

Owing to the great number of studies presented at the Conference and the broad range of subjects covered, it is impossible to discuss in detail even the most important among them. However, it may be useful to give a brief description of the general level of some of the subjects discussed at the Conference.

1. Interest in plasma chemistry is growing rapidly. The topics arousing the greatest interest among scientists are nonequilibrium particle distribution functions, with both elastic and inelastic interactions taken into account; the influence of electronic excitation on the rates of chemical reactions; the multichannel nature of elementary plasmochemical processes; and phenomena related to the absence of thresholds for chemical reactions. Considerable importance is attached to investigations of hydrodynamic turbulent displacement of plasma fluxes at various temperatures, chemical compositions, and specific weights. A prominent position in the fields of theory and fundamental experimental research is held by Soviet scientists, although the United States and the Federal Republic of Germany hold the lead in the industrial application of plasma theory. A great deal of interest was aroused at a plenary meeting by a survey of this subject presented by L. S. Polak (USSR).

2. In the "Elementary Processes" section a prominent place was given to studies on the multiphoton ionization of atoms and molecules under the influence of intense laser radiation. Recent achievements include the first successful comparison of the absolute values of the probabilities of multiphoton processes with the theoretical values, and the investigation of two-stage ionization processes. Some recent theoretical studies indicate that there is a fundamental change in the process of multiphoton ionization when the field of the atom is strongly disturbed by a laser radiation field.

Leaders in research on this subject are the Physics Institute of the Academy of Sciences of the USSR, Voronezh State University, the Applied Physics Institute of the Academy of Sciences of the Moldavian SSR, and the Atomic Physics Center at Saclay.

3. As in the past, great interest is being taken in research on vacuum breakdown. Attention is being concentrated chiefly on the detailed study of the high-speed microprocesses accompanying the development of pulse discharges and on the phenemenon of explosive emission of electrons, which plays a fundamental role in vacuum breakdown and has been widely applied in high-current accelerators and pulsed x-ray sources. A plenary survey report by G. A. Mesyats (USSR) was devoted to an analysis of these problems.

4. There is a steadily growing interest in high-pressure gas-discharge sources. A number of studies submitted to the Conference related to the investigation of plasma produced in high-pressure plasmatrons. Of great practical importance in this connection are the investigations of R. Bauder (United States), who has constructed an argon plasmatron operating at pressures of up to 1000 atm and has studied the effect of high pressure on the optical properties of dense plasma. Also worth noting is a study by K. Goldbach et al. (France), who determined the spectral characteristics of the radiation emitted by high-pressure argon plasma (up to 100 atm).

The greatest amount of attention in these investigations is being devoted to near-electrode phenomena, the processes of radiation transfer, and complex heat exchange (both convective and radiant). It should be pointed out in this connection that liaison was established between the "Discharges at High Pressure" and "Plasma Radiation" sections.

5. There has been a great increase of interest in physical processes taking place in a dense nonideal plasma, i.e., in a plasma for which the average potential energy of particle interaction is of the order of the kinetic energy. Because of this, a new subsection called "Dense Plasma" was organized. A plenary survey report on this subject was presented by Yu. G. Krasnikov, P. P. Kulik, and G. E. Norman (USSR).

At the previous conference in Bucharest there had already been a number of reports on the theoretical investigation of the properties of a dense nonideal plasma. Experimental results presented at the latest Oxford Conference confirmed that dense nonideal plasma has a number of specific properties. One of these

TABLE 1. Relative Numbers of Reports on Various Subjects, %

Subject	1965 (Belgrade)	1967 (Vienna)	1969 (Bucharest)	1971 (Oxford)
Collision of particles	5	5	4	14
Surface phenomena	9	8	7	5
Discharges at low pressure	13	23	20	15
Discharges at high pressure	14	14	11	21
Interaction of waves with plasma	12	14	19	21
Interaction of a beam with plasma	2	4	5	2
Thermodynamics and transfer processes	10	10	10	3
Shock waves	5	3	3	2
Plasma radiation	9	6	3	6
Diagnostics and experimental techniques	21	13	10	10
Plasma sources	3	3	7	0
Mathematical simulation	0	0	1	1

is the sharp increase in the electrical conductivity of a dense nonideal plasma as the temperature increases; the level of metallic conductivity is reached at $T \approx 10^4$°K and $n_e \gtrsim 10^{20}$ cm^{-3}.

The French program for the study of dense nonideal plasma is of great interest, and particularly noteworthy is a report by M. Delpeche on the study of the physics of strongly nonideal plasma in the afterglow of a glow discharge at helium temperatures. Judging by the preliminary experimental and theoretical work presented at the Conference by a number of scientists from the United States, France, and the Federal Republic of Germany, and taking into consideration the development of basic research on dense nonideal plasma in the USSR, we may expect the subject of "Dense Plasma" to be substantially expanded at subsequent conferences.

6. The Conference made it evident that a great deal of interest is being taken in nonlinear processes occurring in plasma. While earlier conferences dealt chiefly with the theoretical problems of such interactions, at this Conference the main attention was devoted to experimental investigations, and a good many examples of agreement between experimental and theoretical results were cited both in the survey reports of K. Etievan (France) and G. Bekefy (United States) and in the original communications.

Among the experiments on nonlinear processes, we should mention the work of scientists from Culham (England), who conducted detailed experimental investigations of the decomposition of a Langmuir wave into another Langmuir wave and an ionic wave and the resulting anomalous absorption of Langmuir waves. A study by G. Hoopman (Netherlands) succeeded for the first time in experimentally discovering and investigating a nonlinear explosive instability under conditions of plasma-beam interaction.

In the problem of the interaction of intense high-frequency fields and laser radiation with plasma and anomalous heating, there is a notable trend toward a study of the role of stochastic fields in the processes of heating and anomalous absorption. Studies conducted by scientists of the Plasma Center at Garching (Federal Republic of Germany) revealed an increase was observed in the interaction of stochastic high-frequency fields with plasma when the interaction frequency was close to the electronic gyrofrequency in the region of a magnetic mirror. This phenomenon may prove very important for an understanding of anomalous heating both as a result of high-frequency fields and as a result of turbulence excited by instability. V. N. Tsitovich and other scientists from the Physcis Institute of the Academy of Sciences of the USSR gave a theoretical discussion of the new effect of anomalous bremsstrahlung and absorption in turbulent plasma.

Among the studies on the heating of plasma by laser radiation, attention should be given to the results obtained by a group of scientists at Limelle (France) who had studied the interaction of laser radiation having a pulse duration of a few nanoseconds and a power of 10 GW with solid deuterium and had found that the total

neutron yield increases as the square of the absorbed energy; this disagrees with the theoretical model of one-dimensional expansion.

In conclusion, it should be remarked that in addition to the indisputably great achievements of the Conference, there was a certain tendency to make the range of subjects narrower than at earlier conferences. For example, no studies were prepared on such problems as thermonuclear synthesis, magnetohydrodynamic generators, or mathematical simulation. The restriction of the Conference's subject matter reduced the interest taken in it; this also seems to be indicated by the fact that there were fewer reports and fewer participants than at previous conferences. At the same time, besides the numerous conferences on narrow problems, there is a need for a broad congress on plasma physics, one of whose goals would be to reveal new directions and promote the mutual enrichment of the individual fields of study. This is especially necessary today, when there is a growing trend toward specialization and the subdivision of various fields of plasma research into narrower branches. The holding of such a congress is made necessary by the widespread impact of plasma physics on many related disciplines (solid-state and liquid physics, astrophysics, outer-space research electronics, mathematical simulation) and the ever-growing application of gas-discharge physics in technology.

It is to be hoped that the tendency toward restriction of subject matter that was observed at the Tenth Conference will be stopped by the new international organizing committee and that future conferences* will become plasma congresses covering a broad range of fundamental subjects and various applications.

*It has been decided that the Eleventh Conference on Phenomena in Ionized Gases will be held in Prague in September, 1973. The chairman of the national organizing committee will be L. Pekarek.

DRESDEN CONFERENCE ON MOSSBAUER SPECTROSCOPY

A. M. Afanas'ev

A conference on Mossbauer spectroscopy was held in Dresden, September 20-25, 1971. This conference was organized by the Physical Society of the German Democratic Republic and by the Central Physical Chemistry Institute of the Academy of Sciences of the German Democratic Republic. This is the fourth such conference on Mossbauer spectroscopy called on the initiative of the socialist countries (the first conference was held in 1962 in the USSR, the second in 1967 in Bulgaria, and the third in 1969 in Hungary).

About 150 scientists took part in the deliberations of the conference.

The scientific agenda of the conference consisted formally of six trends: 1) structural problems and magnetic problems; 2) relaxation phenomena; 3) nature of the chemical bond; 4) research on chemical reactions; 5) unusual aspects; 6) equipment and questions of methodology.

About 80 papers were read. Of these 12 were of a review nature. Most of the presentations were devoted to applications of the Mossbauer effect in research on various problems in solid state physics, in chemistry, and in industrial applications. The most important salient trends in Mossbauer spectroscopy were reflected in the review papers.

The broad opportunities open for applications of the Mossbauer effect in the solution of a wide range of metals science problems, such as phase analysis, studies of the kinetics of phase transitions, research on order – disorder processes, precipitation of new phase, and ageing of alloys, were lucidly demonstrated in a paper presented by T. Zemcik (Czechoslovakia).

A paper submitted by V. I. Gol'danskii (USSR) provided a survey of the work done in the USSR on the study of polymerization processes, stabilization of polymers, phase transformations in polymers, the nature of bonds linking polymeric chains, etc., by Mossbauer spectroscopic techniques. The further outlook for this trend of research was discussed.

J. Dezsy (Hungary) gave an account of research on the chemical structure of solid solutions. The effectiveness of the method in investigations of phase transitions and electron transfer in such systems was demonstrated.

I. P. Suzdalev (USSR) presented a review of research work on the mechanism underlying chemical reactions taking place on the surface of solids, and topochemical reactions. Great advances have been registered in recent years (particularly as a result of work by Soviet physicists) in the field of investigations of elemental events of adsorption and catalysis, with the aid of γ-resonance spectroscopy. The elucidation of the mechanism involved in topochemical reactions makes it possible to devise catalysts with specified catalytic activity.

Results of analysis of specimens of lunar soil obtained by means of the Luna-16 automatic station from the region of the Mare Fecunditatis (Sea of Abundance) were reported by T. V. Malysheva (USSR). These results made it possible to obtain the characteristic distribution of iron with respect to mineralogical phases. A difference between the regalite in the Mare Fecunditatis and the regalite in the Mare Tranquilitatis (Apollo-11 data) and in the Oceanus Procellarum (Apollo-12 data) was detected.

The Bulgarian physicists T. Tomov and T. Ruskov rendered an account of applications of Mossbauer spectroscopy in investigations of the performance of an iron – nickel storage battery.

Magnetic research was represented by a series of brief reports most of which dealt with the now traditional trend in γ-resonance spectroscopy of studying the structural and magnetostructural properties of

Translated from Atomnaya Energiya, Vol. 32, No. 4, pp. 364-365, April, 1972.

ferrites. The Dutch physicists van Kleffens, van der Kraan, and van der Loef presented research findings on the spin flip mechanism in samarium ferrite garnet; a report submitted by the Polish physicists E. Suwalski, E. Piekoszewski, et al., dealt with determinations of the parameters of the exchange interaction in ferrites $Y_{3-2x}Ca_{2x}Fe_{5-x}V_xO_{12}$; this group of physicists also obtained some interesting orderings in Ni – Zn ferrites; Nistor (Rumania) reported research results on several nickel ferrites.

Keen interest was shown in a report by G. Zawadzki (Canada), S. Woekem and van der Woede (Netherlands) on covalent effects in iron compounds. The authors presented a schema for calculating the effect of covalent bonding on the isomeric shift, on hyperfine magnetic fields, and the gradient of the electric field on iron nuclei. The importance of this work is highlighted above all by the fact that the calculations cited can be used in application to a broad class of ferrites.

These authors also presented a report on research into the nature of magnetism in metallic iron, based on a study of the temperature dependence of hyperfine magnetic spectra of iron with slight additions of Mn, Si, Al, and Ni impurities. According to the authors' statements, the degree of reliability of the temperature investigations is far higher than that of measurements of concentration dependences at a fixed temperature. The results obtained indicate the far-reaching nature of the exchange interaction. It is possible that the proposed method will meet with widespread application.

The exceptionally high level of experimental technique attained in investigations of the magnetic properties of ultrathin iron films was demonstrated in a report by J. Walker (USA). The aid of γ-resonance spectrometry was enlisted in detecting the magnetic state of the films down to thicknesses of the order of 7 Å, i.e., about two atomic layers. The magnetic order of the films disappeared starting with the thickness 16 Å.

S. S. Yakimov (USSR) gave an account of experimental detection of the recovery of the magnetic structure of an antiferromagnetic material in an externally applied magnetic field above the Neel point. Similar investigations of ferromagnetic materials were reflected in a paper presented by Sh. Sh. Bashkirov (USSR).

Several papers went into comparisons of the possibilities inherent in other problem-solving methods, applied to problems suitable for study with the aid of γ-resonance spectroscopy. E. Fluck (West Germany) presented a survey of research on the chemical bond in complex compounds, using the method of photoelectron spectroscopy; this research has been undergoing intensive development in recent years. After demonstrating the effectiveness and perspective outlook of the technique, the author emphasized the point that the most complete and reliable information is obtained in those cases where the same substance is investigated by different methods, including Mossbauer spectroscopy. L. Keszthely (Hungary) compared the method of perturbed angular correlations and the method of Mossbauer spectroscopy in studies of magnetic hyperfine interactions.

One of the central positions in Mossbauer spectroscopy is that now occupied by the problem of relaxation spectra. Relaxation processes bring about a sharp increase in the number of qualitatively distinct forms of manifestation of hyperfine structure (HFS), and the interpretation of the corresponding spectra constitutes an involved mathematical problem. Moreover, in some instances the invoking of relaxation processes may provide an alternative explanation of HFS spectra, along with the usual mechanisms in the formation of complex HFS spectra, and may account for the change brought about in HFS spectra by external effects. This last point is responsible for the great practical importance of the problem. All of these questions were touched upon in a review paper by M. Bloom (USA). Several related short reports were also presented.

Among the papers dealing with unusual aspects of Mossbauer spectroscopy, one by Yu. M. Kagan (USSR) is of greatest interest. This paper was devoted to research on the specifics of nuclear reactions in crystals exhibiting a high degree of perfection. The regularity of the arrangement of nuclei in the crystal causes an abrupt change in the character of the nuclear reaction, and an effect of suppression of inelastic channels of the nuclear reaction is possible under certain conditions. This type of research was initiated at the I. V. Kurchatov Institute of Atomic Energy, and is being pursued energetically at the present time. The report provided a detailed theoretical analysis of the problem, and cited results of the experimental detection of that effect recently at the Institute of Atomic Energy (IAE). Reports by J. Walker (USA) and W. Maisel (East Germany) on experimental observations of double nuclear magnetic resonance and γ-resonance were greeted as sensational. Severe and exacting experimental difficulties attend the observation of that double phenomenon. Considering the amount of interest shown at the conference in the

papers mentioned here, an expansion of research on the double resonance can be expected in the coming years.

A report by Yu. Ostanevich (USSR) dealing with an investigation of the Mossbauer effect on the nuclide Zn^{67}, which exhibits a record low line width, was received with great interest. After several years of investigations, this paper brought to light the first work demonstrating the possibility of extensive applications of that unique line.

WARSAW SEPTEMBER 1971 SYMPOSIUM ON NUCLEAR ELECTRONICS

G. P. Zhukov, V. G. Zinov,
I. F. Kolpakov, and A. N. Sinaev

The VI International Symposium on Nuclear Radioelectronics, organized by the JINR in joint sponsorship with the Institute of Nuclear Research at Swierk (Poland), was held in Warsaw in September 1971. Participating in the symposium were about 100 specialists from JINR member-nations, as well as scientists from other countries. The content of over 60 papers delivered at the symposium, and the ensuing floor discussion, highlighted the present state of the art and development trends now extant in nuclear electronics. The article provides brief information on the most essential topics covered in the symposium's agenda.

Proportional Chamber Electronics. Many of the papers submitted on the electronic circuitry of proportional chambers in which information is picked up from each chamber wire dealt with work underway at CERN. Each electronic channel in these chambers is fabricated in the form of a hybrid integrated circuit 4×2 cm in size. The passive circuit elements are fabricated on the basis of thin-film technology, with four blocks of standard integrated circuits used as the active circuit elements. One of the systems developed at CERN was designed for incorporation into a general computer system, and is used to measure the profile of the beam and to save considerable time. Two new systems each containing several thousand wires are being developed for physical experiments. It must be emphasized, however, that the cost of systems incorporating proportional chambers remains high, in the region of ten dollars per wire, i.e., ten times higher than the cost of systems with wire spark chambers.

Time-Measuring Devices. The logic devices developed for time measurements use scintillation counters, and generally satisfy the requirements of physical experiments well enough. Further improvements in the time characteristics of these devices is not a practical requirement for the moment, since no perceptible progress has been made in the performance of the scintillation counters themselves. One exception is provided by devices intended to measure short time intervals. Time – amplitude converters with electric resolving power of 2.2 nsec, and suitable generators for calibrating the converter, have been developed at Grenoble (France). The high resolution stems from the use of new high-speed transistors and tunnel diodes.

Much attention is being given to the development of equipment using semiconductor detectors in time measurements. Precision time correlations to some portion of the incoming pulse is a very important feature for some experiments. The method of constant ratio of amplitude parts is being used widely at the present time. An interesting variant of that method is embodied in a device developed at Debrecen (Hungary). The output signal in this device appears at the instant when the pulse reaches half-amplitude in decay. In a device developed at Saclay (France), pulse-height discrimination is carried out at a low threshold in order to narrow the time spread of the pulses being shaped, while the noise pulses surmounting the threshold are cut off with the aid of additional pulse-width discrimination. The authors of the device proceed from the fact that the duration of the noise pulses is less than the duration of the useful signals above the threshold.

Spectrometric Devices. Better realization of the possibilities inherent in semiconductor detectors is a major problem in the development of equipment for nuclear spectroscopy, and this applies particularly to improving the resolution of the spectrometric part of the system and to achieving faster system response. Attention is centered on reducing the noise of the passive elements in the input circuit, in the design of preamplifiers. Pulse shaping circuits in linear accelerators are being improved in a continuing program, with

Translated from Atomnaya Énergiya, Vol. 32, No. 4, pp. 365-366, April, 1972.

the object of improving the signal/noise ratio. Serious attention is also being given to linear pulse gates and to preselection of pulses for analysis.

The number of channels in amplitude-code converters runs into the range of 8000 to 16,000. This leads added importance to higher speed while keeping other characteristics satisfactory. The address pulse train frequency in the 16,000-channel converter developed at Saclay is 200 MHz. The speed of response of the converter developed at the JINR Neutron Physics Laboratory was improved by using a two-step discharge of the memory capacity.

Serious attention is being given to the design of equipment for calibrating high-precision spectrometer systems. A precision verifying-pulse generator, a device with great promise, was developed at Saclay.

Close attention is being given to the development of various automated devices capable of increasing precision in measurements and monitoring certain system parameters during an experiment. Devices capable of controlling the parameters of linear systems (gain, characteristics of pulse-shaping networks, etc.), with the aid of small computers have been developed at the Hahn and Meitner Institute (West Berlin).

Interfacing Devices. The widespread use of small computers in physics experiments has led to a rapid development of devices performing interfacing functions between the experimental equipment and the computer. Devices conforming to the CAMAC standard have been undergoing particularly vigorous development.

A wide assortment of digital units has been developed at CERN. Close attention is being given to both digital and analog units and modules at Saclay. Impressive advances have been made in the development of various such modules at the Hahn and Meitner Institute, at the Nuclear Research Institute in Swierk, and at the High Energies Laboratory of the Joint Institute for Nuclear Research.

As the devices covered by the CAMAC standard become more complicated, programming acquires increasing significance. A lot of work on standardization of programming and on the devising of special languages is being carried out by the ESONE committee, and similar work is underway at Saclay, at the Hahn and Meitner Institute, and elsewhere.

Applications of Small Computers in Physics Experimentation. In recent years, small desktop computers have come into widespread use in physics experiments. The most commonly used such computers are the RDR-8, NR-2116 (USA), the S11-10020 (France), the TRA (Hungary), etc., all of which feature compactness and convenient channels for communication with off-line equipment. The RDR-11 and NR-2100 computers are among those becoming available in the recent period which show the greatest promise for direct applications in experiments in the coming years. More effective utilization of the high-cost off-line equipment is expedited in many cases by connecting that equipment up to the main computer, to which several data processors for the small computers are also hooked up.

Similar systems, but with some modifications in the structure and types of the computers used, have been developed at physics institutes of some countries in Western Europe and in the USA. For example, the Sigma-7 computer at the Brookhaven laboratory (USA) operates in a time-sharing mode handling several experiments at once. Small computers are also used in experiments being performed in JINR laboratories.

The use of data displays as the most convient means of communication between the experimenter and the computer and experimental equipment is also receiving its due share of attention. Memory tube displays are often used in working with small computers. The Tektronix-611 tube, serving as a basis for the interesting display system develped at the Hahn and Meitner Institute, for example, is now in widespread use. A color display designed around a television picture tube has been developed at the Brookhaven laboratory. The several colors used make it possible to present a lucid visual display of multidimensional spectroscopic information. Clearly, small desktop computers with display devices will find even broader applications in physics experiments in the near future.

Complex electronic facilities used in various areas of experimental physics were also discussed at the symposium.

The proceedings of the symposium will be published by the publishing division of the Joint Institute for Nuclear Research.

IAEA DRAFT REGULATIONS FOR SAFE TRANSPORTATION OF RADIOACTIVE MATERIALS

S. Martynov

A conference of experts meeting in Vienna, October 18 through November 5, 1971, discussed drafts of "Regulations governing safe transportation of radioactive materials" (PL-383) and technical specifications accompanying the "Regulations."

Experts from 13 nations affiliated to IAEA, including Great Britain, the USSR, USA, France, West Germany, and representatives of such interested international agencies as the World Health Organization, the International Standards Organization, the International Aviation Transport Organization, Euratom, and others, took part in the conference.

Recommendations forwarded by nations affiliated to IAEA and by the interested international agencies, bearing on safe conveyance of radioactive materials on all means of transportation, including use of the new system of containerized and prepackaged international cargo shipments for which not only the most highly perfected types of shipping containers, pallets, and packaging means have been developed, but also specialized railway cars and vessels, automotive trailers and semitrailers, were discussed in the course of the conference. The parameters of the containers for that system were recommended by the International Standards Organization. The width and height of all of the containers will be 2438 mm, length 2837, 5924, 8096, and 9144 mm, for gross weights of 10, 20, 25, and 30 tons respectively. Recommendations on safe shipping of radioactive materials through containerized transportation systems were modified in the drafts of the "Regulations" to match those standards.

Such concepts and terminology as packaging, packaging set, packaging sets of types A, B(u), B(m), materials of low-level specific activity, fissionable materials; cargo remitter, cargo receiver, and conveyor of radioactive materials; means of transportation for complete shipments, etc., were specified more precisely in the draft "Regulations." The numerical value of the dose rate of ionizing radiations at a distance of one meter from the external surface of shipping packages belonging to the second transportation category was specified as 1 mrem/h. Earlier parameters for inspection of packaging sets were reviewed and modified. For example, packaging sets of type A for gaseous and liquid radioactive materials are recommended for destructive inspection tests using the impact of an iron ingot falling from a height of 1.7 m.

A graphical system of presentation was decided upon in order to contract the volume of the "Regulations" and simplify their use.

It must be pointed out, however, that the numerical values of some of the parameters of packaging sets in the revised drafts still fall short of optimum conditions. For example, the criteria for calculating numerical values of maximum activity for packaging sets of type A were set somewhat too low, so that the technical capabilities of that type of packaging set are not fully utilized.

The IAEA Secretariat is obligated, by decision of the conference, to present the revised draft "Regulations" to the Council within the shortest feasible time, for approval and publication in 1972.

Translated from Atomnaya Énergiya, Vol. 32, No. 4, p. 367, April, 1972.

V/O IZOTOP AGENCY SEMINARS AND EXHIBITS

A scientific-technical seminar on "Experience in the use of radioisotope techniques and instruments at petrochemical plants" was held in Baku in November, 1971. The seminar was jointly sponsored by V/O Izotop agency, the AzINTI [Azerbaidzham research institute] and the Azneft' association [Azerbaidzhan petroleum association]. Participating in this seminar were representatives of the nation's leading organizations engaged in exploration, processing, and recovery of petroleum and gas, as well as AzfVNIIgeofiziki specialists, specialists from the Azerbaidzhan Petroleum and Gas Institute, organizations engaged in research and development work on instruments for the petrochemical and chemical process industries, and several other organizations in Moscow, Kiev, Ufa, and Dnepropetrovsk. Reports were presented on new instruments and methods in use at oil refining and petrochemical plants.

The seminar participants enjoyed the opportunity of inspecting "Atom for Peace" exhibits set up at Baku under the sponsorship of the USSR State Committee on Peaceful Uses of Atomic Energy [GKIAE].

A scientific-technical conference on "Radioisotope techniques and instruments for process automation and monitoring" held in Leningrad November 24-25, 1971, attracted staffmembers of design and research institutes. The purpose of this seminar was to study the experience gained by advanced institutes in applications of radioisotope equipment and the widespread use of promising radioisotope methods in the design of automatic control systems by design and research institutes in Leningrad. A large fund of positive experience in applications of radioisotope instruments has been accumulated at many of the Leningrad institutes engaged in this work. The list of such institutes includes Giprotsement, LenNIIGiprokhim, Proektavtomatika, Giprotyazhmash, and others.

The conference participants recommend general and all-sided utilization of radioisotope equipment in the designs being developed.

A scientific-technical combined seminar and exhibit on "Applications of isotopes and radioisotope equipment in the national economy" was held in Vladimir, December 8-10, 1971.

The seminar participants heard and discussed reports and communications on applications of isotopes and radioisotope process monitoring devices at plants and organizations in the Vladimir district (at the Khrustal' glass works in Gus'-Khrustal'nyi, the Iskozh plant in Aleksandrov, at the silk combine in Kirzhach, at the Ordzhonikidze plant in Kal'chugin, at the regional printing plant, etc.); they also had opportunities to visit the exhibits, see special film showings, and acquire publicity material and technical data.

Recommendations were to set up a section dealing with radioisotope techniques under the aegis of the Council of assistance on scientific-technical progress of the Vladimir regional committee of the Communist Party of the Soviet Union, and to present a lecture course for workers in industrial plants and organizations on applications of isotopes and radioisotope equipment in the national economy.

A regional combined seminar and exhibit on "Applications of isotope techniques and radioisotope instruments in the national economy" was held in L'vov in December, 1971. The seminar was organized by the Kiev interrepublic division of V/O Izotop jointly with the Center of Scientific-Technical Information and the House of Industry of the NTO [Scientific and Technical Society]. Participating in the work of the seminar were heads of departments of production sections, workers of the monitoring instrumentation services of industrial plants, specialists from research and design institutes, medical and agricultural institutions. Reports were head on applications of γ-ray nondestructive testing and inspection techniques for use on industrial goods, experience in the implementation of radioisotope techniques and instruments at the Donetsk base-level isotope laboratory, on the use of radioisotope instruments at mines of the Ukrzapadugol'

Translated from Atomnaya Énergiya, Vol. 32, No. 4, pp. 367-368, April, 1972.

coal combine, etc. The possibilities and outlook of applications of radioisotope instruments at plants in the L'vov region were discussed. Specimens of radioisotope dosimetric and radiometric instruments and γ-ray nondestructive testing equipment were displayed at the exhibit.

News on the combined seminar and exhibit was broadcast over radio and television. The combined seminar and exhibit is of great significance in expediting the job of getting radioisotope equipment into production use at plants in the L'vov region.

breaking the language barrier

WITH COVER-TO-COVER ENGLISH TRANSLATIONS OF SOVIET JOURNALS

in mathematics and information science

Title	# of Issues	Subscription Price
Algebra and Logic *Algebra i logika*	6	$110.00
Automation and Remote Control *Avtomatika i telemekhanika*	24	$185.00
Cybernetics *Kibernetika*	6	$125.00
Differential Equations *Differentsial'nye uravneniya*	12	$150.00
Functional Analysis and Its Applications *Funktsional'nyi analiz i ego prilozheniya*	4	$ 95.00
Journal of Soviet Mathematics	6	$135.00
Mathematical Notes *Matematicheskie zametki*	12 (2 vols./yr. 6 issues ea.)	$175.00
Problems of Information Transmission *Problemy peredachi informatsii*	4	$100.00
Siberian Mathematical Journal of the Academy of Sciences of the USSR Novosibirski *Sibirskii matematicheskii zhurnal.*	6	$185.00
Theoretical and Mathematical Physics *Teoreticheskaya i matematicheskaya fizika*	12 (4 vols./yr. 3 issues ea.)	$125.00
Ukrainian Mathematical Journal *Ukrainskii matematicheskii zhurnal*	6	$135.00

Back volumes are available.
For further information, please contact the Publishers.

SEND FOR YOUR FREE EXAMINATION COPIES

PLENUM PUBLISHING CORPORATION
Plenum Press • Consultants Bureau
• IFI/Plenum Data Corporation
227 WEST 17th STREET
NEW YORK, N. Y. 10011

In United Kingdom
Plenum Publishing Co. Ltd., Davis House (4th Floor)
8 Scrubs Lane, Harlesden, NW10 6SE, England

breaking the language barrier

WITH COVER-TO-COVER ENGLISH TRANSLATIONS OF SOVIET JOURNALS

in physics

Title	# of Issues	Subscription Price
Astrophysics *Astrofizika*	4	$100.00
Fluid Dynamics *Izvestiya Akademii Nauk SSSR mekhanika zhidkosti i gaza*	6	$160.00
High-Energy Chemistry *Khimiya vysokikh énergii*	6	$135.00
High Temperature *Teplofizika vysokikh temperatur*	6	$125.00
Journal of Applied Mechanics and Technical Physics *Zhurnal prikladnoi mekhaniki i tekhnicheskoi fiziki*	6	$150.00
Journal of Engineering Physics *Inzhenerno-fizicheskii zhurnal*	12 (2 vols./yr. 6 issues ea.)	$150.00
Magnetohydrodynamics *Magnitnaya gidrodinamika*	4	$100.00
Mathematical Notes *Matematicheskie zametki*	12 (2 vols./yr. 6 issues ea.)	$175.00
Polymer Mechanics *Mekhanika polimerov*	6	$120.00
Radiophysics and Quantum Electronics (Formerly Soviet Radiophysics) *Izvestiya VUZ. radiofizika*	12	$160.00
Solar System Research *Astronomicheskii vestnik*	4	$ 75.00
Soviet Applied Mechanics *Prikladnaya mekhanika*	12	$160.00
Soviet Atomic Energy *Atomnaya énergiya*	12 (2 vols./yr. 6 issues ea.)	$150.00
Soviet Physics Journal *Izvestiya VUZ. fizika*	12	$160.00
Soviet Radiochemistry *Radiokhimiya*	6	$145.00
Theoretical and Mathematical Physics *Teoreticheskaya i matematicheskaya fizika*	12 (4 vols./yr. 3 issues ea.)	$125.00

Back volumes are available. For further information, please contact the Publishers.

SEND FOR YOUR FREE EXAMINATION COPIES

PLENUM PUBLISHING CORPORATION
227 WEST 17th STREET
NEW YORK, N. Y. 10011
Plenum Press • Consultants Bureau
• IFI/Plenum Data Corporation

In United Kingdom,
Plenum Publishing Co Ltd., Davis House (4th Floor)
8 Scrubs Lane, Harlesden, NW10 6SE, England